UNIVERSITÀ DEGLI STUDI DI TRIESTE

XXIX CICLO DEL DOTTORATO DI RICERCA IN

CHIMICA

NOVEL ASPARTYL PROTEASE INHIBITORS: SYNTHETIC STUDIES AND PRELIMINARY EVALUATION

Settore scientifico-disciplinare: CHIM/06

DOTTORANDA

Giorgia Regini

COORDINATORE

PROF. Mauro Stener

SUPERVISORE DI TESI

PROF. Fulvia Felluga

ANNO ACCADEMICO 2015/2016

A tutti voi che mi volete bene e
mi riempite la vita di sorrisi

PART 1: Chiral α-allylamines as monomeric units for the synthesis of dipeptide isosters

PART 2: *2-dihydropyrimidines as promising inhibitors of BACE 1*

Experimental Part

ABSTRACT

Aspartic Proteases are proteolytic enzymes involved in a large number of biological processes, playing an essential role in several important diseases. Their inhibitors have emerged as useful drugs in the treatment of cancer, parasitic, fungal and viral infections as well as inflammatory, immunological, respiratory, cardiovascular and neurodegenerative disorders.

Acquired Immunodeficiency Syndrome (AIDS) and Alzheimer Disease (AD) are controlled by aspartic proteases, HIV-Pr and BACE-1 respectively. HIV-Pr plays an essential role in the replication and maturation of the Human Immunodeficiency Virus, while BACE-1 is involved in the production and deposition of amyloid-β-peptide (Aβ), recognized as a possible cause for AD.

Aspartic proteases inhibitors can be classified into the two major categories of peptidomimetic and nonpeptide inhibitors. The former, designed to emulate their natural substrates, are oligopeptides containing a not-hydrolizable dipeptide isostere. Currently, many designed potent and selective protease peptidomimetic inhibitors of the human immunodeficiency virus protease (HIV-1 Pr) are used in the treatment of AIDS as they efficiently slow down or halt disease progression.

Even very potent *in vitro* peptidomimetic BACE-1 inhibitors were developed but their poor pharmacokinetic profile has prevented them from being further developed to oral bioavailable CNS drug. Thus, more recent attempts have been directed towards the discovery of small non peptidic inhibitors, that have higher blood brain barrier penetration and are capable to efficiently bind the active site of the enzyme lowering the production of Aβ protein.

This thesis is divided in two parts.

In the frame of a research activity aimed at the design and synthesis of peptidomimetic HIV-Pr inhibitors, the first part of this work is focused on the synthesis of chiral optically pure α-allylamines as key intermediates for the stereoselective synthesis of dipeptidic isosters. In particular, in chapter 2 the development of a revised version of Julia olefination is described, that allowed the obtainment of a small library of α-aminoalkenes derived from Ala, Ileu, Leu, Phe, Pro, Tyr, Val with good yields and exccellent e.e.s. With respect to the original Julia

reaction, in this modified version α-aminoesters derived from aminoacids are employed as the starting material, this avoiding the use of the aminoaldehydes normally used in the classical olefination methods, whose reproducibility is often affected by the low configurational and chemical stability of α-chiral parent aldehydes.

The second part of the thesis deals with the synthesis and biological evaluation of functionalized 3,4-dihydropyrimidines (DHPMs) as BACE 1 inhibitors. This heterocyclic scaffold is present in many biologically and pharmacologically active compounds and it possesses the requisite features for an effective inhibitory activity against BACE-1, as shown by our preliminary studies run (Chapter 4) on a group of 3,4-dihydropyrimidinones (X = O) e 3,4-dihydropyrimidinthiones (X = S), with measured affinities in the micromolar range.

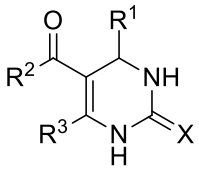

With the aim of obtaining inhibitors with improved potency, the study was extended to 2-iminoDHPMs having a guanidine group embedded in the heterocyclic scaffold, due to the structural features of the guanidine moiety, suitable for an optimal interaction with BACE-1 active site. The library of DHPMs was obtained by Biginelli reaction in which a variety of different aliphatic and aromatic aldehydes, were reacted β-dicarbonylic compounds and with urea, thiourea and guanidine.

Molecular docking experiments (Chapter 5) assisted the choice of the most appropriate substituents to append on the heterocyclic scaffold; inhibitory activity was determined measuring IC_{50} values (Chapter 5), with fluorimetric assays using the FRET technique.

In chapter 5 we describe some preliminary approaches to the obtainment of DHPM as single enantiomers, through resolution techniques or chiral auxiliary based stereoselective synthesis.

ABSTRACT

Le proteasi aspartiche sono enzimi proteolitici coinvolti in un gran numero di importanti processi biologici e svolgono un ruolo chiave in diverse importanti patologie. La loro inibizione è una strategia che si è rivelata utili nel trattamento di malattie fra cui alcuni tipi di tumore, infezioni fungine, parassitiche e virali, nonché malattie infiammatorie, immunologiche, respiratorie cardiovascolari e neurodegenerative.

Sia l'AIDS (Sindrome da Immunodeficienza Acquisita) che il morbo di Alzheimer (AD) sono regolati da proteasi aspartiche, rispettivamente l'HIV-proteasi e la BACE-1. La prima è coinvolta nel processo di maturazione e replicazione del virus da HIV, mentre BACE-1 è alla base dello sviluppo di placche amiloidi, costituite da oligopeptidi di tipo Aβ, e considerate una possibile causa di AD.
Inibitori delle proteasi aspartiche possono essere classificati in due categorie principali, quella dei peptidomimetici e dei non-peptidici. I primi sono piccoli oligopeptidi che mimano il substrato naturale dell'enzima in quanto contengono un isostere dipeptidico non idrolizzabile. Attualmente diversi inibitori di questo tipo sono usati con successo nel trattamento dell'AIDS, per la loro capacità di rallentare o bloccare il progresso della malattia. Al contrario, la strategia basata su inibitori peptidomimetici si è rivelata non produttiva nel caso della BACE-1, in quanto alcuni di questi, pur essendo molto potenti *in vitro*, sono risultati inefficaci *in vivo* a causa del loro elevato peso molecolare e scarso profilo farmacocinetico. L'attenzione si è perciò in questo caso spostata su piccole molecole a carattere non peptidico, in grado di oltrepassare la barriera ematoencefalica e quindi di abbassare la produzione di proteina Aβ anche *in vivo*.

La prima parte di questa tesi di dottorato si sviluppa all'interno di un progetto più ampio rivolto alla progettazione e sintesi di inibitori peptidomimetici dell'HIV-proteasi e riguarda la sintesi di α-allilammine chirali otticamente pure come intermedi chiave nella sintesi stereoselettiva di isosteri dipeptidici.
In particolare nel capitolo 2 è descritta la messa a punto di una variante della reazione di olefinazione di Julia. che ha consentito di ottenere una piccola libreria di α-amminoalcheni derivati da Ala, Ileu, Leu, Phe, Pro, Tyr, Val con buone rese e

eccellenti eccessi enantiomerici. La modifica rispetto alla versione originale della reazione è consistita nell'impiegare α-amminoesteri derivati da amminoacidi naturali come substrati, al posto delle α-amminoaldeidi normalmente usate nelle reazioni di olefinazione, la cui affidabilità e riproducibilità sono spesso condizionate dalla instabilità configurazionale e chimica dei precursori aldeidici con chiralità in posizione alfa.

Nella seconda parte della tesi è descritta la sintesi e valutazione biologica di 3,4-diidropirimidine (DHPMs) funzionalizzate come inibitori di BACE-1. Questo scaffold eterociclico, opportunamente funzionalizzato, è presente in molti sistemi biologicamente e farmacologicamente attivi ed ha le caratteristiche richieste per un'efficace inibizione della BACE 1, come mostrato dai nostri studi preliminari (Capitolo 5) condotti su una libreria di 3,4-diidropirimidinoni (X = O) e 3,4-diidropirimidintioni (X = S) che hanno evidenziato affinità nell'ordine del micromolare.

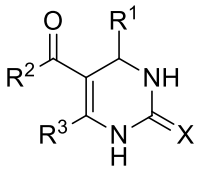

Con l'obiettivo di aumentare l'attività inibitoria abbiamo poi modificato la struttura di questi composti introducendo nello scaffold diidropirimidinico un motivo guanidinico, individuato come unità in grado di interagire più efficacemente con il sito attivo dell'enzima.

L'approccio sintetico utilizzato si basa sulla reazione di Biginelli, in cui oltre che l'urea e la tiourea è stata usata guanidina cloridrato, e come partners di reazione aldeidi alifatiche e aromatiche, e composti β-dicarbonilici..

La scelta dei diversi sostituenti da introdurre sullo scaffold eterociclico è stata supportata da esperimenti di docking molecolare (capitolo 5) mentre l' attività inibitoria è stata valutata tramite misure di IC_{50} eseguite mediante saggi enzimatici di fluorescenza basati sulla tecnica FRET

Nel capitolo 5 sono descritti anche alcuni preliminari approcci all'ottenimento delle DHPMs in forma enantiomericamente pura, attraverso risoluzione delle miscele raceme che risultano dalla reazione o attraverso sintesi stereoselettiva mediata da ausiliarichirali.

Abbreviations

AcOH	Acetic acid
AD	Alzheimer disease
ADME	Absorption, Distribution, Metabolism, Acquired Excretion
AIDS	Immune Deficiency Syndrome
Ala	Alanine
AP	Aspartic proteases
APP	Amyloid precursor protein
Asp	Aspartic acid
Aβ	β-amyloid peptide
BACE1	β-site APP cleaving enzyme 1
Boc	tert-Butoxycarbonyl
br	broad signal
CM	Cross Metathesis
CNS	Central nervous system
d	doublet
DABCYL	4-([4-(Dimethylamino)phenyl]azo) benzoic acid
DCM	Dichloromethane
dd	Doublet of dublets
d.e.	Disteroisomeric excess
DEPT	Distortionless enhancement by polarization transfer
DHPM	Dihydropyrimidine
DMAP	4-Dimethylaminopyridine
DMF	Dimethylformamide
DMSO	Dimethylsulfoxide
EDANS	5-((2-Aminoethyl)amino)naphthalene-1-sulfonic acid
e.e.	Enantiomeric excess
Em	Emission
EtOH	Ethanol
EtOAc	Ethyl acetate
Ex	Excitation
FRET	Förster Resonance Energy Transfer
Gly	Glycine
HIV	Human immunodeficiency virus
HIV-Pr	HIV-1 protease
IC_{50}	Half maximal inhibitory concentration
Ile	Isoleucine

HSQC	Heteronuclear Single Quantum Coherence Spectroscopy
COSY	COrrelation SpectroscopY
HIV-IN	HIV-integrase enzyme
HPLC	High Pressure Liquid Cromatography
iPrOH	Isopropanol
Ki	Equilibrium constant for an inhibited reaction
Leu	Leucine
MeOH	Methanol
m.p.	Melting point
MS	Mass spectrometry
MW	Microwave
MCR	Multicomponent reaction
MRI	Magnetic Resonance Imaging
mRNA	Messenger RNA
NMR	Nuclear Magnetic Resonance
nBuLi	n-Butyl lithium
PAMPA	Parallel Artificial Membrane Permeability Assay
PE	Petroleum ether
Phe	Phenylalanine
Pro	Proline
Py	Pyridine
ppm	Parts per million
PR	Protease
RNA	Ribonucleic acid
r.t.	Room temperature
RT	Reverse Transciptase
Ser	Serine
TFA	Trifluoroacetic acid
THF	Tetrahydrofuran
TLC	Thin layer chromatography
Tyr	Tyrosine
Val	Valine

PART 1

Chiral α-allylamines as monomeric units for the synthesis of dipeptide isosters

Introduction

1. Proteases

Proteases are a class of enzymes that selectively catalyze the hydrolysis of peptide bonds in proteins and polypeptides. The human genome encodes over 500 proteases, making this class one of the largest families of enzymes.[1]

Proteases play a crucial role in physiological as well as in pathological processes related to important diseases. As a consequence, protease inhibitors are emerging as useful drugs in the treatment of cancer, parasitic, fungal and viral infections (e.g. schistosomiasis, malaria, C.albicans, AIDS, hepatitis, herpes), inflammatory, immunological, respiratory, cardiovascular and neurodegenerative disorders including Alzheimer's disease[2].

Proteases can be classified into four classes: aspartic, serine, cysteine and metalloproteases.[3] While cysteine and serine hydrolases use the nucleophilic side chain of an aminoacid residue for the catalytic reaction, in aspartic and metalloproteases the nucleophile attacking the scissile peptide bond is a water molecule which is activated directly, as in aspartic peptidases, or by binding to one or two metal ions, as in the metallopeptidases. Typically, each protease has a dipeptide target (Table 1) and the knowledge of their specific sequences can be an excellent starting point for the design of new inhibitors.[4]

---

[1] H.V Motwani, M. De Rosa; L.R. Odell, A. Hallberg, M. Larhed, *Eur. J. Med. Chem.*, **2015**, 90, 462.

[2] **a.** B. Schmidt, *ChemBioChem* **2003**, 4, 366; **b.** M. S. Craik and C. Debouck, in *Perspectives in Drug Discovery and Design*,: J. H. McKerrow and M. N.G. James, Eds, ESCOM, Leiden,1995, Volume 2, pp 1–125, **c.** C. Seife, *Science,* **1997**, 277, 1602.

[3] O. Kohei, *J. Biochem.*, **2012**, 151, 13.

[4] N. D. Rawlings, G. Salvesen, *Handbook of Proteolytic Enzymes*, Elsevier, **2013**.

Protease	Type	Dipeptide target
BACE1 **(β-site APP cleaving enzyme 1)**	Aspartic human	Leu-Ala
HIV-PR **(Human Immunodeficiency Virus Protease)**	Aspartic viral	Phe-Pro
Gastricsin	Aspartic human	Tyr/Ala, Leu, Ser, Thr
Papain	Viral cysteine	Hydrophobic aa-Arg/Lys
uPA urokinase	Serine human	Arg/Val

Table 1. *Target sequences for representative proteases*

1.1 Aspartyl Proteases

Aspartyl proteases are so named because they use two aspartic acid residues (Asp) to activate the scissile amide bond and a water molecule in the active site, thus promoting the catalytic cleavage of the peptide substrate. These proteases represent the smallest class of peptidases, comprising only 15 members, and they can be classified into two main groups AA and AD according to their tertiary structure. The AA group can be further divided into two families: the A1 family, which includes the classic aspartic proteases (BACE1, BACE2, cathepsin D, cathepsin E, pepsin, pepsin C, renin and napsina), and A2 family, including HIV-PR, which can be integrated in the human genome by retroviruses. The AD group is constituted by presenilin and by other peptidases capable of hydrolysing peptide bonds within a transmembrane region.[5]

Enzymes belonging to the A1 family are monomeric bilobed, with the active site located between the lobes, and an Asp residue on each lobe. The peptidases of the A2 family are homodimers with a single lobe bearing one catalytic Asp. These proteases are active only in dimeric form and the active site is located between the two monomeric units (Figure 1).

[5] J. Eder, U. Hommel, F. Cumin, B. Martoglio and B. Gerhartz, *Current Pharmaceutical Design*, **2007**, 13, 271.

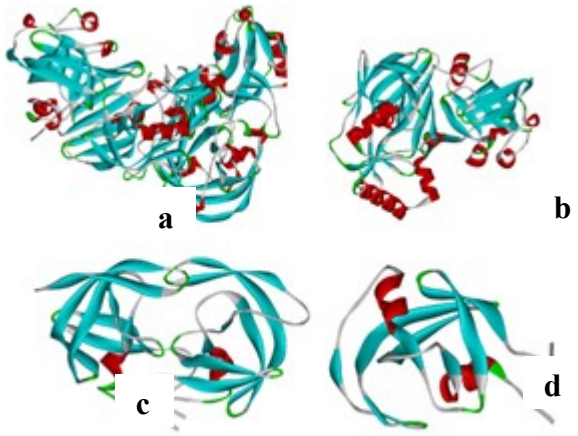

Figure 1.*Schematic structure of monomeric aspartyl proteases (a: renin; b: plasmepsin) and dimeric proteases (c: HIV-1 Pr; d: EIAV protease)*

All aspartic proteases have two triads Asp-Thr/Ser-Gly which form the catalytic site through a network of hydrogen bonds called "fireman's grip". Inside the active site, aspartic proteases generally bind 6-10 aminoacids of their polypeptide substrates.[6] The side chains of the polypeptide substrate are hosted within subsites of the protease catalytic site. According to the nomenclature of Schechter and Berger,[7] the amino acid residues at the N-terminus of the scissile bond are indicated with P1 ... Pn, which correspond to the protease's subsites S1 ... Sn; the residues at C-terminus are indicated with P1 '... .Pn', corresponding to subsites S1'... Sn' (Figure 2).

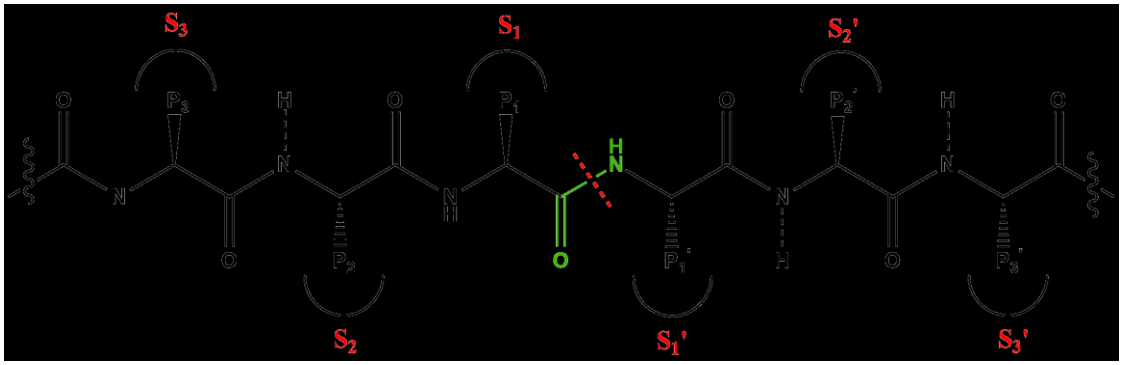

Figure 2. *Schechter and Berger's nomenclature for describing the protease subsites and the side chains of the substrates (the scissile bond is indicated in green).*

[6] M. N. G. James, A. R. Sielecki, *Biological Macromolecules and Assemblies: Active Sites of Enzymes*; John Wiley & Sons: New York, **1987,** Volume 3, 413.

[7] I. Schechter, A Berger. *Biochem. Biophys. Res. Commun.*, **1967**, 27, 157.

Furthermore, some aspartic proteases also have one or more flaps that close down on top of the bound substrate interacting with it and increasing the basis for selectivity.

1.1.1 Hydrolysis Mechanism

The accepted mechanism for aspartic proteases is a general acid-base mechanism involving the coordination of a water molecule between the two aspartate residues. One aspartate activates water by abstracting a proton, enabling the water to attack the carbonyl carbon of the substrate scissile bond, generating a tetrahedral oxyanion intermediate whose rearrangement mediated by the protonated Asp residue finally results in the amine and carboxylic acid fragments[8] (Scheme 1).

Several aspartic proteases are known to be involved in pathological disorders caused by dysfunctions of their proteolytic activity, such as for example BACE 1 whose overexpression is related to the onset of Alzheimer's disease;[9] others are included in viruses that once in the human body alter the normal regulation of biological processes, as for example HIV-PR that is involved in the proliferation and maturation of HIV-virus, the causative agent of AIDS.[10]

---

[8] R. Mannhold, H. Kubinyi, G. Folkers, Wiley-VCH, *Aspartic acid proteases as therapeutic targets*, **2010**, 29.

[9] R. Vassar, B. D. Bennett, S. Babu-Khan, S. Kahn, E. A. Mendiaz, P. Denis, D. B. Teplow, S. Ross, P. Amarante, R. Loeloff, Y. Luo, S. Fisher, J. Fuller, S. Edenson, J. Lile, M. A. Jarosinski, A. L. Biere, E. Curran, T. Burgess, J. Louis, F. Collins, J. Treanor, G. Rogers, M. Citron, *Science*, **1999**, 286, 735.

[10] A. M.J. Wensing, N. M. van Maarseveen, M. Nijhuis, *Antiviral Research,* **2010***,* 85, 59.

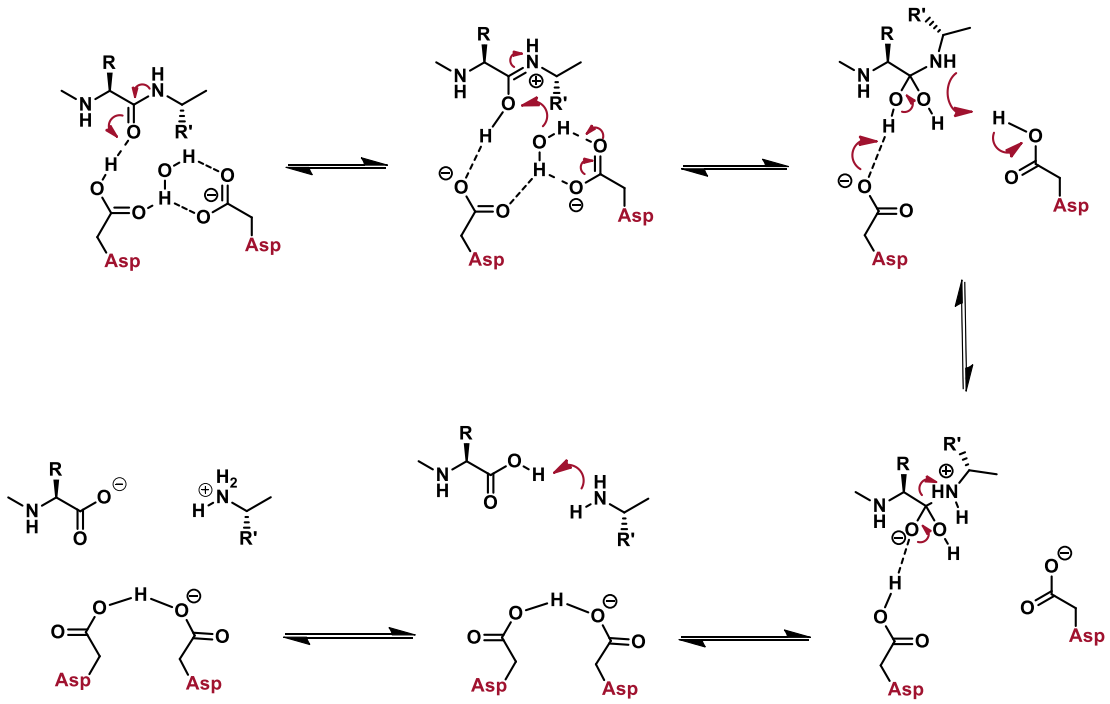

Scheme 1. *Hydrolytic mechanism of aspartyl proteases*

1.2 Human Immunodeficiency Virus (HIV) and AIDS

Acquired Immune Deficiency Syndrome (AIDS) is a severe immunological disease caused by HIV virus, resulting in a defect in cell-mediated immunity that is manifested by increased susceptibility to opportunistic infections and to development of rare cancers, which increases with the progression of the disease. There are many different strains of HIV virus, but HIV-1 is the most common type found worldwide.

HIV-1 belongs to the class of retroviruses, in which the genetic information is enclosed in single strands of RNA. The virus has a spherical structure with a diameter of about 130 nm and is constituted by a lipid bilayer membrane and a core; each viral particle contains 72 glycoprotein complexes integrated into the lipid membrane. The core is a proteic capsid consisting, containing two identical strands of RNA and three enzymes involved in the viral replication, i.e. reverse transcriptase (RT), integrase (IN) and protease (PR).

Three genes encode for the viral proteins: *Gag* encodes for the proteins of the virion core, *Pol* for the three fundamental enzymes, and *Env* for the outer envelope proteins (Figure 3).[11]

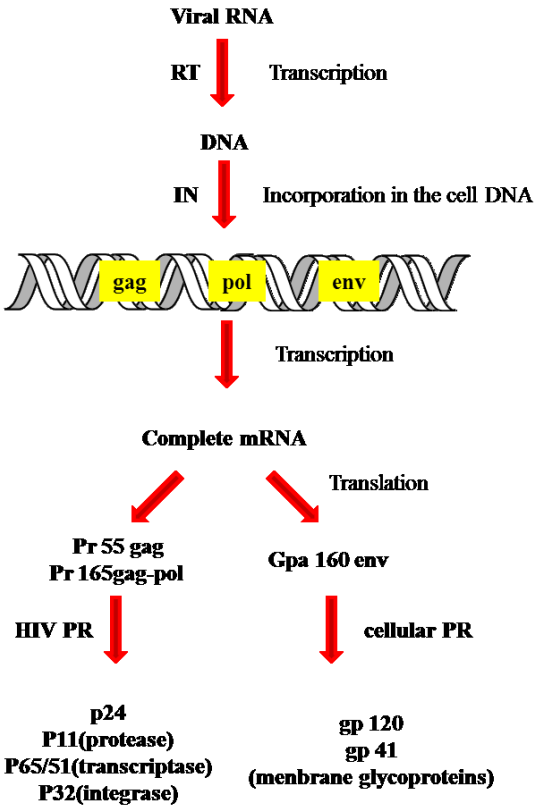

Figure 3. *HIV replication cycle*

Helper T lymphocytes are the host cells for HIV virus. They possess CD4 receptors on the outer membrane, which bind the gp120 glycoprotein of the viral membrane. Subsequently the viral and the cell membrane merge and the core of the virus is released into the host.[12]

Currently there is no cure for AIDS; however, therapies based on the treatment with HIV-PR inhibitors (nelfinavir, ritonavir, and indinavir, etc) in combination with RT inhibitors, have changed the nature of the disease from a terminal illness to a manageable one. Nonetheless, the onset of drug resistance due to mutant viral strains

[11]**a**. F. Barré-sinoussi, A. L. Ross and J. Delfraissy, *Nat. Rev. Microbiol.*, **2013**, 11, 877; **b.** V. W. Pollard M. H. Malim, *Annu. Rev. Microbiol.*, **1998**, 52, 491.

[12] D. C. Chan and P. S. Kim, *Cell*, **1998**, 93, 681.

makes the development of new inhibitors still a strong priority for pharmaceutical research.[10]

1.2.1 HIV Protease (HIV-PR)

HIV-PR plays an essential role in the replication cycle of the HIV-1 virus. HIV-PR cleaves polyproteins PR55*gag* and PR160*gag/pol* (expressed by *gag* and *pol* genes) allowing maturation of a new viral particle. Since HIV-PR is a common target for anti-HIV therapy, it has become one of the most studied enzymes in terms of function and structure.

HIV-PR in its active form is a C2 symmetric homodimer. The monomers, containing 99 amino acid residues, assemble to form a long tunnel closed by two flexible regions (flaps). The active site is located at the centre of the tunnel, with the catalytic Asp residues (Asp25 and Asp25') at the bottom of the cavity.[13] The stability of the dimer mostly depends on a network of intermolecular hydrogen bonds between β sheets located in the proximity of the N- and C-terminals of the two monomers.

The carboxylate groups of the catalytic Asp residues located on each chain are nearly coplanar and show close contacts between two oxygen atoms (2.8-3 Å), indicating the presence of a bridging acidic proton. A water molecule also bridges the carboxylate residues, within hydrogen bond distance to the oxygen atoms of both. Similar water molecules are found also in nonviral proteases and are likely to be the catalytic water in this family of enzymes.

In the presence of a substrate, the flaps open and wrap around the substrate's protein chain, holding it tightly in the tunnel, through interactions responsible for the selectivity observed in catalysis (Figure 4, Figure 5).[14]

---

[13] D. R. Davies, *Annu. Rev. Biophys. Biophys. Chern*, **1990**, 19, 189.

[14] A. Wlodawer and J. Vondrasek, *Annu. Rev. Biophys. Biomol. Struct.,* **1998**, 27, 249.

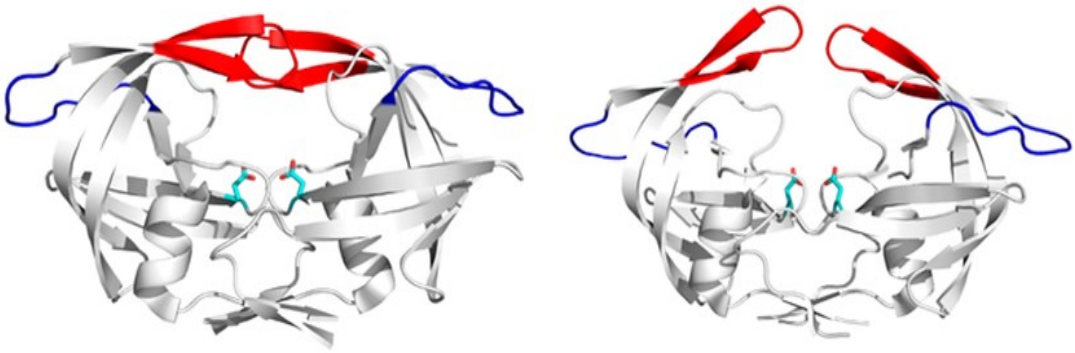

Figure 4. *Crystal structures of HIV-1 PR in the closed and open (PDB 1HVR and 1TW7) conformations. In red the "flaps", in blue the hinge loop, cyan sticks are the catalytic aspartates.*

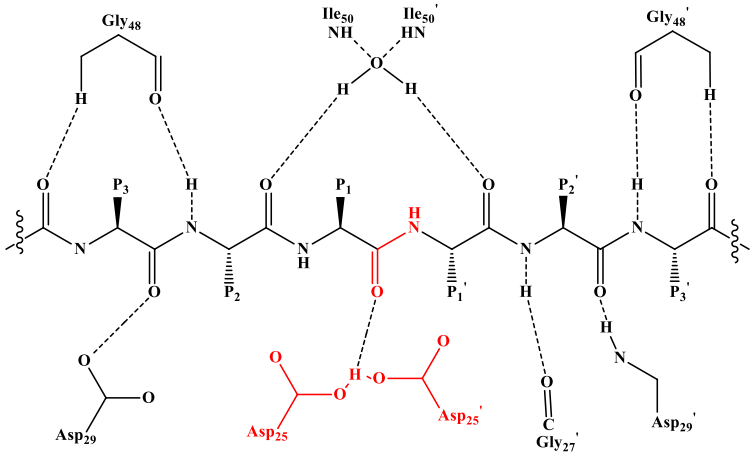

Figure 5. *Schematic diagram of the hydrogen bonds between the active site and the polyprotein*

1.2.2 HIV-PR inhibitors

HIV-PR is among the most studied enzymes in terms of function and structure, and due to its essential role in the maturation and replication cycle of the HIV-1 virus it has become one of the most important therapeutic targets for the treatment of AIDS.

HIV-PR active site, as for the majority of aspartic proteases, does not contain groups that can be chemically modified by irreversible inhibitors. Only strong electrophiles, such as epoxides, can alkylate the catalytic Asp groups, but they are cytotoxic. [15] Therefore, reversible inhibitors were designed and developed with

[15] B. Said, D. C. Matsumoto, A. K. Hamade, R. C. Shank, *Biochem, Biophys, Res. Commun.*, **1999**, 261, 844.

groups that interact with the active site through non-covalent interactions, so as to have higher affinity for the proteolytic site than its natural substrate.

A successful approach to the design of efficient inhibitors, according to Pauling's principle,[16] is based on peptidomimetic structures containing a non-hydrolysable isoster of the scissile dipeptide that mimics the stereo-electronic features of the tetrahedral TS for amide bond hydrolysis (transition state analog).[17] In Figure 6 are shown several transition-state analogs that have been successfully used in the design of aspartic protease inhibitors.[18]

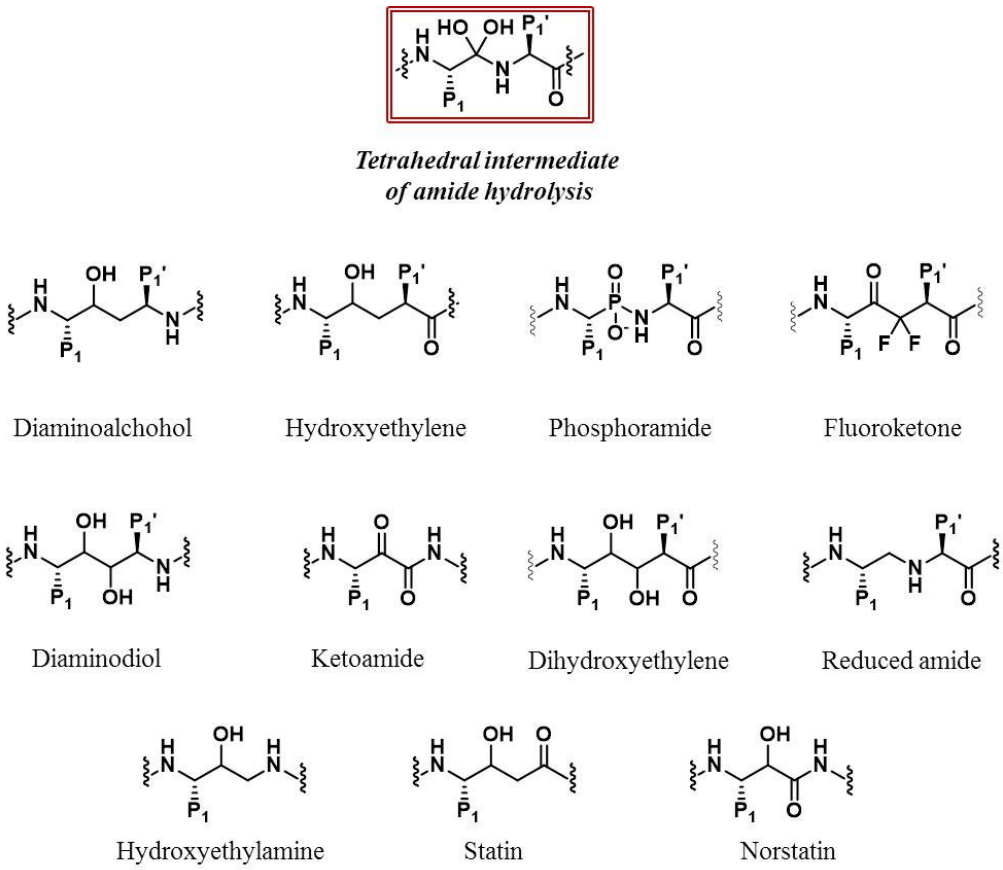

Figure 6. *Some dipeptide isosters*

[16] L. Pauling, *Chem. Eng. News.,* **1946**, 24, 1375.

[17] A. Brik and C-H. Wong ***Org. Biomol. Chem.*, 2003**,**1**, 5.

[18] **a.** A. Wlodawer, J. W. Erickson, , *Annu. Rev. Biochem.,* **1993**, 62, 543; **b.** J. A. Martin, S. Redshaw, G. J.Thomas, *Progress in Medicinal Chemistry,* **1995**, 32, 239; **c.** C. A. Chen, S. M. Sieburth,; A. Glekas, G. W. Hewitt, G. L. Trainor, S. E. Vitanen,; S. S. Garber, B. Cordova; S. Jeffry, R. M.Klabe, *Chem. Biol.,* **2001**, 8, 1161; **d.** J. M. Ahn, N. A. Boyle, M. T. MacDonald, K. D. Janda, , *Mini Rev. Med. Chem.,* **2002**, 2, 463.

HIV-PR selectively performs hydrolysis of peptide bonds between two hydrophobic residues and a bond between an amino acidic residue containing an aromatic ring and a proline is cleaved in three of the nine sites of proteolytic cleavage on the viral polyprotein (Figure 7).[19] The ability to hydrolyze amide bonds to proline (Prolylpeptidase class of enzymes) is a peculiarity of viral proteases; eukaryotic proteases do not have this ability and this has made Phe-Pro and Tyr-Pro isosters good candidates for the selective inhibition of viral proteases.[20]

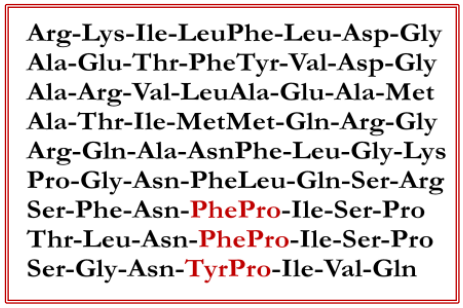

Figure 7. *Cleavage sites of viral polyproteins*

Several representative examples of HIV-PR inhibitors approved by FDA for anti HIV-therapy are shown in Figure 8. It can be seen that the presence of a hydroxylated dipeptide isoster is a peculiar characteristic of many inhibitors. In Saquinavir, Nelfinavir and Indinavir this structural motif is associated to a Phe-Pro dipeptide isoster, in which proline is replaced by larger heterocyclic groups (decahydroisoquinoline in Saquinavir and Nelfinavir; piperazine in Indinavir), that provide better interactions with the protease's S1' sub-site.

---

[19] **a.** P. L. Darket, R. F. Nutt, S. F. Brady, V. M. Garsky, T. M. Ciccarone, C. Leu, P. K. Lumma, R. M. Freidinger, D. F. Veber and I. S. Sigal, *Biochem Biophys Res Commun*, **1988**, 156, 297; **b.** L. Pearl, W. Taylor, *Nature*, **1987**, 328, 482.

[20] N.A. Roberts, J. A. Martin, D.Kinchington, A.V. Broadhurst, J.C. Craig, I.B. Duncan, S.A. Galpin, B.K. Handa, J. Kay, A. Krohn, R.W. Lambert, J.H. Merrett, J.S. Mills, K.E.B. Parkes, S. Redshaw, A.J. Ritchie, D.L. Taylor, G.J. Thomas, P. Machin, *Science,* **1990**, 248, 358.

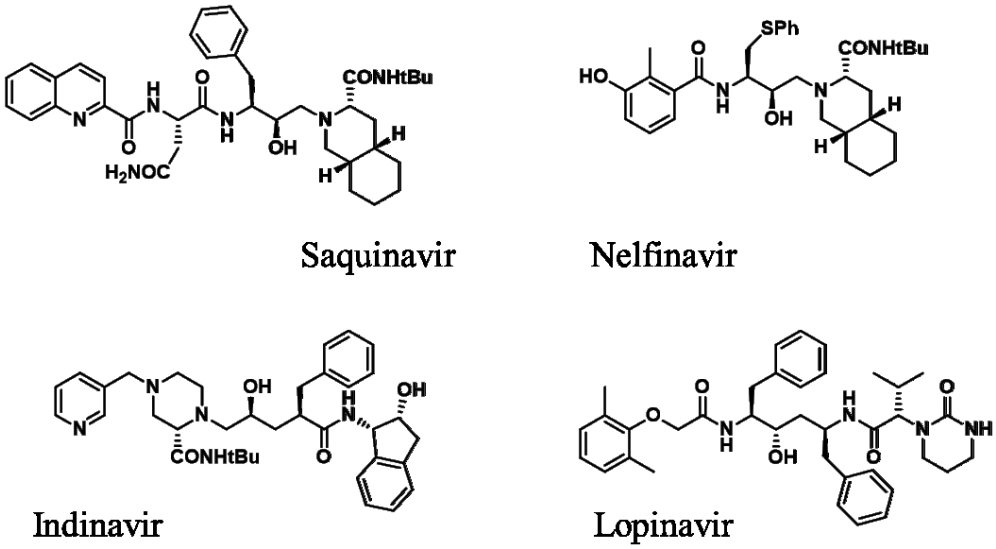

Figure 8. *HIV-Pr inhibitors*

Peptidomimetic inhibitors of HIV-PR contain multiple chiral centres, some of which are located on the central isoster (see, for example, Figure 8). The observation that the absolute configuration of these stereocentres has an important impact on the inhibitor's activity [21] has fostered the development of methodologies for the stereoselective synthesis of hydroxylated dipeptide isosters.[22]

Chiral, enantiomerically pure, 1,4-diaminoalkenes (b, Scheme 2) are interesting in this respect because many methods exist for the stereoselective hydroxylation and dihydroxylation of alkenes[23] which, in this case, would lead to hydroxyethylene(c) and dihydroxyethylene(c') dipeptide isosters, as shown in Scheme 2. Cross-metathesis of chiral allylamines is, in turn, an attractive approach to

---

[21] **a.** K.-H. Budt, A. Peyman, J. Hansen, J. Knolle, C. Meichsner, A. Paessens, D. Ruppert, B. Stowasser, *Bioorg. Med. Chem.* **1995**, 5, 559; **b.** M. V. Hosur, T. N. Bhat, D. J. Kempf, E. T. Baldwin, B. Liu, S. Gulnik, N. E. Wideburg, D. W. Norbeck, K. Appelt, J. W.Erickson, *J. Am. Chem. Soc.* **1994**, 116, 847; **c.** Vondràs˘ek, M. Hradılek,, M. Soucek, I. Pichovà, P. Majer, P. Strop, J. Sedlàcek, A.-M. Heuser, H. Kottler, H.-G. Kräusslich, *Eur. J. Biochem.* **1997**, 250, 559.

[22] A. Tossi, F. Benedetti, S. Norbedo, D. Skrbec, F. Berti, D. Romeo, *Bioorg. Med. Chem.* **2003**, 11, 4719; F. Benedetti, F. Berti, G. Garau, I. Martinuzzi and S. Norbedo *Eur. J. Org. Chem.* **2003**, 1973. F. Benedetti, F. Berti, S. Budal, P. Campaner, F. Dinon, A. Tossi, R. Argirova, P. Genova, V. Atanassov, and A. Hinkov, *J. Med. Chem.* **2012**, *55, 3900.*

[23] **a.** A. K. Ghosh, G. Bilcer, G.Schiltz, *Synthesis* **2001**, 2203; **b.** H. C. Kolb, M.S. VanNieuwenhze, K. B. Sharpless *Chem. Rev.*, 1994, 94, 2483; **c.** D. J. Ager, I. Prakash, and D. R. Schaad, *Chem. Rev*. **1996**, 96, 835.

the synthesis of 1,4-diaminoalkenes [24] (Scheme 2) and is currently being investigated.[25]

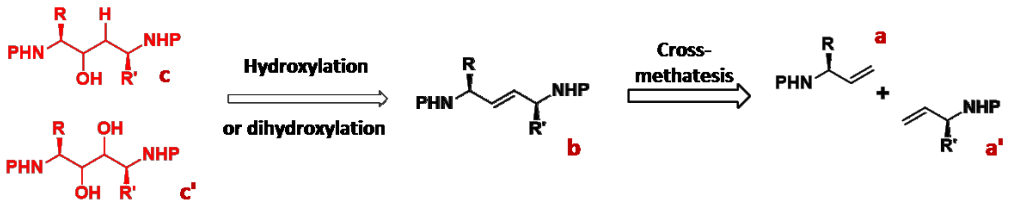

Scheme 2. *Retrosynthesis analysis of hydroxyethylene and dihydroxyethylene dipeptide isosters*

A prerequisite for the approach outlined in Scheme 2 is the availability of reliable and affordable methods for the synthesis of chiral allylamines in enantiomerically pure form, which will be the subject of the first part of this thesis (chapter 2). Chiral allylamines, however, are valuable compounds *per se.* For this reason the subject will be briefly reviewed in the following chapter.

1.3 Chiral allylamines

Allylamines are of significant interest as synthetic intermediates and compounds of biological interst. [26,27,28] The allylamine fragment is present in natural products[29,30,31] and other biologically-active compounds,[32,33,34] including drugs for the treatment of

[24] **a.** H.E. Blackwell, D.J. O'Leary, A.K. Chatterjee, R.A. Washenfelder, D.A. Bussmann, and R. H. Grubbs, *J. Am. Chem. Soc.*, **2000**, 122, 58; **b.** S.J. Connon, S. Blechert, Angew.Chem. Int. Ed. 2003, 42, 1900; **c.** R. H. Grubbs, *Tetrahedron ,* **2004**, 60, 7117; **d.** C. Deraedt, M. d'Halluin and D. Astruc, *Eur. J. Inorg. Chem.* **2013**, 4881.

[25] **a.** A. Ostric, Università di Trieste *Tesi di Dottorato XXIII Ciclo*; **b.** V. Sinisi, unpublished work.

[26] E.M. Skoda, G.C.Davis, P.Wipf, *Org. Process Res. Dev.* **2012**, 16, 26.

[27] S. Nag, S.Batra, *Tetrahedron* **2011**, 67, 8959.

[28] M. Johannsen, K.A. Jørgensen, *Chem. Rev.* **1998**, 98, 1689.

[29] C. Dai, C.R. Stephenson, *J. Org. Lett.* **2010**, 12, 3453.

[30] Y. Nakamura, A.M.Burke, S. Kotani, J.W.Ziller, S.D. Rychnovsky, *Org. Lett.* **2009**, 12, 72.

[31] Z. Ali, I.A. Khan, *Phytochemistry* **2008**, 69, 1037.

[32] Z. Ye, T.F.Brust, V.J Watts, M.Dai, *Org. Lett.* **2015**, 17, 892.

[33] J.S. Foot, M.Deodhar, C.I. Turner, P. Yin, E.M.Van Dam, D.G. Silva, A. Olivieri, A.Holt, I.A. McDonald, *Bioorganic Med. Chem. Lett.* **2012**, 22, 3935.

mycosis (terbinafine, naftifine), [35] depression (zimelidine), [36] motion sickness (cinnarizine),[37] migraine and epilepsy (flunarizine)[38](Figure 9).

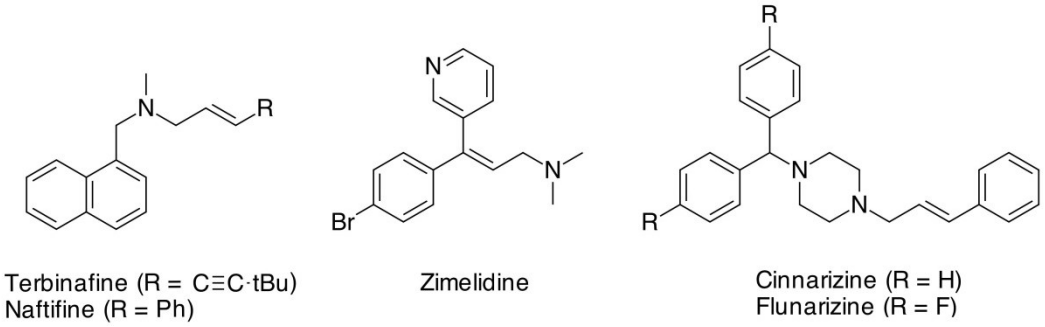

Figure 9. *Bioactive allylamines*

Furthermore, α–chiral allylamines are valuable organic building blocks for the synthesis of optically active compounds, due to the participation of their characteristic bifunctional unit into a wide range of different transformations (aminations, oxidations, metathesis, etc. (Scheme 3).[26,29,39,40]

---

[34] N. Kitahata, S.-Y.Han, N.Noji, T.Saito, M. Kobayashi, T. Nakano, K.Kuchitsu, K. Shinozaki, S. Yoshida, S. Matsumoto, M. Tsujimoto, T.Asami, *Bioorg. Med. Chem.* **2006**, 14, 5555.

[35] A. Stütz, *Angew. Chem. Int. Ed. Engl.* **1987**, 26, 320.

[36] A. Carlsson, *Science* **2001**, 294, 1021.

[37] G.Towse, *J. Laryngol. Otol.* **1980**, 94, 1009.

[38] M. Bebin, T.P.Bleck, *Drugs* **1994**, 48, 153–171.

[39]**a.** S. B. D. Jarvis, A. B. Charette, *Org. Lett.* **2011**, 13, 1830; **b.** T. Moriwake, S. Hamano, S. Saito, S. Torii, S. Kashino *J. Org. Chem.* **1989**, 54, 4114; **c.** R. Jumnah, J. M. J. Williams, A.C. Williams, *Tetrahedron Lett.***1993**, 34, 6619; **d.** J. F. Bower, R. Jumnah, A. C. Williams and J. M. J. Williams, *J. Chem. Soc., Perkin Trans. 1,* **1997**, 19, 1411; **f.** K. Burgess, L.T. Liu, B. Pal *J. Org.Chem.* **1993**, 58, 4758.

[40] **a.** J. R. Luly, J. F. Dellaria, J.J. Plattner, J.L. Soderquist, N. Yi *Org. Chem.* **1987**, 52,1487; **b.** A. Albeck, R. Persky, *J. Org. Chem.* **1994**, 59, 653.

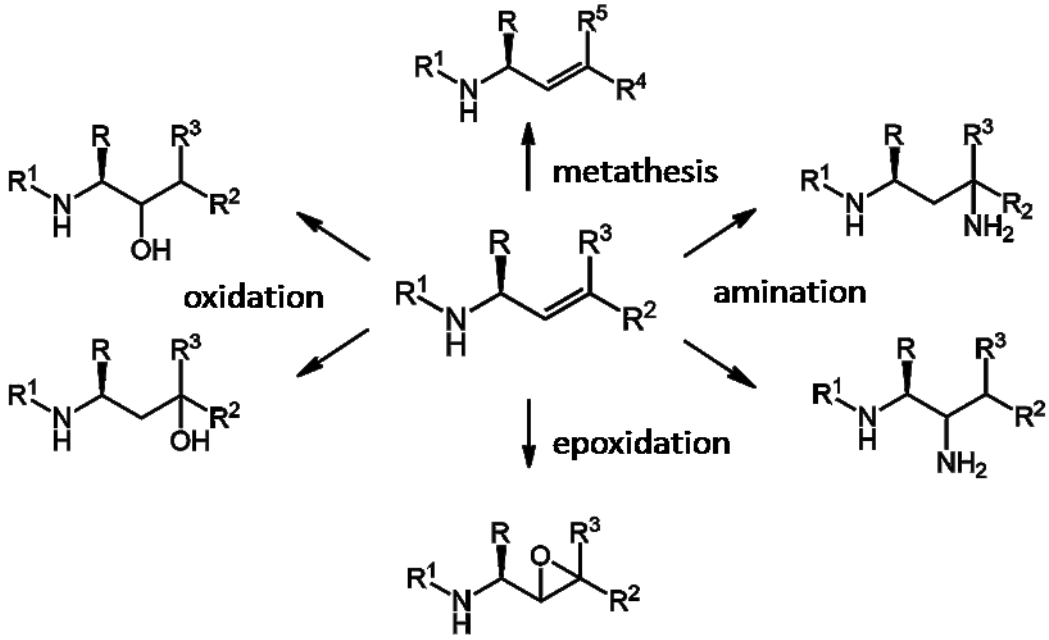

Scheme 3. *Synthetic transformations of allylamines*

The asymmetric synthesis of α-chiral allylamines has been the subject of many studies[41,42] resulting in the development of several approaches, among which the transition metal-catalyzed asymmetric allylic amination has been extensively documented.[41,43,44]

Other methods include the asymmetric vinylation of imines,[42] the Overman rearrangement of allylic imidates,[45] the asymmetric hydrogenation of dienamines,[46] the transition metal-catalyzed asymmetric allylic C-H amination[47] and the nitroso-ene reaction.[48] Despite the recent advances in asymmetric synthesis, the olefination of α-amino aldehydes derived from the chiral pool still remains a valuable synthetic

[41] J.F. Hartwig, L.M. Stanley, *Acc. Chem. Res.* **2010**, 43, 1461.

[42] M.T. Robak, M.A. Herbage, J.A. Ellman, *Chem. Rev.* **2010**, 110, 3600.

[43] C.C. Marvin, *Comprehensive Organic Synthesis*, 2nd ed.; Knochel, P., Molander, G.A., Eds; Elsevier: Amsterdam, The Netherlands, 2014; Volume 6, pp. 34.

[44] G. Helmchen, In *Iridium Complexes in Organic Synthesis*; Oro, L.A., Claver, C., Eds.; Wiley-VCH: Weinheim, Germany, 2009; pp. 145.

[45] L.E. Overman, N.E. Carpenter, *Org. React.* **2005**, 66, doi:10.1002/0471264180.or066.01.

[46] T.-L. Liu, C.-J. Wang, X. Zhang, *Angew. Chem. Int. Ed. Engl.* **2013**, 52, 8416.

[47] T.A. Ramirez, B. Zhao, Y. Shi, *Chem. Soc. Rev.* **2012**, 41, 931.

[48] M. Baidya, H. Yamamoto, *Synthesis* **2013**, 45, 1931.

method as the starting materials can be obtained from the corresponding α-aminoacids.[49,50,51] The synthesis of chiral allylamines by the Wittig,[52,53,54] Julia[55,56,57] and Peterson[58] olefination of α-amino aldehydes has been reported, but these approaches are often limited by the chemical and configurational instability of α-amino aldehydes.[50]

[49] D. Gryko, J. Chalko, J. Jurczak, *Chirality* **2003**, 15, 514.

[50] J. Jurczak, A. Gołebiowski, *Chem. Rev.* **1989**, 89, 149.

[51] M.T. Reetz, *Chem. Rev.* **1999**, 99, 1121.

[52] P. Stallforth, S. Matthies, A. Adibekian, D.G. Gillingham, D. Hilvert, P.H. Seeberger, *Chem. Commun.* **2012**, 48, 11987.

[53] Z.-Y. Wei, E.E. Knaus, *Synthesis* **1994**, 1463.

[54] W.S. Saari, T.E. Fisher, *Synthesis* **1990**, 453.

[55] S. Mirilashvili, N. Chasid-Rubinstein, A. Albeck, *Eur. J. Org. Chem.* **2008**, 2008, 3461.

[56] O. Shirota, K. Nakanishi, N. Berova, *Tetrahedron* **1999**, 55, 13643.

[57] M.K. Gurjar, S. Pal, A.V. Rama Rao, *Tetrahedron* **1997**, 53, 4769.

[58] G. Wei, T. Cohen, *Synlett* **2011**, 2011, 2697.

2. Results and Discussion

Allylamines are versatile building blocks in organic synthesis, because their characteristic bifunctional unit can undergo a wide range of chemical transformations.[26] Chiral allylamines, in particular, are valuable intermediates for the synthesis of a variety of chiral, enantiomerically-pure bioactive compounds.[59,60,61,62]

Among the methods available for their obtainment, the olefination of α-aminoaldehydes derived from aminoacids by Wittig,[52,53,54] Julia[55,56,57] and Peterson[58] olefination, is a procedure of choice. Unfortunately these approaches are often limited by the chemical and configurational instability of the the α-amino aldehydes starting material.[50]

In the classical Julia reaction[63,64] (Scheme 4), a lithiated aryl alkyl sulfone is added to an aldehyde to give the corresponding α-hydroxysulfone A (pathway *a*). This, in turn, is converted into the target alkene by in situ acetylation and treatment of the resulting α-acetoxysulfone with sodium or magnesium amalgam[65] or SmI_2.[66] The same α-hydroxysulfone A, however, can be obtained in two steps by the acylation of the lithiated phenylalkylsulfone with an ester, followed by the reduction of the corresponding α-ketosulfone (Scheme 4, pathway *b*). Chiral allylamines may thus be obtained starting from readily-available α-amino esters that are chemically and configurationally more stable than α-amino aldehydes.[67] Furthermore, the additional step of pathway *b* is not a limitation, as the latter compounds are generally prepared from the corresponding esters in at least one step.[49]

---

[59] P. Szcześniak, S. Stecko, *RSC Adv.* **2015**, 5, 30882.

[60] S. Fustero, A.C. Cuñat, S.Flores, C.Báez, J. Oliver, M.Cynamon, M. Gütschow, M.D. Mertens, O.Delgado, G. Tresadern, A.A.Trabanco, *Chem. - Eur. J.* **2011**, 17, 14772.

[61] A.J. Blacker, M.Roy, S. Hariharan, C. Headley, A.Upare, A. Jagtap, K. Wankhede, S.K. Mishra, D. Dube, S. Bhise, S. Vishwasrao, N. Kadam, *Org. Process Res. Dev.* **2011**, 15, 331.

[62] R. Martín, M.Alcón, M.A. Pericàs, A.Riera, *J. Org. Chem.* **2002**, 67, 6896.

[63] M. Julia, J.-M.Paris, *Tetrahedron Lett.* **1973**, 14, 4833.

[64] I.E. Markó, J. Pospíšil, In *Science of Synthesis*; de Meijere, A., Ed.; Thieme: Stuttgart, Germany; New York, NY, USA, 2009; Volume 47a; pp. 105.

[65] G.H. Lee, H.K. Lee, E.B. Choi, B.T. Kim; C.S. Pak, *Tetrahedron Lett*. **1995**, 36, 5607.

[66] G.E. Keck, K.A. Savin, M. A. Weglarz, *J. Org. Chem.* **1995**, 60, 3194.

[67] A.R. Katritzky, D. Cheng, J. Li, *J. Org. Chem*. **1998**, 63, 3438.

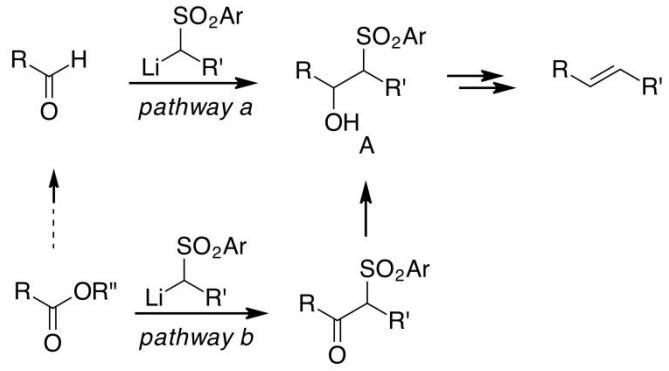

Scheme 4. *Julia olefination.*

This variant of the Julia reaction has been used in the synthesis of *E*-alkene dipeptide isosteres,[68,69] but its wider scope and general applicability is still unexplored. In this study, we have demonstrated that the α-aminoester Julia olefination is a convenient method for the synthesis of terminal and disubstituted allylamines (Scheme 5).

[68] C. Charrier, L. Ettouati, J. Paris, *Tetrahedron Lett.* **1999**, 40, 5705.
[69] B. Lygo, *Synlett* **1992**, 793.

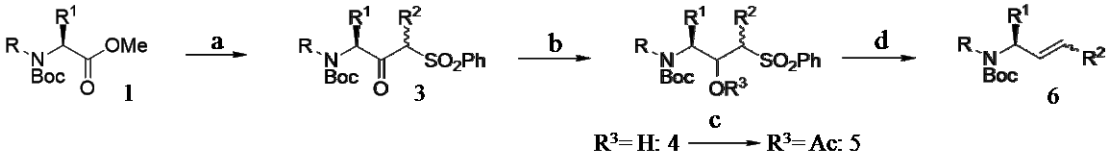

	R	R^1	R^2
a	H	Me	H
b	H	$CH(Me)_2$	H
c	H	CH_2CHMe_2	H
d	H	CHMeEt	H
e	H	CH_2Ph	H
f	H	$CH_2pC_6H_4OTBDMS$	H
g		$(CH_2)_3$	H
h	H	CH_2Ph	Me
i	$(CH_2)_3$	R	Me

a: $PhSO_2CH_3$(2a) or $PhSO_2CH_2CH_3$(2b), nBuLi, THF, -78°C; b: $NaBH_4$, MeOH, 0°C; c: Ac_2O, DMAP, Et_3N, CH_2Cl_2, 0°C; d: Meth. A Mg, cat $HgCl_2$, EtOH and THF (3:1), 25°C, Meth. B Na(Hg), EtOH, -15°C.

Scheme 5. *Julia olefination of chiral α-amino esters.*

2.1 Synthesis of α-Chiral allylamines by a modified Julia olefination reaction

The synthesis started with the reaction between *N*-Boc amino esters **1** and lithiated phenylmethylsulfone **2a**, giving the corresponding ketosulfones **3**. The experimental conditions for this key step were initially optimized, with respect to yields and *ee*, using *N*-Boc alanine methyl ester **1a** as the substrate (Table 2).[70]

[70] As it was not possible to separate the enantiomeric ketosulfones 3, the *ee* were measured after conversion of 3 into the corresponding allylamine 6 (Scheme 5Scheme 4), except for 3f whose *ee* was determined by chiral HPLC.

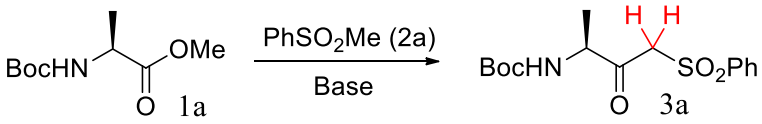

Entry	2a (eq.)	Base (eq.)	T (°C)	Yield [a] %	*ee* [a,b] %
1	1	*n*-BuLi (2)	−78	55	<70
2	1	*n*-BuLi (2)	−30	66	<70
3	1	*n*-BuLi (3)	−78	86	<70
4	2	*n*-BuLi (4)	−78	89	65
5	2	*n*-BuLi (4)	−30	42	<70
6	2	*n*-BuLi/TMEDA (4)	−78	-	-
7	2	KHMDS	−78	-	-
8	2	NaH	−78	-	-
9	2	*n*-BuLi (4)	−78	89 [c]	95 [c]

[a] By addition of **1a** to lithiated **2a**; [b] *ee* determined after conversion to the allylamine **6a**; [c] By the reverse addition of a suspension of lithiated **2a** to **1a**.

Table 2 *Optimized synthesis of the first step of revisited Julia: ketosulfone*

Addition of **1a** to one equivalent of lithiated phenylmethylsulfone **2a,** even in the presence of two equivalents of *n*-BuLi as originally suggested by Lygo,[69,70, 71] resulted in a partial conversion into the ketosulfone **3a** (Table 2, Entries 1 and 2). The low yields are likely due to the presence of ionizable protons, both in the starting amino ester (NHBoc) and in the ketosulfone product (methylene) that can exchange with lithiated **2a**. The yield improved when an excess of BuLi and **2a** was employed (Entries 4 and 5); under these conditions, however, the enantiomeric purity of the ketosulfone **3a** was modest. The use of TMEDA in association with butyllithium[72] (Entry 6) and of other base systems (Entries 7, 8) was not successful. The best results were eventually obtained with two equivalents of sulfone and four equivalents of butyl lithium,[73,74] with the resulting yellow suspension added to the amino ester **1a**, at −78 °C under argon. In this case, complete conversion into the ketosulfone **3a** was

[71] B. Lygo, C.N. Rudd, *Tetrahedron Lett*. **1995**, 36, 3577.
[72] L. Řehová, I. Císařová, J. Ullrich, *Eur. J. Org. Chem*. **2014**, 1461.
[73] R. Rönn, Y.A Sabnis, T. Gossas, E. Akerblom, U.H. Danielson, A. Hallberg, A.Johansson, *Bioorg. Med. Chem.* **2006**, 14, 544.
[74] D. Severi, L. Ettouati, J. Paris, *Lett. Pept. Sci.* **2002**, 9, 11.

achieved, which was isolated in excellent yield and enantiomeric purity (Entry 9). It had been suggested that, under similar conditions, the dilithiated sulfone **8** is formed and is the reactive nucleophile.[73,74] It seems more likely, however, that the monolithiated species **9** is formed following H/Li exchange with the protected aminoester (Scheme 6) and is the actual nucleophile. A second equivalent of **8** is then required for a further H/Li exchange giving the dilithiated product **12**, in agreement with the observed stoichiometry.

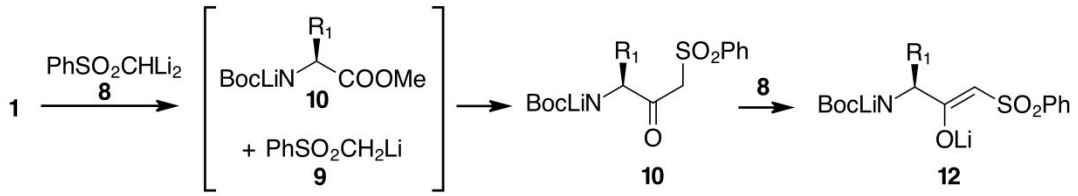

Scheme 6. *Reactions of mono- and bis-lithiated sulfones.*

The optimized reaction conditions were then applied to the *N*-Boc-amino esters **1b–f** (Table 3), giving the corresponding ketosulfones **3** in good to excellent yields and *ee*, with the only exception of the protected tyrosine methyl ester **1f**; repeated attempts under several reaction conditions invariably led to a significant loss in enantiomeric purity for this compound (e.e.: 80%). The e.e.s of **3b-f** were determined via HPLC on a Lux5ucell2 and a Lux5ucell3 column, respectively. Results are reported in Table 3.

With L-proline methyl ester **1g** (Entry 7), where no ionizable protons are present, the best optical purity, albeit at the expenses of a lower yield, was obtained by using two equivalents of $PhSO_2Me$ and BuLi with respect to the aminoester, whereas racemization was observed by employing the usual conditions. This further confirms that the reactive nucleophile in the reaction with the amino esters is the monolithiated species $PhSO_2CH_2Li$, as suggested above (Scheme 6).

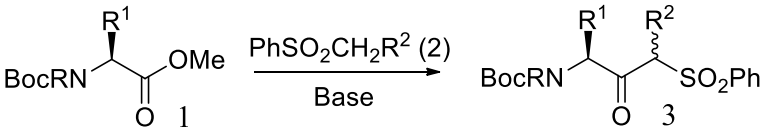

Entry	Sulfone	Aminoester	R^2	Yield(%)	e.e %	Product[a]
1	**1a**	**Ala (1a)**	H	89	95	**3a**
2	**1a**	**Val (1b)**	H	85	97	**3b**
3	**1a**	**Leu (1c)**	H	89	99	**3c**
4	**1a**	**Ile (1d)**	H	86	99	**3d**
5	**1a**	**Phe (1e)**	H	94	95	**3e**
6	**1a**	**Tyr (1f)**[b]	H	78	80	**3f**
7	**1a**[c]	**Pro (1g)**	H	60	n.d.	**3g**
8	**1b**	**Phe (1e)**	Me	77	n.d.[d]	**3h**
9	**1b**[c]	**Pro (1g)**	Me	80	n.d.[e]	**3i**

[a] Reactions were carried out as for entry 9, Table 2; [b] Protected as O-TBDMS; [c] With 2 equivalents of sulfone; [d] 3:2 mixture of diastereoisomers; [e] 55:45 mixture of diastereoisomers.

Table 3. *Reactions between amino esters **2** and lithiated sulfones **1**[a]*

Finally, the same conditions were applied to the reaction of amino esters **1e** and **1g** with phenylethylsulfone **2b** (Table 3, Entries 8 and 9), giving the corresponding ketosulfones **3h** and **3i**, as mixtures of diastereoisomers, in excellent yield.

The ketosulfones **3a**–**g** thus obtained were reduced with $NaBH_4$ (Scheme 5), giving quantitatively the α-hydroxysulfones **4a**–**g** as mixtures of *syn* (*S,S*) and *anti* (*S,R*) diastereoisomers in ratios from approximately 10:1 for branched compounds **4b**–**d** (Val, Leu, Ile) to 3:1 for compounds having linear side chains **4a,e,f** (Ala, Phe,

Tyr) to 1.5:1 for **4g** (Pro), in agreement with previous findings.[75] No attempts were made to optimize the stereoselectivity, as the newly-formed stereogenic center is lost in the final step of the synthesis. Not surprisingly, complex mixtures containing all four possible diastereoisomers were obtained in the reduction of ketosulfones **3h** and **3i**.

Conversion of hydroxysulfones **4** into the allylamines **6** followed the standard protocol of the Julia reaction. Thus, the alcohols **4** were acetylated with acetic anhydride and DMAP, and the corresponding acetoxysulfones **5** were converted to the target aminoalkenes **6** in the final reductive elimination, promoted by sodium amalgam[63] or in situ generated magnesium amalgam[65] (Scheme 5, Table 4). The two methods were shown to proceed with comparable yields and *ee*, except for **5f**: in this case, sodium amalgam caused the deprotection of the phenol group, leading directly to the allylamine **6f′**, while the O-protected product **6f** was smoothly obtained with magnesium amalgam.

[75] F. Benedetti, S. Miertus, S. Norbedo, A. Tossi, P. Zlatoidzky, *J. Org. Chem.* **1997**, 62, 9348.

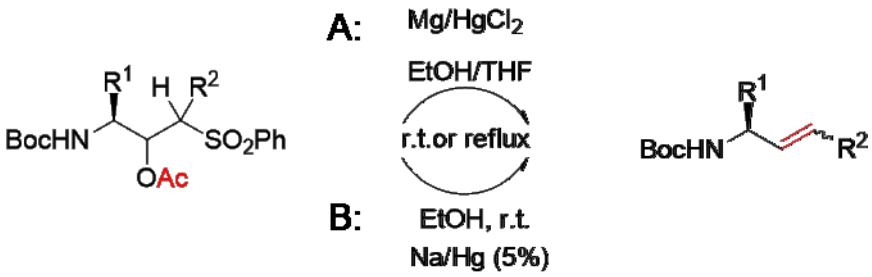

	Allylamine	Method[a]	Yield [b] %	*ee* [c] %
6a	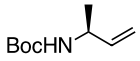	A (1h)	68 (60)	95
6b	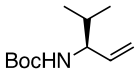	A (2h)	60 (50)	>99
6c	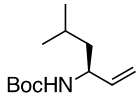	A (2h)	67 (62)	>99
6d	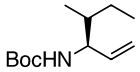	A (3h)	69 (59)	>99
6e	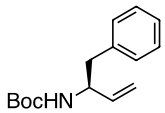	A (2h)	68 (64)	>99
		B (4h)	71 (67)	>99
6f	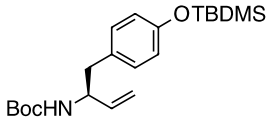	A [d,e] (2h)	65 (52)	80[e]
6f′	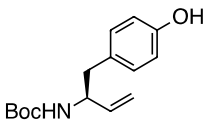	B [d] (4h)	71 (57)	ND

6g	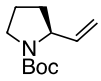	**B (2h)**	**84 (50)**	**>99**
6h	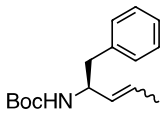	**B (4h)**	**71 [f] (55)**	**ND**
6i	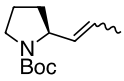	**B (12h)**	**65 [g] (52)**	**ND**

[a] Method A: Mg powder (2.5 eq), $HgCl_2$ (0.1 equiv.), EtOH/THF (3:1), 25 °C; Method B: 5% Na/Hg (3 equiv.), EtOH, −15 °C; [b] Final yields from amino esters **1** in brackets; [c] By chiral HRGC; [d] From O-TBDMS protected sulfone 5f; [e] By chiral HPLC; [f] 80:20 mixture of *E* and *Z* isomers; [g] 85:15 mixture of *E* and *Z* isomers.

Table 4. *Synthesis of allylamines*.

The enantiomeric excess of (S)- allylamines **6a-e** has been determined via chiral high resolution gas-chromatography carried out on β- or γ-cyclodextrin capillary column and were found to be always higher than 99%.
The e.e. of compound **6f** was determined via HPLC on a Lux5ucell 3 column.

The Julia reaction is known to favor the formation of the *E* isomer, when leading to disubstituted alkenes.[63,64] Accordingly, when substituted acetates **5h,i** were subjected to reductive elimination with Na(Hg), the corresponding allylamines **6h,i** were obtained as 4:1 mixtures of *E* and *Z* isomers, as determined by NMR. A complete list of the allylamines synthesized in this study with overall yields and enantiomeric excess is reported in Table 4.

2.2 Conclusions

In this first part of the thesis we have described a general procedure for the synthesis of α-chiral allylamines from readily available α-amino esters, by a simple modification of the Julia olefination reaction. While retaining all of the advantages of the original Julia reaction, this approach avoids using amino aldehydes as precursors in favor of the more readily-available and chemically and configurationally more stable amino esters. Epimerization at the chiral center, which is a frequent problem in the standard Julia and Wittig olefination of N-protected α-amino aldehydes, is thus prevented, and the desired allylamines were obtained in excellent yield and enantiomeric excess. The approach described here for the synthesis of allylamines is quite general and should provide a useful alternative to the classical Julia reaction whenever the starting aldehyde is unstable or, otherwise, not readily accessible. Moreover, its scope might be further expanded by replacing the phenyl alkyl sulfones of this work with benzotriazolylalkyl sulfones or other heteroarylalkyl sulfones, as in the Julia–Kocienski reaction,[76, 77] where the intermediate hydroxysulfones directly collapse to alkenes, thus avoiding the final reduction step.

[76] P.R. Blakemore, *J. Chem. Soc. Perkin Trans. 1* **2002**, 2563.
[77] E. Pfund, T. Lequeux, D. Gueyrard, *Synthesis* **2015**, 47, 1534.

PART 2

2-Dihydropyrimidines as promising BACE 1 inhibitors

Introduction

3. Alzheimer's disease (AD)

Alzheimer's Disease (AD) is a chronic neurodegenerative disease, affecting people in presenile and senile age, resulting in severe cognitive deficits due to loss of neurons and ultimately leading to death. According to the World Health Organization, 48 million individuals suffer from this condition worldwide, and this number is expected to dramatically grow to 115 million by 2050, due to an increase in the average age of the population.[78]

AD was described for the first time in 1906 by the German psychiatrist and neuropathologist Alois Alzheimer, assisted by the Italian neurologist Gaetano Perusini.[79] The disease is characterized by a progressive cognitive and functional deterioration manifesting with short-term memory loss, accompanied by concentration and orientation problems. These early symptoms are often mistaken with those due to aging or stress, and gradually convert into difficulties in the language (aphasia), perception (agnosia) and execution of complex movements (apraxia). Finally, the person loses the ability to interact with the environment and to control his movements, becoming completely dependent on those who provide care. The leading causes of death are the physical deterioration and the action of external agents, to which the patient is completely exposed during the final stage of the disease.

The main neuropathological hallmarks of AD are the presence of extracellular amyloid-β (Aβ) plaques and intracellular neurofibrillary tangles in the brain. Neurofibrillary tangles are insoluble bundles of fibres that locate in the perinuclear cytoplasm and are generally composed of phosphorylated tau protein.[80] Neuritic amyloid plaques are spherical lesions that contain extracellular aggregates of amyloid-β protein (Aβ) and are likely to be the primary lesion in AD.[81] It has been suggested that the appearance of tangles in the AD brain could be due to neuronal

---

[78] C. Reitz, R. Mayeux, *Pharmacology*, **2014**, 88, 640.

[79] A. Alzheimer, *Allgemeine Zeitschrift für Psychiatrie und Psychish-Gerichtliche Medizin*, **1907**, 64, 146.

[80] **a.** D. J. Selkoe, *Physiol. Rev.*, **2001**, 81, 741;**b.** KS. Kosik, C.L. Joachim, D.J. Selkoe *Proc. Natl. Acad. Sci. USA* **1986**, 83, 4044.

[81] D. J. Selkoe, JAMA, *J. Am. Med. Assoc.*, **2000,** 283, 1615.

responses to the formation of plaques.[82,80a] Current therapies are aimed at the management of symptoms and, to date, no disease altering treatment exists for Alzheimer's patients. Currently, Aß peptides and tau proteins are the main therapeutic targets for the treatment of Alzheimer (Figure 10).[83]

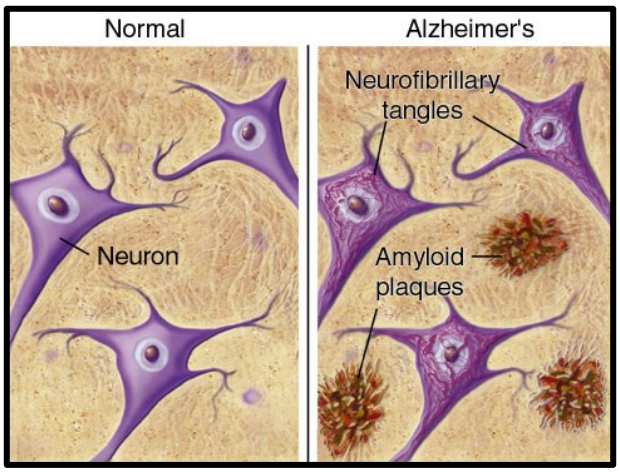

Figure 10. *Comparison between a healthy (left) and an AD affected brain tissue (right).*

The processes that lead to aggregation of the proteins and to neurodegeneration are not yet entirely clear.[78] Distinctive signs of Alzheimer's appear in the peripheral regions of the cortex, centre of cognitive functions such as memory, perception and language, and they are constituted by an enlargement of the ventricles and by a thinning of the cerebral cortex and of the hippocampus (Figure 11).[84]

[82] D. J. Selkoe, *Nature*, **1991**, 354, 432.

[83] P. Tiraboschi, L. A. Hansen, L. J. Thal, and J. Corey-Bloom, *Neurology*, **2004**, 62, 1984.

[84] **a.** N. Schuff, N. Woerner, L. Boreta, T. Kornfield,L. M. Shaw, J. Q. Trojanowski, P. M. Thompson, C. R. Jack, Jr, M. W. Weiner, and the Alzheimer's; Disease Neuroimaging Initiative, Brain, 2009, 132, 1067; **b.** www.brightfocus.org/alzheimers/infographic/brain-alzheimers-disease.

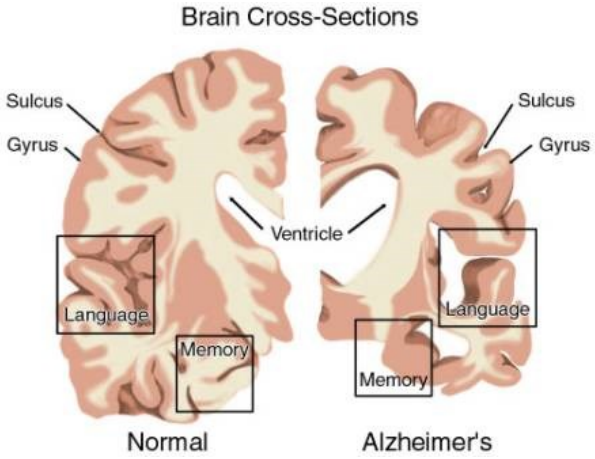

Figure 11. *Brain cross-section of a normal (l) and an AD (r) patient.*

The cause of the atrophy of the brain areas affected by Alzheimer's is the loss of dendrites and axons, which in the beginning undergo a reduction of myelin and at the end lead to the death of neurons.[85] The hippocampus region of a healthy person contains around nine million neurons, while in AD terminal stages more than 80% of these neurons have disappeared and the volume of the brain reduced to less than half.[86] A decrease of the thickness of the medial temporal lobe in AD can be shown by modern imaging techniques, such as MRI (Magnetic Resonance Imaging) and PET (Positron Emission Tomography), that also reveals the presence of β-amyloid fibres (Figure 12).[87] AD affected patients suffering from language dysfunction display a significant reduction in metabolism in the left, frontal, temporal and parietal lobes (blue).

[85] **a.** X. Hu, C. W. Hicks, W. He, P. Wong, W. B. Macklin, B. D. Trapp and R. Yan, *Nature Neurosci.* **2006**, 9, 1520. **b.** S. Barão, D. Moechars, S. F. Lichtenthaler, and B. De Strooper, *Trends in Neurosciences*, **2016**, 39, 158

[86] A.D. Smith, *Proc. Natl. Acad. Sci. USA*, **2002**, 99, 4135.

[87] **a.** R. S. Desikan, H. J. Cabral, C. P. Hess, W. P. Dillon, C. M. Glastonbury, M. W. Weiner, N. J. Schmansky, D. N. Greve, D. H. Salat, R. L. Buckner and B. Fischl, *Brain*, **2009**, 132; 2048; **b.** A.P. Jr Carpenter , M.J. Pontecorvo , F.F.Hefti, D.M. Skovronsky, *Q J Nucl Med Mol Imaging*. **2009**, 53, 387.

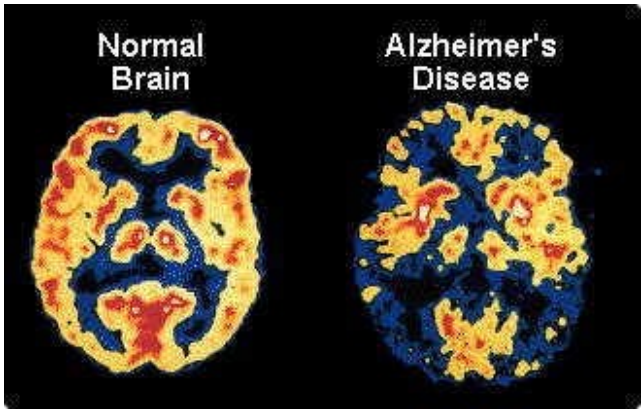

Figure 12. *PET images of a normal (left) and an AD affected(right) brain.*

3.1 Hypotheses for AD pathogenesis

The observation of neurofibrillary tangles and neuritic plaques in the brain of AD patients has led to two theories for the onset of AD, namely the tau and amyloid hypotheses.[88] According to the tau hypothesis, the development of AD is caused by the hyperphosphorylation of the tau proteins as a result of an imbalance in the activity of kinases and phosphatases. The tau proteins are a class of proteins particularly abundant in neurons of the central nervous system; they are linked to microtubules that help to keep the network of interconnections between neurons. Hyperphosphorylation causes the destruction of the network of microtubules, leading to their self-assembly into a β-sheet structure organized into paired helical filaments, which eventually gives rise to neurofibrillary tangles in the perinuclear cytoplasm of the neuron. This causes an alteration of the regular functions of the neuronal transport system, since the biochemical communication between neurons is prevented, thus leading to cellular death (Figure 13).[89]

The hyperphosphorylated tau proteins seem to be in excess in the brain of patients affected of Alzheimer disease than in the healthy people.

---

[88]V. H. Finder, *J. Alzheimers Dis.*, **2010**, 22, 5.

[89] **a.** W. H. Stoothoff, G. V.W. Johnson, *Biochim. Biophys. Acta*, **2005**, 1739, 280; **b.** G. V. W. Johnson and W. H. Stoothoff, *J.Cell Sci.*, **2004**, 117, 5724.

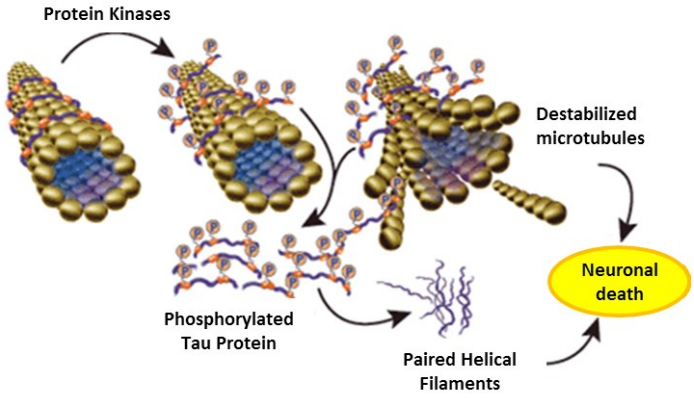

Figure 13. *Hyperphosphorylation of tau proteins.*

This hypothesis has been criticized because other neurodegenerative diseases caused by hyperphosphorylation of tau proteins are known (Pick's disease, Lateral Amyotrophic Sclerosis, etc.), [90] and from recent studies it emerged that hyperphosphorylation follows the formation of β-amyloid aggregates and not the contrary.[91] The most accredited hypothesis for the pathogenesis of AD is the β-amyloid hypothesis that correlates neurodegeneration to the formation of plaques composed of β-amyloid peptides Aβ (Figure 14). The hypothesis is based on the observation that neuron plaques seem to be the primary lesions in order of time in AD. The formation of these plaques initiates a cascade of degenerative processes that eventually result in dementia.[83]

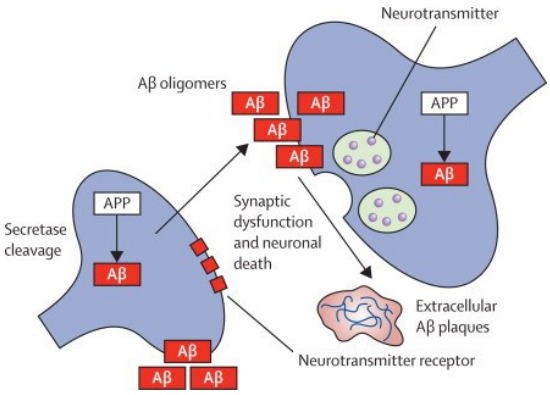

Figure 14. *Schematic cascade of the formation of extracellular Aβ plaques.*[92]

[90] C. Ballatore, V.M. Lee, J.Q. Trojanowski, *Nat. Rev. Neurosci.*, **2007**, 8, 663.

[91] J. Hardy and D. J. Selkoe, *Science*, **2002**, 19, 297, 353.

[92] C. Ballard, S. Gauthier, A. Corbett, C. Brayne, D. Aarsland, E. Jones, *The lancet*, **2011**,377, 1019.

The hyperproduction of β-amyloid peptide is due to an alteration of metabolism of Amyloid Precursor Protein (APP); in the amyloidogenic pathway, Aβ peptide is produced following the sequential cleavage of APP in neurons by two proteases, BACE 1 and γ-secretase.[93] Appropriate choices for a rational approach to the cure of AD are the inhibition of the accumulation of β-amyloid peptide and the selective disaggregation of Aβ plaques, and therefore many research efforts in medicinal chemistry are based on this hypothesis.

3.1.1 Amyloidogenic hypothesis

APP is a bitopic transmembrane protein consisting of 695 to 770 residues (Figure 15) produced in different tissues of the human body, mainly in brain and kidneys.[94] The physiological function of this protein is still not known with precision, but it has been shown that APP and its derivatives contribute to cell-cell and cell-matrix interactions, adhesion and the regulation of intracellular calcium levels within the cells themselves.[94]

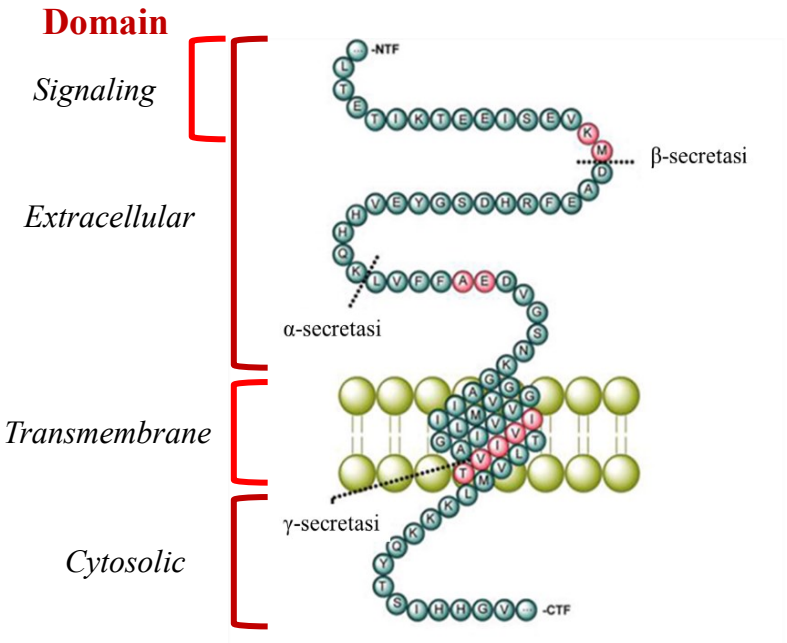

Figure 15. *APP structure.*

[93] Cole, S.L.; Vassar, R. *Mol.Neurodeg.*, **2007**, 2, 22.

[94] A.K. Ghosh and H. Osswald, *Chem. Soc. Rev.*, **2014**, 43, 6765.

Upon arrival of the stimulus to the cell, the signal peptide carries the APP in the endoplasmic reticulum (ER), where it is linked to the membrane by the hydrophobic domain. Proteolysis of APP can take several pathways that give rise to a variety of soluble and membrane fragments. The enzymes responsible for these activities are proteases, called α-secretase, β-secretase and γ-secretase (Figure 16). Cleavage of APP by α-secretase governs the non-amyloidogenic pathway, leading to the formation of the fragment soluble in the matrix (sAPPα) and the C83 C-terminal fragment. Alternatively, APP can undergo a first proteolysis by the β-secretase, which hydrolyses the peptide bond in the extracellular region of APP, 16 aa down from the α-secretase site, releasing the soluble fragment sAPPβ and the C99 C-terminal fragment. The fragments C83 and C99 are further processed by γ-secretase, which acts in the transmembrane region of APP (Figure 16).

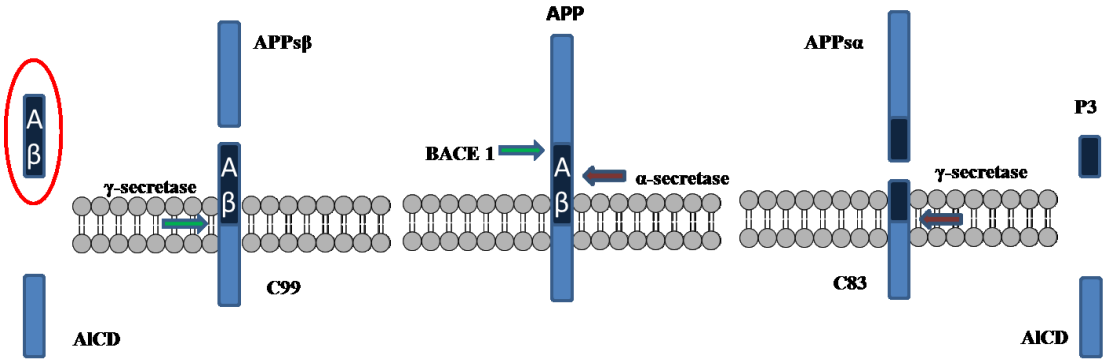

Figure 16. *APP proteolytic pathways. Left: amyloidogenic; right: non amyloidogenic.*

Processing of the C83 fragment by γ-secretase releases the 3 kDa, non-amyloidogenic peptide p3. The action of γ-secretase on the C99 peptide results in the formation of a heterogeneous mixture of Aβ peptides, predominantly 40 and 42 amino acids in length. The latter ($A\beta_{42}$) is more hydrophobic and particularly prone to aggregation,[93] forming oligomers that accumulate in the brain and initiate a cascade of events resulting in neuronal disfunctioning, neurodegeneration and neuronal fatality. Normally, γ-secretase activity favours the formation of less aggregating $A\beta_{40}$ peptides, but mutations of this enzyme (and mutations of the so-called presenilins, which can modulate the activity of γ-secretase, or behave like γ-

secretase) lead to massive formation of $A\beta_{42}$. Accordingly, Aβ plaques are also observed in healthy subjects, but these are completely asymptomatic.[93]

Typical symptoms of AD can also emerge when there is an overexpression of the gene encoding APP. For example, since the gene just mentioned is encoded within the chromosome 21, subjects suffering from trisomy-21 (or Down syndrome) may show signs of neuritic plaques as early as 12 years old, as the accumulation of Aβ begins from birth, this AD being known as Familial AD.[80a] These gene mutations can affect the location of hydrolysis for γ secretase, leading to the formation of an excess of $A\beta_{42}$.

3.2 BACE 1: β-site APP cleaving enzyme 1

β-Secretase (BACE-1) represents the first protease involved in the APP degradation process, leading to production of β-amyloid (Aβ). Silencing BACE-1 can reduce $A\beta_{42}$ production thus slowing or stopping disease progression and therefore it represents a viable therapeutic strategy for AD.

BACE 1 is a type 1 transmembrane aspartic protease with a bilobate structure, made of 501 aa. It is built in the Golgi apparatus from modification and cleavage of the immature glycosylated polypeptide pro-BACE1 in the endoplasmic reticulum. BACE 1 exhibits optimum proteolytic activity between pH 4 and 5, suggesting that this enzyme does not act at the cell surface but in the endosomes, on the way to the cell surface.[94,95]

BACE 1 can assume two thermodynamically stable conformations, the open flap and closed flap conformation (red and blue, respectively, in Figure 17). The free enzyme preferentially assumes the open flap conformation, in which the active site is exposed to accommodate the substrate. When it is bound to the substrate, the enzyme adopts the closed flap conformation.[96]

---

[95] C. Venugopal, C. M. Demos, K. S. J. Rao, M. A. Pappolla, and K. Sambamurti, *Neurol Disord Drug Targets*, **2008**, 7, 278.

[96] L. Hong, J. Tang, *Biochemistry*, **2004**, 43, 4689.

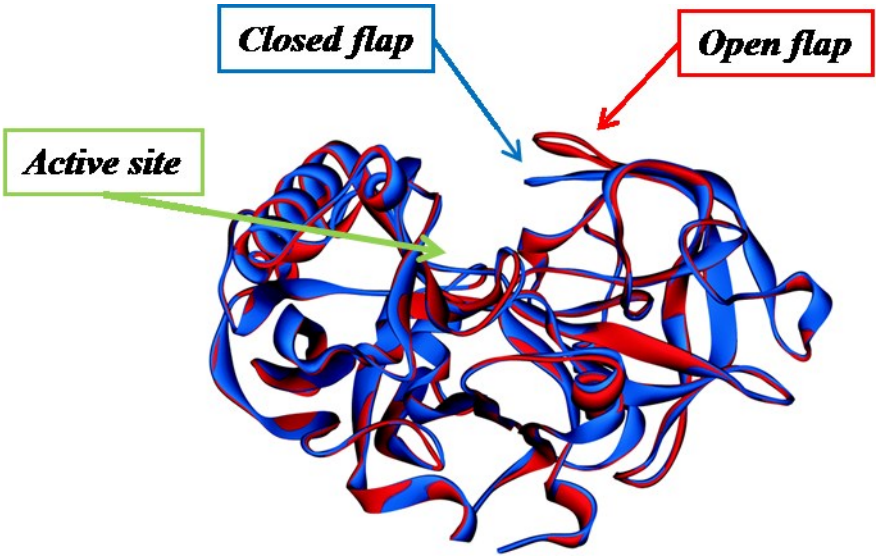

Figure 17.*BACE1 conformations: open flap (red) and closed flap (blue).*

The conformational shift open - closed flap is accompanied by the breaking of several hydrogen bonds. This destabilization, however, is compensated by interactions between the enzyme and the substrate, as well as by interactions between the side chains.[94] The two catalytic aspartates (Asp32 and Asp228) are located in the center of the proteolytic pocket and are surrounded by a network of hydrogen bonds. In the presence of a substrate their carboxylate groups are not perfectly coplanar.[97]

While BACE 1 inhibition is a promising approach to fight Alzheimer's disease, one must be aware of several possible adverse effects:

1. there is another enzyme (BACE 2) with a sequence similar to BACE 1 (68% homology) and with the same structural organization, but differing in the tissue distribution, localization and substrate specificity.[95] While BACE 2 function is not completely understood, its activity, considering the structural similarities, might be affected by BACE 1 inhibitors.
2. Another function of BACE 1 is the proteolytic processing of Neuregulin 1 that regulates axon myelination in the peripheral nervous system.[85]
3. Amyloid β peptide appears to participate in the activation of kinase enzymes, [98] regulation of cholesterol transport, [99] protection against

[97] L. Hong, G. Koelsch, X. Lin, A.K. Gosh, X.C. Zhang, J. Tang, J. *Science*, **2000**, *290*, 150.

[98] M. A. Bogoyevitch, I. Boehm, A. Oakley, A. J. Ketterman, R.K. Barr, *Biochim. Biophy. Acta*, **2004**, 1697, 89.

[99] Z. Yao and V. Papadopoulos, *J. FASEB*, **2002,** doi: 0.1096/fj.02-0285fje.

oxidative stress, [100] and others, but especially it may fight other syndromes.[101]

Therefore the degree of BACE 1 inhibition is a matter of great importance, depending on the advancement of the disease. *In vivo* tests allow to estimate that 50% inhibition may circumvent mechanism-based side effects and, yet, provide sufficient Aβ reduction for therapeutic efficiency. [102]

[100] M. Hiltunena, T. van Groenb and J. Jolkkonen, *J. Alzheimer Dis.*, **2009**, 18, 401.

[101] **a.** D. K. Kumar, S. H. Choi, K. J. Washicosky, W. A. Eimer, S. Tucker, J. Ghofrani, A. Lefkowitz, G. McColl, L. E. Goldstein, R. E. Tanzi, R. D. Moir, *Science Translational Medicine,* **2016**, 8, 340; **b.** M. R. White, R. Kandel, S. Tripathi, D. Condon, L. Qi, J. Taubenberger, K. L. Hartshorn, *PLOS One*, **2014**, 9, 101364.

[102] R. Vassar, *Alzheimer's Res. Ther.*, **2014**, 6, 89.

3.2.1 BACE 1 inhibitors

The crystal structure of BACE 1 co-crystallized with different ligands reveals the basic requirements and the key features needed for enzyme inhibition.

Following a well-established approach to protease inhibition, in earlier attempts, peptidomimetic BACE-1 inhibitors were designed mimicking the conformation of the transition state for hydrolysis of the substrate.[103] In this approach, a hydroxyl group on the transition state isostere displaces the catalytic water molecule and forms tight hydrogen bonds with the catalytic aspartic acid residues, thus precluding catalytic activity. Peptidomimetics containing statine, hydroxyethylene, and hydroxyethylamine transition states isosters were extensively investigated and their properties optimized. Their major drawback is related to the poor pharmacokinetic profile, limited specificity and pharmacological properties *in vivo*, such as blood brain barrier crossing, oral bioavailability, susceptibly to transport P-glycoprotein, which have prevented them from being further developed to orally bioavailable CNS drugs.

The most detailed study on the complex BACE1-inhibitor was reported by Shimzu, with the highly peptidic inhibitor OM99-2.[104]
The authors have obtained the structures of active and inactive forms of the enzyme. The maximum catalytic activity and the maximum binding of OM-99-2 occur both at pH 5, and the analysis of the crystal structures of the enzyme from crystallizations carried out at different pHs reveal that a major conformational change can also be identified by raising or lowering the pH. The crystal structure at pH 5 can therefore be used to map the binding subsites of the proteases, and to set a reference interaction scheme (Figure 18).

[103] A.K. Ghosh, M. Brindisi, J. Tang, *J. Neurochem.*, **2012**, 120, 71.

[104] H. Shimizu, A. Tosaki, K. Kaneko, T. Hisano, T. Sakurai, N. Nukina, *Mol Cell Biol*. **2008**, 28, 3663.

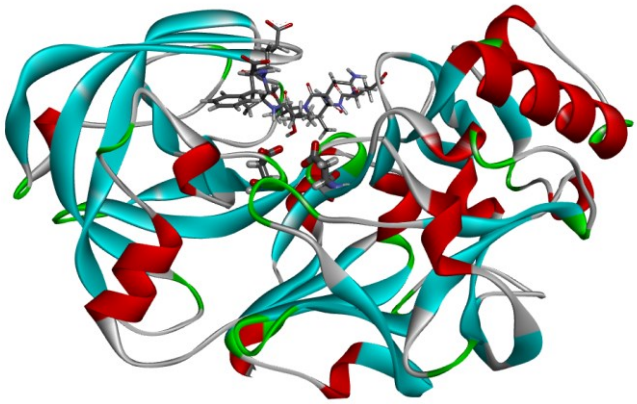

a

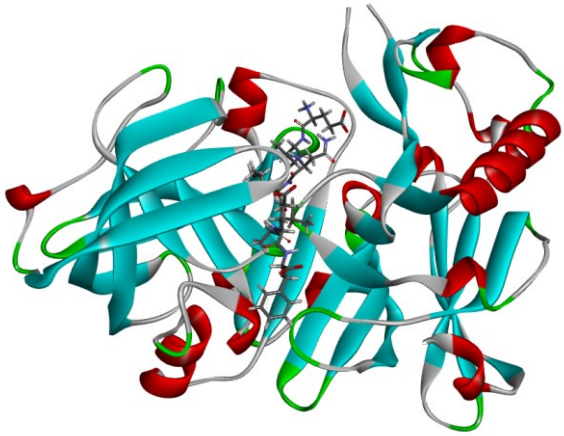

b

Figure 18. *a: side and b: top views of the complex of BACE-1 with the pseudopeptide inhibitor OM99-2.*

The substrate analogue inhibitor is hosted by a channel in contact with eight aminoacid residues spanning from P4' to P4, and the catalytically active aspartyl residues 32 and 228 are buried inside the catalytic site. In the empty enzyme they interact with the conserved water residues, which lies in the same position occupied by the hydroxyl group of the pseudopeptide moiety of the inhibitor. A large flap made by an antiparallel b-sheet strand and by its loop covers the catalytic site in the empty enzyme, while a major conformational change occurs in the complex, where the flap is shifted towards the P2 residue of the inhibitor. This allows the interaction of the pseudopeptide at all the binding channel subsite. A map of such interactions is reported in Figure 19.

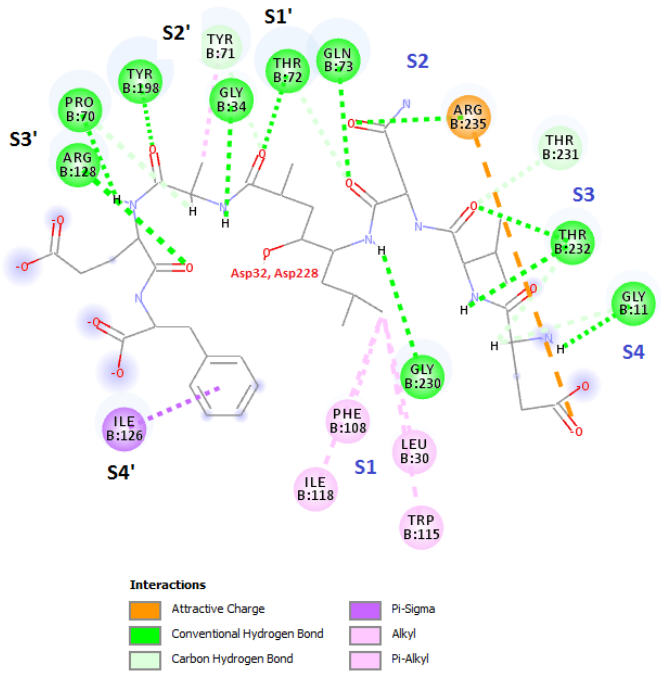

a

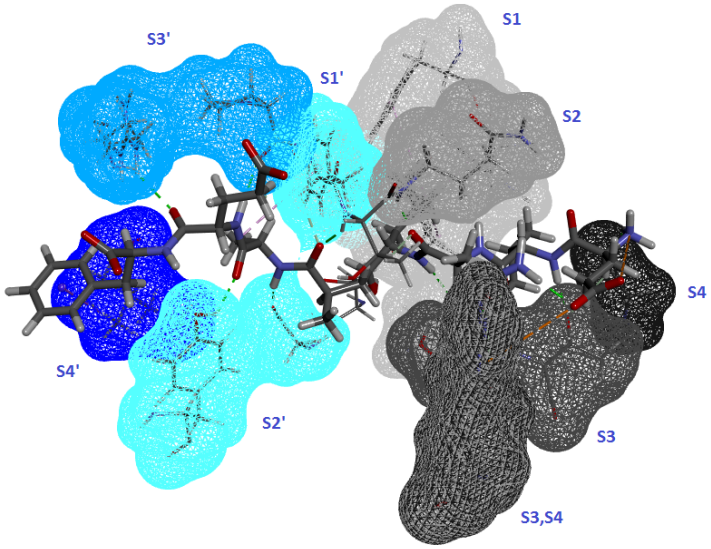

b

Figure 19. *a: map of the interactions of the pseudopeptide inhibitor OM99-2 at the S4' ÷ S4 subsite level; b: view of the subsite from the crystallographic structure (pdb id. 2ZHR).*

The binding mode is highly unsymmetrical, and most of the interactions are found at the P1-P4 side. S1 is a large a well-defined site, where the P1 isoleucine is in contact with four hydrophobic side chains (Leu30, Phe 108, Trp 115, Ile 118). Conversely, S1' is smaller and less accessible, and no hydrophobic contacts are clearly identified for the alanine residue at P1'. S2 is a very polar and cationic subsite, as it shares Arg 235 with S4, and this residue interacts on one side with the asparagine side chain of

P2 and with the carboxyl terminus on the other side. On the contrary, S2' is small and hydrophobic. Polar S2 is followed by the very hydrophobic subsite S3, where interactions take place with P3 valine, while hydrophobic S2' is followed by the very polar S3' subsite, where Arg 128 binds P3' glutamate. The last polarity inversion is then found at S4 (very polar to bind P4 aspartate) and S4' (hydrophobic to bind P4' isoleucine).

More recent attempts have been directed towards the discovery of non peptidic, small molecule BACE-1 inhibitors,[105] designed to have optimal interactions with the enzyme, higher metabolic stability, and higher blood-brain-barrier penetration ability.[102]

Recently, a significant number of these 2nd generation BACE-1 inhibitors has been developed as small-molecule candidates possessing drug-like features.

While no one of those have has been approved for clinical use as yet, however some of them have gone through various stages of clinical trials, as shown in Table 5. AZD3293 and MK-8931 are currently at an advanced state of clinical sperimentation.

Company	Compound	Clinical trial phase
AstraZeneca/Lilly	**AZD3293**	**Phase 2/3**
CoMentis	CTS-21166	Phase 1
Eisai/Biogen	Idec E2609	Phase 2
High Point	HPP854	Phase 1
Merck	**MK-8931**	**Phase 2/3**
Pfizer	PF-05297909	Phase 1
Takeda	TAK-070	Phase 1
Vitae/Boehringer Ingelheim	VTP-37948	Phase 1

Table 5. *Phases of clinical sperimentation of BACE1 inhibitors.*

MK-8931 (Verubecestat)[106] developed by Merck, was tested for safety and tolerability as well as pharmacokinetic and pharmacodynamic properties in moderate

[105] R. Silvestri, *Med Res Rev.*, **2009**, 29, 295

[106] R. Yan, *Transl. Neurodegen*. **2016**, 5, 13.

to mild symptomatic AD patients. The core of the molecule is a 3-aminothiadiazine group (Figure 20).

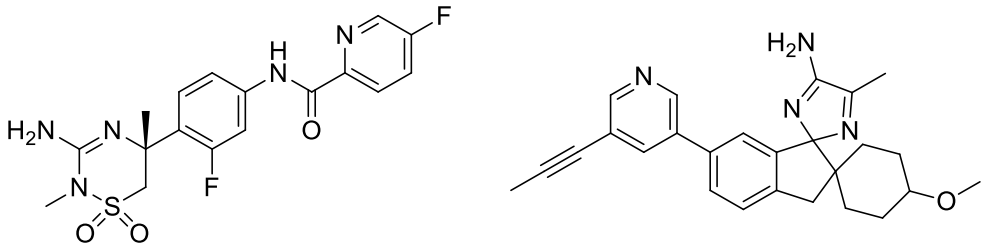

Figure 20. *MK-8931 (left) and AZD- 3293 (right).*

MK-8931 reduces $A\beta_{40}$ peptides in cells with IC_{50} = 13 nM and K_i =7.8 nM. This inhibitor showed positive results in the 1 and 1b clinical phase; the combined phases 2 and 3 will be concluded in the 2018.

AZD3293, also known as LY3314814, has been shown in Phase 1 studies to reduce levels of amyloid-beta in the cerebro-spinal fluid of Alzheimer's patients and healthy volunteers. A pivotal Phase 2/3 clinical trial started in 2014 and is planned to end in June 2019.

4. *Small molecules as non peptidomimetic inhibitors for BACE1*

Several chemical scaffolds have been proposed in the design of BACE 1 inhibitors (Figure 21), all of which contain structural motifs that can establish efficient hydrogen bond interactions with the catalytic aspartates.[107] The synthesis and biological evaluation of inhibitors based on a different heterocyclic scaffold, namely the dihydropyrimidinone scaffold, is described in the second part of this thesis.

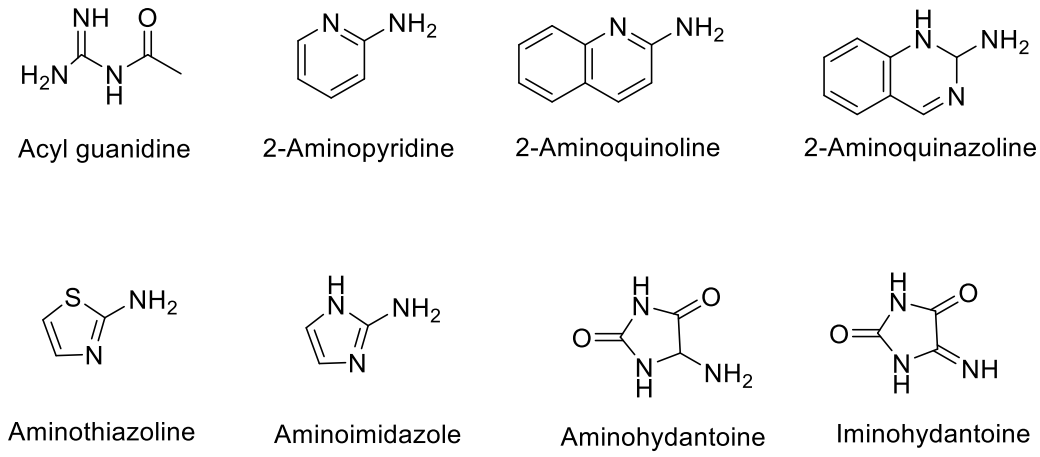

Figure 21. *Scaffolds for BACE-1 inhibitors.*

4.1 *3,4-Dihydropyrimidin-2(1H)-ones (DHPMs) and their 2-thia and 2-aza analogues*

Recently, interest in multifunctionalized 3,4-dihydropyrimidin-2(1*H*)-ones, (DHPMs) has surged rapidly, owing to the biological and pharmacological properties associated with this heterocyclic scaffold.

Properly functionalized DHMPs derivatives have been identified, for example, as excellent calcium channel modulators,[108] mitotic Kinesin inhibitors, adrenergic receptor antagonists, antibacterials, antivirals, as extensively reviewed.[109].

---

[107] **a.** S. J. Stachel, *J Drug Develop. Res.* **2009**, 70, 101; **b.** Y. Niu, H. Gao, F. Xu, C. Wang, P. Liu, G. Yang, Q. Sun, P. Xu, *Chem. Biol. Drug Des*. **2012**, 80, 775.

[108] **a.** K.S. Atwal, B.N. Swanson, S.E. Unger, D.M. Floyd, S. Moreland, A. Hedberg, B.C. O'Reilly, *J. Med. Chem.*, **1991**, 34, 806; **b.** G. C. Rovnyak, K. S. Atwal, A. Hedberg, S. D. Kimball, S. Moreland, J. Z. Gougoutas, B. C. O'Reilly, J. Schwartz, M. F. Malley, *J. Med. Chem.* **1992**, 35, 3254.

[109] C. O. Kappe, *Eur. J. Med. Chem*. **2000,** 35, 1043–1052

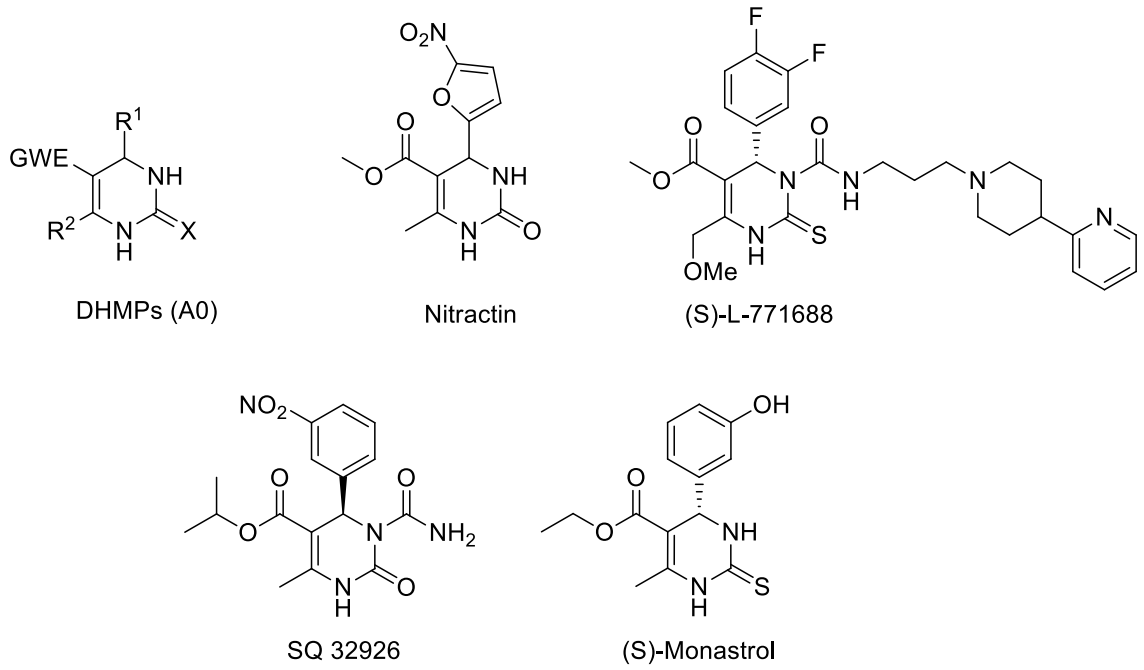

Figure 22. *The DHMP scaffold and two medicinally relevant dihydropirimidinones.*

Nitractin (Figure 22) has excellent antiviral activity against the viruses of the trachoma group. The same compound also exhibits modest antibacterial activity.[110]
The aminopropyl-4-arylpiperidine group attached via a C-5 amide to the 2-thio DHPM scaffold, as for compound (S)-L-771688 (Figure 22), has proved to be an excellent template for selective α1A receptor subtype antagonists for the treatment of benign prostatic hyperplasia.
Besides, (S)-Monastrol (Figure 22) has been identified as an inhibitor of a mitotic kinesin Eg5 and a potential new lead compound for the treatment of cancer.[111]

Moreover, Atwal and co-worker demonstrated that the compound SQ 32926, (Figure 22) has antihypertensive properties in *vivo*.[108a]

The interest in DHMPs is also related to their easy accessibility by the well known three component Biginelli reaction,[112] and the possibility of structural

[110] E.W. Hurst, R.J. Hull, *Med. Pharm. Chem. Gem. 3*, **1961**, 215; T. Matsuda, I. Hirao, *Nippon Kag. Zass*. **1965**, 86, 1195.

[111] U. Mayer, T.M. Kapoor, S.J. Haggarty, R.W. King, S.L. Schreiber, T.J. Mitchison, *Science,* **1999**, 286, 971.

[112] P. Biginelli, *Gazz. Chim. Ital*. 23, **1893**, 360.

modifications introducing various chemical substituents in different positions of the ring, this providing remarkable changes in pharmacological profile.

4.2 Biginelli Reaction

The Biginelli reaction is one of the first examples of multicomponent reactions (MCRs), a class of increasing importance in organic and medicinal chemistry.[113] The convergent approach characteristic of MCRs offers significant advantages over conventional linear-type synthesis and can provide products with the diversity needed for the discovery of new lead compounds using combinatorial chemistry techniques.

In 1893, the Italian chemist Pietro Biginelli reported the acid catalyzed cyclocondensation reaction of ethyl acetoacetate, benzaldehyde, and urea.[112] The reaction was carried out in refluxing ethanol in the presence of a catalytic amount of HCl. The product of this one-pot, three-component reaction was identified as ethyl 6-methyl-4-phenyl-3,4-dihydropyrimidin2(1*H*)-one 5-carboxylate (Scheme 7).

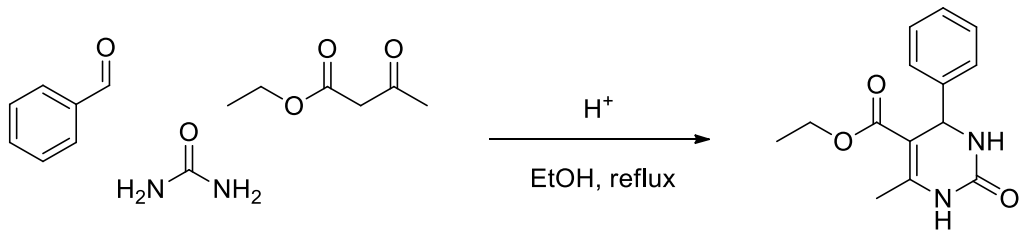

Scheme 7. *Biginelli reaction.*

While the early examples of the Biginelli reaction were limited to the use of aromatic aldehydes, urea and a β-ketoester, the scope of the reaction has been significantly extended by variation of all three reaction partners, giving access to a broad range of different dihydropyrimidine compounds of the type A0 (Figure 23).

[113] J. Zhu, H. Bienayme, *Multicomponent Reaction*, WILEY-VCH, **2005.**

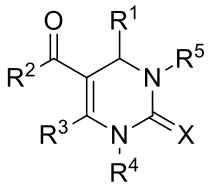

Figure 23. *The DHPM scaffold (A0).*

Variations in the aldehyde component have been explored extensively. The reaction generally tolerates well aromatic aldehydes, substituted in all position of the aromatic rings by electron withdrawing or donating groups, and also with heteroaromatic aldehydes derived from furan, thiophene, and pyridine. With aliphatic aldehydes lower yields are observed under the classical conditions but better results were achieved by the use of Lewis acids and solvent free conditions.

Regarding the 1,3-dicarbonyl compound, in addition to alkyl acetoacetates also other types of 3-oxoalkanoic esters or thioesters were employed successfully.[114] Primary, secondary and tertiary acetoacetamides can be used to afford pyrimidine-5-carboxamides.[115] Linear and cyclic 1,3-diketones, [116] and nitroacetone have also been used.[117]

The urea component is the most limiting in terms of structural variations allowed. Monosubstituted ureas have been employed in regiospecific reactions affording the N-1 substituted DHPMs. Isomeric N-3 substituted derivatives are not obtained with monoalkyl ureas under Biginelli conditions, and N,N'-disubstituted ureas do not react.[118] With thiourea and monosubstituted thioureas similar results are observed leading to the formation of the corresponding thiopyrimidinones. [119]
Biginelli reactions with guanidine and protected guanidine have been reported,[119] giving access to 2-iminoDHPMs (Scheme 8). The optimized reaction conditions were decribed by Kappe, [120] with guanidine hydrochloride, in DMF at 80°C, in the

[114] R. Pe ´rez, T. Beryozkina, O. I. Zbruyev, W. Haas, C. O. Kappe, *J. Comb. Chem*. **2002**, 4, 501.

[115]Y. S. Sadanandam, M. M. Shetty, P. V. Diwan, *Eur. J. Med. Chem.* **1992**, 27, 87.

[116] K. K. Mayer, S. Dove, H. Pongratz, M. Ertan, W. Wiegrebe, *Heterocycles* **1998**, 48, 1169

[117] G. Y. Remenikov, *Khim. Geterotsikl. Soedin*. **1997**, 1587.

[118] C.O. Kappe, *Tetrahedron lett*. **1993**, 49, 6937

[119] C.O. Kappe, *Multicomponent Reactions*, Wiley-VCH, Edited by Jieping Zhu, Hugues Bienayme, **2005**.

[120] J.J.V Eynde, N. Hecq, O. Kataeva, C. O. Kappe, *Tetrahedron Lett*. **2001**, 57, 1785.

presence of $NaHCO_3$ for 3hrs. The reaction times can be further reduced by the recent use of ultrasonic irradiation.[121]

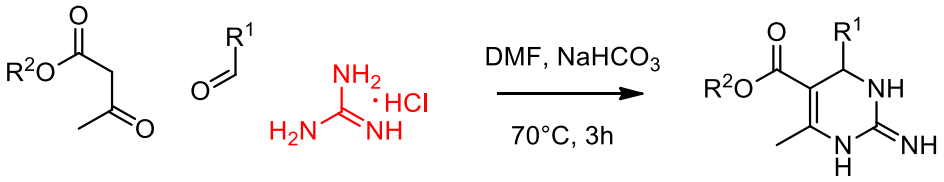

Scheme 8. *Biginelli-type reaction with guanidine.*

More recent developments of the Biginelli reactions are in the field of solid phase synthesis, combinatorial chemistry and the synthesis of natural products.[122]

A great variety of experimental conditions have been reported for this reaction, exploring the use of different solvents, acidic catalyst and temperature, as extensively reported in the published reviews.[118]

4.2.1 Mechanistic studies

Starting from the early work of Johnoson and Folkers,[123] the mechanism of the Biginelli condensation has been extensively investigated and three possible mechanisms have been proposed (iminium, enamine and Knoevenagel).[124]

[121] M.J. Ahmad; S.F. Hassan, R.U. Nisa; K.Ayub,; M.S Nadeem, S.Nazir, F.L.Ansari, N.A.Qureshi, U. Rashid *Med. Chem Res.* **2016** ,25, 1877-1894.

[122] C.O. Kappe, *Acc. Chem. Res.*, **2000**, 33, 879

[123] K. Folkers, T.B. Johnson, J. Am. Chem. Soc., **1933**, 55, 3781

[124] G. O. H. Alvim, E. N. J da Silva Junior and B. A. D. Neto, *RSC Adv*, **2014**, 4, 54282.

Folkers and Johnson privileged the "enamine mechanism" (Scheme 9) that involves the condensation between ethylacetoacetate (A1) and urea (A2), in the first, rate determining step, followed by addition to the aldehyde.

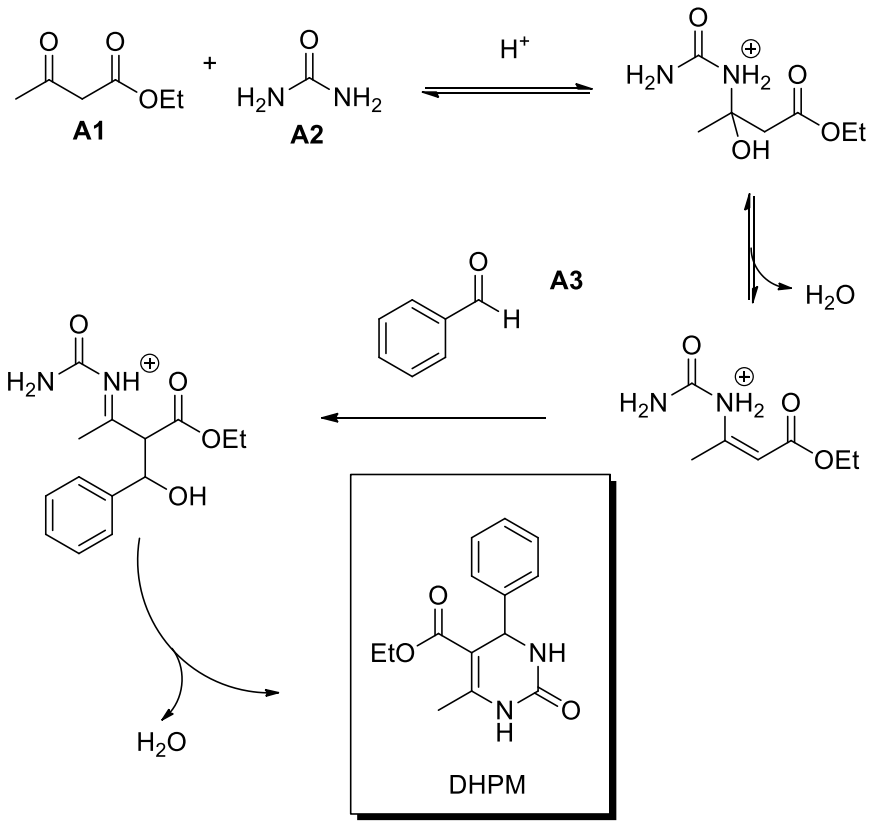

Scheme 9. *The Enamine-based mechanism for the Biginelli reaction*.

Interestingly, in 2007 Cepanec and coworkers [125] presented a series of experiments showing that the three components reaction proceeds via the enamine mechanism when catalysed by $SbCl_3$ and other Lewis acids in anhydrous aprotic solvents.

The so-called Knoevenagel mechanism (Scheme 10) is based on the findings of Sweet and Fissekis,[126] and it postulates that a Knoevenagel adduct, formed by the condensation between benzaldehyde and ethyl acetoacetate is the key intermediate. Although the Knoevenagel-based mechanism is still accepted, further evidences indicate other preferred reaction pathways in most cases.

[125] I. Cepanec, M. Litvic, M. Filipan-Litvic, I. Grungold, *Tetrahedron*, **2007**, 63, 11822

[126] F. Sweet, J.D. Fissekis, *J. Am. Chem. Soc.*, **1973**, 95, 8741.

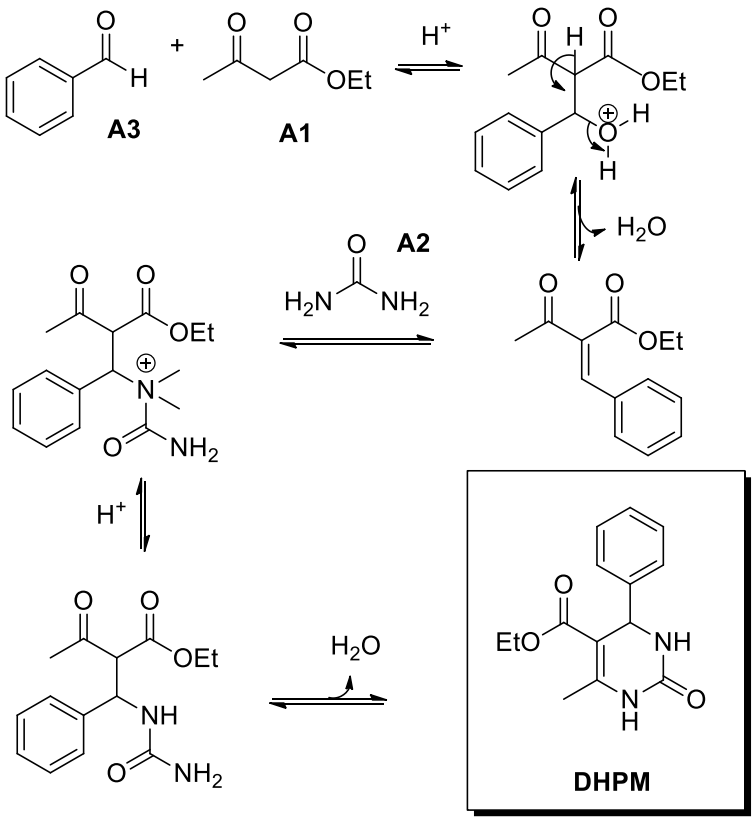

Scheme 10. *Knovenagel mechanism for the Biginelli reaction.*

In 1997 Kappe[127] reported a detailed re-investigation of the mechanism of the Biginelli reaction using ^{1}H and ^{13}C NMR spectroscopy and trapping experiments, providing strong evidences for the iminium mechanism (Scheme 11). This is based on the formation of an *N*-acyliminium intermediate from the acid-catalyzed reaction of the aldehyde (A3) and urea (A2) which is intercepted in the following step by the enol form of the dicarbonyl component, giving an open chain ureide precursor of the Biginelli compound (Scheme 11). The reaction mechanism can therefore be classified as α-amidoalkylation.

[127]C. O. Kappe, *J. Org. Chem*. **1997**, 62, 7201.

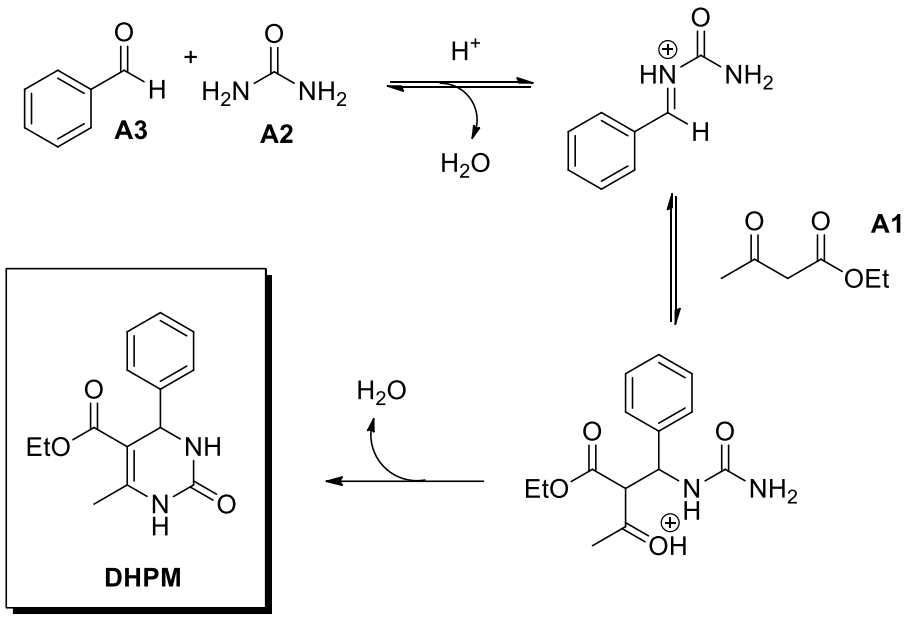

Scheme 11. *Iminium* mechanism of *Biginelli reaction.*

The elucidation of the mechanism of the Biginelli reaction prompted a renewed interest in improving the efficiency of this process and a great variety of experimental conditions have been reported for this reaction, exploring the use of different solvents and acid catalyst as extensively reported. [128] Solvent-free procedures [129] [130] as well as microwave enhanced protocols, [131] and solid-phase methods suitable for combinatorial chemistry have also been described.[132]

4.3 Chiral, enantioenriched dihydropyrimidines

4-Substituted-dihydropyrimidines arising from the Biginelli reaction are chiral molecules and, not surprisingly, the absolute configuration at C-4 was found to

---

[128] C.O. Kappe, A. Stadler *Org.Reactions*, **2004**, vol. 63, chapt. 1, The Biginelli Dihydropyrimidine Synthesis, Ed.by L.Overman et al., Published by John Wiley & Sons.,

[129] A. Shaabani, Bazgir and F. Teimouri, *Tetrahedron Lett*. **2003**, 44, 857.

[130]H. G. O. Alvim, T. B. Lima, A. L. de Oliveira, H. C. B. de Oliveira, F. M. Silva, F. C. Gozzo, R. Y. Souza, W. A. da Silva, and B. A. D. Neto *J. Org. Chem*. **2014**, 79, 3383.

[131] M. Nuchter, B. Ondruschka, *Mol. Diversity* **2003**, 7, 253.

[132] **a.** P. Wipf, A. Cunningham, A. *Tetrahedron Lett.* **1995**, 36, 7819; **b.** A. Studer, P. Jeger, P. Wipf, D.P. Curran, *J. Org. Chem.* **1997**; 62, 2917-2924; **c.** C. O. Kappe, *Bioorg. Med. Chem. Lett.* **2000**, 10, 49, **d.** J. J. Vanden Eynde, N. Labuche, Y. Van Haverbeke, L. Tietze, *Arkivoc* **2003**, 15, 22.

greatly influence their pharmacological properties. For example, the (*R*)-enantiomer of the calcium channel blocker SQ 32926 exhibits >400-fold more potent antihypertensive activity *in vitro* than the (*S*)-enantiomer (Figure 22).[108a]

Similarly, the (*S*)-enantiomer of the well-known antitumor lead compound monastrol (Figure 22) has been found to have a considerably higher activity than the (*R*)-enantiomer, both *in vitro* and *in vivo*.[133] The (*S*) enantiomer of L-771,688 (Figure 22), an α1A-adrenoceptor antagonist active against benign prostatic hyperplasia (BPH), is 100-fold more potent and selective than its enantiomer.[134]

Due to their important biological and pharmaceutical properties, access to optically pure DHPMs is in great demand. Although still lacking a broad application scope, several approaches have been developed, based either on the resolution of racemic mixtures or on asymmetric synthesis; these have been mainly applied to the synthesis of enantioenriched 2-oxo or 2-thiapyrimidinones, while, to our knowledge, a single example of optically pure aza analogs has been reported to date.[135]

4.3.1 Resolution

Initially, optically pure dihydropirimidinones were obtained only by the fractional crystallization of diastereoisomeric salts of chiral amines,[136] or by separation of covalently bonded diastereoisomeric compounds.[137, 138], For instance, the chiral resolution of racemic Monastrol was carried out on a preparative scale (ca. 100 mg),

[133] Y. Yan,V. Sardana, B. Xu,C. Homnick, W. Halczenko, C.A. Buser, M. Schaber, G.D. Hartman, H.E. Huber, L.C. Kuo, *J. Mol. Biol.*, **2004**, 335, 547.

[134] J. C. Barrow, P. G. Nantermet, H. G. Selnick, K. L. Glass, K. E. Rittle, K. F. Gilbert, T. G. Steele, C. F. Homnick, R. M. Freidinger, R. W. Ransom, P. Kling, D. Reiss, T. P. Broten, T. W. Schorn, R. S. L. Chang, S. S. O'Malley, T. V. Olah, J. D. Ellis, A. Barrish, K. Kassahun, P. Leppert, D. Nagarathnam, and C. Forray *J. Med. Chem.* **2000**, 43, 2703.

[135] N. Li, X-H. Chen, J. Song, S.-W. Luo,W. Fan and Z. Gong, *J. Am. Chem. Soc.* **2009**, 131, 15301.

[136] C. O. Kappe, G. Uray, P. Roschger, W. Lindneq, C. Kratky, and W. Keller, *Tetrahedron,* **1992**, 48, 5473

[137] A. Dondoni, A. Massi and S. Sabbatini, *Tetrahedron Lett.*, **2002**, 43, 5913.

[138] K. Singh , K. Singh, H. Kaur, *Tetrahedron* **2012**,68,6169.

through the separation of diastereomeric N-3 ribofuranosyl amides. These were obtained from the regioselective acylation of the racemic substrate with the chloride of the β-linked C-glycosyl carboxylic acid (8c,Scheme 12). After chromatographic separation of the diastereoisomeric amides and N-3 deprotection, the individual stereoisomers of monastrol were isolated wit >97% optical purity and good total yield. CD spectra proved the absolute C-4 configuration of each enantiomer.[137]

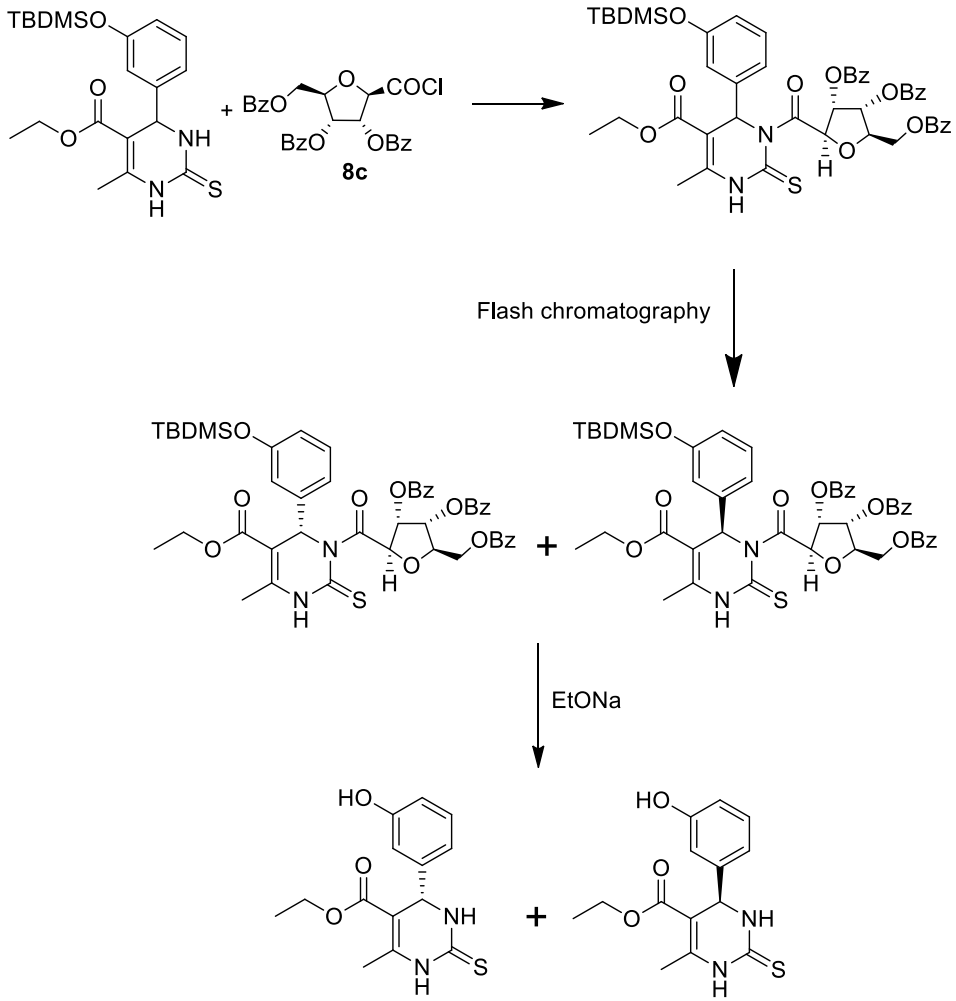

Scheme 12. *Separation of Monastrol enantiomers.*

More recently[139] Singh reported the chemical resolution of some DHPMs by appending an enantiopure chiral auxiliary derived from phenylalanine at the N-1 or N-3 positions of the heterocycles, leading to the formation of two diastereomers that were separated by chromatography to obtain both enantiomers of DHPMs, after removal of the auxiliary, with ee up to 99.9%. However, although being efficient in the reported cases, these methods turned out to be of limited general applicability.

Biocatalytic kinetic resolution of a precursor of (*S*)-L-771,668 was performed[139] employing *subtilisin* for the selective hydrolysis of C-5 (*R*)-methyl ester, leading to the recovery of the desired (*S*)-enantiomer in 80-90% chemical yield and high (98%) enantioselectivity. Similarly, the preparation of optically pure DHPMs by a lipase-catalyzed kinetic resolution of the corresponding N-3-acetoxymethylated derivatives has been reported by Kappe (Scheme 13).[140]

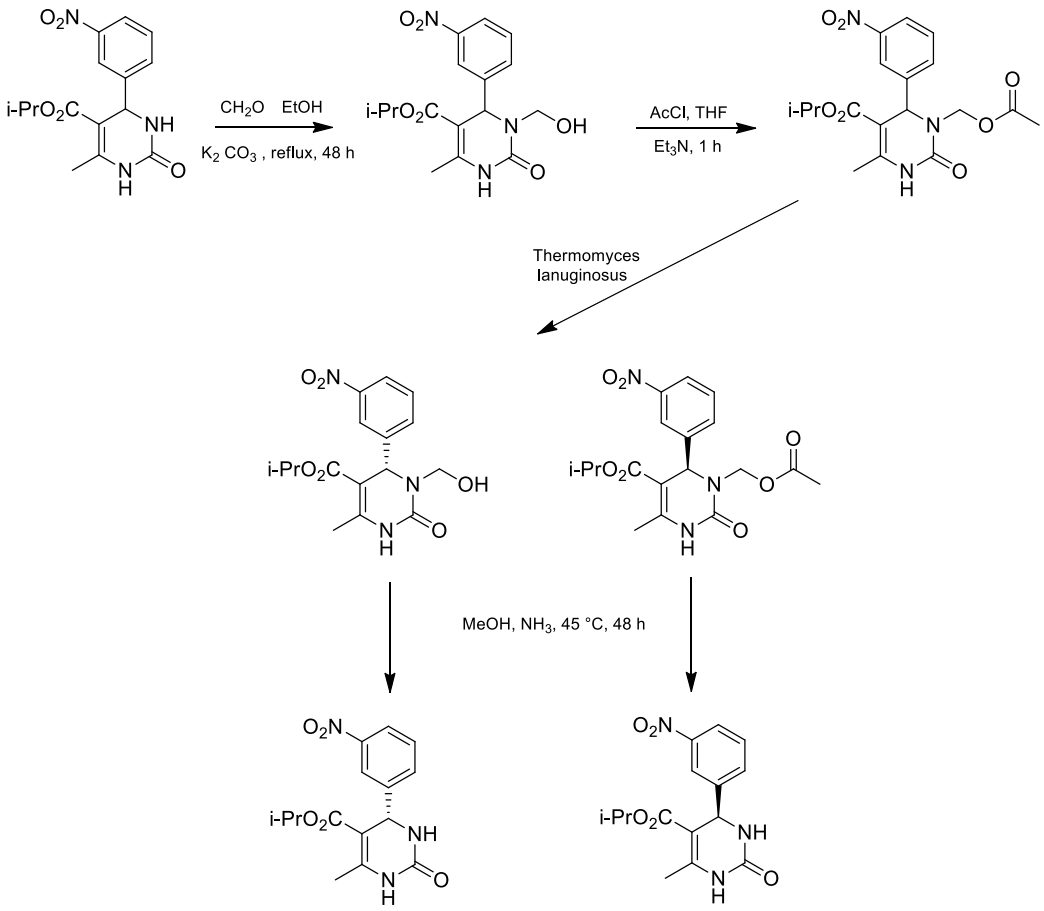

Scheme 13. *Lipase catalyzed kinetic resolution of racemic DHMPs.*

On the analytical scale, the separation of DHMP derivatives was achieved by HPLC on a variety of different chiral stationary phases,[141] and also by capillary electrophoresis[142] with chiral modifiers and buffers.

---

[139] D. R. Sidler, N. Barta, W. Li, E. Hu, L. Matty, N. Ikemoto, J.S. Campbell, M. Chartrain, K. Gbewonyo, r. Boyd, E. Corley, R.G. Ball, R.D. Larsen, P. Reider, *J. Can. J. Chem.* **2002**, 80, 646.

[140] B. Schnell, W. Krenn, K. Faber and C. O. Kappe, *J. Chem. Soc. Perkin Trans. 1*, **2000**, 4382

[141] O.P. Kleidernigg, C.O. Kappe *Tetrahedron: Asymmetry* **1997**, 8, 2057.

4.3.2 Asymmetric synthesis

The asymmetric version of the Biginelli reaction has not been available until recently. Complementarily to the resolution procedures described above, direct asymmetric version of the Biginelli reaction using chiral starting materials or auxiliaries have been developed. (-)-Menthyl acetoacetate[136] and glycosylated aldehydes (hexoses or pentoses)[143] have been used as chiral reactants, providing DHPMs, albeit with poor stereoselectivities.

A breakthrough in the catalytic asymmetric Biginelli reaction came in 2005 when Zhu and co-workers[144] found that a novel, recyclable chiral ytterbium catalyst provided efficient control on the enantioselectivity of Biginelli reactions involving different aldehydes, β-ketoesters and urea/thiourea, yielding DHPMs with good to excellent chemical and optical yields. Later, a 1-glycyl-3-methyl imidazolium chloride copper (II) complex was reported to promote the three-component reaction of different benzaldehydes, ethyl acetoacetate and urea under solvent-free conditions, although its application scope was limited to a few urea-derived DHPMs.[145]

The very fast progress of organocatalysis as a powerful tool in asymmetric synthesis has provided significant advances also in the enantioselective Biginelli reaction, which were reviewed in 2013[146] and 2014.[147] The first organocatalytic highly enantioselective Biginelli reaction was reported by Gong and co-workers in 2007 using a BINOL-derived phosphoric acids as catalyst.[148] Different aryl/alkyl aldehydes, alkyl acetoacetates, and thiourea/urea were used allowing a broad range

---

[142] Wang, F.; Loughlin, T.; Dowling, T.; Bicker, G.; Wyvratt, J. *J. Chromatogr. A.*, **2000**, 872, 279.

[143] A. Dondoni, A. Massi, E. Minghini, S. Sabbatini, V. Bertolasi, V. *J.Org. Chem.* **2002**, 67, 6979.

[144] Y. Huang, F. Yang, C. Zhu, *J. Am. Chem. Soc.*, **2005**, 127, 16386.

[145] P. Karthikeyan, S. A. Aswar, P. N. Muskawar, P. R. Bhagat, S. S. Kumar, *J. Organometal. Chem.*, **2013**, *723*, 154.

[146] M.M. Herawi, S. Asadi, B:M. Lashkariani, *Mol. Divers.* **2013**, 17, 389.

[147] J.-P. Wan, J. Lin, Y. Liu, *Current organic chemistry* **2014**, 18, 687.

[148] X.-H. Chen, X.-Y. Xu, H.Liu, L.-F. Cun, and L.-Z. Gong, *J. Am. Chem. Soc.* **2006**, 128 , 14802.

of functionalized DHPMs to be synthesized with good to excellent enantioselectivity. Further development on the use of chiral Brønsted acids led to the enantioselective synthesis of MCH1-R inhibitor SNAP-7941 with 91%e.e and 96% yield (Figure 24).[149]

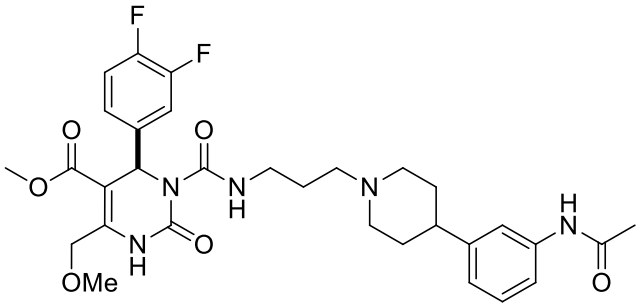

Figure 24. *SNAP-7941.*

An alternative approach was based on the use of proline-derived secondary amines[150] in combination with achiral Brønsted acids as catalysts to promote the Biginelli reaction, with enantioselectivities controlled by a dual activation protocol involving the enamine-type activation (via the condensation of the chiral amine and the β-keto ester) and the Brønsted acid-catalyzed formation of urea-based imines.[151] A broad range of secondary amines has been employed in the organocatalytic Biginelli rection.[147] Later, chiral primary amines, especially of the cinchona alkaloid class, have also attracted great interests. In 2010, the Zhao[152] and Lai[153] groups reported the enantioselective Biginelli reaction via dual activation using chiral primary amines with an acid as additive to activate the enamine intermediate. Recently, Wang and co-workers used a derivative of cyclohexane-1,2-diamine for the synthesis of enantiomerically enriched DHPMs via the Biginelli reaction.[154]

---

[149] J. M. Goss, S. E. Schaus, *J. Org. Chem*. **2008**, 73, 7651.

[150] **a.** J. G. Xin, L. Chang, Z. R. Hou, D. J. Shang, X. H. Liu, X. M. Feng, *Chem.Eur.J.* **2008**, 14, 3177; **b.** R. Gonzalez-Olvera, P. Demare, I. Regla, E. Juaristi, *Arkivoc* **2008**, 4, 61.

[151] **a.** J. H. Sohn, H. M. Choi, S. Lee, S. Joung, H.Y. Lee, *Eur. J. Org. Chem*. **2009**, 3858; **b.** Y.Y. Wu, Z. Chai, X.Y. Liu, G. Zhao, S.W. Zhao, *Eur. J. Org. Chem*. **2009**, 904.

[152] D. Ding, C.-G. Zhao, *Eur. J. Org. Chem.*, **2010**, 3802.

[153] Y.-F. Cai, H.-M. Yang, L. Li, K.-Z. Jiang, G.-Q. Lai, J.-X. Jiang, L.W. Xu, *Eur. J. Org. Chem*. **2010**, 4986.

[154] D.-Z. Xu, H. Li, Y. Wang, *Tetrahedron*, **2012**, 68, 7867.

Chiral thioureas have been developed as another major class of organocatalysts; their ability to induce enantioselectivity in a variety of different reactions has been mainly attributed to the ability to form strong hydrogen bonds with reactants and/or intermediates. The use of thioureas in enantioselective Biginelli reaction has been investigated, among others, by Miao and Chen[155] they reported that a gluco-2-aminocyclohexylthiourea (BPAT(I)), combined with with tert-butylammonium trifluoroacetate ((t-$BuNH_2$)·TFA) as a Brønsted acid additive, in dichloromethane at room temperature, provided DHPMs with (*R*)- configuration via the transition state proposed in Scheme 14.

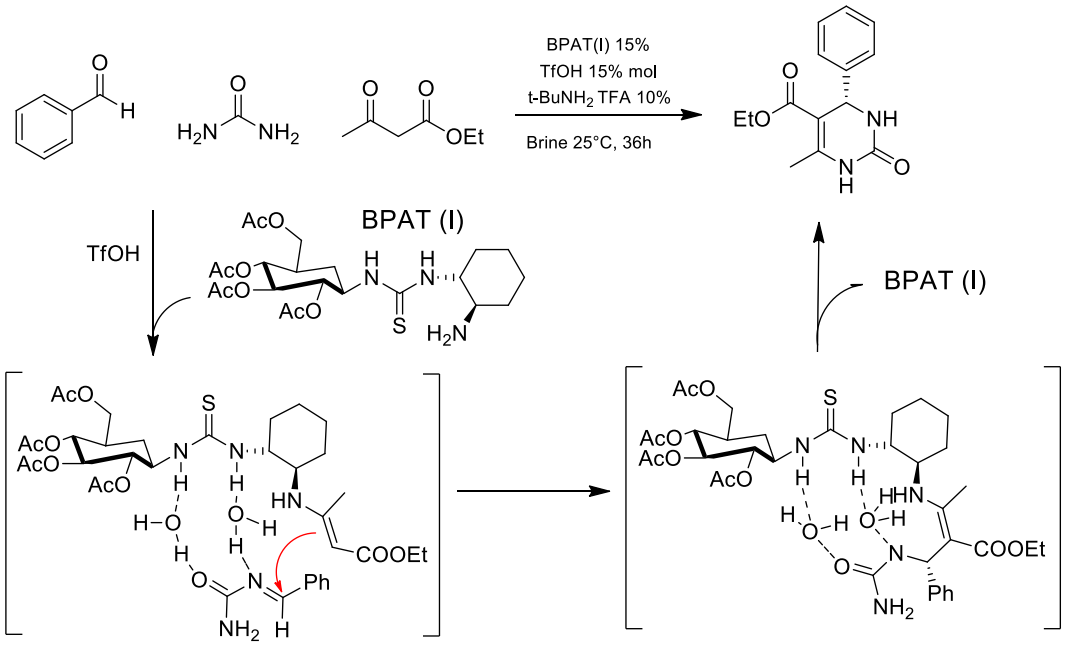

Scheme 14. *Mechanism of the BPAT(I)-catalyzed Biginelli reaction.*

The opposite (*S*) enantiomers of the same DHMPs were produced by the stereoisomeric catalyst BPAT(II), differing in the configuration at the cyclohexyl stereogenic carbon atoms (Figure 25). Later the same authors discovered that the same bifunctional thiourea-amine-TfOH system could be used in aqueous solution, as a chiral phase transfer catalyst.

[155] Y. Wang, H. Yang, J. Yu, Z. Miao, R. Chen, *Adv. Synth. Catal.* **2009**, 351, 3057.

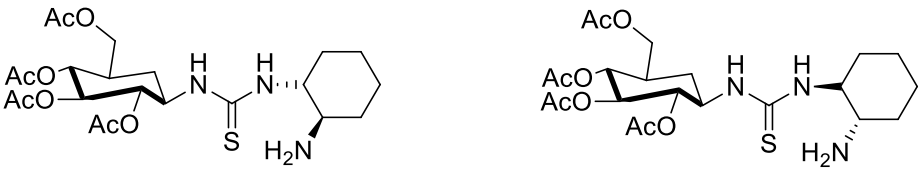

BPAT (I) BPAT (II)

Figure 25. *Thiourea catalysts BPAT(I) and BPAT(2).*

Results and Discussion

5. Biginelli reaction with urea and thiourea

The synthesis of 3,4-dihydropyrimidin-2-(1*H*)-ones (**O1-O16**) and thiones (**S1-S8**), was run following a very simple, inexpensive, solvent free method, reported in the literature in 2003 as a "green" version of the Biginelli reaction.[129] The reaction was carried out by heating at 100 °C for three hours the reactants in the absence of solvent, with ammonium chloride as the catalyst. This protocol is reported to give the products in good yields, avoiding the problems associated with the use of solvents, in shorter reaction times compared with the traditional methods. Moreover at the reaction temperature of 100°C, water by-product evaporates.

Highest yields were obtained with a 0.5:1:1:1.5 ratio of ammonium chloride, aldehyde, 1,3-dicarbonyl compound and urea or thiourea.

The work-up simply involves addition of water in which the DHPMs precipitate and subsequent isolation of the products by filtration.

Under these conditions a series of aldehydes, acetoacetic esters and acetoacetamide were reacted with urea and thiourea for 3hrs to give the corresponding DHPMs. Good yields were achieved with aromatic aldehydes, either unsubstituted or bearing electron-withdrawing (entries 5, 14, 20) and donating groups (entries 6, 7), and with heteroaromatic aldehydes (entries 8, 9, 12, 13, 21).

Even the reaction of aliphatic aldehydes (entries 1 and 2) which normally proceeds to give the products in extremely poor yields under classical conditions, furnished the final heterocyclic products in 50 and 60% yields respectively.

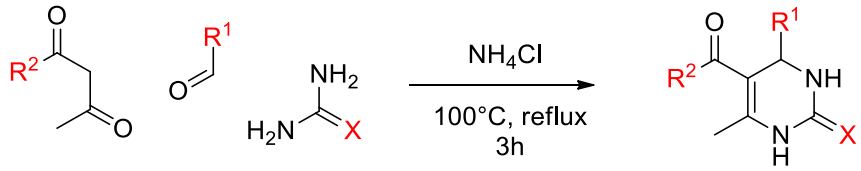

Entry	X	R^1	R^2	Product	Yield (%)
1	O	Methyl	EtO	**O1**	60
2	O	Butyl	EtO	**O2**	50
3	O	Phenyl	EtO	**O3**	92
4	O	Phenyl	MeO	**O4**	90
5	O	4-fluoro-phenyl	EtO	**O5**	70
6	O	4-hydroxy-3-methoxyphenyl	EtO	**O6**	78
7	O	4-methoxyphenyl	EtO	**O7**	72
8	O	Benzothiophen-2-yl	EtO	**O8**	85
9	O	3-benzothiophenyl	EtO	**O9**	73
10	O	2-Naphtyl	EtO	**O10**	87
11	O	1-Naphtyl	EtO	**O11**	89
12	O	2-thiophenyl	EtO	**O12**	61
13	O	3- thiophenyl	EtO	**O13**	58
14	O	2-(2-NO2- thiophenyl)	EtO	**O14**	50

15	O	Phenyl	BnO	**O15**	90
16	O	Phenyl	NH_2	**O16**	47
17	S	Phenyl	EtO	**S1**	85
18	S	Phenyl	MeO	**S2**	87
19	S	Phenyl	BnO	**S3**	85
20	S	4-fluoro-phenyl	EtO	**S4**	68
21	S	Benzothiophen-2-yl	EtO	**S5**	73
22	S	2-Naphtyl	EtO	**S6**	88
23	S	1-Naphtyl	EtO	**S7**	87
24	S	Phenyl	(-)MenthylO	**S8**	54

Table 6. *"Solvent free" Biginelli reaction.*

All the reaction products were isolated as pure crystalline solids and characterized by NMR spectroscopy. They show in the ^{1}H NMR spectrum the peak of the hydrogen linked to the C-4 that typically resonates in the range 5.0 - 5.5 ppm (Figure 26). Only in **O1-O2**, carrying an alkyl substituent at C-4, the same signal is moved upfield, around 4.0 ppm. In **O11** on the contrary, it resonates at 6.06 ppm.

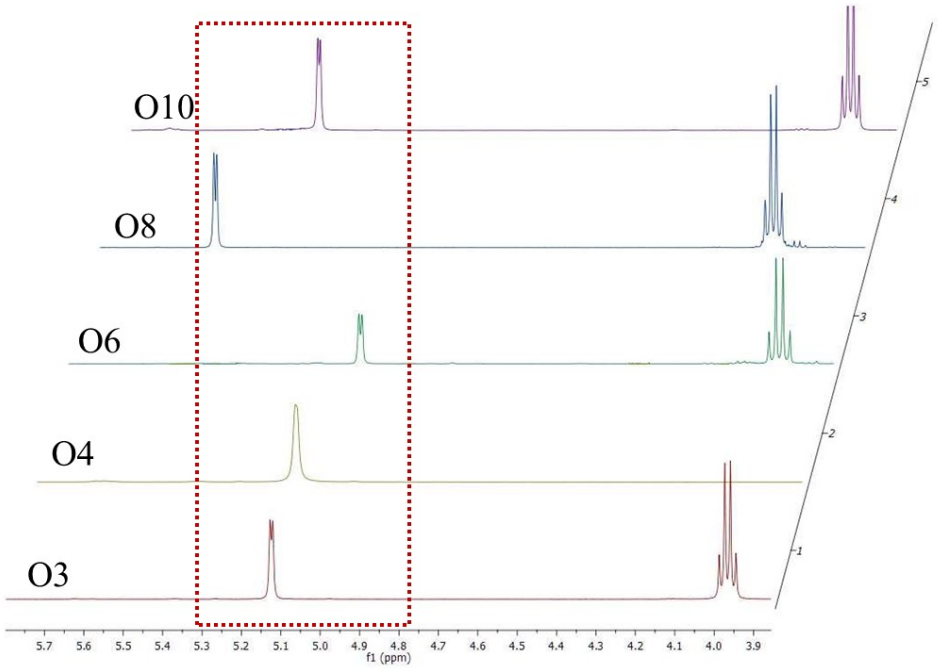

Figure 26. *^{1}H-NMR spectra of compounds O3/O4/O6/O8/O10 in the region from 3.9 to 5.7 ppm. In the red box is shown the peak of H-4 for each compound.*

The signal of the C-6 methyl group resonates near 2.25 ppm. Furthermore, from the correlation with H-4 in the COSY spectra, it is possible to identify the characteristic peak of the hydrogen N(3)-H which usually resonates between 7.3-8.0 ppm in the pyrimidinones and is shifted downfield in the range 9.6-9.9 ppm in the case of thiopyrimidinones.

Moreover, from **O15** the corresponding carboxylic acid **O17** was derived by hydrogenolysis carried out in MeOH over 10% Pd/C, at room temperature under H_2 atmophere.

In turn, the carboxylic acid **O17** was employed as the starting material for the synthesis of amides **O18**, **O19** (Figure 27), by reaction with piperidine or n-propilamine, under standard amide coupling conditions (TBTU and DIPEA (N, N-diisopropylethylamine)).

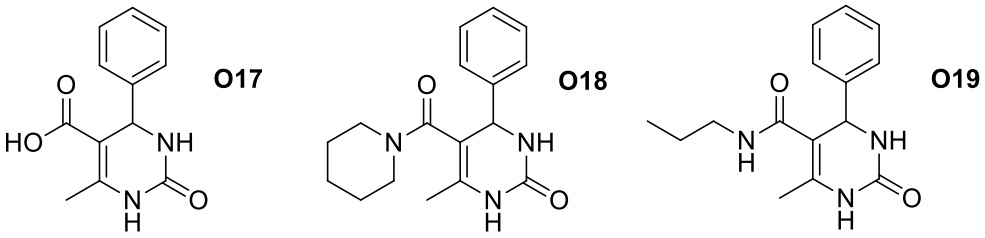

Figure 27. *Compounds O17, O18, O19.*

5.1 Biological activity assays

The *in vitro* BACE 1 inhibitory activity was determined by enzymatic Fluorescence Resonance Energy Transfer (FRET) assay.

The principle of the BACE 1 FRET assay is as follows: the protease substrate is a decapeptide connecting a fluorescence donor group (EDANS, 5- (2-aminoethylamino) naphthalene-1- sulfonic acid; Ass. 345 nm, Em. 505 nm) and a fluorescence acceptor (DABCYL, 4 - ((4-aminophenyl) diazenil) benzoic acid, abs. 505 nm), Figure 28.

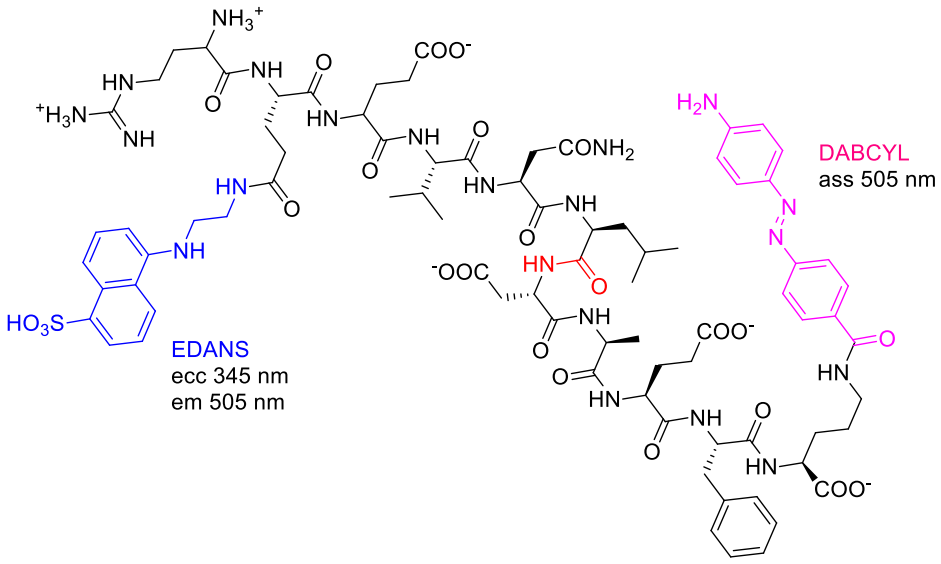

Figure 28. *Peptide substrate of the β-secretase. Scissile bond is in red.*

The distance between these two groups has been selected so that upon light excitation, the donor fluorescence energy is significantly quenched by the acceptor through resonance energy transfer. Upon cleavage by the protease, the fluorophore is

separated from the quenching group, restoring the full fluorescence yield of the donor. The increase in fluorescence is linearly related to the rate of proteolysis (blue line, Figure 29).

Upon addition of the inhibitor **N3** the fluorescence intensity stops increasing and remains constant over time. (green line, Figure 29).

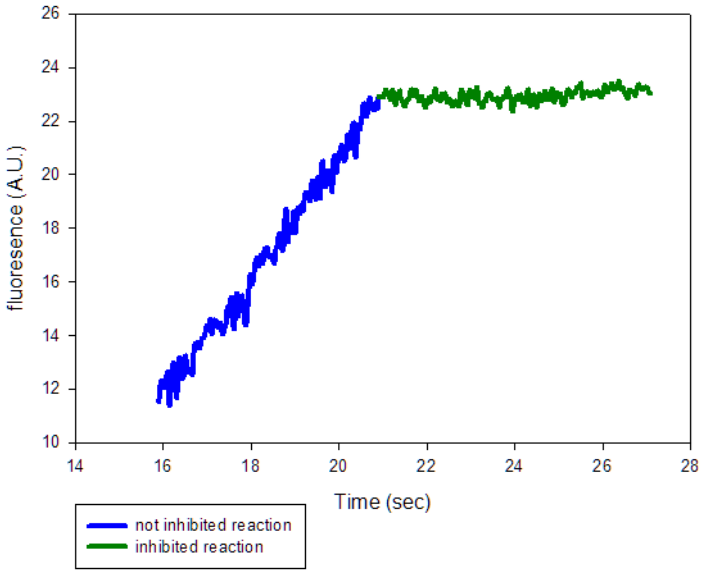

Figure 29. *Fluoresence intensity variation, Blue line: substrate + enzyme; green line: substrate + enzyme + inhibitor.*

The rate of the hydrolysis reaction is obtained by linear interpolation of the fluorescence curves and it is represented by the slope of these curve. From the relationship between the rate of the inhibited (green line) and not-inhibited reaction (blue line) is derived the residual enzyme activity, allowing the determination of the IC_{50} (the half maximal inhibitory concentration).

5.1.1 Inhibition results

The IC_{50} values were measured for the 2-oxoDHPMs (**O2-O14** and **O16-O18**) and 2-thioDHPMs (**S1, S2** and **S4-S7**). All these compounds were found to be active as BACE 1 inhibitors. Among them, **O4, O10, S4** and **S7** were found to be the most active agents, with IC_{50} ranging from 0.20 – 0.50 µM. The others all showed IC_{50} in

the micromolar range with exception of the compounds **O7**, **O9** and **O17** that were two order of magnitude less active.

Scaffold	Product	X	R^1	R^2	IC_{50}(µM)
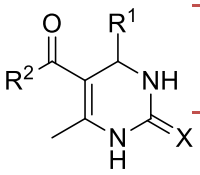	**O2**	O	Butyl	EtO	2.26±0.18
	O3	O	Phenyl	EtO	2.81±0.10
	O4	O	Phenyl	MeO	0.32±0.06
	O5	O	4-fluoro-phenyl	EtO	1.72±0.38
	O6	O	4-hydroxy-3-methoxyphenyl	EtO	0.65±0.03
	O7	O	4-methoxyphenyl	EtO	46.00
	O8	O	Benzothiophen-2-yl	EtO	1.35±0.09
	O9	O	Benzothiophen-3-yl	EtO	71.00
	O10	O	2-Naphtyl	EtO	0.51±0.05
	O11	O	1-Naphtyl	EtO	3.07±0.45
	O12	O	2-thienyl	EtO	2.20
	O13	O	3-thienyl	EtO	3.20
	O14	O	2-(2-NO_2-thienyl)	EtO	1.20
	O16	O	Phenyl	NH_2	1.60±0.03

Scaffold	Product	X	R^1	R^2	IC_{50}(µM)
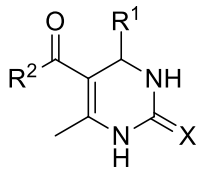	**O17**	O	Phenyl	OH	34.00±0.82
	O18	O	Phenyl	$(CH_2)_5N$	1.60±0.08
	S1	S	Phenyl	EtO	1.48±0.36
	S2	S	Phenyl	MeO	0.85±0.03
	S4	S	4-fluoro-phenyl	EtO	0.24±0.05
	S5	S	Benzothiophen-2-yl	Ethoxy	0.67±0.11
	S6	S	2-Naphtyl	Ethoxy	1.09±0.04
	S7	S	1-Naphtyl	Ethoxy	0.34±0.08

Table 7. *Determined IC_{50} for 2-oxoDHPMs (O2-O14 and O16-O18) and 2-thioDHPMs (S1, S2 and S4-S7).*

An important structural variation at the DHPM scaffold is represented by the introduction of a guanidine unit in the heterocyclic ring. Guanidine functional groups are found in numerous biologically active natural products, several drugs and drug candidates [156, 157] that include cardiovascular, antihistamine, anti-inflammatory, antidiabetic, antibacterial, antiviral, and antineoplastic drugs. The diversity in activity of these compounds likely derives, in part, from the ability of guanidinium cations to recognize receptors by a variety of noncovalent interactions, including hydrogen-bonding, electrostatic, and π-stacking associations.

[156] J. V. Greenhill, P. Lue, *Prog. Med. Chem.* **1993**, 30, 203.

[157] R. G. S. Berlinck, M. H. Kossuga, *Nat. Prod. Rep.* **2005**, 22, 516.

The guanidine-containing six-member heterocyclic structural subunit is present for example in Rosuvastatin (member of the drug class of statins), the anticancer agent Imatinib, the antibiotic sulfadiazine, and trimethoprim[158, 159] (TMP). This latter compound, initially considered as an antimalarial agent, is now known as highly effective against bacterial infections, especially in synergistic combination with sulfamethoxazole.

Also marine natural alkaloids possessing guanidine functionalities embedded in complex structural architectures are known, displaying a considerable array of biological activity and not surprisingly have attracted considerable synthetic interest.[160]

5.2 *Biginelli reaction with guanidine*

The condensation of guanidine, an aldehyde, and a β-ketoester to form the corresponding substituted 2-imino-3,4-dihydropyrimidines, is much less documented than the classical Biginelli reaction involving urea and thiourea.

Examples of Biginelli adducts of this type were described by Cho[161] and Atwal[162] as resulting from the reactions between the Knoevenagel product of ethyl acetoacetate and 3-nitrobenzaldehyde with guanidine or methylguanidine, although in low yields (14-25%).

Milcent in 1997[163] showed that yields could be improved by replacing acetyl- with benzoyl acetate $PhCOCH_2CO2Et$ as the β-ketoester. He afforded a series of 4-aryl-

---

[158] I.M. Lagoja *Chem Biodivers* **2005**, 2, 1.

[159] **a.** M. Watanabe, H. Koike, T. Ishiba, T. Okada, S. Seo, K. Hirai *Bioorg Med Chem* **1997**, 5, 437; **b.** R. Capdeville, E. Buchdunger, J. Zimmermann, A. Matter *Nat Rev Drug Discov* **2002**, 1, 493.

[160] L. Heys, C.G. Moore and P.J. Murphy *Chem. Soc. Rev.* **2000**, 29, 57

[161] H. Cho, K. Shima, M. Hayashimatsu, Y. Ohnaka, A. Mizuno, Y.Takeuchi, *J. Org. Chem.* **1985**, 50, 4227.

[162] K. S. Atwal, G. C. Rovnyak, J. Schwartz, S. Moreland, A. Hedberg, J. Z. Gougoutas, M. F. Malley, D. M. Floyd, *J. Med. Chem.* **1990**, 33, 1510.

[163] R. Milcent, J.-C. Malanda, G. J. Barbier, *Heterocycl. Chem.* **1997**, 34, 329.

3,4-dihydro-2-imino-6-phenylpyrimidines-5-carboxylate by reacting guanidine hydrochloride with the Knoevenangel adduct resulting from the other two carbonylic partners, in the presence of $NaHCO_3$ and reaction times ranging from 8 to 48 hrs (Scheme 15).

Scheme 15. *Synthesis of 4-aryl-3,4-dihydro-2-imino-6-phenylpyrimidines-5-carboxylates proposed by Milcent.*

However, in these reactions the formation of double Biginelli adducts [diethyl-2,4,6,8-tetraaryl-4,6-dihydro-1H-pyrimido-[1,2a]pyrimidine-3,7-dicarboxylates], arising from a competitive Michael type condensation between two molecules of ester and guanidine was observed (Figure 30).

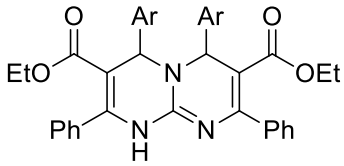

Figure 30. *Diethyl-2,4,6,8-tetraaryl-4,6-dihydro-1H-pyrimido-[1,2a]pyrimidine-3,7-dicarboxylates.*

Kappe in 2001[120] reported optimized microwaves and solvent-free conditions to use guanidine in a traditional three-component Biginelli reaction to give the cyclocondensation compounds in satisfactory yields while avoiding byproducts, but the authors claimed that the presence of the phenyl group on the ketone carbonylic function of the β-ketoester was an essential condition.

2-Imino-5-carboxy-3,4-dihydropyrimidines were described to be obtained in high yield even working with alkyl acetoacetates by the method proposed by Overman in 2006.[164] He reported a four step sequence utilizing pyrazole carboxamidine as a

[164] B. L. Nilsson and L.E. Overman, *J.Org. Chem.* **2006**, 71, 7706.

masked guanidine reactant, smoothly reacting in a Biginelli-type condensation with aldehydes and β-ketoesters.

After **N-3** Boc protection, these products were subjected to ammonolysis and acidic deprotection to generate 2-imino-3,4-dihydropyrimidines in good yields (Scheme 16).

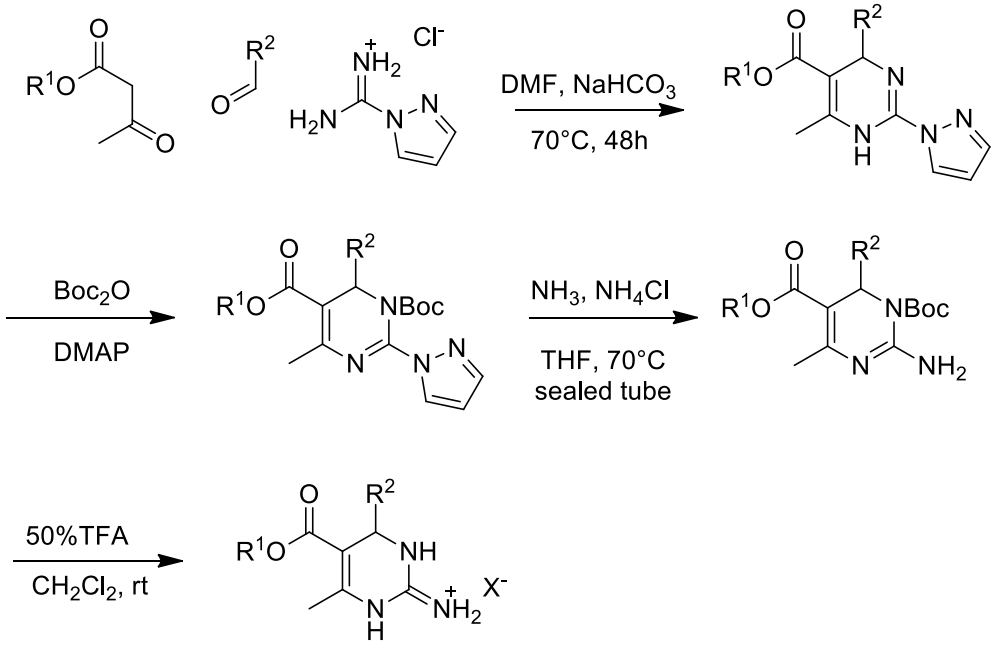

Scheme 16. *Synthesis of Biginelli-type products using the procedure proposed by Overman.*[164]

In 2009 an improved Biginelli reaction using urea/thiourea/guanidine was described using a phase transfer catalysis method.[165] Finally, multistep Biginelli/ammonolysis strategies in which isoureas or isothioureas are used as guanidine precursors to access 2-imino-3,4-dihydropyrimidines after treatment with ammonia have been described in the literature by Atwal[166] and later modified by Kappe,[167] who prepared 2-imino-3,4-dihydropyrimidines by ammonolysis of resin-bound isothiourea Biginelli adducts.

[165]B. Ahmeda, R.A. Khanb, Habibullah, M. Keshari *Tetrahedron Letters* **2009**, 50 2889.

[166]**a.** D.A. Arnold, M.G. LaPorte, S.M. Anderson, P. Wipf *Tetrahedron* **2013**, 69, 7719; **b.** K. S. Atwal, G.C. Rovnyak, B.C. O'Reilly, J. Schwartz, *J. Org. Chem.* **1989**, 54, 5898.

[167] C. O. Kappe, *Bioorg. Med. Chem. Lett.* **2000**, 10, 49.

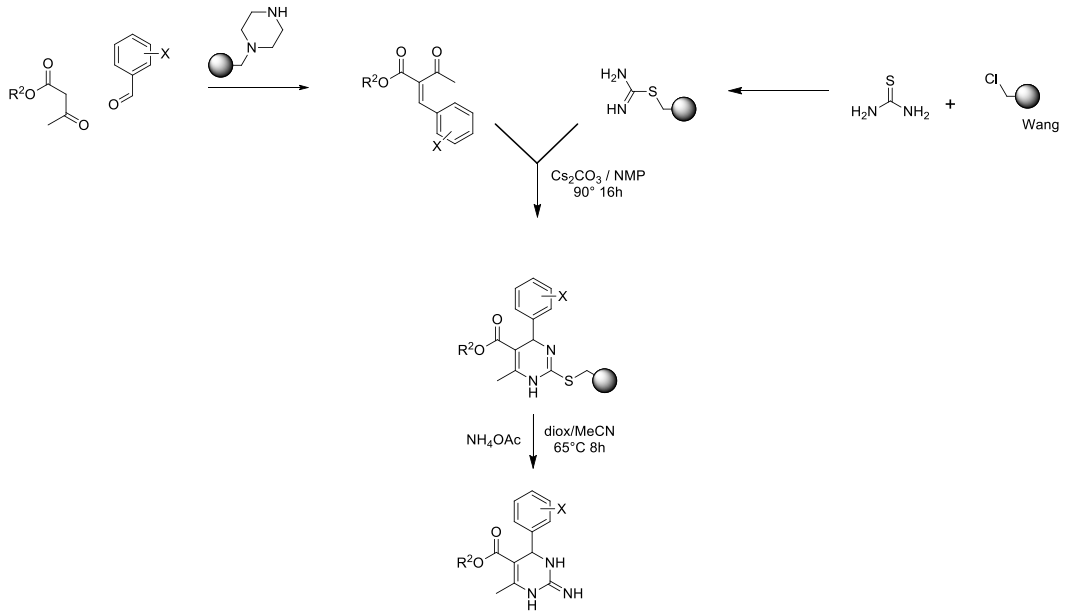

Scheme 17. *Synthesis of 2-imino-3,4-dihydropyrimidines through the procedure proposed by Kappe.*[167]

In our hands, and contrarily to what reported in the literature,[120] ethyl acetylacetate (or 1,3-dicarbonyl compound) reacted smoothly with guanidine hydrochloride and different aromatic aldehydes under the conditions (DMF, 70°C, excess $NaHCO_3$) Kappe had reported for the reaction of ethyl 2-benzoylacetate, to give the corresponding 2-imino-dihydropyrimidines (Scheme 18) [120] with very good yields, provided the reaction time did not exceeded three hours.

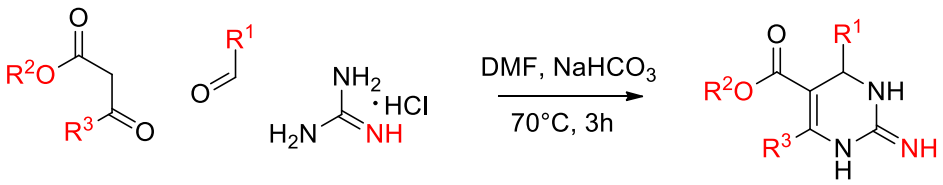

Scheme 18. *Biginelli reaction with guanidine hydrochloride (R^1 and R^2 are summarized in* Table 8*).*

More prolonged reaction times infact resulted in the formation of the double adducts (Figure 30) thus limiting the yield of the process.

Under these conditions we prepared a library of 2-imino-dihydropyrimidines **N1-N14**, that were obtained with the yields reported in Table 8, and whose structure was confirmed by spectroscopic analysis.

Product	R^1	R^2	Yield
N1	Phenyl	Ethyl	83
N2	Benzothiophen-2-yl	Ethyl	80
N3	2-Naphtyl	Ethyl	71
N4	Phenyl	Methyl	80
N5	Phenyl	Isobutyl	73
N6	Phenyl	Benzyl	47
N7	Methyl	Ethyl	40
N8	Butyl	Ethyl	53
N9	4-fluoro-phenyl	Ethyl	
N10	1-Naphtyl	Ethyl	76
N11	Biphen-4-yl	Methyl	74
N12	4-(pyridin-2-yl) phenyl	Methyl	58
N13	Benzyl	Ethyl	69
N14*	Phenyl	Ethyl	80

*R^3= Phenyl

Table 8 *Yields and IC_{50} values of 2-iminoDHPMs (N1-14)(R^3= Methyl).*

Similarly to what described for the urea- and thiourea analogs, the ^{1}H-NMR spectra (recorded in DMSO-d_6) showed characteristic peaks relative to the H-4 proton around 5.5 ppm, and the singlet of the CH_3 near 2.17-2.24 ppm. A single broad peak between 6.00 and 6.50 ppm is attributed to the N(3)-H and the hydrogen of the C=NH imino group.[120]

The carboxylic acid **N15** (Figure 31) was obtained by hydrogenolysis of the benzylester **N6**, under the reaction conditions described above for compound **O17**.

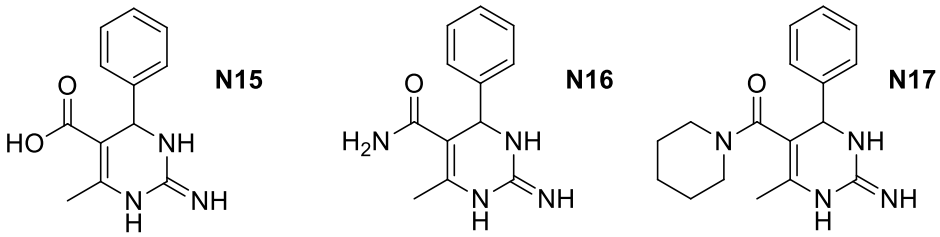

Figure 31. *Compounds N15, N16, N17.*

The amide **N16** could not be obtained by the Biginelli reaction of acetoacetamide with benzaldehyde and guanidine as under the usual conditions only the corresponding double adduct was formed quantitatively (Figure 32).

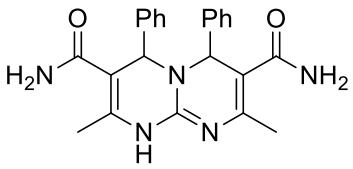

Figure 32. *Double adduct.*

For this reason we used the indirect procedure proposed by Atwal,[166b] involving the conversion of a 2-thio Biginelli cicloadduct into a 2-imino analog through a S-methylation/ammonolysis reaction (see chapter 5.7.1, d).

On the contrary, the piperidine amide **N17** could be obtained under microwave irradiation, at 120°C for ten minutes in ethanol (**N17**, Figure 31), in the presence of $NaHCO_3$.

A preliminary comparative screening run on a small series of analog 2-oxo (**O3, O8, O10**), 2-thio (**S1, S5, S6**) and 2-iminopyrimidines (**N1, N2,N3**), having the same substitution pattern revealed that the latter compounds have the highest inhibitory activity. The results are reported in Table 9, in which the IC_{50} values determined by fluorimetric assay for the DHPMs with R^1 = Ph (**O3, S1, N1**), R^1 = benzothiophenyl (**O8, S5, N2**) and R^1 = 2-naphtyl (**O10, S5, N2**) are compared.

R^1	Scaffold	IC_{50} (μM): X		
		O	**S**	**N**
Phenyl	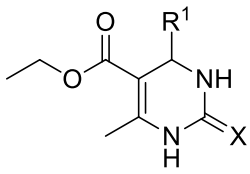	2.81±0.10(**O3**)	1.48±0.36(**S1**)	0.53±0.09(**N1**)
Benzothiophen-2-yl		1.35±0.09(**O8**)	0.67±0.11(**S5**)	0.30±0.05(**N2**)
2-Naphtyl		0.51±0.05(**O10**)	1.09±0.04(**S6**)	0.19±0.05(**N3**)

Table 9. *Comparison of IC_{50} values between the 2-oxo,2- thio and 2-iminoDHPMs.*

Even in these cases, the inhibition values are all in a sub-micromolar range (**N1, N2, N3**, Table 9).

The behaviour of the oxygen and sulphur compound is not linear, infact **O10** (R^1 = 2-naphtyl, IC_{50} = 0.51±0.05 μM) shows a better inhibition activity than the corresponding 2-thioDHPMs **S6** (R^1 = 2-naphtyl;1.09±0.04 μM), but the same trend is not observed when comparing compounds **O3** (R^1 =Phenyl) with **S1** (R^1 =Phenyl) and **O8** (R^1 = Benzothiophen-2-yl) with **S5** (R^1 = Benzothiophen-2-yl) respectively Interestingly, it is possible to observe that in each triad the 2-iminoDHPMs are always more active than the oxygen and thio analogs, and in this series the compound **N3**, bearing a 2-naphthyl group at position C4 proved the most active (IC_{50} = 0.19±0.05μM).

5.3 Crystallographic structures of BACE1-inhibitor complexes present in PDB

In order to rationalize these results we studied the crystallographic structures of non peptidomimetic BACE 1-inhibitor complexes present in the Protein Data Bank. This study was run on 302 crystallographic structures that were organized in four groups according to the presence of urea, thiourea, amidine and guanidine motives in their structure.

No inhibitors having a thiourea unit and only 13 based on the urea group were found in the PDB. On the contrary, 62 molecules having the guanidine and 60 the amidine group have emerged by this research, and they are reported to have a higher inhibition activity than the oxo compounds (Figure 33).

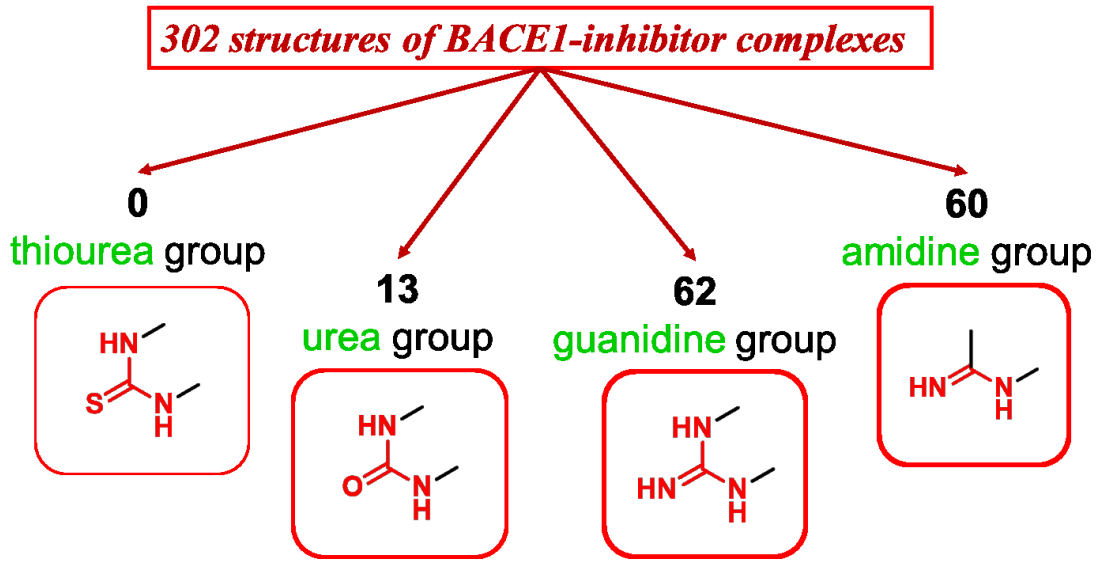

Figure 33. *Non peptidomimetic BACE 1-inhibitosr organized in four groups according to the presence of urea, thiourea, amidine and guanidine motives in their structure.*

In the following table (Table 10) are shown some representative members belonging to each collection.

Inhibitor	pdb	IC_{50}(μM)	Group	Subgroup
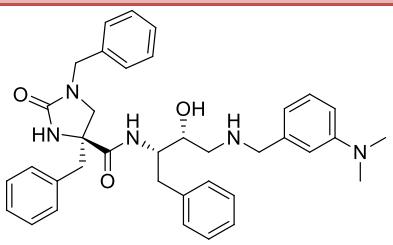	3CKR	5.000	urea	2-Imidazolidinone
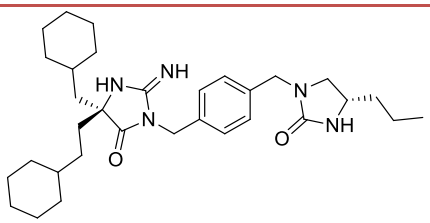	3L5E	0.027	guanidine	2-Iminoimidazolidinone
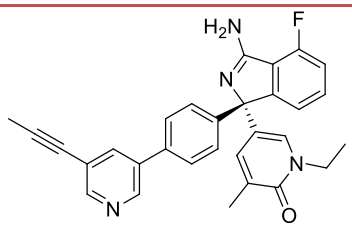	4B00	0.0025	amidine	2-Aminopyrrole

Table 10 *Three BACE-1 inhibitors of known BACE-1 complexes based on urea, guanidine and amidine unit.*

The crystallographic structures of these ligands, complexed with BACE 1 active site, showed that the amidine and guanidine motive interacts with the enzyme pocket through a stable network of 4 H-bonds with the catalytic aspartates. At the working pH of the enzyme (4-5) probably the iminic nitrogen is protonated, as well as one of the aspartic groups. In Figure 34 and Figure 35 are represented the weak interactions between the enzyme and two selected inhibitors, namely BDV and I6X (corresponding to the pdb file: 3L5E and 4B00, that were found to be among the most active (3L5E, IC_{50}= 0.027 μM; 4B00, IC_{50}=0.0025 μM).

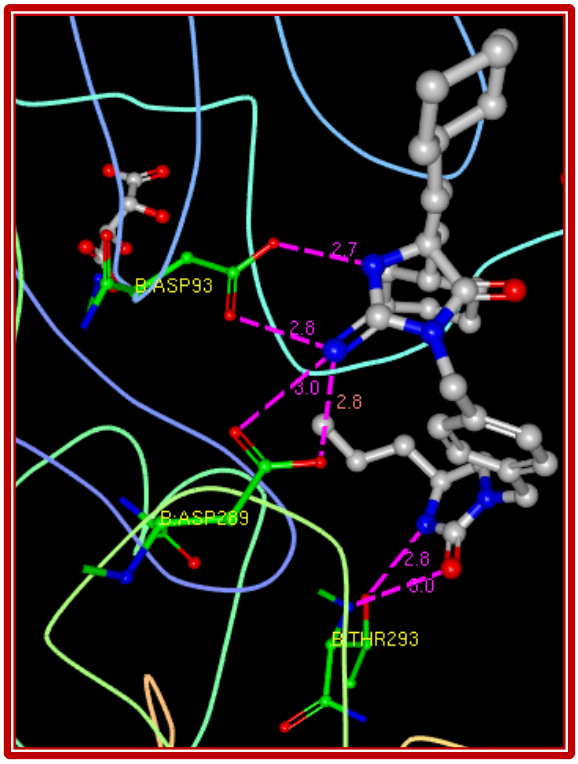

Figure 34. *BACE 1/ BDV complex (pdb file: 3LCE): H-bonds interactions in pink (guanidine group).*

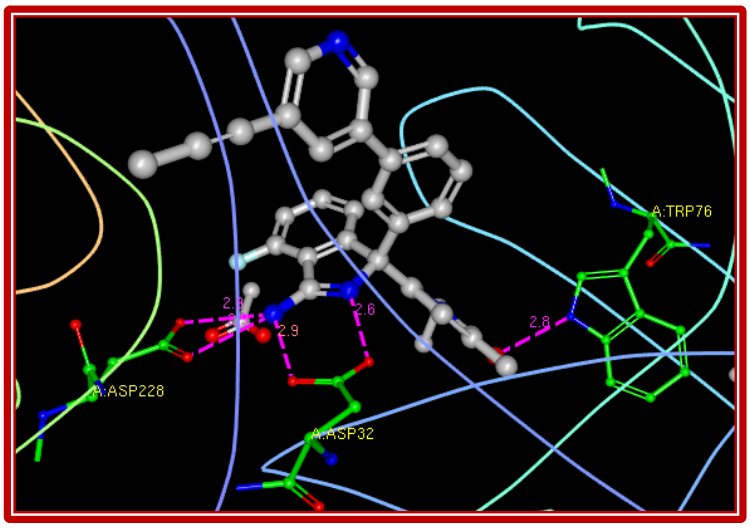

Figure 35 *BACE 1/ I6X complex (pdb file: 4B00): H-bonds interactions in pink (amidine group).*

An analogous array of hydrogen bonds is not allowed with the –NHCONH- group that is not protonated at the same pH value. Another structural feature of these inhibitors is the “butterfly shape” with two large substituents pointing towards opposite directions, and therefore filling the two large hydrophobic pockets of the

enzyme binding site. Figure 36 and Figure 37, show each the structures of five overlapped inhibitors having IC_{50} from 0.008 to 0.0003 µM. (pdb files: 4rcf 4wtu 4rce 4b00 4frk (Figure 36) and 4djy 4frs 4h1e 4h3f 4h3g 4h3i (Figure 37).

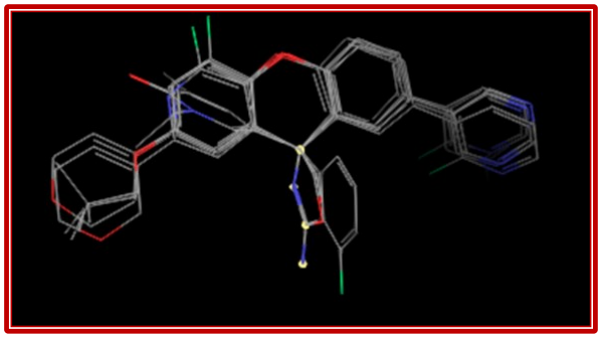

Figure 36 *Superimposition of 5 inhibitors of BACE 1*
(PDB files 4rcf 4wtu 4rce 4b00 4frk , IC_{50} 0.003, 0.003, 0.002, 0.003, 0.008µM)-guanidine group.

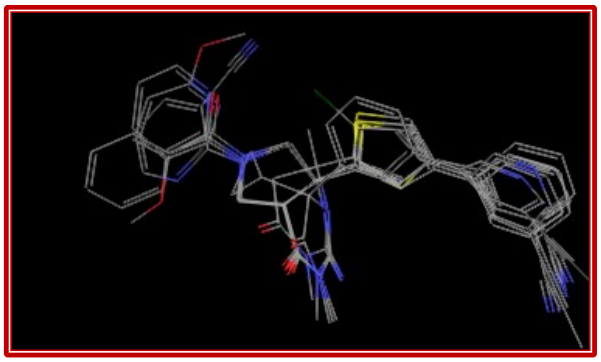

Figure 37. *Superimposition of 5 inhibitors of BACE 1*
(PDB files 4djy 4frs 4h1e 4h3f 4h3g 4h3i, corresponding IC_{50} 0.005, 0.002, 0.003, 0.001, 0.006, 0.003 µM)-amidine group.

5.4 Structure –activity relationship: 2-iminoDHPMs and BACE1

To gain a deeper insight into the relationship between the structure and activity of the 2-iminoDHPMs, we extended our studies to the other 2-iminoDHPM, bearing different R^1, R^2, and R^3 substituents.

Product	R^1	R^2	Yield	IC_{50}(µM)
N1	Phenyl	EtO	83	0.50±0.1
N2	Benzothiophen-2-yl	EtO	80	0.30±0.1
N3	2-Naphtyl	EtO	71	**0.20±0.1**
N4	Phenyl	MeO	80	0.50±0.1
N5	Phenyl	i-PrO	73	1.06±0.19
N6	Phenyl	BnO	47	Inactive
N7	Methyl	EtO	40	/
N8	Butyl	EtO	53	1.06±0.19
N9	4-fluorophenyl	EtO	70	0.30±0.14
N10	1-Naphtyl	EtO	76	1.50±0.1
N11	Biphen-4-yl	MeO	74	4.65±0.68
N12	4-(pyridin-2-yl) phenyl	MeO	58	0.72±0.13
N13	Benzyl	EtO	69	/
N14*	Phenyl	EtO	80	0.28±0.19
N15	Phenyl	OH	50	0.69±0.05
N16	Phenyl	NH_2	57	2.15±0.82

* R^3= Phenyl

Table 11. *Yields and IC_{50} values of 2-iminoDHPMs (N1-14).*

The effect of the structural variations at the heterocyclic scaffold can be synthetized as follows:

a) Effect of the variation of the ester function: It is possible to observe that the variation at the alkoxy group of the ester function in going from methoxy (**N4**) to ethoxy (**N1**) to isobutoxy (**N5**) does not affect the inhibition activity, which remains in the order of sub-micromolar; by further extending the size

of the alkoxy group as in the benzylester **N-6**, no inhibitory activity was observed. IC_{50} for the carboxylic acid **N15** was found to be of the same order as the methyl and ethylesters **N1** and **N4**, while a lower inhibitory activity was measured for **N16**.

b) Effect of the C4 substituent: Considering **N1** as the a reference compound (IC_{50} = 0.50±0.1 μM), a decrease in the activity was shown when the phenyl substituent at C-4 was replaced by an alkyl group, as in **N7**, R1 = methyl, and **N8**, R2 = butyl.). On the contrary an increase in the inhibitory activity was observed when a fluorine atom was present on the aromatic group at C4 in para position (**N9**). Larger aromatic groups, as benzothiophen-2-yl (**N2**), and 2-naphtyl (**N3**, IC_{50} = 0.2μM) increased the activity but with 1-naphtyl (**N10**), biphen-4-yl (**N11**), 4-(pyrid-2-yl)phenyl (**N12**) the activity decreased. The difference in activity between **N3** and **N10** shows that the orientation of the large aromatic with respect to the dihydropyrimidine group plays a role, and the result observed with **N11** and **N12** suggests the presence of a tight pocket in which groups with larger rotational freedom are less favourably accommodated.

The increased activity in going from **N11** (biphen-4-yl) to **N12** (4-(pyridin-2-yl) phenyl) indicates that the presence of the nitrogen atom on the pyridyl group could favour the interaction with the binding site trough additional hydrogen bonds.

c) Effect of substituent at C-6: All compounds shown carry a methyl group at C-6. A dihydropyrimidinone was synthetized with R^1 = Ph, R^2 = Et, and carrying a Ph substituent at C-6 (**N14**). This variation was found to not significantly affect the inhibitory activity that is slightly higher (IC_{50} 0.28 μM).

A point of interest concerning small inhibitors of BACE 1 is the permeability across Blood Brain Barrier, that was estimated for some representative DHPMs by PAMPA test.

5.5 BBB Permeability test: In vitro PAMPA (Parallel Artificial Membrane Permeability) assay

The drug's penetration into the BBB at therapeutic concentrations is one of the major problem in the pharmacological treatment of central nervous system (CNS) diseases. The BBB is a complex semipermeable barrier between blood and the CNS. It strictly controls the exchanges between the brain and blood compartments.[168] The endothelial cells are the main unit of this "wall"; they protect the CNS from endogenous materials which could damage it, and this is why they are located in such a way as to have tight junctions between them.[169] The majority of CNS drugs enter the brain by transcellular passive diffusion, due to the tight junction structure and limited transport pathways. At the early drug discovery stage, evaluation of ADME (Absorption, Distribution, Metabolism, Excretion) properties is of crucial importance to reduce attrition in development process. Parallel Artificial Membrane Permeability Assay (PAMPA) is a high throughput technique developed to predict passive permeability through biological membranes. We used the PAMPA-BBB method described by Di et al, to determine the ability of a few compounds to penetrate into the brain.[170] The assay employs a brain lipid porcine membrane. Through the equation below it is possible to determine the permeability of drugs (Equation 1).

$$P_e = \frac{Vd \times Vr}{(Vd+Vr)St} \; Ln \; \frac{100\,Vd}{100Vd - \%T(Vd+Vr)}$$

Equation 1 *Equation for the determination of the permeability in the PAMPA assay (in brakets are reported the experimental values used)*

[168] F. L. Cardoso, D. Brites, M. A. Brito, *Brain Res. Dev.*, **2010**, 64, 328.

[169] J. Van Asperen, U. Mayer, O. Van Tellingen, J. H. Beijnen, *J. Pharm. Sciences*, **1997**, 86, 881

[170] L. Di, E. H. Kerns, K. Fan, O. J. McConnell, G. T. Carter *Eur. J. Med. Chem.*, **2003**, 38, 223.

At first, the method was validated by comparing reported permeability values of commercial drugs (listed in Table 12) with experimental data. Figure 38, the shows the good correlation between experimental and reported values, IS (R^2= 0.898).

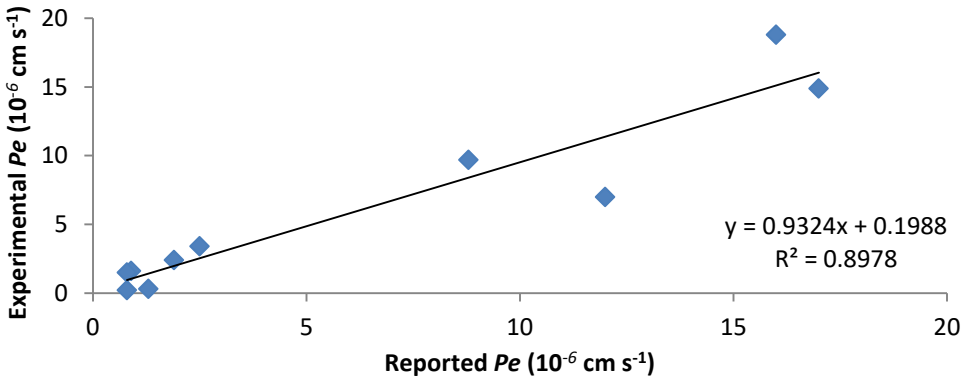

Figure 38 *Linear correlation between experimental and reported permeability data, of PAMPA-BBB assay, of commercial drugs (reported in table).*

From Equation 1 and following the pattern established in the literature for BBB permeation prediction[171] we could classify compounds as CNS+ when they present a permeability > $3.9 \cdot 10^{-6}$ cm s^{-1} and CNS– when they present a permeability < $2.1 \cdot 10^{-6}$ cm s^{-1}.

Based on these results we can consider that compounds **O10, S6** and **N3** are able to cross the BBB by passive permeation (Table 12), with expected decreasing permeability in going from **S10** to **O10** to **N3**.

[171] P. Crivori, G. Cruciani, B. Testa, *J. Med. Chem.,* **2000**, 43, 2204.

Compound	Bibl.170	*Pe* (10^{-6} cm s^{-1})[c]	Prediction
Atenolol	0.8	0.2 ± 0.3	**CNS -**
Caffeine	1.3	0.3 ± 0.2	**CNS -**
Desipramine	12	7.0 ± 0.4	**CNS +**
Enoxacin	1.6	0.4 ± 0.1	**CNS -**
Hydrocortisone	2.4	1.0 ± 0.3	**CNS -**
Ofloxacine	0.8	1.5 ± 0.2	**CNS -**
Piroxicam	2.5	3.4 ± 0.4	**CNS +**
Promazine	8.8	9.7 ± 1.1	**CNS +**
Testosterone	17	14.9 ± 0.6	**CNS +**
Verapamil	16	18.8 ± 0.1	**CNS +**
O10	/	8.3 ± 0.3	**CNS +**
S6	/	9.8 ± 1.0	**CNS +**
N3	/	6.9 ± 3.5	**CNS +**

[a]PBS:EtOH (70:30) was used as solvent. [b]Data are an average ± SD of two independent measurments.

Table 12 *Permeability (Pe 10^{-6} cm s^{-1}) in the PAMPA-BBB assay for 10 commercial drugs (used in the experiment validation) and **O10**, **S6**, **N3** with their predictive penetration in the CNS.*[a]

5.6 Docking experiment

Small, non-peptidic inhibitors as those that inspired our work, have only a minority of the interactions found on the OM99-2 complex (Chapter 4), but nevertheless, the affinity is fully conserved if not improved, as in the case of the 2-amino-3,4-dihydroquinazoline described by Baxter and colleagues in 2007 (Figure 39). [172]

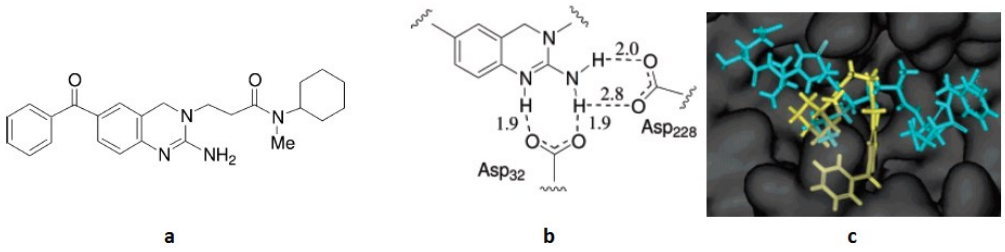

Figure 39. *a: structure of the Baxter's inhibitor; b: its network of interactions with the catalytic aspartyl residues; c: overlay of its complex with BACE-1 and the complex of OM99-2, showing that the N-cyclohexyl substituent lies inside the S1 subsite (pdb id. 2Q15).*[172]

The guanindine-like structure of the inhibitor allows to establish a full network of interactions with the catalytic aspartyl residues, both by hydrogen bonding and charge complementarity. In order to fill the S1 subsite, the chain connecting the core of the molecule with the cyclohexyl ring is folded in order to allow the hydrophobic end to fill into subsite S1'. No other subsites are involved in the interaction, and the side of the inhibitor sticks out the substrate channel forcing the flap to change its conformation to a more open one.

In order to obtain a preliminary indication on the interactions of our inhibitors with BACE-1, we have built several computational models by a molecular dynamics – based docking protocol. The crystallographic structure of the BACE-1-Baxter inhibitor was chosen as our starting point, and several models were obtained for inhibitors of the guanidine series. The set comprises both the R and S enantiomers of the most active compound, **N3**, and the R enantiomers of its 6-phenyl analogue (**N18**), of the compound **N10**, of **N1** and of its 6-phenyl analogue **N14**. To build the models, file 2Q15 was downloaded from the Protein Data Bank, and after adding all

[172] E. W. Baxter, A. K. Conway, L. Kennis, F. Bischoff, M. H. Mercken, H. L. De Winter, C. H. Reynolds, B. A. Tounge, C. Luo, M. K. Scott, Y. Huang, M. Braeken, S. M. A. Pieters, D. J. C. Berthelot, S. Masure, W. D. Bruinzeel, A. D. Jordan, M. H. Parker, R. E. Boyd, J. Qu, R. S. Alexander, D. E. Brenneman, and A. B. Reitz J. Med. Chem. **2007**, 50, 4261.

the hydrogens including the polar ones (setting the pH to 5), the structure was relaxed by an energy minimization of 50000 steps of steepest descent method, keeping first frozen the protein backbone and then allowing the whole structure to relax. The minimization was carried out with the OPLS3 forcefield [173] as implemented in the Schrödinger suite. [174] The ligands were then manually docked inside the enzyme and a starting geometry was obtained by superimposing the guanidine group of each inhibitor onto that of the Baxter inhibitor in the relaxed structure of its model. At least two starting models for each inhibitor were obtained by different superimposition ways. The starting models of each inhibitor-BACE1 complexes were then thermalized by a molecular dynamic run carried out in the NTP ensemble at 300 °K for 100 ns. The dynamics outcomes were then analyzed, and the lowest energy conformation for each run was chosen for the final optimization of the complexes, carried out as described above for the initial one, but using the conjugate gradient optimization algorithm. Binding energies were calculated according to eq. 2.

$$\Delta E_b = E_{EI} - E_E^0 - E_I^0 \quad eq\ 2$$

Where E_{EI} is the OPLS3 energy of the optimized enzyme – inhibitor complex, E_E^0 is the OPLS3 energy of the empty enzyme after relaxation down to its closest energy minimum (chosen as the same for each model), and E_I^0 is the OPLS3 energy of the free ligand in its absolute minimum energy conformation as obtained from a conformational search. In this preliminary study all the optimizations were carried out in vacuo and no solvation effects were carried into account. The resulting binding energies are reported in Table 13.

[173] E. Harder, W. Damm, J. Maple, C. Wu, M. Reboul, J.Y. Xiang, L. Wang, D. Lupyan, M.K. Dahlgren, J.L. Knight, J.W. Kaus, D.S. Cerutti, G. Krilov, W.L. Jorgensen, R. Abel, R.A. Friesner, *J. Chem. Theory Comput.*, **2015**, DOI: 10.1021/acs.jctc.5b00864

[174] Schrödinger Release 2016-4**:** Maestro, Schrödinger, LLC, New York, NY, 2016.

Inhibitor	Experimental IC_{50}* (nM)	Rel ΔE_b** (Kcal mol^{-1})
R-N3	200	0
S-N3		5.2
R-18	/	-1.5
R-N10	150	5.6
R-N1	500	2.3
R-N14	300	2.3

Table 13. **racemic mixture. **relative to the binding energy of R-N3.*

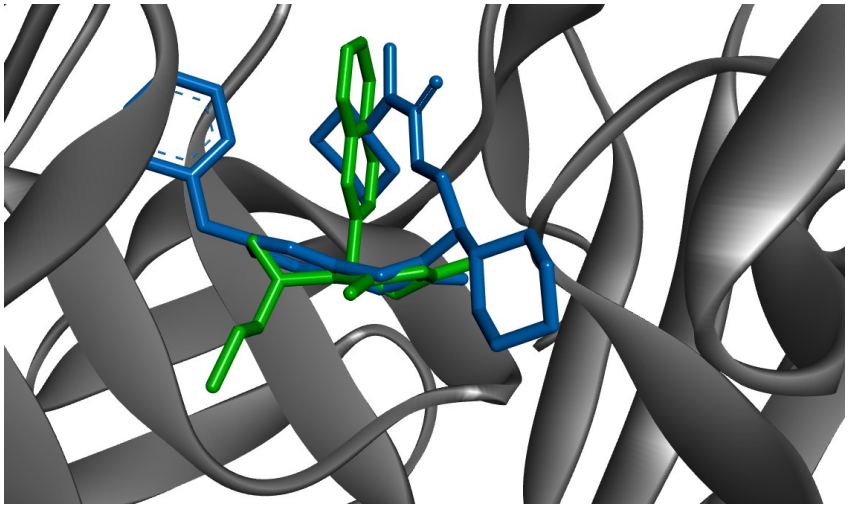

Figure 40. *overlay of the crystal structure of the complex of BACE with the Baxter inhibitor (blue) and the best calculated pose of R-N3 (green).*

Inhibitor **R-N3** ranks second in binding energy within the series, and its pose inside the catalytic site resembles strictly that of the Baxter inhibitor (Figure 40), with the 2-naphtyl group well placed inside S1.

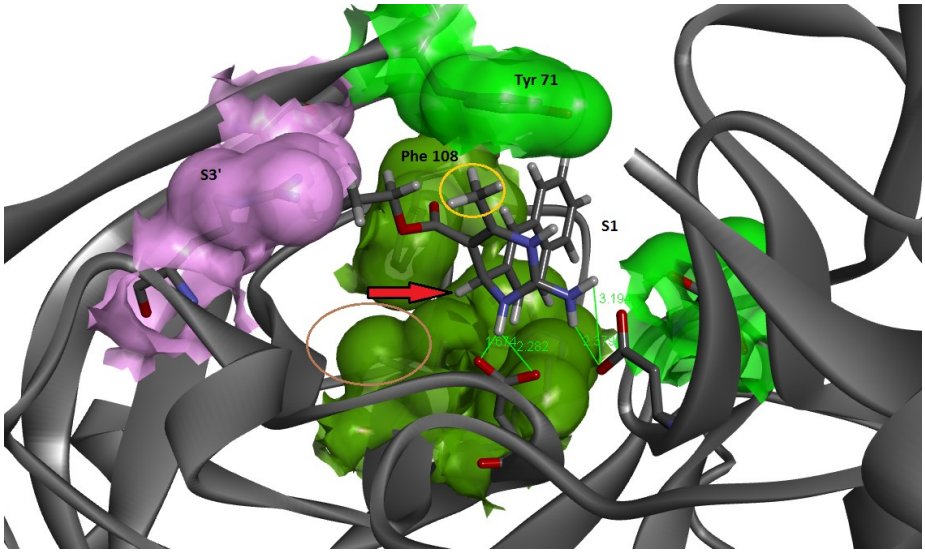

Figure 41. *the best pose of R-N3 and its interactions. Green surfaces: Connoly surface of subsite S1; pink surface: Connoly surface of subsite S3'; red arrow: the pro-S hydrogen of the inhibitor; yellow circle: the 6-methyl group of the inhibitor; brown circle: the empty area of S1'-S2'.*

The main interactions of R-N3 are shown in Figure 41. The guanidinium system interacts with the two aspartyl residues in a very good fashion, and a full network of hydrogen bonds could be established, resembling that of the Baxter inhibitor. The 2-naphtyl group is at hydrophobic contact distance with most of the residues of S1, namely Phe 108, Tyr 71 on the upper flap, Leu 30, Trp 115 and Ile 118 at the bottom of the subsite. The ethyl ester group of the inhibitor points towards the surface of S3', with some minor clashes that lead to a certain change in the local conformation of the flap (likely causing a decrease in the affinity).

The S-enantiomer of the same inhibitor is predicted to bind less favorably. Actually none of the poses of this molecules lead to optimal interactions. The pro-S hydrogen of the inhibitor (red arrow in Figure 41) points towards a very unfavorable position, and its replacement with the 2-napthyl group leads to severe bumping with the bottom residues of S1. Any solution to this bumping leads to a loss in binding energy, either at the aspartyl residues level, either at S1 subsite which cannot be filled by the napthyl group in the same way as in the R-enantiomer. The observed activity of the racemic mixture on N3 is thus likely due to the R-enantiomer alone.

Having therefore established that the R-enantiomer allows the better interaction, the analyses on the other compounds were carried out on the same configuration only.

The 1-naphtyl analogue of **R-N3**, **R-N10** is about one order of magnitude less active, and its predicted binding energy is coherently less favorable. In this case, the different orientation of the aromatic system makes impossible to keep at the same time the interactions of the guanidinum system and those at S1 without clashes with Tyr 71.

R-N1, with a phenyl ring replacing the naphtyl moiety, is found inside the catalytic site almost in the same pose of **R-N3**, and its slightly minor activity can be simply explained by the reduced amount of hydrophobic surface in contact with S1.

The other two compounds in the series bear a phenyl ring at position 6, where a methyl group is found in **R-N3** (yellow circle in Figure 41). This position points mostly outside, and the phenyl rings of compounds **N18** and **N14** remains partly exposed to the solvent. However, they can establish two very favorable interactions, namely a π-stacking with Tyr 71 and a cation-π stacking with Arg 128 on the other side, without affecting the overall pose of the molecules, and this can explain the good measured affinity of these compounds (Figure 42).

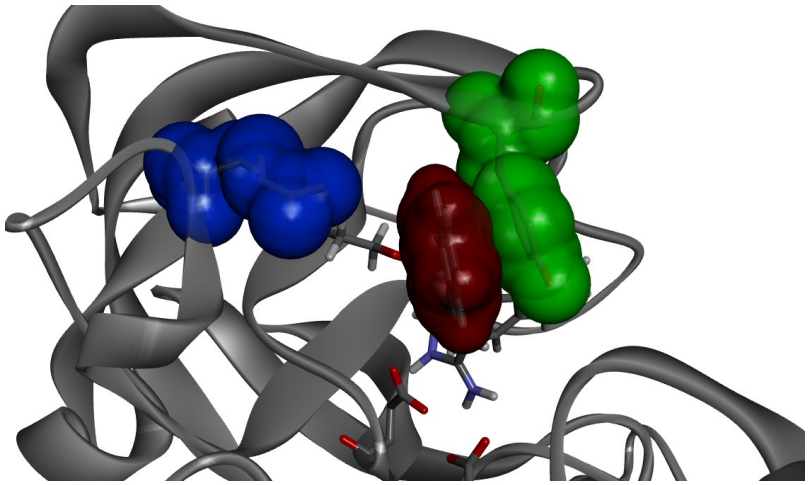

Figure 42. *the extra π-stacking and cation- π interactions of inhibitor R-N18 (red surface) with Tyr 71 (green surface) and Arg 128 (blue surface).*

Finally, we note that it seems difficult to place on the core of our molecules some group capable to bring extra interactions at the S1'-S2' level (brown circle in Figure 41) without affecting the other interactions. It is also difficult to carry out a rational design to solve this problem, as the available IC_{50} data on the whole series of compounds prepared in this thesis span on a rather narrow range of affinities. This

makes them poorly significant as candidates for a training set, and a calibration curve of a quantitative model built only on the knowledge of such compounds would lead to very large errors in the predicted affinity of novel compounds. However, from the inspection of the models, it seems that the only way to reach the S1'-S2' region would be via a flexible chain at C5. This could be eventually obtained by replacing the ester moiety with an aliphatic ketone one.

Following this study we planned to run the synthesis and the evaluation of the inhibitory activity for the individual enantiomers of DHMPs .

5.7 Approaches to the synthesis of enantiomeric 2-iminoDHPMs

Possible pathways reported for the obtainment of 2-oxo and 2-thiooxoDHPM enantiomers are shown in Scheme 12, Scheme 13, Scheme 14, comprising chemical and enzymatic resolution, use of substrate-based chiral auxiliary reaction and organocatalysis, that were already mentioned in the introduction.

The obtainment of 2-iminopyrimidines in enantiomeric form is not documented to our knowledge, apart from a single example in which an optically pure thiopyrimidinone was converted into the related chiral 2-pyrrolidinoguanidine through S-methylation followed by ammonolysis.[175]

In the last part of this PhD thesis, we describe some preliminary approaches to the synthesis of chiral 2-iminopyrimidines as single enantiomers.

Following what reported in the literature for the analog 2-oxo and 2-thioderivatives, some attempts were made to obtain the reference compound 2-iminoDHPM **N1** (R^1 = Ph) as a single enantiomer.

5.7.1 Asymmetric substrate-based Biginelli reaction

For the synthesis of DHMP in optically pure form, we considered first the effect of a chiral β-ketoester on the Biginelli reaction. When (-)-menthyl and (-)-borneylacetoacetate were reacted with guanidine hydrochloride and benzaldehyde under the optimized conditions described above,[120] the expected Biginelli-type

[175] J.-P. Wan, Y. Lin and Y. Liu. *Curr.Org.Chem*. **2014**, 18, 687.

guanidines were obtained as diastereoisomeric mixtures with 20% and 10% d.e. respectively, as determined by integration of the appropriate distinguishable signals in the ^{1}H NMR spectra (Figure 43). Chiral acetylacetate were prepared by boric acid mediated transesterification reaction of ethyl acetoacetate with (-) – menthol (-) - borneol[176]

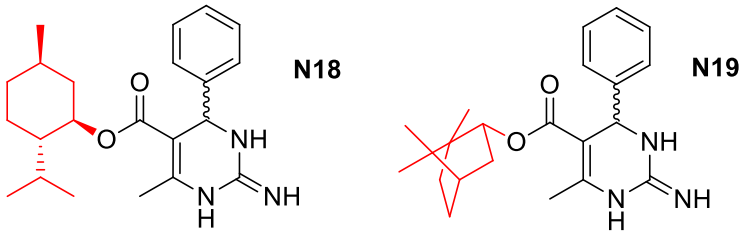

d.e. = diasteroisomeric excess

Figure 43. *Compounds N18 and N19.*

The diastereoisomers could unfortunately not be separated by cristallization or by chromatographic techniques.

5.7.2 Resolution methods

a) Classical chemical resolution by formation of diastereoisomeric salts

The presence of the basic guanidine substituent was exploited for the formation of diastereoisomeric salts, by reaction with an optically active enantiopure carboxylic acid. Mandelic, acetylmandelic, Mosher, and tartaric acid were used but none of them afforded the expected salts in a crystalline, separable form.

Alternatively, we envisaged that a Biginelli compound with a free acidic group could serve as a suitable starting material for a resolution by reaction with a chiral amine. The carboxylic acid (**N15,** Figure 44), not described in the literature, was obtained by hydrogenolysis of the corresponding benzyl ester (**N6**) over 10% Pd/C, carried out in MeOH overnight at room temperature under atmospheric H_2 pressure.

[176] G.C.M. Kondaiah, L.A. Reddy, K.S. Babu, V.M. Gurav, K.G. Huge, R. Bandichhor, P.P. Reddy, A. Bhattacharya, R.V. Anand, *Tetrahedron. Lett.*, **2008**, 49, 106.

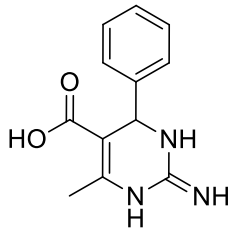

Figure 44 *Compound N15.*

However, subsequent reaction with (R)-(+)-α-phenylethylamine and (+) or (-)-cinchonine did not afford any product prone to crystallization.
Alternatively, a classic chemical resolution with formation of diastereoisomeric compounds was tried, by the use of suitable chiral auxiliaries to append to the 2-iminopyridines, as described in the following paragraph.

b) Classical chemical resolution by formation of diastereoisomeric compounds

Following a procedure suggested by Singh[138] for the chemical resolution of enantiomers of 3,4-dihydropyrimidin-2(1H)-ones (see chapter 4), we reacted the enantiopure (2S)-3-phenyl-2-phthalimidylpropanoyl chloride (**8a**) derived from phenylalanine, with **N1** (Scheme 19). In the literature procedure this reaction occurs, after lithiation with BuLi at N-1 affording N-acylated diastereomeric DHPMs, which after chromatographic separation and removal of the chiral auxiliary by $LiAlH_4$ furnished both enantiomers of DHPMs.

Considering the basic nature of the guanidine group we run this reaction directly on the substrate (**N1**) at room temperature, in the presence of an equimolar amount of Et_3N. Acylation occurred at **N3** with formation of the corresponding product as diastereoisomeric 1:1 mixture, that did not resolve on TLC nor on chromatographic column.

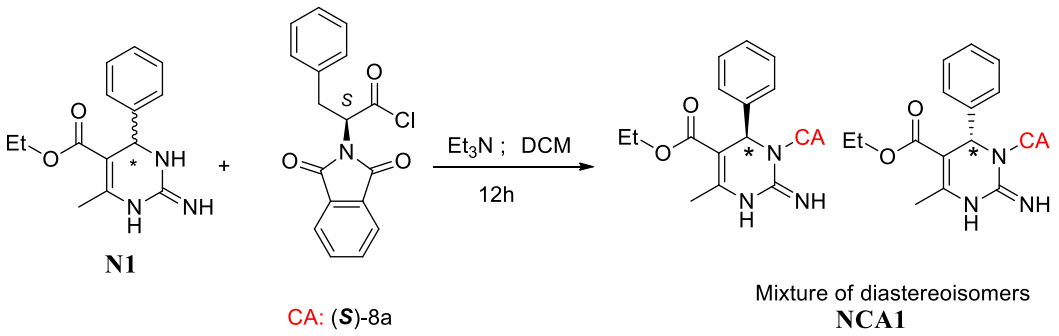

Scheme 19. *Synthesis of NCA1.*

N-3 acylation was attempted on the protected guanidine (**NP1**), described by Overman.[164] This 5-ethoxycarbonyl-6-methyl-4-phenyl-3,4-dihydropyrimidin-2(1H-pyrazol-1-yl)-imine was described to be quite easily N-Boc protected at N-3 by reaction with Boc_2O under standard condition. This suggested us the possibility to employ an enantiopure acid chloride as the electrophile to acylate this position, with formation of diastereoisomeric derivatives. NP1 was quantitatively obtained by reacting the masked guanidine 1*H*-Pyrazole-1-carboxamidine hydrochloride in a Biginelli type reaction in DMF at 70°C with $NaHCO_3$ to give **NP1** quantitatively (Scheme 20).

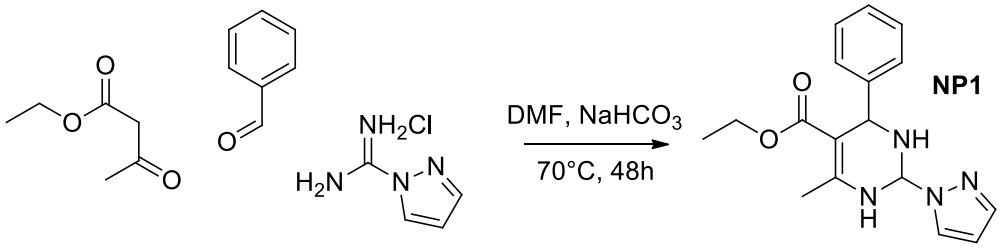

Scheme 20. *Synthesis of NP1.*

NP1 was reacted with the three different chiral auxiliaries **8a**, **8b** and **8c** (Scheme 21).[137] The reaction of NP1 with **8a** gave a diasteroisomeric mixture in a 1:1 ratio (**NPCA1)** that could unfortunately not be separated by chromatography.

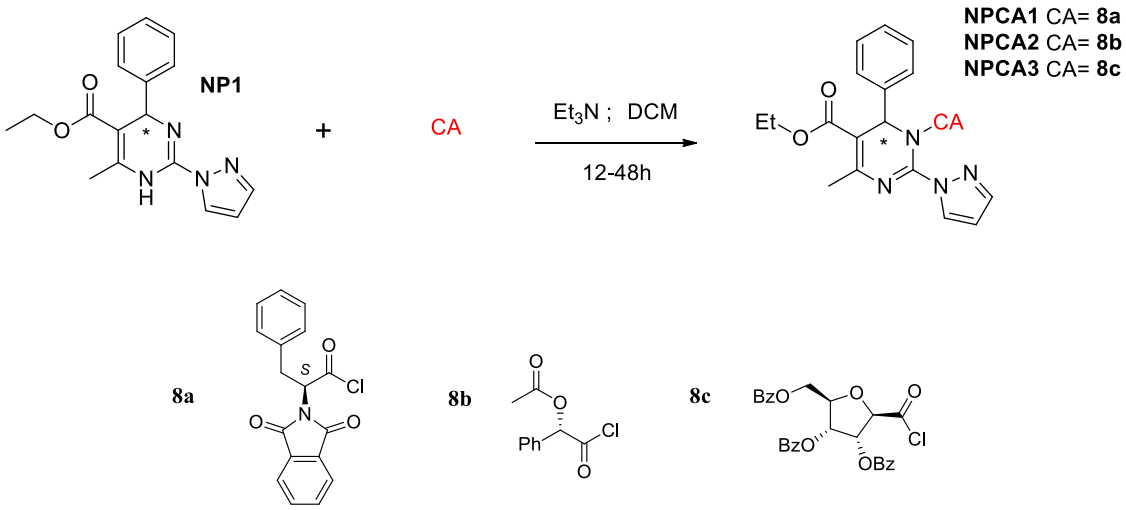

Scheme 21 *Synthesis of NPCA.*

On the other hand **NPCA2**, obtained by reaction of NP1 with **8b**, lead to a diasteroisomeric mixture from which it was possible to separate one diasteroisomer with flash chromatography, the second diastereoisomer remaining in admixture. The compound was fully characterized spectroscopically, and was optically active. ($[\alpha]_D^{20}$= + 50.4, $CHCl_3$, c=1). This single diasteroisomer (+)-**NPCA2** was treated with an ammonia aqueous solution for 30min, leading to the corresponding deacylated compound (+)-**NP1.** To transform this compound into **N1** in an optically active form it is necessary to remove the pyrazolic group as described in the literature, after N-Boc reprotection at N3 (see Scheme 16).[164] These final steps are in due course. The opposite enantiomer could be obtained either from the second diastereoisomer of NPCA2 mixture, or by carrying by derivatization of NP1 with the opposite R enantiomer of acetilmandelic acid (R-8b). This synthesis is currently under investigation.

c) Enzymatic resolution

Inspired by numerous successful examples of enzymatic resolutions via hydrolysis of esters with a stereogenic center in β-position, we took into account this type of reaction as an alternative to the chemical resolution. However, when screening a set of commercially available hydrolases such as, for example, lipases from Aspergillus niger, Candida antarctica B (CAL-B), subtilisine, α-chymotripsine and PLE (esterase from porcine liver), we could not identify a suitable biocatalytic system for the

hydrolysis at the C-5 ester function. In all cases infact the reactions stopped within 5% conversion, that were reached after days. Due to the lack of a significant activity of this process, further process development has not been carried out.

d) Convesion of 2-thioDHMP into 2-imino DHPM

The conversion of 2-thioDHMPs into their 2-imino analogs is a documented reaction, and it occurs by a convenient *one-pot* S-methylation/ammonolysis procedure. Optimized conditions for the methylation step involve the use of methyl triflate in chlorobenzene as the solvent, at 100°C, under sealed tube conditions.[166a] The following ammonolysis with NH_3/NH_4Cl smoothly proceeds to give the target guanidine with good yields, also on a multigram scale. (Scheme 22).

Our idea, represented in Scheme 22, was to exploite this indirect method to afford enantiomerically pure guanidine from chiral thiopyrimidinones, whose obtainment is reported, at least for some specific cases (Scheme 22).[175]

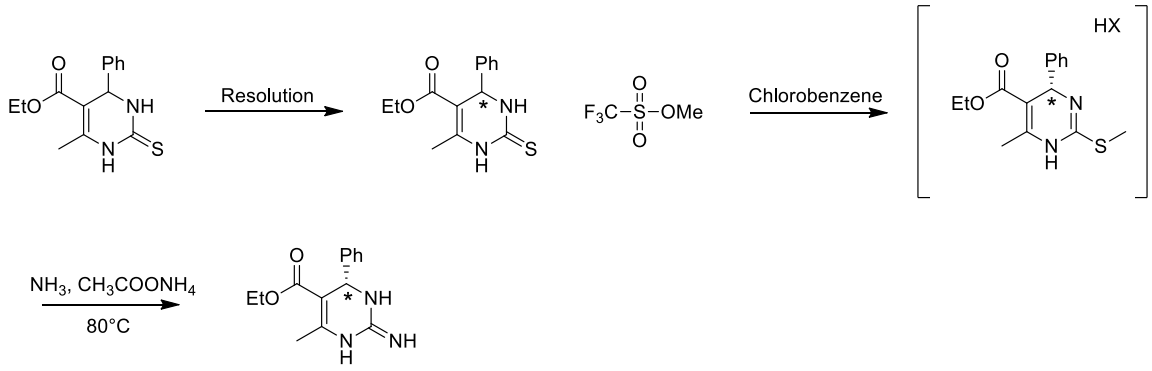

Scheme 22. *Possible strategy for the synthesis of enantiomeric 2-imiopyrimidines through resolution of DHMPs-thiones followed by methylation/ammonolysis.*

Possible pathways reported for the achievement of 2-thioDHPM enantiomers involve chemical and enzymatic resolution, use of chiral substrate-based reactions and organocatalysis.

a) The enzymatic resolution of compound **S1** was attempted as in the literature,[134] by the use of subtilisine and α-chimotrypsine as the biocatalyst for the hydrolysis of the ester function, in aqueous phosphate buffer at pH 7.4

also with addition of co-solvents but the reaction did not proceed beyond very low conversion values.

b) Resolution via diastereoisomeric compounds via derivatization with optically pure acid chlorides **8a**, **8b**, **8c** (see Scheme 23). The chiral auxiliaries were reacted in refluxing toluene. With **8a** compound SCA1 was obtained as a not separable mixture of diastereoisomers, with **8b** and **8c** the reactions are currently under investigation.

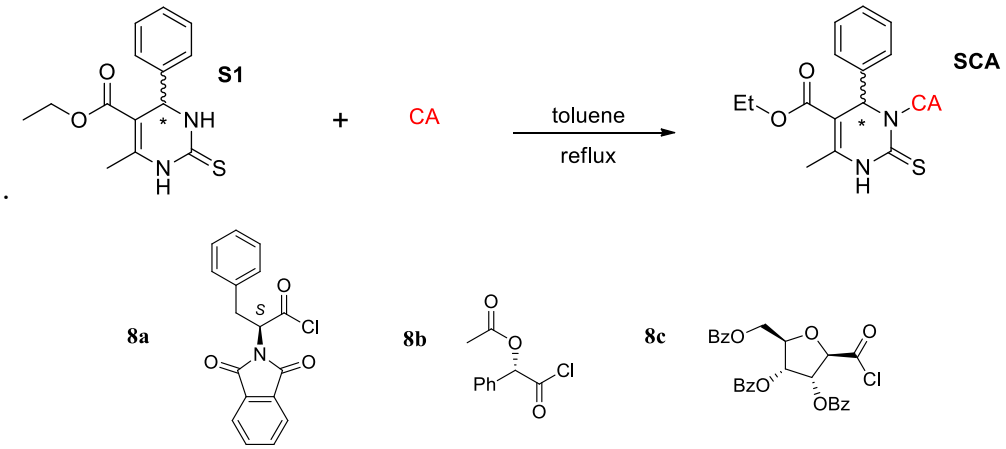

Scheme 23 *Synthesis of diasteroisomeric compounds with optically pure active chlorides 8a, 8b, 8c.*

c) Asymmetric synthesis at starting from (-)-menthylacetoacetate 7a was also attempted, but similarly to the case of the reaction with urea, the Biginelli cyclocondensation with thiourea led to a 1:1 diastereoisomeric mixture that could not be separated.

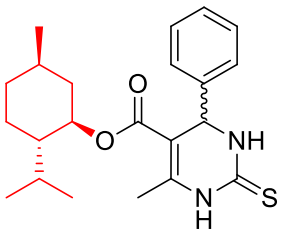

Figure 45. *Compound S8.*

5.8 Conclusions

By an inexpensive and simple synthetic method, a series of functionalized 3,4-dihydropyrimidin-2(1*H*)-ones, 3,4-dihydropyrimidin-2(1*H*)-thiones, and 3,4-dihydropyrimidin-2(1*H*)-imines were obtained under Biginelli conditions, combining urea/thiourea/guanidine with β-ketoesters and different aromatic, heteroaromatic and alkyl aldehydes. They were shown to be promising inhibitors of BACE-1 with IC_{50} values in the micromolar and sub-micromolar range.

Guanidine derived DHPM-2-imines were found to be in general more active than the corresponding DHPM-2-ones and DHMP-2-thiones, probably due to the ability of the protonated guanidine residue to directly target the catalytic aspartates of the enzyme. This hypothesis, supported by docking experiments (Figure 41), suggested that the 2-imino-DHPM scaffold may represent a privileged motif for the design of new and efficient BACE1 inhibitors.

It has been observed that small structural changes in the 2-iminoDHPM scaffold resulted in a variation of the inhibitory activity of the respective compounds. The best inhibition activity was observed with a 2-naphtylic substituent at C-4, as a result of an optimal fitting of this group into a narrow hydrophobic pocket due to the its dimension and orientation.

Based on docking experiments indicating more favorable interactions of the (*R*)-enantiomer, we have started our research on the achievement of the DHPMs in optically pure forms exploring so far chemical and enzymatic resolution technique and asymmetric synthesis with the use of a chiral β-ketoester. This part will be developed in the future.

Chapter 5

Experimental Part

6 *Instruments and materials*

IR spetra were recorded on a Nicolet Avatar FT-IR spectrometer (Thermo Fisher Scientific), as thin film or Nujol mull on NaCl.

NMR spectra were obtained on a Varian 500 MHz spectrometer in $CDCl_3$ or DMSO-d_6 or $(CD_3)CO_2$, unless otherwise stated, at 500 MHz (^1H) and 125.68 MHz (^{13}C); chemical shifts are in ppm (δ) with chloroform (δ = 7.26 for ^{1}H-NMR and 77.16 for ^{13}C-NMR), DMSO (δ = 2.50 for ^{1}H NMR and 39.52 for ^{13}C NMR), or acetone as the reference (δ = 2.05 for ^{1}H-NMR and 29.84 for ^{13}C-NMR) as the reference. Coupling constants *J* are given in hertz. ^{1}H and ^{13}C-NMR resonances have been assigned by a combination of DEPT, COSY and HSQC spectra. The resonances multiplicity is described as *s* (singlet), *d* (doublet), *t* (triplet), *q* (quartet), *m* (multiplet), *dd* (doublet of doublets), *br* (broad signal).

Electrospray (ESI) mass spectra were obtained on a Bruker Daltonics Esquire 4000 spectrometer.

HRMS analysis were carried out in the ESI mode on a TOF-MS instrument (bruker Corporation).

Chiral High Resolution GC analyses were carried out on a Shimadzu GC-14B instrument, the capillary columns being ChiraldexTM type G-TA, γ-cyclodextrin (40m X 0.25mm,carrier gas Helium, 180 KPa, split 1:100), or DiMePe β-cyclodextrin (25m X0.25mm,carrier gas He, 110 KPa, split 1:50).

HPLC were run on a HP 1100 series instrument with a UV detector at λ = 280 nm, using chiral columns (Lux5uCellulose 1 to 4) eluting with nHex/iPrOH mixture in different ratios as indicated, flow 1mL/min.

M.p. (melting points) were measured on a *Büchi* 510 apparatus and are uncorrected

Column chromatography were carried out with Merck silica gel 60 (230-240 Mesh)

TLC analysis were carried out on silica gel plates using UV light as the visualizing agent and $KMnO_4$ and I_2 as the developing agent. TLC were pre-coated plastic sheets with 0.25mm Merck silica gel 60F-254.

Optical rotations ([α]) were measured at 20 °C with a Jasco P-2000 polarimeter (Jasco Inc, Easton, MD, USA).

Commercial reagents and solvents were purchased from Sigma-Aldrich (Milan, Italy);

Anhydrous solvents: THF was distilled over sodium benzophenone ketyl under argon, CH_2Cl_2 and EtOH were distilled over CaH_2 under argon. Glassware were oven-dried before use.

BACE1 assays:

Fluorescence spectra were recorded from 350 to 600 nm on a Perkin Elmer LS50B spectrofluorimeter in a quartz cell (optical path 5 mm).
Human-β-secretase (1.140 mg / mL aqueous solution) was purchased from Sigma-Aldrich. Substrate (Arg-Glu(EDANS)-(Asn^{670},Leu^{671})-Amyloid β/A4 Protein Precursor$_{770}$ (668-675)-Lys(DABCYL)-Arg trifluoroacetate salt) was purchased from BACHEM.

PAMPA assay

UV measurements were recorded in a 96-well plate UV reader (Tecan Infinite M1000).
Ten commercial drugs, phosphate buffer saline solution at pH 7.4 (PBS), ethanol and dodecane were purchased from Sigma Aldrich and Alfa Aesar. Porcine polar brain lipid (PBL) (catalog no. 141101) was purchased from Avanti Polar Lipids, donor plate (a 96-well filtrate plate, Multiscreen® IP Sterile Plate PDVF membrane, pore size is 0.45 μM, catalog no. MAIPS4510), the acceptor plate (an indented 96-well plate, Multiscreen®, catalog no. MAMCS9610) and filter PDVF membrane units (diameter 30 mm, pore size 0.45 μm) from Millipore.

6.7 Synthesis of the α-Chiral allylamines

6.7.1 General method for the Synthesis of α-Ketosulfones (3a-i)

$PhSO_2Me$ and $PhSO_2Et$ were prepared by reaction of sodium phenylsulfinate with appropriate iodoalkene according to the literature.[177]

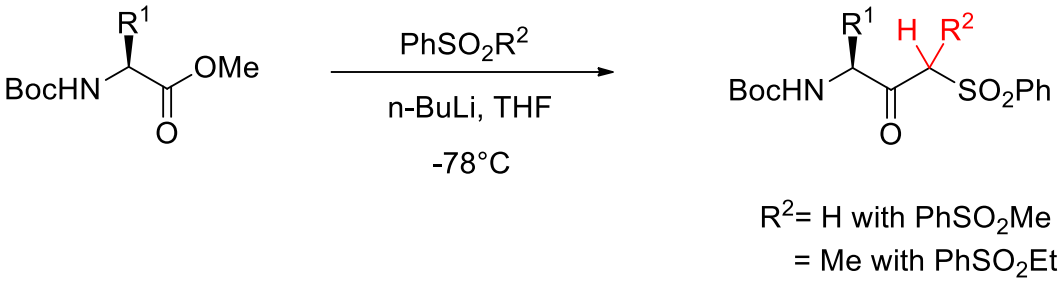

The sulfone 2a-b (2.0 mmol) was dissolved in dry THF (1.5 mL), the solution was cooled to −5 °C, under Ar. Subsequently 1.6 M *n*-BuLi in hexane (2.5 mL, 4 mmol for **3a**–**f,h**; 1.25 mL, 2 mmol for **3g,i**) was slowly added, and the mixture was stirred at −5 °C for 30 min (4 h for reactions with sulfone 2**b**). The resulting yellow suspension was transferred via a syringe to a three-necked flask, containing a 2.5M solution in dry THF of the N-Boc amino ester 2 (1 mmol, 1M only for **3h,i**), at −78 °C, under an Ar atmosphere, with stirring. The mixture was stirred overnight and allowed to reach 25 °C, then it was partitioned between water and ethyl acetate. The organic phase was extracted with saturated $NaHCO_3$ and brine, dried over Na_2SO_4 and evaporated to give a solid that was purified by flash chromatography (eluent AcOEt/petroleum ether from 0% to 15%). NMR spectra were recorded in $CDCl_3$, unless otherwise stated.

[177] S. H. Hwang and M. J. Kurth, *Tetrahedron Lett*. **2002**, 43, 53.

(3S)-3-(tert-Butoxycarbonylamino)-1-(phenylsulfonyl)-2-butanone **(3a):**

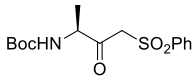

Yield 89%; white solid, mp 115–117 °C, $[\alpha]_D^{25}$ −36 (*c* 0.8, $CHCl_3$).

IR: 3387, 1736, 1700, 1288, 1148 cm^{-1}.

^{1}H-NMR (500 MHz): δ 1.35 (d, *J* = 7.0 Hz, 3H, CH_3), 1.44 (s, 9H, $C(CH_3)_3$), 4.24 (d, *J* = 14.0 Hz, 1H, CH_2SO_2Ph), 4.33 (m, 1H, CHNH), 4.44 (d, *J* = 14.0 Hz, 1H, CH_2SO_2Ph), 5.15 (br, 1H, NH), 7.58 (m, 2H, Ph), 7.69 (m, 1H, Ph), 7.90 (m, 2H, Ph) ppm.

^{13}C-NMR (125.68 MHz): δ 16.1, 28.1, 55.9, 63.2, 80.2, 128.4, 129.3, 134.3, 139.0, 155.3, 198.4 ppm.

ESI-MS: *m*/*z* 350 $[M + Na]^+$.

(3S)-3-(tert-Butoxycarbonylamino)-4-methyl-1-(phenylsulfonyl)-2-pentanone **(3b):**

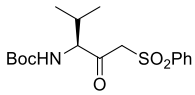

yield 85%; white solid, mp 85–88 °C, $[\alpha]_D^{25}$ −34 (*c* 1, $CHCl_3$).

IR: 3372, 1709, 1506, 1323, 1160 cm^{-1}.

^{1}H-NMR (500 MHz): δ 0.80 (d, *J* = 7.0 Hz, 3H, $CH(CH_3)_2$), 0.98 (d, *J* = 7.0 Hz, 3H, $CH(CH_3)_2$), 1.44 (s, 9H, $C(CH_3)_3$), 2.29 (m, 1H, $CH(CH_3)_2$), 4.20 (d, *J* = 14.5, 1H, CH_2SO_2Ph), 4.25 (dd, *J* = 4.6, 8.7 Hz, 1H, CHNH), 4.43 (d, *J* = 14.5 Hz, 1H, CH_2SO_2Ph), 5.10 (d, *J* = 8.7 Hz, 1H, NH), 7.57 (m, 2H, Ph), 7.67 (m, 1H, Ph), 7.93 (m, 2H, Ph) ppm.

^{13}C-NMR (125.68 MHz): δ 17.0, 19.9, 28.4, 28.9, 64.0, 65.2, 80.5, 128.6, 129.4, 134.4, 139.1, 156.0, 197.8 ppm.

ESI-MS: *m*/*z* 378 $[M + Na]^+$, 394 $[M + K]^+$.

(3S)-3-(tert-Butoxycarbonylamino)-5-methyl-1-(phenylsulfonyl)-2-hexanone (3c):

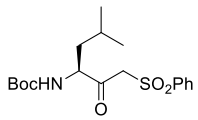

Yield 89%; white solid, mp 76–78 °C; $[\alpha]_D^{25}$ −43 (*c* 1.6, $CHCl_3$).

IR: 3369, 1708, 1511, 1323, 1159 cm^{-1}.

^{1}H-NMR (500 MHz): δ 0.93 (d, *J* = 6.1 Hz, 3H, $CH(CH_3)_2$), 0.94 (d, *J* = 6.1 Hz, 3H, $CH(CH_3)_2$), 1.44 (s, 9H, $C(CH_3)_3$), 1.67 (m, 2H, $CH_2CH(CH_3)_2$), 4.21 (d, *J* = 13.9 Hz, 1H, CH_2SO_2Ph), 4.28 (m, 1H, CHN), 4.49 (d, *J* = 13.9 Hz, 1H, CH_2SO_2Ph), 5.06 (d, *J* = 7.1 Hz, 1H, NH), 7.58 (t, 2H, Ph), 7.67 (t, 1H, Ph), 7.94 (dd, *J* = 8.0, 1.5 Hz, 2H, Ph) ppm.

^{13}C-NMR (125.68 MHz): δ 21.4, 23.1, 24.8, 28.2, 39.1, 58.9, 63.3, 80.5, 128.4, 129.2, 134.2, 138.9, 155.5, 198.6 ppm.

ESI-MS: *m/z* 392 $[M + Na]^+$, 408 $[M + K]^+$.

Anal. Calcd. for $C_{18}H_{27}NO_5S$: C, 58.51; H, 7.37; N, 3.79. Found C, 58.50; H, 7.43; N, 3.86.

***(3S,4S)-3-(tert-Butoxycarbonylamino)-4-methyl-1-(phenylsulfonyl)-2-hexanone* (3d):**

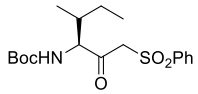

Yield 86% ; white solid, mp 83–85 °C; $[\alpha]_D^{25}$ –0.2 (*c* 0.9, $CHCl_3$).

IR: 3368, 1708, 1504, 1323, 1156 cm^{-1}.

^{1}H-NMR (500 MHz): δ 0.87 (t, *J* = 7.1 Hz, 3H, CH_2CH_3), 0.95 (d, *J* = 6.5 Hz, 3H, CH_3), 1.05 (m, 1H, CH_2CH_3), 1.27 (m, 1H, CH_2CH_3), 1.42 (s, 9H, $C(CH_3)_3$), 1.99 (m, 1H, $CHCH_2CH_3$), 4.20 (d, 1H, CH_2SO_2Ph), 4.27 (dd, *J* = 5.0, 8.7 Hz, 1H, CHNH), 4.43 (d, *J* = 14.5 Hz, 1H CH_2SO_2Ph), 5.08 (d, *J* = 8.7 Hz, 1H NH), 7.56 (m, 2H, Ph), 7.67 (m, 1H, Ph), 7.92 (m, 2H, Ph) ppm.

^{13}C-NMR (125.68 MHz): δ 11.6, 16.1, 24.3, 28.4, 35.7, 64.1, 65.0, 80.5, 128.6, 129.4, 134.3, 139.1, 155.9, 197.9 ppm.

ESI-MS: *m/z* 392 $[M + Na]^+$, 408 $[M + K]^+$.

Anal. Calcd. for $C_{18}H_{27}NO_5S$: C, 58.51; H, 7.37; N, 3.79. Found C, 58.42; H, 7.40; N, 3.91.

(3S)-3-(tert-Butoxycarbonylamino)-4-phenyl-1-(phenylsulfonyl)-2-butanone **(3e):**

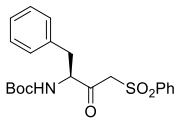

Yield 94%; white solid, mp 137–139 °C; $[\alpha]_D^{25}$ –22 (*c* 1, $CHCl_3$).

IR: 3386, 1732, 1691, 1295, 1147 cm^{-1}.

^{1}H-NMR (500 MHz): δ 1.38 (*s*, 9H, $C(CH_3)_3$), 2.91 (dd, *J* = 8.5, 14.0 Hz, 1H, CH_2Ph), 3.16 (dd, *J* = 5.5, 14.0 Hz, 1H, CH_2Ph), 4.22 (d, *J* = 14.0 Hz, 1H, CH_2SO_2Ph), 4.35 (d, *J* = 14.0 Hz, 1H, CH_2SO_2Ph), 4.47 (m, 1H, CHNH), 5.12 (d, *J* = 6.0 Hz, 1H, NH), 7.15 (m, 2H, Ph (Phe)), 7.23–7.31 (m, 3H, 1H, Ph (Phe) and 2H Ph (Phe)), 7.56 (m, 2H, Ph), 7.67 (m, 1H, Ph), 7.86 (m, 2H, Ph) ppm.

^{13}C-NMR (125.68 MHz): δ 28.2, 36.3, 61.4, 63.7, 80.6, 127.1, 128.4, 128.8, 129.3, 134.3, 136.2, 138.8, 155.4, 197.4 ppm.

ESI-MS: *m*/*z* 426 $[M + Na]^+$, 442 $[M + K]^+$.

(3S)-3-(tert-Butoxycarbonylamino)-4-[4-(tert-butyldimethylsilyloxy)phenyl]-1-(phenylsulfonyl)-2-butanone **(3f):**

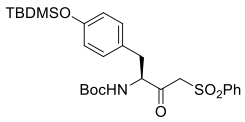

Yield 78%; *ee* 81%; white solid, mp 111–113 °C; $[\alpha]_D^{25}$ −21(*c* 1, $CHCl_3$).

IR: 3369, 1709, 1609, 1584, 1511 cm^{-1}.

^{1}H-NMR (500 MHz): δ 0.19 (s, 6H, $Si(CH_3)_2C(CH_3)_3$), 0.98 (s, 9H, $Si(CH_3)_2C(CH_3)_3$), 1.39 (s, 9H, $COC(CH_3)_3$), 2.86 (dd, *J* = 8.6, 14.6 Hz, 1H, CH_2Ph), 3.18 (dd, *J* = 5.7, 14.6 Hz, 1H, CH_2Ph), 4.17 (d, *J* = 13.9 Hz, 1H, CH_2SO_2Ph), 4.32 (d, *J* = 13.9 Hz, 1H, CH_2SO_2Ph), 4.42 (*m*, 1H, CHNH), 5.04 (d, *J* = 6.4 Hz, 1H, NH), 6.77 (d, *J* = 8.0 Hz, 2H, Ph(Tyr)), 7.00 (d, *J* = 8.0 Hz, 2H, Ph(Tyr)), 7.57 (t, *J* = 7.8 Hz, 2H, Ph), 7.68 (t, *J* = 7.8 Hz, 1H, Ph), 7.87 (d, *J* = 7.8 Hz, 2H, Ph) ppm.

^{13}C NMR (125.68 MHz): δ 4.4, 18.2, 25.6, 28.2, 35.7, 61.5, 63.9, 80.6, 120.4, 128.4, 128.5, 129.2, 130.9, 134.2, 138.8, 154.8, 197.6 ppm.

ESI-MS: *m*/*z* 556.2 $[M + Na]^+$, 572 $[M + K]^+$.

Anal. Calcd. for $C_{27}H_{39}NO_6SSi$: C, 60.76; H, 7.37; N, 2.62. Found C, 60.81; H, 7.38; N, 2.55.

***1-((2S)-1-(tert-Butoxycarbonyl)-2-pyrrolidinyl)-2-(phenylsulfonyl)-1-ethanone* (3g):**

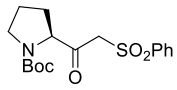

Yield 60%; yellow oil; $[\alpha]_D^{25}$ −43.1 (*c* 1.6, $CHCl_3$).

IR: 1698, 1693, 1323, 1157 cm^{-1}.

^{1}H-NMR (500 MHz, mixture of rotamers): δ 1.36 and 1.43 (2s, 9H, $C(CH_3)_3$), 1.85–1.96 (m, 2H, CH_2CH_2), 2.00–2.24 (m, 2H, CH_2CH_2), 3.46 and 3.55 (m, 2H, CH_2N), 4.18–4.42 (m, 3H, 2H CH_2SO_2Ph and 1H CHN), 7.58 (m, 2H, Ph), 7.67 (m, 1H, Ph), 7.94 (m, 2H, Ph) ppm.

^{13}C-NMR (125.68 MHz, Mixture of rotamers): δ 23.9, 24.8, 28.4 and 28.5, 47.0 and 47.2, 62.8 and 64.1, 65.7 and 66.3, 80.6 and 81.1, 128.6, 129.3 and 129.4, 134.2 and 134.4, 139.3, 153.7 and 155.0, 198.1 and 198.6 ppm.

HRMS (ESI) *m/z* Calcd. for $C_{17}H_{23}NNaO_5S$ $[M + Na]^+$ 376.1195, found 376.1192.

***(2S,4S) and (2S,4R)-2-(tert-Butoxycarbonylamino)-1-phenyl-4-(phenylsulfonyl)-3-pentanone* (3h):**

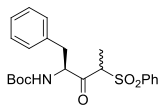

A 3:2 (*a* and *b*) was obtained in 77% yield; white solid.

IR: 3390, 1737, 1700, 1286, 1150 cm^{-1}.

^{1}H-NMR (500 MHz, mixture of diastereoisomers): δ 1.28 and 1.37 (2d, 3H,$CHCH_3$ *a* and *b*), 1.39 (s, 5.4H, *b* $C(CH_3)_3$), 1.44 (s, 3.6H, *a* $C(CH_3)_3$), 2.85 (dd, *J* = 9.6, 14.0 Hz, 0.67H, *a* CH_2SO_2Ph), 3.02 (dd, *J* = 7.8, 13.8 Hz, 0.33H, *b* CH_2SO_2Ph), 3.22 (dd, *J* = 5.0, 13.8 Hz, 0.33H, *b* CH_2SO_2Ph), 3.33 (dd, *J* = 5.0, 14.0 Hz, 0.67H, *a* CH_2SO_2Ph), 4.40–4.55 (m, 1H, *a* CHNH), 4.65–4.75 (m, 1H, *b* CHNH), 4.97 (d, 0.67H, *a* NH), 5.40 (d, 0.33H, *b* NH), 7.17–7.35 (m, 5H, Ph *a* and *b*), 7.52–7.77 (m, 5H, Ph *a* and *b*) ppm.

^{13}C-NMR (125.68 MHz): δ 12.1 (*b*), 12.5 (*a*), 28.0 (*a*), 28.1 (*b*), 35.0 (*a*), 37.7 (*b*), 61.5 (*a*), 61.6 (*b*), 65.9 (*b*), 66.5 (*a*), 80.2 (*b*), 80.7 (*a*), 126.8 (*a*), 127.1 (*b*), 128.3 (*b*), 128.7, 129.1, 129.2, 129.3, 129.5, 129.6, 129.7, 134.3, 134.5, 135.9, 136.0, 136.3, 137.3, 155.4, 155.7, 200.8, 202.2 ppm.

ESI-MS: *m*/*z* 440 $[M + Na]^+$, 456 $[M + K]^+$.

Anal. Calcd. for $C_{22}H_{27}NO_5S$: C, 63.29; H, 6.52; N, 3.35. Found C, 63.23; H, 6.38; N, 3.38.

(2S) and (2R) 1-((2S)-1-(tert-Butoxycarbonyl)-2-pyrrolidinyl)-2-(phenylsulfonyl)-1-propanone **(3i):**

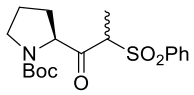

A 55:45 mixture of two diastereoisomers (*a* and *b*) was obtained in 80% yield. Yellow oil.

IR: 1700, 1689, 1322, 1157 cm^{-1}.

^{1}H-NMR (500 MHz, DMSO-d_6, 80 °C): δ 1.30 (d, *J* = 7.4, 1.65H, *a* CH_3), 1.34 (d, *J* = 7.4 Hz, 1.35H, *b* CH_3), 1.35 (s, 4.95H, *a* $C(CH_3)_3$), 1.41 (s, 4.05H, *b* $C(CH_3)_3$), 1.59–2.25 (m, 4H, CH_2CH_2, *a* and *b*), 3.28–3.45 (m, 2H, CH_2N *a* and *b*), 4.55 (dd, *J* = 3.0, 8.0 Hz, 0.55H, *a* $CHCH_3$), 4.67 (br, 0.45H, *b* CHNH), 4.73 (m, 0.45H, *b* $CHCH_3$), 4.85 (br, 0.55H, *a* CHNH), 7.67 (m, 2H, Ph *a* and *b*), 7.78 (m, 1H, Ph *a* and *b*), 7.88 (m, 2H, Ph *a* and *b*) ppm.

^{13}C-NMR (125.68 MHz, $DMSOd_6$, 80 °C): δ 12.1 (*b*), 12.3 (*a*), 22.7 (*a* and *b*), 27.6 (*a* or *b*), 27.7 (*a* or *b*), 46.1 (*b*), 46.3 (*a*), 64.3, 64.7, 65.7, 78.8 (*a*), 79.0 (*b*), 128.5, 128.6 and 128.8, 133.7 (*b*), 133.8 (*a*), 137.0, 153.0, 201.6 ppm.

HRMS (ESI) *m*/*z* Calcd. for $C_{18}H_{25}NNaO_5S$ $[M + Na]^+$ 390.1351, found 390.1342.

6.7.2 General method for the Synthesis of Allylamine from Ketosulfones

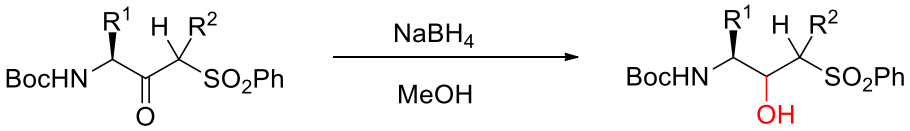

The ketone **3a-i** (1 mmol) was dissolved in MeOH (5 mL)and $NaBH_4$ (0.04 g, 1 mmol) was added portion-wise, at 0 °C. When the reaction was complete (TLC), the solvent was removed *in vacuo*. Aqueous workup and extraction with ethyl acetate gave the β-hydroxysulfones(4a-i) as mixtures of diastereoisomers (the ratio were determined by NMRanalysis).

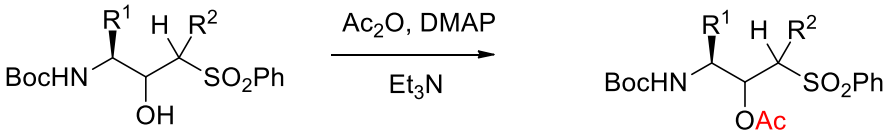

In the minimum amount of dry dichloromethane, the crude mixture of diasteroisomeric alcohols was dissolved, **4a-i**. The solution was cooled down at 0 °C and 2-dimethylaminopyridine (0.01 mmol), triethylamine (10 mmol) and acetic anhydride (5 mmol) were sequentially. The reaction mixture was stirred at room temperature until the formation of the product was complete (TLC: AcOEt/petroleum ether 2:8), extracted with 10% aqueous citric acid, saturated $NaHCO_3$ and brine, dried over Na_2SO_4 and evaporated. If necessary, co-evaporation with toluene was performed to completely remove the excess anhydride. The crude acetates **5a-i** were obtained in quantitative yield and were used in the final step without further purification. NMR spectra were recorded in $CDCl_3$, unless otherwise stated.

6.7.3 Acetoxysulfones were transformed into the corresponding allylamines by two methods (6a-i).

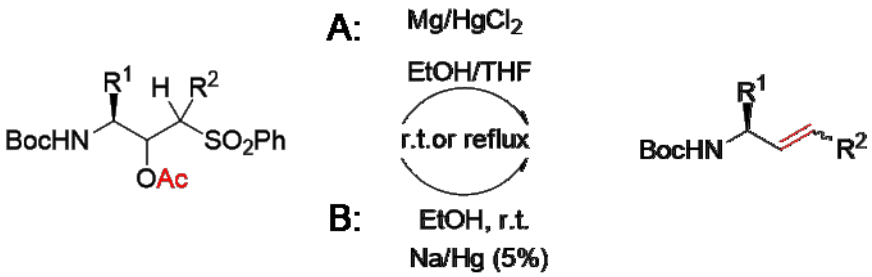

Method A: in a Schlenk reactor filled with Ar, sulfone **5i-f** (1mmol, mixture of diastereoisomers) was dissolved in 3:1 EtOH/THF (0.2 M solution). Mg powder (2.5 mmol) and $HgCl_2$ (0.1 mmol) were added, in the order. The reaction mixture was stirred at room temperature monitoring the progress by TLC (petroleum ether/diethyl ether 8:2). To the completed reaction was added 10% aqueous citric acid, and the aqueous phase was extracted with ethyl acetate. The combined organic layers were washed with brine, dried over Na_2SO_4 and evaporated. The crude product (6a-f) was purified by column chromatography using 9:1 petroleum ether/Et_2O as the eluent.

Method B: in a round-bottomed flask, under an Ar atmosphere, sulfone **5e-i** (1 mmol) was dissolved into anhydrous, degassed ethanol (0.5 M solution). 5% Na/Hg amalgam (3 mmol of Na) was added, at −15 °C, to the stirred solution. The reaction mixture was left at room temperature monitoring the progress by TLC (petroleum ether/diethyl ether 8:2); water was added, and the same workup as above gave the crude allylamines **6e, 6f', 6g-i**

***(3S)-3-(tert-Butoxycarbonylamino)-1-butene* (6a):**

tert -butyl (S)-3-hydroxy-4-(phenylsulfonyl)butan-2-ylcarbamate(4a)

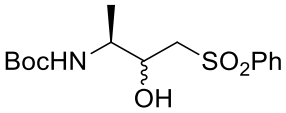

3:1 mixture of *syn* (*s*) and *anti* (*a*) diastereoisomers, pale yellow oil.

IR: 3370, 1693, 1304, 1146 cm^{-1}.

^{1}H-NMR (500 MHz): δ 1.13 (d, J = 8.5 Hz, 2.25H, *s* CH_3), 1.21 (d, J = 8.5 Hz, 0.75H, *a* CH_3), 1.40 (s, 9H, $C(CH_3)_3$), 3.21 (m, 1.5H, *s* CH_2SO_2Ph), 3.26

(m, 0.5H, *a* CH_2SO_2Ph), 3.64 (br, 2H, NHCH and OH), 4.10 (br, 1H, CHOH), 4.73 (br, 1H, NH), 7.59 (m, 2H, Ph), 7.69 (m, 1H, Ph), 7.92 (m, 2H, Ph) ppm.

^{13}C-NMR (125.68 MHz): δ 15.4 (*s*), 18.1 (*a*), 28.3, 50.1, 59.8 (*s*), 60.5 (*s*), 68.5 (*s*), 68.9 (*s*), 79.9, 127.3 (*s*), 127.9 (*s*), 129.3 (*a*), 129.4 (*s*), 133.7 (*a*), 134.1 (*s*), 139.1, 155.5 ppm.

ESI-MS: *m/z* 296 $[M + Na]^+$, 368 $[M + K]^+$.

tert -butyl (S)-3-acetoxy-4-(phenylsulfonyl)butan-2-ylcarbamate (5a)

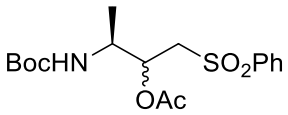

3:1 mixture of *syn* (*s*) and *anti* (*a*) diastereoisomers, white solid, mp 110–111 °C.

IR: 3358, 1742, 1712, 1521 cm^{-1}.

^{1}H-NMR (500 MHz): δ 1.06 (d, *J* = 7.0 Hz, 0.75H, *a* CH3), 1.09 (d, *J* = 7.0 Hz, 2.25H, *s* CH3), 1.40 (s, 6.75H, *s* $C(CH_3)_3$), 1.42 (s, 2.25H, *a* $C(CH_3)_3$), 1.82 (s, 2.25H, *s* $COCH_3$), 1.95 (s, 0.75H, *a* $COCH_3$), 3.37 (m, 2H, CH_2SO_2Ph), 3.86 (br, 1H, CHNH), 4.43 (br, 0.75H, *s* CHOAc), 4.52 (br, 0.25H, *a* CHOAc) 5.21 (br, 0.75H, *s* NH), 5.34 (br, 0.25H, *a* NH), 7.57 (m, 2H, Ph), 7.66 (m, 1H, Ph), 7.91 (m, 2H, Ph) ppm.

^{13}C-NMR (125.68 MHz): δ 16.3 (*s*), 18.1 (*a*), 20.6, 28.3, 48.3 (*s*) 49.4 (*a*), 56.7 (*s*), 57.8 (*a*), 69.5 (*a*), 70.2 (*s*), 80.0, 128.3, 129.3, 133.9, 139.2, 155.1, 169.8 ppm.

ESI-MS: *m/z* 394 $[M + Na]^+$.

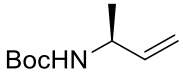

Method **A**: final yield 68%, oil, *ee* 95% (by GLC); $[\alpha]_D^{25}$ –6.0 (*c* 0.45, $CHCl_3$).

^{1}H-NMR (500 MHz): δ 1.20 (d, *J* = 8.5 Hz, 3H, CH_3), 1.44 (s, 9H, $C(CH_3)_3$), 4.22 (br, 1H, CHNH), 4.45 (br, 1H, NH), 5.10 (m, 2H, $=CH_2$), 5.81 (m, 1H, CH=) ppm.

^{13}C NMR (125.68 MHz): δ 20.7, 28.4, 48.1, 79.3, 113.6, 140.1, 155.1 ppm.

ESI-MS: *m/z* 194 $[M + Na]^+$.

***(3S)-3-(tert-Butoxycarbonylamino)-4-methyl-1-pentene (6b)*:**

tert -butyl (3S)-2-hydroxy-4-methyl-1-(phenylsulfonyl)pentan-3-ylcarbamate

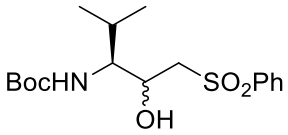

(4b)

10:1 mixture of *syn* (*s*) and *anti* (*a*) diastereoisomers, yellow oil.

IR: 3368, 1691, 1304, 1146 cm^{-1}.

^{1}H-NMR (500 MHz, *syn* diastereoisomer): δ 0.87 (d, *J* = 7.0 Hz, 3H, $CH(CH_3)_2$), 0.90 (d, *J* = 7.0 Hz, 3H, $CH(CH_3)_2$), 1.40 (s, 9H, $C(CH_3)_3$), 2.18 (m, 1H $CH(CH_3)_2$), 3.23 (m, 1H, CH_2SO_2Ph), 3.32 (m, 1H, CH_2SO_2Ph), 3.48 (m, 1H, CHNH), 3.56 (d, *J* = 2.9 Hz, 1H, OH) 4.12 (m, 1H, CHOH), 4.41 (d, *J* = 9.7 Hz, 1H, NH), 7.59 (m, 2H, Ph), 7.68 (m, 1H, Ph), 7.92 (m, 2H, Ph) ppm.

^{13}C-NMR (125.68 MHz, (2*S*,3*S*) diastereoisomer): δ 15.7, 20.0, 27.1, 28.3, 58.5, 60.4, 67.4, 80.1, 128.1, 129.7, 134.4, 139.6, 156.7 ppm.

ESI-MS: *m*/*z* 380 $[M + Na]^+$, 396 $[M + K]^+$.

tert -butyl (3 S)-2-acetoxy-4-methyl-1-(phenylsulfonyl)pentan-3-ylcarbamate (5b)

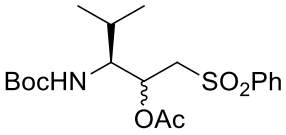

syn isomer: white solid, mp: 98–100 °C; $[\alpha]_D^{25}$ −5 (*c* 0.6, $CHCl_3$).

IR: 3365, 1744, 1712, 1523 cm^{-1}.

^{1}H-NMR (500 MHz): δ 0.86 (d, *J* = 8.5 Hz, 3H, $CH(CH_3)_2$), 0.90 (d, *J* = 8.5 Hz, 3H, $CH(CH_3)_2$), 1.41 (s, 9H, $C(CH_3)_3$), 1.62 (m, 1H, $CH(CH_3)_2$), 1.75 (s, 3H, $COCH_3$), 3.33 (d, *J* = 18.3 Hz, 1H, CH_2SO_2Ph), 3.44 (dd, *J*= 12.5, 18.3 Hz, 1H, CH_2SO_2Ph), 3.63 (m, 1H, CHNH), 4.35 (d, *J* = 13.0 Hz, 1H, NH), 5.29 (m, 1H, CHOAc), 7.57 (m, 2H, Ph), 7.66 (m, 1H, Ph), 7.90 (m, 2H, Ph) ppm.

^{13}C-NMR (125.68 MHz): δ 17.1, 19.6, 20.6, 28.3, 56.6, 57.3, 68.1, 79.9, 127.4, 128.3, 129.1, 133.9, 139.1, 155.6, 169.7 ppm.

ESI-MS: *m/z* 422 $[M + Na]^+$, 438 $[M + K]^+$.

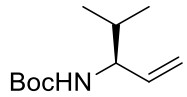

Method **A**: final yield 60%, oil, *ee* > 99.5% (by GLC); $[\alpha]_D^{25}$ + 28 (*c* 0.85, $CHCl_3$), lit. $[\alpha]_D^{25}$
+25 ($CHCl_3$).

^{1}H-NMR (500 MHz): δ 0.88 (d, *J* = 7 Hz, 3H, CH_3), 0.90 (d, *J* = 7 Hz, 3H, CH_2CH_3), 1.44 (s, 10H, $C(CH_3)_3$ and CH_2CH_3), 1.77 (m, 1H, $CHCH_2CH_3$), 3.98 (br, 1H, CHNH), 4.50 (br, 1H, NH), 5.12 (m, 2H, $=CH_2$), 5.73 (m, 1H, -CH=) ppm.

^{13}C-NMR (125.68 MHz): δ 18.2, 18.8, 28.6, 32.4, 58.1, 79.3, 115.2, 137.5, 155.7 ppm.

ESI-MS: *m/z* 222 $[M + Na]^+$, 237 $[M + K]^+$.

(3S)-3-(tert-Butoxycarbonylamino)-5-methyl-1-hexene **(6c):**

tert -butyl (3 S)-2-hydroxy-5-methyl-1-(phenylsulfonyl)hexan-3-ylcarbamate (4c)

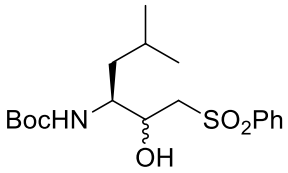

7:1 mixture of *syn* (*s*) and *anti* (*a*) diastereoisomers, orange oil.

IR: 3368, 1694, 1305, 1146 cm^{-1}.

^{1}H-NMR (500 MHz): δ 0.85 (d, *J* = 6.7 Hz, 3H, $CH(CH_3)_2$), 0.90 (d, *J* = 6.7 Hz, 3H, $CH(CH_3)_2$), 1.31 (m, 2H CH_2CH), 1.39 (s, 9H, $C(CH_3)_3$), 1.60 (m, 1H, CH(CH3)2), 3.25 (m, 1.76H, *s* CH_2SO_2Ph), 3.27 (m, 0.24H, *a* CH_2SO_2Ph), 3.49 (br, 0.12H, *a* CHNH), 3.56 (br, 0.88H, *s* CHNH), 3.74, (br, 0.12H, *a* OH), 3.78 (br, 0.88H, *s* OH), 4.10 (m, 1H, CHOH), 4.55 (br d, *J* = 7.3 Hz, 0.88H, *s* NH), 4.72 (br d, *J* = 9.0 Hz, 0.12H, *a* NH), 7.57 (t, 2H, Ph), 7.66 (t, 1H, Ph), 7.92 (d, 2H, Ph) ppm.

^{13}C-NMR(125.68 MHz): δ 21.5 (*s*), 22.0 (*a*), 23.0 (*a*), 23.6 (*s*) 24.6 (*s*), 24.7 (*a*), 28.2 (*s*), 28.3 (*a*), 38.9 (*s*), 41.3 (*a*), 52.6 (*a*), 52.9 (*s*), 59.8 (*s*), 60.3 (*a*),

67.8 (*s*), 69.4 (*a*), 79.6 (*s*), 79.8 (*a*), 127.9 (*s*), 128.0 (*a*), 129.4 (*s*), 129.5 (*a*), 134.0 (*a*), 134.1 (*s*), 134.2 (*a*), 139.2 (a), 139.3 (*s*), 156.1 ppm.

ESI-MS: *m/z* 394 $[M + Na]^+$, 410 $[M + K]^+$.

tert -butyl (3 S)-2-acetoxy-5-methyl-1-(phenylsulfonyl)hexan-3-ylcarbamate (5c)

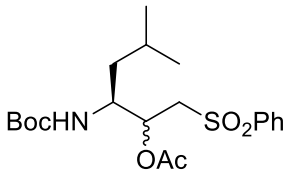

7:1 mixture of *syn* (*s*) and *anti* (*a*) diastereoisomers, white solid.

IR: 3372, 1745, 1707, 1519 cm^{-1}

^{1}H-NMR (500 MHz): δ 0.86 (d, *J* = 6.6 Hz, 3H, $CH(CH_3)_2$), 0.91 (d, *J* = 6.6 Hz, 3H, $CH(CH_3)_2$), 1.13–1.25 (m, 2H, CH_2CH), 1.41 (s, 7.9H, *s* $C(CH_3)_3$) 1.43 (s, 1.1H, *a* $C(CH_3)_3$), 1.60 (m, 1H, $CH(CH_3)_2$), 1.78 (s, 2.6H, *s* CH_3CO), 1.96 (s, 0.4H, *a* CH_3CO), 3.35 (m, 1H, CH_2SO_2) 3.44 (m, 1H, CH_2SO_2), 3.76 (m, 0.13H, *a* CHN), 3.89 (br, 0.87H, *s* CHN), 4.33 (d, *J* = 10.0 Hz, 0.9H, *s* NH), 4.45 (d, *J* = 10.0 Hz, 0.1H, *a* NH), 5.18 (m, 0.9H, *s* CHO), 5.37 (dbt, *J* = 9.4, 2.5 Hz, 0.1H, *a* CHO), 7.58 (t, 2H, Ph), 7.67 (t, 1H, Ph), 7.91 (dd, *J* = 8.0, 1.5 Hz, 2H, Ph) ppm.

^{13}C-NMR (125.68 MHz): δ 20.6, 21.6 (*s*), 21.8 (*a*), 23.1 (*a*), 23.2 (*s*), 24.6 (*a*), 24.7 (*s*), 28.2 (*s*), 28.3 (*a*), 39.5 (*s*), 41.1 (*a*), 50.6 (*s*), 52.0 (*a*), 56.3 (*s*), 57.8 (*a*), 69.1 (*a*), 70.1 (*s*), 79.8 (*a*), 79.9 (*s*) 128.26 (*s*), 128.33 (*a*), 129.27 (*s*) 129.33 (*a*), 133.8, 139.3, 155.4, 169.7 ppm.

ESI-MS: *m/z* 436 $[M + Na]^+$, 452 $[M + K]^+$.

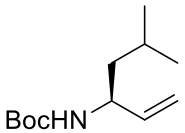

Method **A**: final yield 67% oil, *ee* > 99.5% (by GLC); $[\alpha]_D^{25}$ +3.5 (*c* 1.0, $CHCl_3$).

^{1}H-NMR (500 MHz): δ 0.89 (d, *J* = 6.7 Hz, 3H, $CH(CH_3)_2$) 0.90 (d, *J* = 6.7 Hz, 3H, $CH(CH_3)_2$), 1.31 (m, 2H, CH_2), 1.42 (s, 9H, $C(CH_3)_3$), 1.65 (sept, 1H, $CH_2CH(CH_3)_2$), 4.12 (br, 1H, CHNH), 4.62 (br, 1H, NH), 5.03 (d, *J* = 9.9 Hz, 1H,

=CH_2), 5.12 (d, *J* = 15.8 Hz, 1H, =CH_2), 5.71 (ddd, *J* = 6.9, 9.9, 15.8 Hz, 1H, -CH=) ppm.

^{13}C NMR (125.68 MHz): δ 22.0, 22.7, 24.4, 28.1, 44.7, 51.0, 79.2, 113.9, 139.4, 155.1 ppm.

ESI-MS: *m*/*z* 236 $[M + Na]^+$.

***(3S,4S)-3-(tert-Butoxycarbonylamino)-4-methyl-1-hexene* (6d):**

tert -butyl (3 S , 4S)-2-hydroxy-4-methyl-1-(phenylsulfonyl)hexan-3-ylcarbamate (4d)

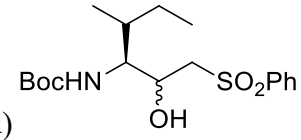

94:6 mixture of *syn* (*s*) and *anti* (*a*) diastereoisomers, pale yellow oil.

IR: 3370, 1693, 1304, 1146 cm^{-1}.

^{1}H-NMR (500 MHz): δ 0.85 (t, 0.18H, *a* CH_2CH_3), 0.90 (d, *J* = 7.0 Hz, 3H, *s* CH_3), 0.92 (t, *J* = 7.0 Hz, 0.82H, *s* CH_2CH_3), 0.99 (m, 1H, CH_2CH_3), 1.39 (s, 9H, $C(CH_3)_3$), 1.54 (m, 1H CH_2CH_3), 1.85 (m, 1H, $CHCH_2CH_3$), 3.27 (m, 2H, CH_2SO_2Ph), 3.50 (m, 1H, CHOH), 3.58 (br, 1H, OH), 4.18 (m, 1H, CHNH), 4.40 (d, *J* = 9.5 Hz, 0.94H, *s* NH), 4.84 (d, *J* = 10.0 Hz, 0.06H, *a* NH), 7.58 (m, 2H, Ph), 7.68 (m, 1H, Ph), 7.92 (m, 2H, Ph) ppm.

^{13}C-NMR (125.68 MHz): δ 11.1 (*a*), 11.8 (*s*), 15.6 (*a*), 16.3 (*s*), 23.1 (*s*), 25.7 (*a*), 28.4, 31.0 (*a*) 34.2 (*s*), 58.8 (*a*), 59.0 (*s*), 60.4 (*s*), 60.7 (*a*), 65.2 (*s*), 67.2 (*s*), 80.1, 127.5 (*a*), 128.0 (*s*), 129.4 (*a*), 129.6 (*s*), 133.8 (*a*), 134.2 (*s*), 139.6, 156.6 ppm.

ESI-MS: *m*/*z* 394 $[M + Na]^+$, 410 $[M + K]^+$.

tert -butyl (3 S , 4 S)-2-acetoxy-4-methyl-1-(phenylsulfonyl)hexan-3-ylcarbamate (5d)

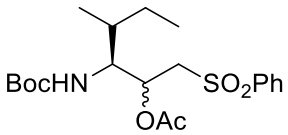

94:6 Mixture of *syn* (*s*) and *anti* (*a*) diastereoisomers, white solid, mp 108–110 °C; $[\alpha]_D^{25}$ −3.8 (*c* 1.5, $CHCl_3$).

IR: 3367, 1746, 1708, 1518 cm^{-1}.

^{1}H-NMR (500 MHz): δ 0.84 (t, *J* = 7.2 Hz, 3H, CH_2CH_3), 0.89 (d, *J* = 6.5 Hz, 3H, CH_3), 1.00 (m, 1H, CH_2CH_3) 1.30 (m, 1H, $CHCH_2CH_3$), 1.41 (s, 8.5H, *s* $C(CH_3)_3$), 1.43 (s, 0.5H, *a* $C(CH_3)_3$), 1.50 (m, 1H, CH_2CH_3), 1.73 (s, 2.8H, *s* $COCH_3$), 1.98 (s, 0.2H, *a* $COCH_3$), 3.29 (d, *J* = 15Hz, 1H, CH_2SO_2Ph), 3.43 (dd, *J* = 9.5, 15.0 Hz, 1H, CH_2SO_2Ph), 3.68 (m, 1H, CHNH), 4.31 (d, 1H, *J* = 10.0 Hz, 0.94H, *s* NH), 4.55 (d, *J* = 10.5 Hz, 0.06H, *a* NH), 5.34 (dt, *J* = 6.3, 1.2 Hz, 0.94H, *s* CHOAc), 5.55 (dt, *J* = 9.3, 2.2 Hz, 0.06H, *a* CHOAc), 7.57 (m, 2H, Ph), 7.66 (m, 1H, Ph), 7.90 (m, 2H, Ph) ppm.

^{13}C NMR (125.68 MHz, *syn* diastereoisomer): δ 10.8, 15.5, 20.6, 24.2, 27.9, 35.1, 56.3, 56.4, 67.9, 80.0, 128.1, 129.1, 133.6, 139.0, 155.5, 169.7 ppm.

ESI-MS: *m/z* 436 $[M + Na]^+$, 452 $[M + K]^+$.

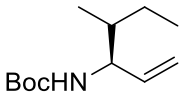

Method **A**: yield 69%, oil, *ee* > 99.5% (by GLC). $[\alpha]_D^{25}$ + 32 (*c* 1.0, $CHCl_3$).

^{1}H NMR (500 MHz): δ 0.85 (d, *J* = 6.5 Hz, 3H, CH_3,), 0.89 (t, *J* = 7.5 Hz, 3H, CH_2CH_3), 1.10 (m, 1H CH_2CH_3), 1.43 (s, 9H, $C(CH_3)_3$), 1.40–1.53 (m, 2H, CH_2CH_3), 4.05 (br, 1H, CHNH), 4.54 (br, 1H, NH), 5.12 (m, 2H, $=CH_2$), 5.70 (m, 1H, CH=) ppm.

^{13}C-NMR (125.68 MHz): δ 11.7, 15.0, 25.3, 28.4, 38.6, 56.9, 78.9, 115.2, 136.8, 155.5 ppm.

ESI-MS: *m/z* 236 $[M + Na]^+$, 252 $[M + K]^+$.

***(3S)-3-(tert-Butoxycarbonylamino)-4-phenyl-1-butene* (6e):**

tert -butyl (S)-3-hydroxy-1-phenyl-4-(phenylsulfonyl)butan-2-ylcarbamate (4e)

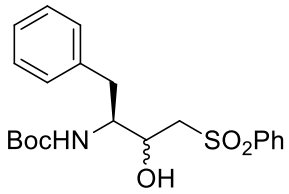

3:1 mixture of *syn* (*s*) and *anti* (*a*) diastereoisomers, white solid, mp 130–131 °C.

IR: 3370, 1692, 1304, 1146 cm^{-1}.

^{1}H-NMR(500 MHz): δ 1.30 (s, 6.75H, *s* $C(CH_3)_3$), 1.35 (s, 2.25H, *a* $C(CH_3)_3$), 2.78–3.01 (m, 2H, CH_2Ph), 3.16–3.33 (m, 2H, CH_2SO_2Ph), 3.62–3.92 (multiplets, 2H, CHNH and OH), 4.07 (br, 0.25H, *a* CHOH), 4.14 (br, 0.75H, *s* CHOH), 4.55 (br, 0.75H, *s* NH), 4.93 (d, *J* = 9.5 Hz, 0.25H, *a* NH), 7.16–7.29 (m, 5H, Ph(Phe)), 7.51 (m, 0.5H, *a* Ph), 7.57 (m, 1.5H, *s* Ph), 7.64 (m, 0.25H, *a* Ph), 7.68 (m, 0.75H, *s* Ph), 7.82 (m, 0.5H, *a* Ph), 7.89 (m, 1.5H, *s* Ph) ppm.

^{13}C NMR (125.68 MHz): δ 28.1 (*s*), 28.2 (*a*), 35.8 (*s*), 38.3 (*a*), (55.1 (*s*), 55.8 (*a*), detected in HSQC only) 59.8 (*s*), 60.3 (*a*), 65.7 (*a*), 68.1 (*s*), 79.8 (*s*) 80.0 (*a*), 126.5 (*s*), 126.7 (*s*), 127.8 (*a*) 127.9 (*s*), 128.4 (*a*), 128.5 (*s*), 129.2 (*s*), 129.3 (*a*), 129.4 (*a*), 129.5 (*s*), 134.1 (*a*), 134.2 (*s*), 136.9, 139.1, 155.7 ppm.

ESI-MS: *m/z* 428 $[M + Na]^+$.

tert -butyl (2 S)-3-acetoxy-1-phenyl-4-(phenylsulfonyl)butan-2-ylcarbamate (5e)

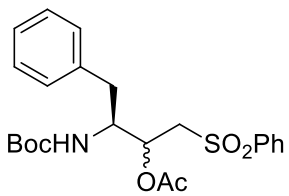

syn isomer: white solid, mp 122–124 °C; $[\alpha]_D^{25}$ −7 (*c* 1, $CHCl_3$).

IR: 3336, 1732, 1705 cm^{-1}.

^{1}H-NMR (*syn* isomer, 500 MHz): δ 1.28 (s, 9H, C(CH_3)$_3$), 1.84 (s, 3H, $COCH_3$), 2.61 (m, 1H, CH_2Ph), 2.84 (dd, J = 5.5, 14.0 Hz, 1H, CH_2Ph), 3.41 (m, 2H, CH_2SO_2Ph), 4.08 (br, 1H, CHNH), 4.40 (m, 1H, NH), 5.30 (m, 1H, CHOAc), 7.12–7.29 (m, 5H, Ph (Phe)), 7.52–7.57 (m, 2H, Ph), 7.66 (m, 1H, Ph), 7.81–7.89 (m, 2H, Ph) ppm.

^{13}C NMR(125.68 MHz): δ 20.6, 28.1, 36.8, 53.5, 56.7, 69.7, 80.0, 126.8, 128.2, 128.6, 129.0, 129.3, 133.8, 136.5, 139.3, 155.3, 169.8 ppm.

ESI-MS: *m/z* 470 $[M + Na]^+$, 486 $[M + K]^+$.

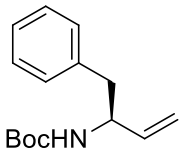

Method **B**: yield 70% white solid, mp 72–74 °C; *ee* > 99.5%. $[\alpha]_D^{25}$ + 15 (*c* 0.85, $CHCl_3$);

^{1}H-NMR (500 MHz): δ 1.44 (s, 9H, C(CH_3)$_3$), 2.83 (d, J = 6.3 Hz, 2H, CH_2Ph), 4.47 (br, 2H, CHNH and CHNH), 5.08 (m, 2H, =CH_2), 5.80 (m, 1H,CH=), 7.17–7.29 (m, 5H, Ph) ppm.

^{13}C NMR (125.68 MHz): δ 28.3, 41.3, 53.3, 79.1, 114.5, 126.2, 128.1, 129.7, 137.1, 137.9, 155.3 ppm.

ESI-MS: *m/z* 270 $[M + Na]^+$.

(3S)-*3-(tert-Butoxycarbonylamino)-4-[4-(tert-butyldimethylsilyloxy)phenyl]-1-butene* (6f):

tert -butyl (S)-3-hydroxy-1-(4-OTBDS-phenyl)-4-(phenylsulfonyl)butan-2-ylcarbamate (4f)

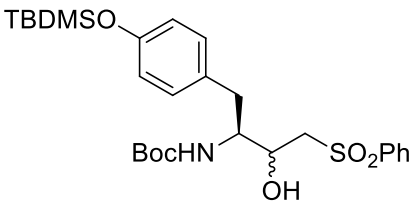

5:1 mixture of *syn* (*s*) and *anti* (*a*) diastereoisomers, white solid, mp 107–109 °C.

IR: 3369, 1693, 1610, 1511, 1256, 1145 cm^{-1}.

^{1}H-NMR (500 MHz): δ 0.17 (s, 7.5H, *s* $Si(CH_3)_2C(CH_3)_3$) and 0.18 (s, 1.5H, *a* $Si(CH_3)_2C(CH_3)_3$), 0.97 (s, 5H, *s* $Si(CH_3)_2$) and 0.98 (s, 1H, *a* $Si(CH_3)_2$,), 1.32 (s, 7.5 H, *s* $C(CH_3)_3$) and 1.35 (s, 1.5H, *a* $C(CH_3)_3$), 2.67–2.95 (m, 2H, CH_2Ph), 3.14–3.35 (m, 2H, CH_2SO_2Ph), 3.56–3.92 (m, 2H, CHNH and OH), 4.05 (br, 0.17H, *a* CHOH) and 4.11 (br, 0.83H, *s* CHOH), 4.51 (br, 0.83H, *s* NH) and 4.89 (d, *J* = 8.6, 0.17H, *a* NH), 6.71 (d, 0.36H, *a* Ph(Tyr)) and 6.75 (d, 1.64H, *s* Ph(Tyr)), 7.01 (overlapping d, 2H, Ph(Tyr)), 7.61 (m, 2H, SO_2Ph), 7.67 (m, 1H, SO_2Ph), 7.83 (d, 0.36H, *a* SO_2Ph) and 7.90 (d, 1.64H, *s* SO_2Ph), ppm.

^{13}C-NMR (125.68 MHz): δ −4.45, 18.2, 25.7, 28.2, 35.0 (*s*), 37.5 (*a*), 55.3 (*s*), 55.9 (*a*), 59.9 (*s*), 60.4 (*a*) 65.7 (*a*), 68.1 (*s*), 79.7, 120.0 (*a*), 120.1 (*s*), 127.8 (*a*), 127.9 (*s*), 129.4, 130.1, 130.4, 134.1, 139.1, 154.4 (*s*), 155.7 (*a*) ppm.

ESI-MS: *m/z* 558.2 $[M + Na]^+$, 574.2 $[M + K]^+$.

tert -butyl (3 S)-3-acetoxy-1-(4-OTBDS-phenyl)-4-(phenylsulfonyl) butan-2-ylcarbamate (5f)

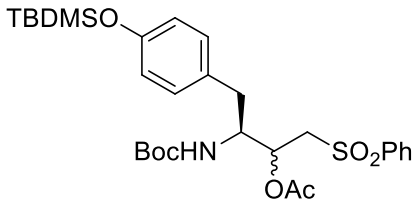

syn isomer, white solid, mp 159–161 °C; $[\alpha]_D^{25}$ −6.7 (*c* 1.5, $CHCl_3$).

IR: 3369, 1747, 1705, 1609, 1512 cm^{-1}.

^{1}H-NMR (500 MHz): δ 0.16 (s, 6H, $Si(CH_3)_2$), 0.96 (s, 9H, $Si(CH_3)_2C(CH_3)_3$), 1.30 (s, 9H, $C(CH_3)_3$) 1.80 (s, 3H, OCOCH3), 2.45 (m, 1H, CH_2Ph), 2.84 (m, 1H, CH_2Ph), 3.43 (m, 2H, CH_2SO_2Ph), 4.04 (br, 1H, CHNH), 4.48 (br, 1H, NH), 5.29–5.34 (m, 1H, CHOAc) 6.73 (d, *J* = 8.3 Hz, 2H, Ph(Tyr)), 6.98 (d, *J* = 8.3 Hz, 2H, Ph(Tyr)), 7.56 (t, 2H, SO_2Ph), 7.65 (m, 1H, SO_2Ph), 7.88 (d, *J* = 7.5 Hz, 2H, SO_2Ph) ppm.

^{13}C-NMR (125.68 MHz): δ −4.5, 18.2, 20.6, 25.6, 28.1, 35.9, 53.5, 56.6, 69.7, 79.9, 120.1, 128.2, 129.0, 129.3, 129.9, 133.8, 139.3, 154.4, 155.3, 169.8 ppm.

ESI-MS: *m/z* 600 $[M + Na]^+$, 616.2 $[M + K]^+$.

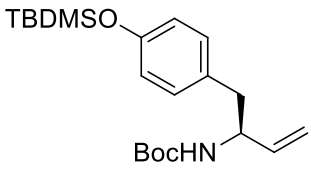

Method **A**: yield 76% white solid, mp 51–53 °C; *ee* = 80% (by HPLC); $[\alpha]_D^{25}$ + 1.2 (*c* 1, $CHCl_3$).

IR 2957, 2930, 2858, 1702, 1610, 1510 cm^{-1}.

^{1}H-NMR(500 MHz): δ 0.19 (s, 6H, $Si(CH_3)_2$), 0.98 (s, 9H, $Si(CH_3)_2C(CH_3)_3$), 1.41 (s, 9H, $C(CH_3)_3$), 2.76 (m, 2H, CH_2Ph), 4.36 (br, 1H, CHNH), 4.47 (br, 1H, NH), 5.06 (dt, *J* = 10.3, 1.2 Hz, 1H, $=CH_2$), 5.09 (dt, *J* = 17.4, 1.2 Hz, 1H, $=CH_2$), 5.78 (ddd, *J* = 10.3, 17.4, 5.5 Hz, 1H, CH=), 6.76 (d, 2H, Ph), 7.02 (d, 2H, Ph) ppm.

^{13}C-NMR (125.68 MHz): δ −4.8, 18.0, 25.7, 28.4, 40.4, 79.0, 114.5, 119.9, 130.0, 130.1, 130.4, 138.2, 154.2 ppm.

ESI-MS: *m/z* 400 $[M + Na]^+$.

Anal. Calcd for $C_{21}H_{35}NO_3Si$: C, 66.80; H, 9.34; N, 3.71. Found: C, 66.88; H, 9.26; N, 3.73.

(3S)-3-(tert-Butoxycarbonylamino)-4-[4-(hydroxy)phenyl]-1-butene **(6f'):**

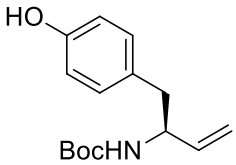

Method **B** from 5f: 81%, white solid, mp 82–84 °C; $[\alpha]_D^{26}$ +21.5 (*c* 1.5, $CHCl_3$).

IR = 3339, 1683, 1615, 1516 cm^{-1}.

^{1}H-NMR (500 MHz): δ 1.41 (s, 9H, $C(CH_3)_3$), 2.75 (m, 2H, CH_2Ph), 4.35 (br, 1H, CHNH), 4.50 (br, 1H, NH), 5.07 (dd, *J* = 10.3, 1.2 Hz, 1H, $=CH_2$), 5.10 (dd, *J* = 17.4, 1.2 Hz, 1H, $=CH_2$), 5.60 (br, 1H, OH), 5.78 (ddd, *J* = 17.4, 10.3, 5.5 Hz, 1H, CH=), 6.75, (d, 2H, Ph), 7.01 (d, 2H, Ph) ppm.

^{13}C-NMR (125.68 MHz): δ 28.4, 40.6, 53.7, 79.7, 114.7, 115.3, 129.0, 130.6, 138.1, 154.6, 155.5 ppm.

ESI-MS: *m/z* 286.1 $[M + Na]^+$, 302 $[M + K]^+$.

Anal. Calcd for $C_{15}H_{21}NO_3$: C, 68.42; H, 8.04; N, 5.32; O, 18.23; Found: C, 68.41; H, 8.10; N, 5.24.

***(2S)-1-(tert-Butoxycarbonyl)-2-vinylpyrrolidine* (6g):**

tert -butyl (S)-2-(1 hydroxy-2-(phenylsulfonyl)ethyl)pyrrolidine-N-carboxylate (4g)

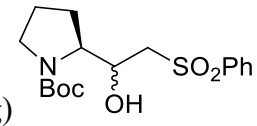

3:2 mixture of *syn* (*s*) and *anti* (*a*) diastereoisomers, pale yellow oil.

IR: 3493, 1687, 1305, 1148 cm^{-1}.

^{1}H-NMR (500MHz, DMSO-d_6, 80 °C): δ 1.38 (s, 5.4H, *s* $C(CH_3)_3$), 1.39 (s, 3.6H, *a* $C(CH_3)_3$), 1.66–1.92 (m, 2H, CH_2CH_2), 3.08–3.40 (m, 4H, CH_2N and CH_2SO_2Ph), 3.66 (m, 0.6H, *s* CHN), 3.80 (m, 0.4H, *a* CHN), 4.25 (br, 1H, CHOH), 4.84 (d, J = 6.0 Hz, 0.4H, *a* OH), 4.91 (d, J = 6.5 Hz, 0.6H, *s* OH), 7.63 (m, 2H, Ph), 7.70 (m, 1H, Ph), 7.89 (m, 2H, Ph) ppm.

^{13}C-NMR (125.68 MHz, DMSO-d_6, 80 °C): δ 22.9 (*a*), 24.7 (*s*), 26.2 (*s*), 27.6 (*a*), 27.8 (*s*), 30.0 (*a*), 46.2 (*s*), 46.7 (*a*), 58.8 (*a*), 59.8 (*s*), 60.4 (*a*), 60.8 (*s*), 65.6 (*s*), 66.8 (*a*), 78.1 (*s*), 78.3 (*a*), 126.3 (*a*), 127.1 (*s*), 128.6 (*s*), 128.8 (*a*), 132.8 (*a*), 132.9 (*s*), 140.26 (*a*), 140.27 (*s*), 153.5 (*s*), 153.8 (*a*) ppm.

ESI-MS: *m/z* 378 $[M + Na]^+$, 394 $[M + K]^+$.

tert -butyl (S)- 2-(1-acetoxy-2-(phenylsulfonyl)ethyl)pyrrolidine-N-carboxylate (5g)

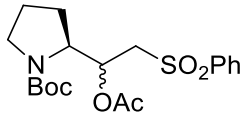

syn isomer: white solid, mp 140–143 °C; $[\alpha]_D^{25}$ –33.1 (*c* 1.25, $CHCl_3$).

IR: 1747, 1692, 1520 cm^{-1}.

^{1}H-NMR (500MHz, DMSO-d_6, 80 °C): δ 1.38 (s, 9H, $C(CH_3)_3$), 1.67–1.87 (m, 4H, CH_2CH_2), 1.76 (s, 3H, OCH_3), 3.04 (m, 1H, CH_2N), 3.31 (m, 1H, CH_2N), 3.60, 3.65 (part AB of an ABX system, J = 4.1, 7.9, 15.0 Hz, 2H, CH_2SO_2Ph), 3.84 (br, 1H, CHN), 5.73 (m, 1H, CHOAc), 7.65 (m, 2H, Ph), 7.74

^{13}C-NMR (125.68 MHz DMSO-d_6, 80 °C): δ 19.5, 22.4, 24.7, 27.2, 45.7, 55.6, 58.8, 66.9, 78.0, 127.2, 128.2, 133.0, 139.1, 153.2, 168.1 ppm.

ESI-MS: *m/z* 378 $[M + Na]^+$, 394 $[M + K]^+$.

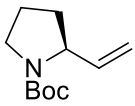

Method **B**: yield 84%, oil, *ee* > 99.5% (by GLC); $[\alpha]_D^{25}$ −15 (*c* 0.75, $CHCl_3$), lit. $[\alpha]_D^{25}$ −15.7 (*c* 0.55, $CHCl_3$).

^{1}H-NMR (500 MHz, rotamers): δ 1.43 (s, 9H, $C(CH_3)_3$), 1.69 (m, 1H, CH_2CH_2), 1.77–1.79 (m, 2H, CH_2CH_2), 2.02 (m, 1H, CH_2CH_2), 3.38 (m, 2H, CH_2N), 4.27 (br, 1H, CHN), 5.04 (m, 2H,=CH_2), 5.73 (m, 1H, CH=) ppm.

^{13}C-NMR (125.68 MHz, rotamers): δ 22.6 and 23.2, 28.3, 31.4 and 31.8, 46.0 and 46.4, 59.0, 79.0, 113.6, 138.8 and 139.0, 154.8 ppm.

ESI-MS: *m/z* 220 $[M + Na]^+$.

(4S)-4-(tert-Butoxycarbonylamino)-5-phenyl-1-butene **(6h):**

tert-butyl ((2S)-3-hydroxy-1-phenyl-4-(phenylsulfonyl)pentan-2-yl) carbamate (4h)

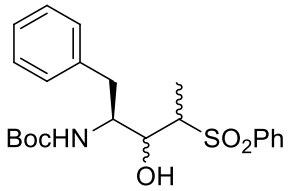

mixture of 4 diastereoisomers in approximately 1:1:3:3 ratio, white solid.

IR: 3372, 1704, 1297, 1142 cm^{-1}.

^{1}H-NMR (500MHz): δ [1.03, 1.06, 1.20 (d, 3H, $CHCH_3$)], [1.23, 1.29, 1.31, 1.36 (s, 9H, $C(CH_3)_3$)], 2.75–3.15 (multiplets, 2H, CH_2Ph), 3.20–3.30 (m, 1H, $CH(CH_3)$), [3.70, 3.85, 3.98 (multiplets, 1H, CH(NH))], [3.80, 4.06, 4.15 (multiplets, 1H, CH(OH))], [4.38, 4.50 (br, 1H, OH)], [4.85, 4.99, 5.05 (d, 1H, NH)], 7.20–7.30 (m, 5H, Ph(Phe)), 7.53–7.73 (m, 3H, Ph(Phe)), 7.80–7.91 (m, 2H, Ph(Phe)).

^{13}C-NMR (125.68 MHz): δ [7.1, 11.0, 11.4, 11.7 (CH_3CH)], [28.0, 28.17, 28.22, 28.25 (tBu)], [34.2, 36.8, 38.9, 39.8 (CH_2)], [52.4, 52.7, 53.0, 54.8 (CHNH)], [60.6, 63.1, 63.4, 63.6 ($CHSO_2Ph$)], [69.1, 69.4, 70.0, 72.3 (CHOH)], [79.4, 79.7, 79.8 (tBu)], [126.4–137.7 (CAr)], [155.1, 155.4 (CO)].

ESI-MS: *m/z* 442 $[M + Na]^+$, 458 $[M + K]^+$.

(2S)-2-((tert-butoxycarbonyl)amino)-1-phenyl-4-(phenylsulfonyl) pentan-3-yl acetate (5h)

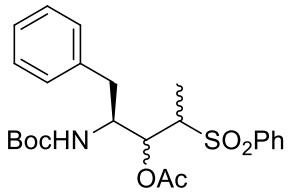

white solid, mixture of four diastereoisomers.

IR: 3369, 1747, 1704, 1513 cm^{-1}.

^{1}H-NMR (500 MHz): δ [1.12, 1.16, 1.24, 1.28 (s, 9H, $C(CH_3)_3$), [1.17, 1.44 (d, 3H, CH_3)], [1.99, 2.02, 2.28, 2.35 (s, 3H, $COCH_3$)], 2.45–2.90 (m, 2H, CH_2Ph), 3.38 (m, 1H, $CHSO_2Ph$), 3.90–4.10 (m, 1H, CHNH), [4.64, 4.67, 4.77, 4.82 (m, 1H, NH)], 5.25–5.40 (m, 1H, CHOAc), 7.07–7.90 (m, 5H, Ph(Phe)), 7.45–7.60 (m, 3H, Ph), 7.76–7.83 (m, 2H, Ph) ppm.

^{13}C-NMR (125.68 MHz): δ [10.8, 12.0, 13.0, 14.2, 20.9, 21.2, 22.1, 22.8, 27.9, 28.0, 28.3, 28.4 (*C*H_3)], [36.4, 37.6, 39.8, 40.7 (*C*H_2)], [52.3, 52.7, 53.1, 54.6 (*C*HNH)], [60.2, 60.7, 61.1, 61.3 (*C*HSO_2Ph)], [70.5, 71.7, 71.9, 73.9 (*C*HOAc)], [79.8, 80.1, 80.5, (tBu)], 126.4–138.2 (*C*Ar), [155.0, 155.4, 155.5 (*C*O)], [170.0, 170.1, 170.3 (*C*O)] ppm.

ESI-MS: *m/z* 484 $[M + Na]^+$, 500 $[M + K]^+$.

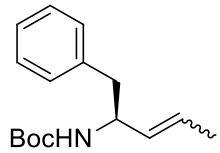

Method **B**: 8:2 mixture of *E* and *Z* isomers, yield 60%, pale yellow oil.

IR: 3340, 1692, 1390, 1365, 1255 cm^{-1}.

^{1}H-NMR(500 MHz): δ 1.40 (s, 7.2H, *E* $C(CH_3)_3$), 1.42 (s, 1.8H, *Z* $C(CH_3)_3$), 1.47 (d, *J* = 7.5 Hz, 0.6H, *Z* CH_3), 1.65 (d, *J* = 7.4 Hz, 2.4H, *E* CH_3), 2.65–2.95 (m, 2H, CH_2Ph), 4.23–4.66 (br, 2H, CHNH and NH), 5.21 (m, 0.2 H, *Z* $=CH_2$), 5.30 (m, 0.8H, *E* $=CH_2$), 5.52 (m, 1H, CH=), 7.10–7.34 (m, 5H) ppm.

^{13}C-NMR (125.68 MHz): δ 13.1 (*Z*), 17.7 (*E*), 28.36 (*Z*), 28.37 (*E*), 42.0, 53.2, 79.3, 126.2, 126.3, 128.17 (*E*) 128.20 (*Z*), 129.6 (*E*), 129.7 (*Z*), 130.9, 137.7 (*E*), 137.8 (*Z*), 155.0 (*Z*), 155.1 (*E*) ppm.

HRMS (ESI) *m/z* Calcd, for $C_{16}H_{23}NNaO_2$ $[M + Na]^+$ 284.1626, found 284.1628.

1-[(2S)-1-(tert-Butoxycarbonyl)-2-pyrrolidinyl]-1-propene **(6i):**

(2S)-tert-butyl 2-(1-hydroxy-2-(phenylsulfonyl)propyl)pyrrolidine-1-carboxylate (4i)

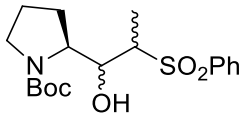

Mixture of diastereoisomers, yellow oil.

IR: 3420, 1687, 1302, 1148 cm^{-1}.

^{1}H-NMR (500 MHz, major diastereoisomer) δ: 1.37 (d, 3H, CH_3), 1.44 (s, 9H, $C(CH_3)_3$), 1.70–1.90 (m, 3H, CH_2CH_2), 2.18 (m, 1H, CH_2CH_2), 3.30 (m, 1H, CH_2N), 3.37 (m, 1H, $CHCH_3$), 3.50 (m, 1H, CH_2N), 3.73 (m, 1H, CHOH), 4.40 (m, 1H, CHN), 5.18 (m, 1H, OH), 7.53 (m, 2H, Ph), 7.64 (m, 1H, Ph), 7.93 (m, 2H, Ph) ppm.

^{13}C-NMR (125.68 MHz, major diastereoisomer) δ: 13.2, 24.3, 27.8, 29.9, 48.1, 60.1, 63.8, 77.4, 80.3, 129.0, 130.1, 134.1, 157.5 ppm.

ESI-MS: *m/z* 392 $[M + Na]^+$, 408 $[M + K]^+$.

(2S)-tert-butyl 2-(1-acetoxy-2-(phenylsulfonyl)propyl)pyrrolidine-1-carboxylate (5i)

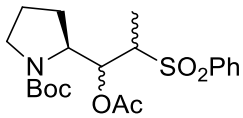

yellow oil, mixture of diastereoisomers.

IR: 3496, 1744, 1691 cm^{-1}.

^{1}H-NMR (500 MHz, major diastereoisomer): δ 1.40 (br, 12H, $C(CH_3)_3$ and CH_3), 1.76 (s, 3H, CH_3CO), 1.80–2.05 (m, 4H, CH_2CH_2), 3.07–3.67 (m, 3H, CH_2N and $CHSO_2Ph$), 4.2–4.4 (m, 1H, CHN), 5.12 (m, 1H, CHOAc), 7.53 (m, 2H, Ph), 7.64 (m, 1H, Ph), 7.93 (m, 2H, Ph).

^{13}C-NMR (125.68 MHz, major diastereoisomer): δ 11.9 (*C*H$_3$), 21.1 (*C*H$_3$CO), 23.7 (*C*H$_2$), 28.4 (tBu), 29.4 (*C*H$_2$), 46.9 (*C*H$_2$N), 56.9 (*C*HN), 61.8 (*C*HSO$_2$Ph), 73.4 (*C*HOAc), 79.5 (tBu), 128.8, 129.0, 133.5, 139.0, 155.4, 170.2 ppm.

ESI-MS: *m/z* 434 $[M + Na]^+$, 450 $[M + K]^+$.

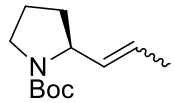

Method **B**: 85:15 mixture of *E* and *Z* isomers, yield 65%, pale yellow oil.

IR: 1695, 1394, 1365, 1252 cm^{-1}.

^{1}H-NMR (500MHz, DMSO- d$_6$, 80 °C): δ 1.39 (s, 7.65H, C(CH$_3$)$_3$), 1.40 (s, 1.35H, C(CH$_3$)$_3$), 1.51 (m, 0.15 H, CH$_2$CH$_2$), 1.60–1.65 (m, 0.85H, CH$_2$CH$_2$), 1.64 (d, 3H, CH$_3$), 1.75 (m, 2H, CH$_2$CH$_2$), 1.94 (m, 0.85H, CH$_2$CH$_2$), 2.04 (m, 0.15H, CH$_2$CH$_2$), 3.20–3.34 (m, 2H, CH$_2$N), 4.14 (m, 0.85H, CHN), 4.48 (m, 0.15H, CHN), 5.30–5.50 (m, 2H, CH= and =CHCH$_3$).

^{13}C-NMR (125.68 MHz, DMSO- d$_6$, 80 °C): δ 12.2 (*Z*), 16.6 (*E*), 22.3 (*Z*), 22.8 (*E*), 27.8 (*E,Z*), 31.3 (*E*), 32.0 (*Z*), 45.5 (*E*), 45.6 (*Z*), 53.3 (*Z*), 57.5 (*E*), 77.5 (*E*), 77.6 (*Z*), 122.3 (*Z*), 123.6 (*E*), 131.9 (*E*), 132.5 (*Z*), 153.2 (*E,Z*).

HRMS (ESI) *m/z* Calcd. for C$_{12}$H$_{21}$NNaO$_2$ $[M + Na]^+$ 234.1470, found 234.1477.

6.8 *Biginelli Reaction: dihydropyrimidines*

6.8.1 Synthesis of β-ketoesters – transesterification (7a-c)

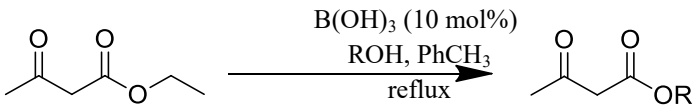

Reagent: ROH	Product name
(1R,2S,5R)-(−)-Menthol	7a
(−)-Ethyl-L-lactate	7b
(-)Borneol	7c

Table 14 *synthesis of β-ketoesters*

To a 0.5M solution of ethylacetoacetate(1mmol) in toluene was added the alcohol (1.5mmol) and 10% of boric acid (0.1mmol) were added.

The solution was heated to reflux and stirred for 6 h, ethanol was removed with a Dean-Stark apparatus. Once the reaction was complete (TLC, ethylacetate/PE: 20/80). The mixture was cooled to r.t., neutralized with saturated $NaHCO_3$ solution, and extracted with AcOEt . The organic layers were washed with brine, dried on Na_2SO_4, and concentrated *in vacuo*. The residue was purified by flash chromatography (siliga gel, AcOEt 10% in PE), leading to 7a-c.

(1R,2S,5R)-2-isopropyl-5-methylcyclohexyl 3-oxobutanoate (7a)

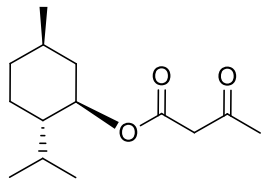

Yield 99%, transparent oil.

IR: 2957, 2871, 1741, 1716, 1646, 1243, 1149 cm^{-1}

^{1}H-NMR (500 MHz, $CDCl_3$): δ, 0.76 (d, 3H, *J* = 7 Hz, $CH(CH_3)_2$), 0.89 (d, 3H, *J* = 7.2 Hz, $CH(CH_3)_2$), 0.91 (d, 3H, *J* = 6.5 Hz, $C(5)HCH_3$), 2.05-0.92 (m, 9H, C(1/2)H, $C(3/4/6)H_2$), 2.26 (s, 3H, $C(O)CH_3$), 3.42 (d, 2H, *J* = 2 Hz, CH_2CO), 4.73 (dt, 1H, *J* = 11.1, 4.5 Hz, OC(1)H) ppm.

^{13}C-NMR (125.68 MHz, $CDCl_3$): δ 16.1, 20.7, 22.0, 23.3, 26.1, 30.0, 31.4, 34.1, 40.7, 46.9, 50.5, 75.5, 166.7, 200.6 ppm.

ESI-MS: (m/z) 263.4 $[M+H]^+$.

(S)-1-ethoxy-1-oxopropan-2-yl 3-oxobutanoate (7b)

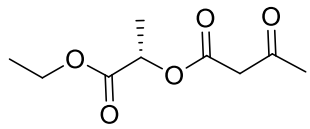

Yield 74%, pale-yellow oil.

IR: 2989, 2943, 1747, 1720, 1633, 1210, 1098 cm^{-1}

^{1}H-NMR (500 MHz, $CDCl_3$): δ, 1.19 (t, 3H, *J* = 8.7 Hz, CH_2CH_3), 1.40 (d, 3H, *J* = 9 Hz, $CHCH_3$), 2.20 (s, 3H, $C(O)CH_3$), 3.66 (d, 2H, *J* = 4 Hz, $C(O)CH_2C(O)$), 4.13 (qd, 2H, *J* = 8.8, 2 Hz, CH_2CH_3), 5.03 (q, 1H, *J* = 8.6 Hz, $CHCH_3$).

^{13}C-NMR (125.68 MHz, $CDCl_3$): δ, 14.4, 17.0, 30.4, 49.8, 61.5, 69.5, 167.4, 170.8, 201.7 ppm.

ESI-MS: (m/z) 225.4 $[M+H]^+$.

1,7,7-trimethylbicyclo[2.2.1]heptan-2-yl 3-oxobutanoate(7c)

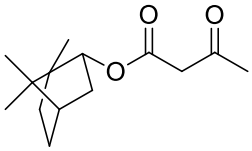

Yield 71%, incolor oil.

IR: 2956, 2881, 1739, 1716, 1650, 1245, 1152 cm^{-1}

^{1}H-NMR (500 MHz, $CDCl_3$): δ 0.84 (s, 3H, $CHC(CH_3)CH_2$), 0.87 (s, 3H, $C(CH_3)_2$), 0.90 (s, 3H, $C(CH_3)_2$), 2.28 (s, 3H, $C(O)CH_3$), 1.90-0.94 (m, 5H, $CHCH_2CH_2$), 2.37 (m, 2H, $CHCH_2CH$), 3.46 (s, 2H, $C(O)CH_2C(O)$), 4.95 (dd, 1H, J = 10.0, 3.6 Hz, CHO) ppm.

^{13}C-NMR (125.68 MHz, $CDCl_3$): δ 13.6, 19.0, 19.8, 27.2, 28.1, 30.3, 36.8, 45.0, 48.0, 49.0, 50.6, 81.4, 167.6, 200.8 ppm.

ESI-MS: (m/z) 260.5 $[M+H]^+$.

6.8.2 *Synthesis of 3,4-dihydropyrimidin-2(1H)-ones (O1-16) and 3,4-dihydropyrimidin-2(1H)-thiones (S1-8).*[129]

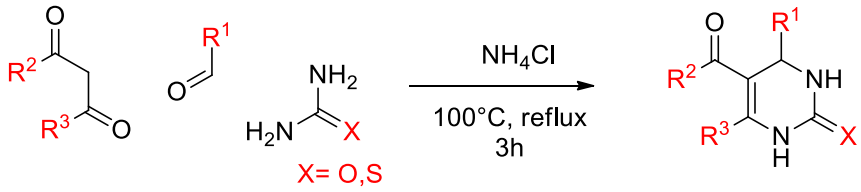

Following a literature procedure a mixture of the appropriate aldehyde (1 mmol), β-ketoester or acetoacetamide (1 mmol), urea or thiourea (1.5 mmol) and NH_4Cl (0.4 mmol) was heated at 100°C for 3 h. under stirring. The reaction mixture was allowed to reach r.t. and cold water was added to it (25 mL). The solid precipitated was filtered off and recrystallized from ethyl acetate:*n*-hexane (1:3). NMR spectra were recorded in DMSO- $d_{6,}$ unless otherwise stated.

6.8.2.1 *3,4-dihydropyrimidin-2(1H)-ones O1-11 (Table 15)*

R^1	R^2	Product name
Methyl	EtO	**O1**
Buthyl	EtO	**O2**
Phenyl	EtO	**O3**
Phenyl	MeO	**O4**
4-fluoro-phenyl	EtO	**O5**

4-hydroxy-3-methoxyphenyl	EtO	**O6**
4-methoxyphenyl	EtO	**O7**
Benzothiophen-2-yl	EtO	**O8**
3-benzothiophenyl	EtO	**O9**
2-Naphtyl	EtO	**O10**
1-Naphtyl	EtO	**O11**
2-thienyl	EtO	**O12**
3-thienyl	EtO	**O13**
2-(2-NO_2-thienyl)	EtO	**O14**
Phenyl	BnO	**O15**
Phenyl	NH_2	**O16**

[a] R^3= methyl

Table 15 *2-oxoDHPMs synthetized*[a].

5-Ethoxycarbonyl-4, 6-dimethyl-3,4-dihydropyrimidin-2(1H)-one (O1)

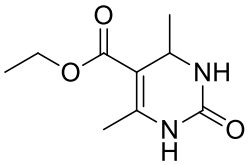

Yield 60%, white solid, mp 192-194°C

IR: 3265, 3110, 1704, 1651 cm^{-1}

^{1}H-NMR (500 MHz, DMSO-d_6): δ 1.08 (d, 3H, *J*= 6 Hz, $CHCH_3$), 1.18 (t, 3H, *J*= 7 Hz CH_2CH_3), 2.14 (s, 3H, C(6)CH_3), 4.07 (*m*, 3H, CH_2CH_3 and C(4)CH_3) 7.19 (*s*, 1H, N(3)H), 8.97 (*s*, 1H, N(1)H)ppm.

^{13}C-NMR (100 MHz, DMSO-d_6): δ 14.3, 17.7, 23.4, 46.3, 59.1, 100.5, 147.8, 152.5, 165.3 ppm

ESI-MS: (m/z) 199.3 $[M+H]^+$.

5-Ethoxycarbonyl-4- butyl-6-methyl-3,4-dihydropyrimidin-2(1H)-one (O2)

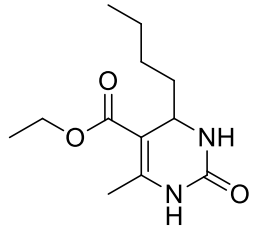

Yield 50%, white solid, mp 178-183°C

IR: 3255, 3123, 2938, 1720, 1655 cm^{-1}

^{1}H-NMR (500 MHz, DMSO-d_6): δ 0.86 (t, 3H, *J*= 8.5 Hz, $CH_2CH_2CH_3$), 1.16 (t, 3H, *J*= 9 Hz, OCH_2CH_3), 1.22 (m, 4H, $CH_2CH_2CH_3$), 1.36 (m, 2H, C(4)CH_2), 2.14 (*s*, 3H, C(6)CH_3), 4.01(m, 3H, OCH_2CH_3 and C(4)CH_3) 7.29 (s, 1H, N(3)H), 8.90 (s, 1H, N(1)H)ppm.

^{13}C-NMR (125.68 MHz, DMSO-d_6): δ 14.0, 14.2, 17.7, 21.9, 25.9, 36.4, 50.0, 59.0, 99.4, 148.3, 152.8, 165.4 ppm.

ESI-MS: (m/z) 241 $[M+H]^+$, 263 $[M+Na]^+$, 279 $[M + K]^+$.

5-Ethoxycarbonyl-6-methyl-4-phenyl-3,4-dihydropyrimidin-2(1H)-one (O3)

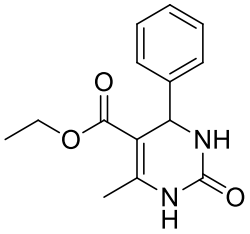

Yield 92%, white solid, mp 205-206°C

IR: 1724, 1700, 1646, 1221, 1089 cm^{-1}

^{1}H-NMR (500 MHz, DMSO-d_6): δ 1.09 (t, 3H, *J*= 10 Hz, CH_2CH_3), 2.24 (*s*, 3H, C(6)CH_3), 3,91 (*q*, 2H, CH_2CH_3); 5.14 (d, 1H, *J*= 2.5 Hz, CH(4)Ph), 7.20-7.36 (*m*, 5H, Ph), 7.74 (*s*, 1H, N(3)H); 9.20 (*s*, 1H, N(1)H) ppm.

^{13}C-NMR (125.68 MHz, DMSO-d_6): δ 14.53, 18,24 , 54.49, 59.74, 99.87, 129,08-126,92, 145,58, 149,09, 152.87, 166.09 ppm.

ESI-MS: (m/z) 261.5 $[M+H]^+$, 283.4 $[M+Na]^+$.

5-Methoxycarbonyl- 6-methyl-4-phenyl-3,4-dihydropyrimidin-2(1H)-one(O4)

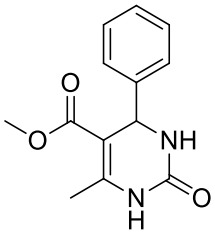

Yield 90%, cream-white powder, mp 207-209°C

IR: 1693, 1642, 1406 , 1335 , 1272 , 1228, 1088 cm^{-1}.

^{1}H-NMR (500 MHz, DMSO-d_6):δ 2.25 (*s*, 3H, C(6)CH_3), 3.53 (*s*, 3H, OCH_3), 5.14 (*d, J*= 1 Hz, 1H, C(4)H), 7.23-7.34 (*m*, 5H, Ph), 7.74 (*s*, 1H, N(3)H), 9.20 (*s*, 1H, N(3)H).

^{13}C-NMR (125.68 MHz, DMSO-d_6): δ 17.71, 50.83, 53.85, 99.30, 126.6, 127.73, 128.90, 145.21, 149.22, 152.73, 166.45 ppm.

ESI-MS: (m/z) 269.4 $[M+Na]^+$.

5-ethoxycarbonyl 4-(4-fluorophenyl)-6-methyl-3,4-dihydropyrimidine-2(1H)-one (O5)

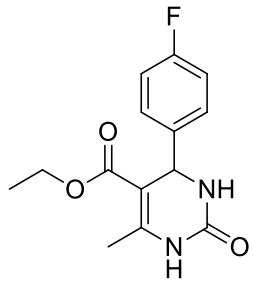

Yield 70%, yellow solid, mp 189-191°C

IR: 3285, 2374, 1700, 1088 cm^{-1}

^{1}H-NMR (500 MHz, DMSO-d_6): δ 1,09 (t, 3H, J = 9.0 Hz, CH_2CH_3), 2.25 (*s*, 3H, C(6)CH_3), 3,98 (*q*, 2H, J= 9.0 Hz, CH_2CH_3); 5.15 (d, 1H, J= 4.5 Hz, CH(4)), 7.11-7.18 (*m*, 2H, Ph), 7.24-7.29(*m*, 2H, Ph), 7.75 (*s*, 1H, N(3)H); 9.22 (*s*, 1H, N(1)H) ppm.

^{13}C-NMR (125.68 MHz, DMSO-d_6): δ 14.1, 17.7, 53.4, 59.2, 99.1, 115.1(d, ^{2}J = 21.0 Hz), 128.2 (d, ^{3}J = 8.0 Hz), 141.1 (d, ^{4}J = 3.0 Hz), 150.3 (d, ^{1}J = 345.0 Hz), 160.1, 165.2 ppm.

ESI-MS: (m/z) 279 $[M+H]^{+}$.

5-Ethoxycarbonyl 4-(4-hydroxy-3-methoxyphenyl)-6-methyl-3,4-dihydropyrimidine-2(1H)-one (O6)

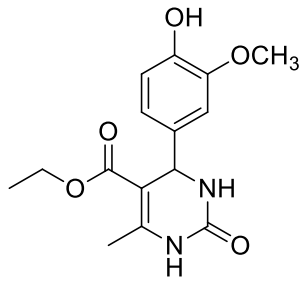

Yield 78%, yellow solid, mp 234-236°C

IR: 3248, 3114, 1701, 1647, 1518 cm^{-1}

^{1}H-NMR (500 MHz, DMSO-d_6): δ 1.11 (t, 3H, J = 10.0 Hz, CH_2CH_3), 3.72 (*s*, 3H, OCH_3), 2.23 (*s*, 3H, C(6)CH_3), 3.99 (*q*, 2H, J = 9.0 Hz, CH_2CH_3), 5.15 (d, 1H, J= 4.0 Hz, CH(4)), 6.55-6.83 (*m*, 3H, Ph), 7.62 (*s*, 1H, N(3)H), 8.89 (*s*, 1H, OH), 9.11 (*s*, 1H, N(1)H) ppm.

^{13}C-NMR (125.68 MHz, DMSO-d_6): δ 14.2, 17.7, 53.6, 55.6, 59.1, 99.5, 135.9, 145.8, 147.2, 147.9, 152.2, 165.5 ppm

ESI-MS: (m/z) 307 $[M+H]^+$.

5-Ethoxycarbonyl-4-(4-methoxyphenyl)-6-methyl-3,4-dihydropyrimidin-2(1H)-one (O7):

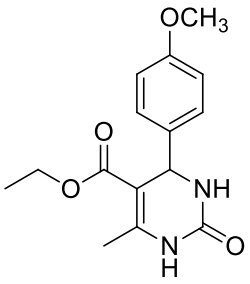

Yield 72%, white solid, mp 202-203°C

IR: 3237, 3115, 1701, 1648, 1516, 1281, 1221, 1086, 786cm^{-1}

^{1}H-NMR (500 MHz, DMSO-d_6): δ 1.15 (t, 3H, J = 7.1 Hz, CH_2CH_3), 2.22 (*s*, 3H, C(6)CH_3), 3.70 (*s*, 3H, OCH_3), 3.89 (*q*, 2H, J= 7.1 Hz, CH_2CH_3), 5.20 (s, 1H, C(4)H), 6.83 (d, 2H, J = 7.6 Hz, Ph),7.16 (d, 2H, J = 7.6 Hz, Ph), 7.63 (*s*, 1H, N(3)H), 9.20 (*s*, 1H, N(1)H) ppm.

ESI-MS: (m/z) 291.5 $[M+H]^+$.

5-Ethoxycarbonyl-4-(benzo[b]thiophen-2-yl)-6-methyl-3,4-dihydropyrimidin-2(1H)-one (O8)

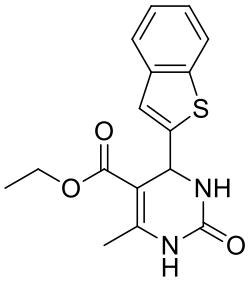

Yield 85%, white solid, mp 260-262 °C (dec).

IR: 3188, 3091, 2916, 1704, 1645, 1285, 1221, 1089 cm^{-1}.

^{1}H NMR (500 MHz, DMSO-d_6): δ 1.19 (t, 2H, J = 7.1 Hz, CH_3CH_2), 2.24 (s, 3H, C(6)CH_3), 4.09 (q, 3H, J =7.1 Hz, CH_3CH_2O), 5.50 (d, 1H, J = 3.5 Hz, C(4)H), 7.19 (s, 1H, thiophenyl CH=C), 7.28-7.36 (m, 2H, ArH), 7.79 (d, 1H, J = 7.2 Hz, ArH),

7.88 (d, 1H, *J* = 7.2 Hz, ArH), 8.01 (bdd, 1H, *J* = 1.6, 3.5 Hz, N(3)H), 9.39 (bd, *J* = 1.6Hz, 1H, N(1)H);

^{13}C NMR (125.68 MHz, DMSO-d_6): δ 14.2, 17.7, 50.0, 59.5, 99.0, 119.9, 122.5, 123.5, 124.2, 124.4, 138.6, 139.0, 149.2, 149.25, 152.2, 159.6, 164.0 ppm.

ESI-MS: *m/z*: 317.4 $[M+H]^+$.

5-Ethoxycarbonyl-4-(3-benzothiophenyl)-6-methyl-3,4-dihydropyrimidin-2(1H)-one (O9):

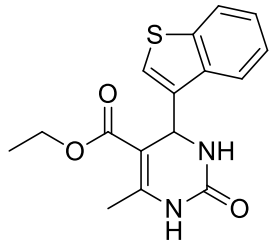

Yield 73%, yellow solid, mp

^{1}H-NMR(500 MHz, DMSO-d_6): 0.98 (t, *J*= 7.2 Hz, 3H, CH_3CH_2), 2.30 (s, 3H, C(6)CH_3), 3.92 (q, J=7.2 Hz, 2H, CH_3CH_2), 5.58 (s, 1H, C(4)H), 7.39-7.35 (m, 4H, Ph), 7.82 (s, 1H, N(3)H), 7.99-7.97 (m, 1H, thiophenyl CH=C), 9.29 (s, 1H, N(1)H).

^{13}C-NMR(125.68 MHz, DMSO-d_6): δ 14.30, 18.06, 48.66, 59.70, 79.27, 98.77, 122.37, 123.37, 124.49, 124.70, 124.79, 138.99, 140.55, 146.03, 152.44, 165.68 ppm.

ESI-MS: *m/z*:317.5 $[M+H]^+$.

5-Ethoxycarbonyl-6-methyl-4-(naphthalen-2-yl)-3,4-dihydropyrimidin-2(1H)-one (O10)

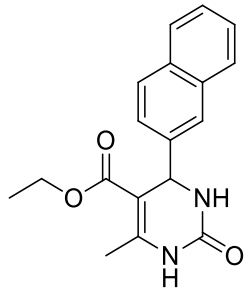

Yield 87 %, yellow solid, mp 211-213°C,

IR: 3247, 3123, 2975, 1719, 1658, 1459, 1292, 1226, 1088 cm^{-1}.

^{1}H NMR (500 MHz, DMSO-d_6): δ 1.08 (t, 3H, *J* = 7.0 Hz, CH_3CH_2), 2.29 (s, 3H, C(6)CH_3), 3.97 (q, 2H, *J* = 7.0 Hz, CH_3CH_2O), 5.32 (d, 1H, *J*= 3.0, C(4)H), 7.42-

7.53 (m, 4H, ArH), 7.67 (s, 1H, ArH), 7.82(bs, 1H, N(3)H), 7.85-7.91 (m, 3H, ArH), 9.24(s, 1H, N(1)H) ppm.

^{13}C NMR (125.68 MHz, DMSO-d_6): δ 14.1, 17.9, 54.3, 59.18, 99.01, 124.6, 124.9, 125.9, 126.3, 127.5, 127.8, 128.3, 132.3, 132.7, 142.15, 148.5, 152.01, 165.3 ppm.

ESI-MS, *m/z 311* $[M+H]^+$ 333.5 $[M+Na]^+$.

5-Ethoxycarbonyl-6-methyl-4-(naphthalen-1-yl)-3,4-dihydropyrimidin-2(1H)-one (O11)

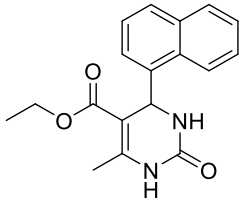

Yield 89%, yellow solid , mp 251-252°C,

IR: 3239, 3110, 2987, 2931, 1707, 1649, 1467, 1315, 1223, 1086, 793, 779 cm^{-1}.

^{1}H NMR (500 MHz, DMSO-d_6): δ 0.81 (t, 3H, J = 7.0 Hz, CH_3CH_2), 2.35 (s, 3H, C(6)CH_3), 3.80 (q, 2H, CH_3CH_2O), 6.06 (d, 1H, J= 3.0, C(4)H), 7.45-7.64 (m, 1H, ArH), 7.80 (s, 1H, N(3)H), 7.85 (m, 2H, ArH), 7.94 (t, 2H, J = 8 Hz, ArH), 8.05 (d, 1H, J = 8.5 Hz, ArH), 8.30 (d, 1H, J = 8.0 Hz, ArH), 9.25(s, 1H, N(1)H) ppm.

^{13}C NMR (125.68 MHz, DMSO-d_6): δ 13.8, 17.8, 49.8, 56.5, 99.1, 122.43, 123.28, 123.42, 127.74, 128.43, 128.50, 140.4, 148.7, 151.6, 157.30, 159.53, 165.27 ppm.

ESI-MS, *m/z* 311.4 $[M+H]^+$ 333.4 $[M+Na]^+$.

5-ethoxycarbonyl-4-(2-thienyl)-6-methyl-3,4-dihydropyrimidin-2(1H)-one (O12)

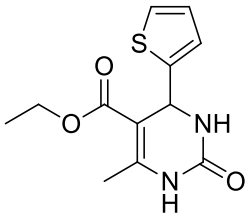

Yield 61%, yellow solid.

^{1}H-NMR (500 MHz, DMSO-d_6): δ 1.15 (t, 3H, *J*= 7.2 Hz, CH_2CH_3), 2.20 (s, 3H, C(6)CH_3), 4.05 (q, 2H, *J*= 7.2 Hz, CH_2CH_3); 5.40 (d, 1H, *J*= 3.2 Hz, C(4)H), 6.49-6.87 (m, 2H, thyenyl), 7.35-7.33 (m, 1H, thyenyl), 7.90 (s, 1H, N(3)H); 8.31 (s, 1H, N(1)H) ppm.

^{13}C-NMR (125.68 MHz, DMSO-d_6): δ 14.62, 18.14, 49.79, 59.85, 79.62, 100.24, 123.99, 125.116, 127.15, 149.13, 152.72, 165.50. ppm.

5-ethoxycarbonyl-4-(3-thienyl)-6-methyl-3,4-dihydropyrimidin-2(1H)-one (O13)

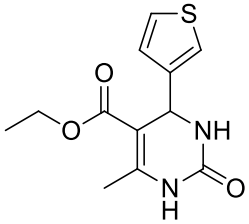

Yield 58%, yellow solid.

^{1}H-NMR (500 MHz): δ 1.14 (t, 3H, *J*= 7.2 Hz, CH_2CH_3), 2.20 (s, 3H, C(6)CH_3), 4.03 (q, 2H, *J*= 7.2 Hz, CH_2CH_3); 5.19 (d, 1H, *J*= 3.2 Hz, C(4)H), 6.97 (d, 1H, *J*= 4.8 Hz, thyenyl), 7.14 (s, 1H, thyenyl), 7.45 (t, 3H, *J*= 4.8 Hz, thyenyl), 7.75 (s, 1H, N(3)H); 9.19 (s, 1H, N(1)H) ppm.

^{13}C-NMR (125.68 MHz): δ 14.50, 18.07, 49.74, 59.63, 99.83, 121.09, 126.46, 126.99, 146.06, 148.77, 152.96, 165 ppm.

5-ethoxycarbonyl-4-(2-NO2-thienyl)-6-methyl-3,4-dihydropyrimidin-2(1H)-one (O14)

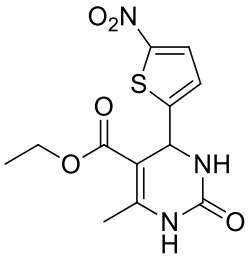

Yield 50%, yellow solid.

^{1}H-NMR (500 MHz): δ 1.20 (t, 3H, *J*= 7.2 Hz, CH_2CH_3), 2.22 (s, 3H, C(6)CH_3), 4.10 (q, 2H, *J*= 7.2 Hz, CH_2CH_3); 5.43 (d, 1H, *J*= 3.2 Hz, C(4)H), 7.2 (s, 1H, thyenyl), 8.00 (d, 1H, *J*= 5 Hz, thyenyl), 8.18 (s, 1H, N(3)H); 9.58 (s, 1H, N(1)H) ppm.

5-Benzyloxycarbonyl-6-methyl-4-phenyl-3,4-dihydropyrimidin-2(1H)-one (O15)

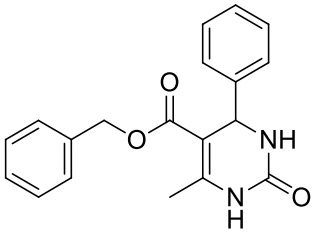

Yield 90 %, white solid, mp 168 – 170 °C.

IR: 3358, 3115, 3028, 1705, 1686, 1497, 1376, 1176, 1138, 1107, 1085 cm^{-1}.

^{1}H NMR (500 MHz, DMSO-d_6): δ 2.27 (s, 3H, C(6)-CH_3), 5.01 (d, 1H, *J* = 12.8 Hz, $PhCH_2$), 5.05 (d, 1H, *J* = 12.8 Hz, $PhCH_2$), 5.17 (d, 1H, *J* = 3.2 Hz, C(4)H), 7.10-7.35(m, 10H, 2xPh), 7.74 (bs, 2H, N(3)H), 9.25 (bs, 2H, N(1)H) ppm.

ESI-MS, *m/z*: 323 $[M+H]^+$.

6-methyl-2-oxo-4-phenyl-1,2,3,4-tetrahydropyrimidine-5-carboxamide (O16)

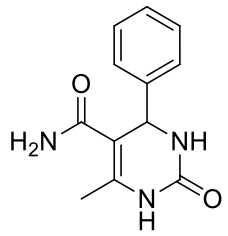

Yield 47 %, white solid, mp 220 – 222 °C.

^{1}H NMR (500 MHz, DMSO-d_6): δ 2.06 (s, 3H, C(6)-CH_3), 5.23 (d, 1H, J = 3 Hz, C(4)H), 6.90 (bs, 2H, C(=O)NH_2), 7.21-7.35(m, 6H, Ph), 7.49 (s, 1H, N(3)H), 8.55(s, 1H, N(1)H) ppm.

^{13}C NMR (125.68 MHz, DMSO-d_6): δ 17.54, 55.13, 126.83, 127.61, 128.75, 139.24, 144.88, 153.12, 168.59 ppm.

ESI-MS, *m/z*: 232 $[M+H]^+$.

6.8.2.2 3,4-dihydropyrimidin-2(1H)-thiones S1-8 (Table 16)

R^1	R^2	Product name
Phenyl	EtO	**S1**
Phenyl	MeO	**S2**
Phenyl	BnO	**S3**
4-fluoro-phenyl	EtO	**S4**
Benzothiophen-2-yl	EtO	**S5**
2-Naphtyl	EtO	**S6**
1-Naphtyl	EtO	**S7**
Phenyl	(-)MenthylO	**S8**

Table 16 *2-thioDHPMs synthesized (R^3= methyl)*

5-Ethoxycarbonyl-6-methyl-4-phenyl-3,4-dihydropyrimidin-2(1H)-thione (S1)

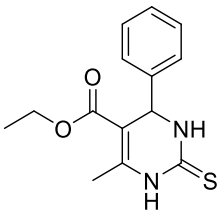

Yield 85%, white solid, mp 206-208 °C,

IR: 1668, 1573, 1462, 1283, 1195, 1117 cm^{-1}.

^{1}H NMR (500 MHz, DMSO-d_6): δ 1.10 (t, 3H, J = 7.0 Hz, OCH_2CH_3), 2.29 (s, 3H, $C(6)CH_3$); 4.01 (q, 2H, J = 7.0 Hz, CH_2CH_3); 5.17 (d, 1H, J = 3.5 Hz, C(4)H); 7.21-7.36 (m, 5H, Ph), 9.64 (s, 1H, N(3)H); 10.32 (s, 1H, N(1)H) ppm.

^{13}C NMR (125.68 MHz, DMSO-d_6): δ 14.5, 18.2, 54.5, 60.0, 101.1, 128.8, 128.1, 129.0, 143.9, 145.5, 165.6, 174.7 ppm.

ESI-MS, *m/z*: 277.4 $[M+H]^+$; 299.4 $[M+Na]^+$.

5-Methoxycarbonyl-6-methyl-4-phenyl-3,4-dihydropyrimidin-2(1H)-thione (S2)

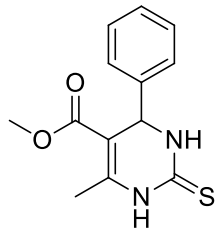

Yield 87 %, light yellow solid, mp 220-222 °C,

IR: 1711, 1572, 1459, 1318, 1280, 1180, 1113 cm^{-1}.

^1H NMR (500 MHz, DMSO-d_6): δ 2.29 (s, 3H, C(6)CH_3), 3.56 (s, 3H, OCH_3), 5.18 (d, 1H, J = 3.5 Hz, C(4)H), 7.21-7.36 (m, 5H, Ph), 9.66 (s, 1H, N(3)H), 10.35 (s, 1H, N(1)H) ppm.

^{13}C NMR (125.68 MHz, DMSO-d_6): δ 17.2, 51.1, 53.9, 100.4, 126.3, 127.7, 128.6, 143.3, 145.3, 165.6, 174.25 ppm.

ESI-MS, *m/z*: 263.4 $[M+H]^+$; 285.4 $[M+Na]^+$.

5-Benzoxycarbonyl-6-methyl-4-phenyl-3,4-dihydropyrimidin-2(1H)-thione **(S3)**

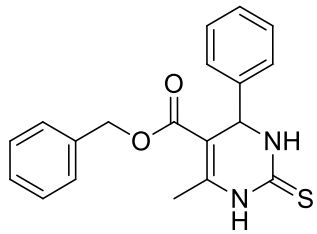

Yield %, yellow solid, mp 157-159°C,

^1H NMR (500 MHz, DMSO-d_6): δ 2.31 (s, 3H, C(6)CH_3), 5.02 (d, 1H, J = 12.5 Hz, $PhCH_2$), 5.09 (d, 1H, J = 12.5 Hz, $PhCH_2$) 5.20 (d, J = 4.0 Hz, 1H, C(4)H), 7.84-8.36 (m, 10H, Ph), 9.63 (s, 1H, N(3)H), 10.38 (s, 1H, N(1)H) ppm.

ESI-MS, *m/z*: 339.4 $[M+H]^+$.

5-Ethoxycarbonyl-4-(4-fluorophenyl)-6-methyl-2-thioxo-3,4-dihydropyrimidine-2(1H)-thione (S4)

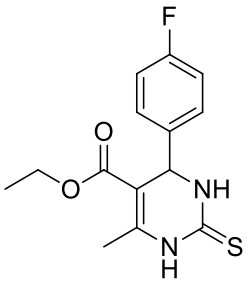

Yield 68%, light yellow solid, mp 188-190°C,

IR: 3391, 1711, 1586 cm^{-1}.

^{1}H NMR (400 MHz, DMSO-d_6): δ 1.9 (t, 3H, J = 7.0 Hz, OCH_2CH_3), 2.29 (s, 3H, $C(6)CH_3$), 4.00 (m, 2H, CH_2CH_3), 5.17 (d, 1H, J = 4.0 Hz, C(4)H), 7.11-7.29 (m, 5H, Ph), 9.65 (s, 1H, N(3)H), 10.36 (s, 1H, N(1)H) ppm.

^{13}C NMR (100 MHz, DMSO-d_6): δ 14.0, 17.2, 53.4, 59.6, 100.6, 115.3(d, ^{2}J = 17.0 Hz), 128.4 (d, ^{3}J = 7 Hz), 139.8 (d, ^{4}J = 2.0 Hz), 161.5 (d, ^{1}J = 194.0 Hz), 165.0, 174.2 ppm.

ESI-MS, *m/z*: 295 $[M+H]^{+}$.

5-Ethoxycarbonyl-4-(benzo[b]thiophen-1-yl)-6-methyl-3,4-dihydropyrimidin-2(1H)-one (S5)

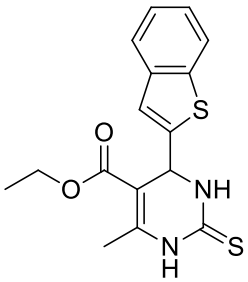

Yield 73%, pale orange solid, mp 211-213 °C (dec).

IR: 3272, 3167, 2978, 1705, 1558, 1310, 1182, 1100 cm^{-1}.

^{1}H NMR (500 MHz, DMSO-d_6): δ 1.19 (t, 2H, J = 7.1 Hz, CH_3CH_2), 2.30 (s, 3H, $C(6)CH_3$), 4.11 (q, 3H, J = 7.1 Hz, CH_3CH_2O), 5.52 (d, 1H, J = 3.5 Hz, C(4)H), 7.19 (s, 1H, thiophenyl CHC=), 7.29-7.38 (m, 2H, ArH), 7.81 (d, J = 8.2 Hz, 1H, ArH), 7.90 (d, J = 8.2 Hz, 1H, ArH), 9.87 (s, 1H, N(3)H), 10.56 (s, 1H, N(1)H) ppm.

^{13}C NMR (125.68 MHz, DMSO-d_6): δ 14.1, 17.1, 50.0, 59.85, 100.5, 120.5, 122.6, 123.7, 124.4, 124.5, 138.7, 138.9, 145.8, 147.4, 164.7, 174.9 ppm.

ESI-MS, *m/z*: 333.3 $[M+H]^+$.

5-Ethoxycarbonyl-6-methyl-4-(naphthalen-2-yl)-3,4-dihydropyrimidin-2(1H)-thione (S6)

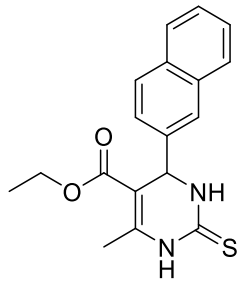

Yield 88 %, yellow solid, mp 183°C,

IR: 3435, 3209, 3097, 2961, 1693, 1559, 1461, 1335, 1214, 1146, 1023 cm^{-1}.

^1H NMR (500 MHz, , DMSO-d_6): δ 1.11 (t, 3H, J = 7 Hz, CH_3CH_2), 2.33 (s, 3H, C(6)CH_3), 4.00 (m, 2H, CH_3CH_2O), 5.34 (d, J= 3.5 Hz, C(4)H), 7.45(m, 1H, ArH), 7.54 (m, 2H, ArH), 7.71 (s, 1H, ArH), 7.93(m, 1H, ArH), 7.96 (m, 3H, Ph), 9.73 (s, 1H, N(3)H), 10.37 (s, 1H, N(1)H) ppm.

^{13}C NMR (125,68 MHz, DMSO-d_6): δ 14.47, 17.7, 54.8, 60.03, 100.92, 125.2, 125.4, 126.9, 126.6, 128.0, 128.3, 129.0, 132.9, 133.1, 141.2, 145.7, 165.6, 174.6 ppm.

ESI-MS, m/z 327 $[M+H]^+$ 349 $[M+Na]^+$.

5-Ethoxycarbonyl-6-methyl-4-(naphthalen-1-yl)-3,4-dihydropyrimidin-2(1H)-thione (S7)

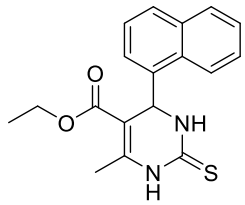

Yield 87 %, yellow powder, mp 223-225°C,

IR: 3427, 3208, 2967, 1695, 1562, 1454, 1334, 1210, 1143, 1021 cm^{-1}.

^1H NMR (500 MHz, DMSO-d_6): δ 0.83 (t, 3H, J = 7.0 Hz, CH_3CH_2), 2.39 (s, 3H, C(6)CH_3), 3.83 (m, 2H, CH_3CH_2O), 5.08 (d, 1H, J= 3.5 Hz, C(4)H), 7.38 (d, J = 7.0 Hz, 1H, ArH), 7.55 (m, 3H, ArH), 7.88 (d, J = 8.0 Hz, 1H, ArH), 7.95 (d, J = 8 Hz,

1H, ArH), 8.37 (d, *J* = 8 Hz, 1H, ArH), 9.64 (s, 1H, N(3)H), 10.37 (s, 1H, N(1)H) ppm.

^{13}C NMR (125.68 MHz, DMSO-d_6): δ 13.7, 17.1, 14.1, 49.7, 59.4, 100.8, 130.0, 133.4, 139.2, 145.3, 165.0, 173.7 ppm.

ESI-MS, m/z 327 $[M+H]^+$, 349 $[M+Na]^+$, 365 $[M+K]^+$.

(-)-Menthyl α-6-methyl-(4R,4S)-4-phenyl-3,4-dihydropyrimidin-2(1H)-thion-5-carboxylate (S8)

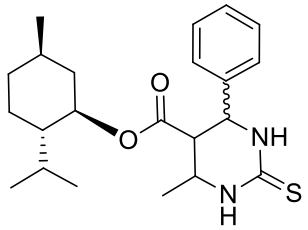

Yield 54%, white solid, d.e. 0% (*a* and *b*).

^{1}H NMR (500 MHz, DMSO-d_6): δ 0.37 (d, *a*, 1.5H, *J* = 9.0 Hz, $CHCH(CH_3)_2$), 0.52 (d, *a*, 1.5H, *J* = 8.5 Hz, $CHCH(CH_3)_2$), 0.67 (d, *b*, 1.5 H, *J* = 9.0 Hz, $CH(CH_3)_2$),), 0.70 – 2.00 (m, *a* and *b*, 10.5H, CH and CH_2 mentyl), 2.16 (s, *b*, 1.5H, C(6)-CH_3), 2.43 (s, *a*, 1.5H, C(6)-CH_3), 4.47-4.80 (m, *a* and *b*, 2H, OCH), 5.16 (d, *a*, 0.5H, *J* = 4.5 Hz, C(4)H), 5.17 (d, *a*, 0.5H, *J* = 4.5 Hz, C(4)H), 7.18-8.01 (m, *a* and *b*, 10H, Ph) ppm, 10.02 (s, *a* and *b,* 1H, NH).

6.8.3 *Synthesis of 3,4-dihydropyrimidin-2(1H)-imine derivatives (N1-19)*

Method A[120]***:***

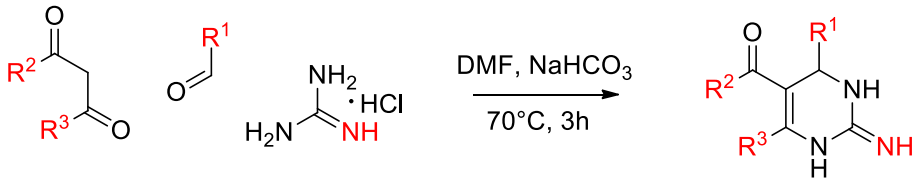

To a 0.5 M DMF solution of the appropriate aldehyde (1mmol), β-ketoester (1.1mmol), guanidine hydrochloride (1.5 mmol), and sodium hydrogen carbonate (4mmol) were added and the mixture stirred at 70°C for 3.5 hours (1.5 for **N14**). After cooling to room temperature, the mixture was poured into crushed ice. The solid formed was filtered, washed with cold water and finally triturated with diisopropyl ether or crystallized from hexane/ ethyl acetate (3:1), leading to **N1-19**.

Method B:

To a 0.5 M EtOH solution of the appropriate aldehyde (1mmol), were added the 1,3-dicarbonyl compound (1.1mmol), guanidine hydrochloride (1.5 mmol), and sodium hydrogen carbonate (4 mmol). The mixture was irradiated for ten minutes in a microvave oven at 120°C. For compound N1 the reaction mixture was poured into cold water and left in the fridge for 30min until complete precipitation of the product. The solid formed was filtered, washed with cold water and finally triturated with diisopropyl ether. In the case of compound **N17** the mixture was filtered and the solvent evaporated *in vacuo*, to give a residue that was crystallized from AcOEt.

Method C[137,166a]***:***

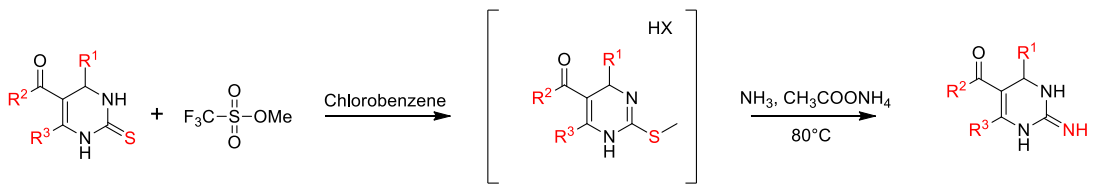

2-thio-DHPM (1mmol) was dissolved in chlorobenzene in a sealed reaction tube, then methyl trifluoromethansulfonate was added to the solution at 0°C in one portion. The reaction was stirred at r. t. and monitored by ^{1}H-NMR. After completation ammonium acetate (10mmol) was added to the mixture and ammonia gas was bubbled at 0°C for 30min, then the solution was heated at 100°C for 24h.

The sealed tube was cooled to r. t., opened and the suspension stirred in a current of argon to drive off the mercaptan by-product (take precautions). The solid was filtered and washed with water, then it was triturated with a NaOH solution (0.2M), left at 0°C for one hour and refiltered, leading to N1.

*6.8.3.1 3,4-dihydropyrimidin-2(1H)-imine N1-19 (*Table 17*)*

R^1	R^2	Product name
Phenyl	EtO	**N1**
Benzothiophen-2-yl	EtO	**N2**
2-Naphtyl	EtO	**N3**
Phenyl	MeO	**N4**
Phenyl	i-PrO	**N5**
Phenyl	BnO	**N6**
Methyl	EtO	**N7**
Buthyl	EtO	**N8**
4-fluoro-phenyl	EtO	**N9**
1-Naphtyl	EtO	**N10**
Biphenyl-4-yl	MeO	**N11**
4-(pyridin-2-yl) phenyl	MeO	**N12**
Benzyl	EtO	**N13**
Phenyl	EtO	**N14**[a]
Phenyl	NH_2	**N16**
Phenyl	$(CH_2)_5N$	**N17**
Phenyl	(-)MenthylO	**N18**
Phenyl	(-)BorneylO	**N19**

[a] R^3= Phenyl

Table 17 *2-iminoDHPMs synthesized (R^3 = phenyl)*[a]

Synthesized by Method A unless otherwise stated.

5-Ethoxycarbonyl-6-methyl-4-phenyl-3,4-dihydropyrimidin-2(1H)-imine (N1)

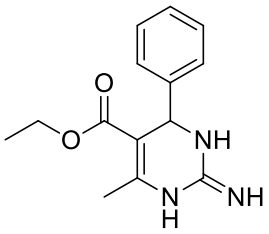

Method A: Yield 83.2%, white solid, mp 175-178°C.

Method B: Yield 65%, white solid, mp 175-178°C.

Method C: Yield 70%, white solid, mp 175-178°C.

IR: 3285, 1713, 1665, 1612, 1093 cm^{-1}.

^{1}H-NMR (500 MHz, DMSO-d_6): δ 1.05 (t, 3H, J = 7.3 Hz, CH_2CH_3), 2.17 (s, 3H, C(6)CH_3), 3.89 (q, 2H, J = 7.3 Hz CH_2CH_3), 5.17 (s, 1H, C(4)H), 6.16 (br, 2H, N(3)H and C(2)=NH), 7.15-7.30 (*m*, 5H, Ph), 7.39 (*s*, 1H, N(1)H) ppm.

^{13}C NMR (125.68 MHz, DMSO-d_6): δ 14.8, 23.9, 53.2, 58.65, 97.9, 126.9, 127.6, 128.8, 147.4, 155.9, 161.3, 166.9 ppm.

ESI-MS, *m/z*: 260.4 $[M+H]^+$.

5-Ethoxycarbonyl-4-(benzo[b]thiophen-2-yl)-6-methyl-3,4-dihydropyrimidin-2(1H)-imine (N2)

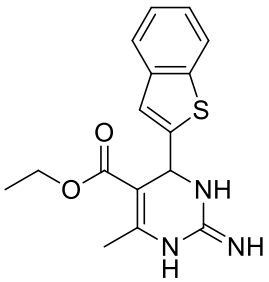

Yield 80%, light brown solid, mp 130-132 °C (dec).

IR: 3340, 3112, 1710, 1559, 1244, 1096 cm^{-1}.

^{1}H NMR (500 MHz, DMSO-d_6): δ 1.16 (t, 2H, J = 7.2 Hz, CH_3CH_2), 2.18 (s, 3H, C(6)CH_3), 4.02 (q, 3H, J = 7.2 Hz, CH_3CH_2O), 5.57 (s, 1H, C(4)H), 6.45 (bs, 2H,

N(1)H and C(2)=NH), 7.11(s, 1H, N(3)H), 7.22-7.35 (m, 2H, ArH), 7.65 (s, 1H, N(3)H), 7.74 (d, J = 7.8 Hz, 1H, ArH), 7.85 (d, J = 7.8 Hz,1H, ArH) ppm.

^{13}C NMR (125.68 MHz, DMSO-d_6): δ 14.5, 23.6, 48.8, 58.3, 97.0, 118.9, 122.5, 123.2, 123.9, 124.2, 138.8, 139.1, 151.4, 155.5, 161.6, 165.7 ppm.

ESI-MS, *m/z*: 316.4 $[M+H]^+$.

5-Ethoxycarbonyl-6-methyl-4-(naphthalen-1-yl)-3,4-dihydropyrimidin-2(1H)-imine (N3)

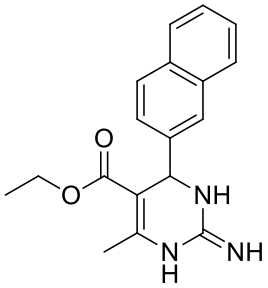

Yield 71%, light brown solid, mp 165.2–167.3 °C.

IR: 3350, 2923, 2854, 1703, 1661, 1602, 1094 cm^{-1}.

^{1}H NMR (500 MHz, DMSO-d_6): δ 1.06 (t, 3H, J = 7.4 Hz, CH_3CH_2), 2.24 (s, 3H, C(6)CH_3), 3.92 (q, 2H, J = 7.4 Hz, CH_3CH_2O), 5.38 (s, C(4)H), 6.24 (s, 2H, N(1)H, C(2)=NH), 7.43-7.51 (m, 4H, ArH), 7.64 (s, 1H, ArH), 7.85 (m, 3H, ArH and N(3)H) ppm.

^{13}C NMR (125.68 MHz, DMSO-d_6): δ 14.8, 23.6, 53.4, 58.7, 97.8, 124.7, 125.6, 126.1, 126.6, 127.9, 128.2, 128.6, 132.7, 133.1, 144.1, 155.3, 160.3, 166.5 ppm.

ESI-MS, *m/z:* 310.1 $[M+H]^+$.

5-Methoxycarbonyl-6-methyl-4-phenyl-3,4-dihydropyrimidin-2(1H)-imine (N4)

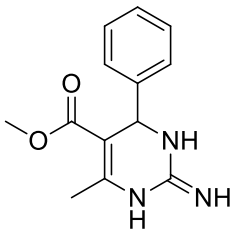

Yield 80%, yellow solid, mp 112-118°C.

IR: 3030, 2950, 1697, 1626, 1557, 1495, 1431, 1345, 1238, 1188, 1087 cm^{-1}.

^{1}H NMR (500 MHz, DMSO-d_6): δ 2.20 (*s*, 3H, CH_3), 3.46 (*s*, 3H, OCH_3), 5.19 (*s*, 1H, C(4)H), 6.21 (br, 2H, N(1)H) and C=NH), 7.21-7.30 (*m*, 5H, Ph), 7.41 (*s*, 1H, N(3)H) ppm.

^{13}C NMR (125 MHz, DMSO-d_6): δ 23.8, 49.9, 52.4, 96.7, 126.1, 126.9, 128.2, 146.5, 155.45, 161.4, 166.6 ppm.

ESI-MS, *m/z*: 246.4 $[M+H]^+$.

5-Isobutoxycarbonyl-6-methyl-4-phenyl-3,4-dihydropyrimidin-2(1H)-imine (N5)

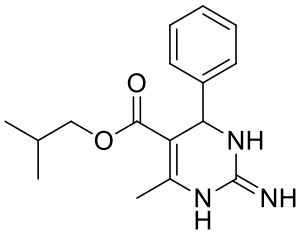

Yield 73 %, yellow solid, mp 115-117 °C.

IR: 3316, 2958, 1692, 1626, 1598, 1493, 1470, 1376, 1230, 1080 cm^{-1}.

^{1}H NMR (500 MHz, DMSO-d_6): δ 0.72 (d, J = 3.5 Hz, 3H, CH_2CHCH_3), 0.74 (d, J = 3.5 Hz, 3H, OCH_2CHCH_3), 1.71 (m, 1H, $CH(CH_3)_2$), 2.20 (*s*, 3H, C(6)-CH_3), 3.64 (dd, J = 10.6, 6.3 Hz, 2H, OCH_2CHCH_3), 5.18 (s, 1H, C(4)H),6.13 (s, 2H, N(1)H and C(2)=NH),7.16-7.29 (*m*, 6H, N(3)H and Ph) ppm.

^{13}C NMR (125.68 MHz, DMSO-d_6): δ 19.46, 19.49, 24.2, 27.9, 53.1, 68.9, 97.2, 126.7, 127.4, 128.6, 146.9, 155.7, 161.9, 166.6 ppm.

ESI-MS, *m/z*: 288.4 $[M+H]^+$.

5-Benzyloxycarbonyl-6-methyl-4-phenyl-3,4-dihydropyrimidin-2(1H)-imine (N6)

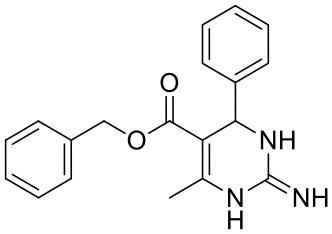

Yield 47 %, ocher solid, mp 142 – 145 °C.

IR: 3435, 3359, 3030, 1701, 1629, 1454, 1376, 1232, 1076, 1028, 833, 732, 696 cm^{-1}.

^{1}H NMR (500 MHz, $CDCl_3$): δ 2.31 (s, 3H, C(6)-CH_3), 4.99 (d, 1H, J = 12.6 Hz, $PhCH_2$), 5.07 (d, 1H, J = 12.6 Hz, $PhCH_2$), 5.33 (s, 1H, C(4)H), 5.91 (bs, 2H, N(1)H and C(2)=NH), 6.95-7.45(m, 12H, 2xPh and N(3)H) ppm.

^{13}C NMR (125.68 MHz, $CDCl_3$): δ 22.6, 53.9, 65.8, 101.4, 126.6,127.9, 128.4, 128.8, 136.1 143.4, 152.6, 165.5 ppm.

ESI-MS, *m/z*: 322.5 $[M+H]^+$.

5-Ethoxycarbonyl-4, 6-dimethyl-3,4-dihydropyrimidin-2(1H)-imine (N7)

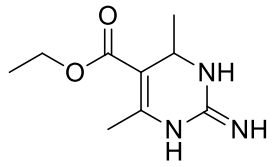

Yield 40%, white solid, mp 195-197°C

IR: 3392, 3305, 3090, 2977, 1663, 1587, 1228, 1156, 1094, 1067 cm^{-1}

^{1}H-NMR (500 MHz, DMSO-d_6): δ 0.97 (d, 3H, J = 6.0 Hz, CH(4)CH_3), 1.16 (t, 3H, J = 7.0 Hz CH_2CH_3), 2.10 (s, 3H, C(6)CH_3), 3.99 (m, 2H, CH_2CH_3) 4.18 (q, 1H, J= 6 Hz C(4)H), 6.05 (b*s*, 1H, N(3)H), 6.81 (*s*, 1H, N(1)H) ppm.

^{13}C-NMR (125.68 MHz, DMSO-d_6): δ 15.0,. 23.8, 23.9, 45.4, 58.4, 98.7, 155.8, 160.6, 166.5 ppm.

ESI-MS: (m/z) 198 $[M+H]^+$.

5-ethoxycarbonyl-4-butyl-6-methyl-3,4-dihydropyrimidin-2(1H)-imine (N8)

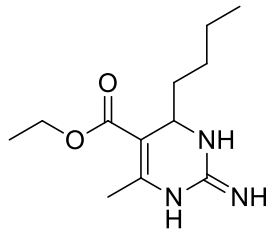

Yield 53%, light yellow solid, mp 110-115°C,

IR: 3300, 1710, 1670, 1616, 1458, 1376, 1257, 1094 cm^{-1}.

^{1}H NMR (400 MHz, DMSO-d_6): δ 0.85 (t, 3H, J = 7.2 Hz, $CH_3(CH_2)_3$), 1.16 (t, 3H, J = 7.2 Hz, CH_3CH_2O), 1.17-1.35 (m, 6H, $CH_3(CH_2)_3$), 2.10 (s, 3H, C(6)CH_3), 3.90-4.05 (m, 2H, CH_3CH_2O), 4.09 (d, 1H, J = 6.5 Hz, C(4)H), 6.01 (bs, 2H, N(1)H and C=NH,), 6.90 (bs, 1H, N(3)H) ppm.

^{13}C NMR (100 MHz, DMSO-d_6): δ 14.0, 14.5, 22.0, 23.4, 25.8, 36.5, 48.9, 57.9, 97.4, 155.6, 165.1, 166.1 ppm.

ESI-MS, *m/z*: 240.1 $[M+H]^+$.

5-Ethoxycarbonyl-4-(4-fluorophenyl)-6-methyl-3,4-dihydropyrimidine-2(1H)-imine(N9)

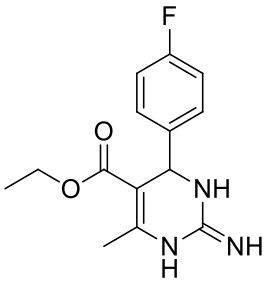

Yield 70%, yellow solid, mp 113-115°C.

IR: 3300, 1710, 1664, 1232, 1089, 832 cm^{-1}.

^{1}H-NMR (500 MHz, DMSO-d_6): δ 1.07 (t, 3H, J = 7.3 Hz, CH_2CH_3), 2.20 (s, 3H, C(6)CH_3), 3.91 (q, 2H, J = 7.3 Hz CH_2CH_3), 5.20 (s, 1H, C(4)H), 6.29 (br, 2H, N(3)H and C(2)=NH), 7.05-7.30 (*m*, 5H, Ph + N(1)H) ppm.

^{13}C NMR (125 MHz, DMSO-d_6): δ 14.3, 23.5, 52.0, 58.1, 97.1, 114.8 (d, ^2J = 21.3 Hz), 128.1 (d, ^3J = 8.8 Hz), 143.0 (d, ^4J = 2.5 Hz), 155.1, 161.1 (d, ^1J = 236.0 Hz), 166.1 ppm.

ESI-MS, *m/z*: 278.4 $[M+H]^+$.

5-Ethoxycarbonyl-6-methyl-4-(naphthalen-1-yl)-3,4-dihydropyrimidin-2(1H)-imine (N1O)

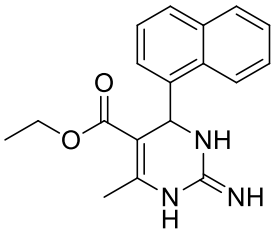

Yield 76%, pale yellow solid, mp 165.2-167.3 °C.

IR: 3380, 3187, 1652, 1585, 1071 cm^{-1}.

^{1}H NMR (500 MHz, DMSO-d_6): δ 0.82 (t, 3H, J = 7.4 Hz, CH_3CH_2), 2.32 (s, 3H, CH_3), 3.77 (m, 2H, J = 7.4 Hz, CH_3CH_2O), 5.98 (bs, 1H, NH), 6.08 (s, 1H, C(4)H), 7.24 (bs, 1H, NH), 7.35 (bd, 1H, J = 6.2 Hz, NH), 7.45 (t, 1H, J = 7.9 Hz, ArH), 7.52

(t, 1H, *J* = 7.1 Hz, ArH), 7.59 (t, 1H, *J* = 7.5 Hz, ArH), 7.81 (d, 1H, *J* = 7.9 Hz, ArH), 7.93 (d, 1H, *J* = 7.1 Hz, ArH), 8.35 (d, 1H, *J* = 7.5 Hz, ArH) ppm.

^{13}C NMR (125.68 MHz, DMSO-d_6): δ 14.2, 23.4, 48.7, 58.1, 96.4, 123.5, 124.4, 125.5, 125.8, 126.2, 127.5, 128.6, 130.1, 133.6, 141.3, 154.7, 166.2 ppm.

ESI-MS, *m/z*: 310.2 $[M+H]^+$.

5-Methoxycarbonyl-4-([1,1'-biphenyl]-4-yl)-6-methyl-3,4-dihydropyrimidine-2(1H)-imine (N11)

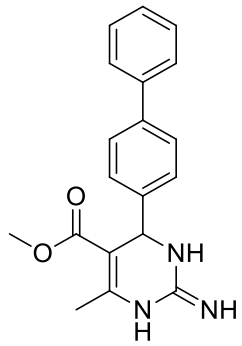

Yield 74%, orange solid, mp 152-157 °C.

IR: 3289, 1698, 1651, 1598, 1463, 1342, 1234, 1085 cm^{-1}.

^{1}H-NMR (400 MHz, DMSO-d_6): δ 2.26 (s, 3H, C(6)CH_3), 3.50 (s, 3H, CH_3O), 5.27 (s, 1H, C(4)H), 7.30-7.36 (m, 3H, ArH, N(3)H), 7.42-7.50 (m, 3H, ArH), 7.57-7.72 (m, 5H, ArH, N(1)H, C(2)=NH) ppm

^{13}C-NMR (125.68 MHz, DMSO-d_6): δ 22.4, 50.4, 52.2, 79.6, 98.2, 126.7, 126.8, 126.9, 127.4, 128.9, 139.2, 140.0, 155.0, 166.4 ppm.

ESI-MS, *m/z*: 322.1 $[M+H]^+$

5-Methoxycarbonyl-6-methyl-4-(4-(pyridin-2-yl)phenyl)-3,4-dihydropyrimidine-2(1H)-imine (N12)

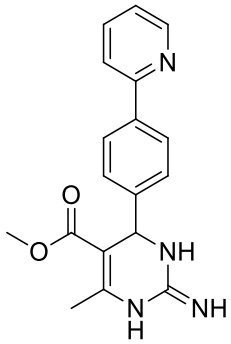

Yield 58%, light-orange solid, mp 137-142 °C.

IR: 3288, 1710, 1668, 1464, 1377, 1242 cm^{-1}.

^{1}H-NMR (500 MHz, DMSO-d_6): δ 2.22 (s, 3H, C(6)CH_3), 3.48 (s, 3H, CH_3O), 5.25 (s, 1H, C(4)H), 6.23 (bs, 2H, N(1)H, C(2)=NH), 7.33 (d, 2H, J = 7.5Hz, ArH), 7.46 (bs, 1H, N(3)H), 7.81 - 7.92 (m, 3H, ArH), 7.99 (d, 2H, J = 8.5 Hz, ArH), 8.64 (s, 1H, NArH) ppm.

^{13}C-NMR (125.68 MHz, DMSO-d_6): δ 23.3, 50.1, 52.8, 97.1, 120.2, 122.5, 126.6, 126.6, 137.2, 149.5, 137.6, 147.0, 155.0, 155.9, 166.5 ppm.

ESI-MS, *m/z*: 323.1 $[M+H]^+$

5-Ethoxycarbonyl-4-benzyl-6-methyl-3,4-dihydropyrimidine-2(1H)-imine(N13)

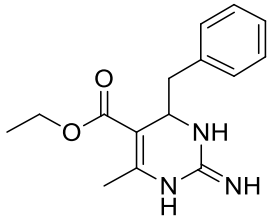

Yield 69%, ocher solid, mp 125-130°C (dec).

IR: 3385, 1702, 1661, 1494, 1456, 1377, 1239, 1089, 1030 cm^{-1}.

^{1}H-NMR (500 MHz, DMSO-d_6): δ 1.95 (t, 3H, J = 7.1 Hz, CH_3CH_2O), 2.21 (s, 3H, C(6)CH_3), 3.62-3.65 (m, 2H, CH_3CH_2O), 2.68-2.80 (m, 2H, CH_2Ph), 4.50-4.54 (m, 1H, C(4)H), 7.15-7.45 (m, 5H, ArH), 7.12 – 7.51 (s, 1H, N(1)H; s, 1H, C=NH; s, 1H, N(3)H) ppm.

^{13}C-NMR (125.68 MHz, DMSO-d_6): δ 20.6 23.1, 43.5, 50.9, 52.3, 71.2, 127.1, 128.9, 130.4, 138.3, 148.9, 154.8, 166.8 ppm.

ESI-MS (m/z): 261.1 $[M+H]^+$

5-Ethoxycarbonyl-4,6-diphenyl-3,4-dihydropyrimidin-2(1H)-imine (N14)

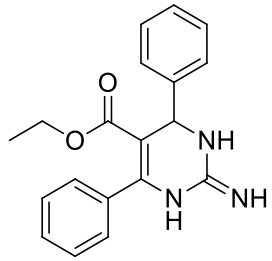

Yield 80%, solid, mp 242-245°C.

IR: 3393, 1670, 1228, 1076, 760, 697cm^{-1}.

^{1}H NMR (500 MHz, DMSO-d_6): δ 0.74 (t, 3H, J = 7.5 Hz, CH_3CH_2), 3.67 (m, 2H, J = 7.5 Hz, CH_3CH_2O), 5.30 (s, 1H, C(4)H), 6.31 (bs, 1H, NH), 7.30 (m, 11H, 2x Ph and NH) ppm.

^{13}C NMR (125.68 MHz, DMSO-d_6): δ 13.6, 52.9, 58.1, 97.6, 126.3, 126.8, 127.0, 127.1, 128.1, 128.3, 142.4, 146.2, 155.3, 161.0, 166.2. ppm

ESI-MS, *m/z*: 322 $[M+H]^+$.

2-Imino-6-methyl-4-phenyl-1,2,3,4-tetrahydropyrimidine-5-carboxamide (N16)

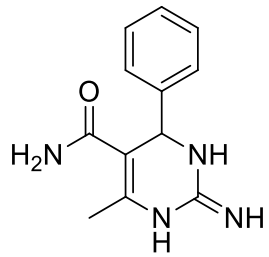

Method C: Yield 57 %, white solid.

^{1}H NMR (500 MHz, DMSO-d_6): δ 2.10 (s, 3H, C(6)CH_3), 5.35 (s, 1H, C(4)H), 6.94 (br, 2H, C(=O)NH_2), 7.28-7.48 (m, 8H, Ph+ 3xNH) ppm.

^{13}C NMR (125.68 MHz, DMSO-d_6): δ 18.86, 56.75, 109.73, 130.14, 131.10, 139.24, 131.15, 146.95, 155.73, 172.11, 179.80 ppm.

2-Imino-6-methyl-4-phenyl-5-(piperidin-1-carbonyl)-3,4-tetrahydropyrimidina (N17)

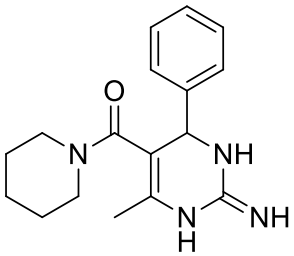

Method B: Yield 60 %, white solid.

^{1}H NMR (400 MHz, DMSO-d_6): δ 1.13 (bs, 4H, CH_2 piper), 1.35(bs, 4H, CH_2 piper), 1.56 (s, 3H, C(6)CH_3), 3.00 (bs, 2H, pCH_2piper), 5.11 (s, 1H, C(4)H), 5.50(br, 2H, 2xNH), 6.80 (br, 1H, NH), 7.10-7.38 (m, 5H, Ph) ppm.

^{13}C NMR (125.68 MHz, DMSO-d_6): δ 14.1, 20.9, 24.0, 25.4, 59.6, 103.6, 126.1, 127.1, 128.4, 145.8, 169.2, 170.3 ppm.

(-)-Menthyloxycarbonyl-α-6-methyl-(4R,4S)-4-phenyl-3,4-dihydropyrimidin-2(1H)-imine-5-carboxylate (N18)

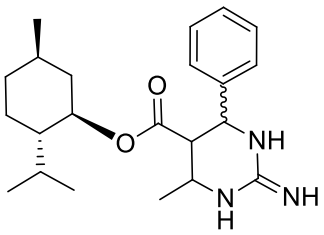

Yield 54%, white solid, d.e. 18% (major =**M**, minor= **m**).

IR: 3324, 2954, 2925, 2869, 1694, 1652, 1622, 1494, 1456, 1373, 1231, 1080, 961 cm^{-1}.

^{1}H NMR (500 MHz, DMSO-d_6): δ 0.40 (d, **M**, 1.77H, J = 7.0 Hz, $CHCH(CH_3)_2$) 0.52 (d, **M**, 1.77H, J = 7.0 Hz, $CHCH(CH_3)_2$, 0.69 (d, **m**, 1.23H, J = 7.0 Hz, $CH(CH_3)_2$),), 0.73 – 2.00 (m, **m**+**M**, 10H, CH and CH_2 menthyl), 2.18 (s, **m**, 1.23H, C(6)-CH_3), 2.23 (s, **M**, 1.77H, C(6)-CH_3), 4.46 (m, **m**+**M**, 1H, OCH), 5.16 (s, **M**, 0.59H, C(4)H), 5.18 (s, **m**, 0.41H, C(4)H), 6.07 (s, **M**, 1H, N(1)H and C(2)=NH), 6.13 (s, **m**, 1H, N(1)H and C(2)=NH), 7.24 (m, **m**+**M,** 6H, N(3)H and Ph) ppm.

^{13}C NMR (125 MHz, DMSO-d_6): δ 15.9, 16.9, 21.1, 21.3, 22.37, 22.42, 22.8, 23.6 , 23.8, 25.0, 26.5, 31.3, 31.4, 34.28, 34.31, 41.2, 41.8, 47.1, 47.3, 53.25, 53.30, 71.2,

71.6, 97.4, 98.0, 126.7, 126.8, 127.26, 127.29, 128.5, 128.6, 146.9, 147.1, 155.2, 155.4, 160.2, 161.1, 165.9, 166.1 ppm.

ESI-MS, *m/z*: 370.5 $[M+H]^+$.

(-)-Borneyloxycarbonyl 6-methyl-4-phenyl-1,2,3,4- tetrahydropyrimidine -2-imine-5- carboxylate (N19)

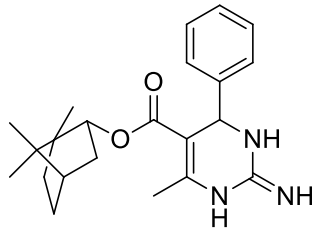

Yield 69%, light yellow solid, d.e. 9%(major =**M**, minor= **m**).

IR: 3330, 2954, 1654, 1624, 1492, 1454, 1375, 1230, 1077 cm^{-1}.

^1H NMR (400 MHz, $CDCl_3$): δ 0.41 (s, **M**, 1.62H, $C(CH_3)$). 0.75 (s, **m**, 1.38H, $C(CH_3)$), 0.77 (s, **M**, 1.62H, $C(CH_3)_2$), 0.79 (s, **m**, 1.38H, $C(CH_3)_2$), 0.80 (s, **m**, 1.38H, $C(CH_3)_2$), 0.82 (s, **M**, 1.62H, $C(CH_3)_2$), 0.86 (m, **m+M**, 2H, $CHCH_2CH$), 0.90 – 2.20(m, **m+M**, 5H, CCH_2CH_2CH), 2.23 (s, **M**, 1.62H, C(6)-CH_3), 2.24 (s, **m**, 1.38H, C(6)-CH_3), 4.61 (dt, **m**, 0.46H, J = 9.3, 2.3 Hz, OCH), 4.73 (dt, **M**, 0.54H, J = 9.3, 2.3 Hz, OCH), 5.24 (s, **m**, 0.46H, C(4)H), 5.25 (s, **M**, 0.54H, C(4)H), 6.12 (s, **m+M**, 1H, N(1)H), 7.00 – 7.34 (m, **m+M**, 7H, N(3)H, N(2)H and Ph) ppm.

^{13}C NMR (100 MHz, $CDCl_3$): δ 13.0, 13.5, 18.60, 18.63, 19.49, 19.52, 23.7, 26.8, 27.2, 27.4, 27.7, 36.4, 37.0, 44.1, 44.2 , 47.2 , 47.3, 48.07, 48.15, 52.66, 52.69, 76.8, 77.2, 126.3, 126.3, 126.9, 127.0, 128.2, 146,4, 155.0, 160.64, 161.5, 166.2 ppm.

ESI-MS, *m/z*: 368.5 $[M+H]^+$.

6.8.4 Hydrolysis of DHPMs

6.8.4.1 3,4-Dihydropyrimidin-2(1H)-thione

To a 0.34M ethanol solution of the 2-oxo or 2-thio-DHPM (1mmol) a 1M aqueous NaOH (5.88 mmol) was added. The resulting solution was refluxed under stirring and monitored by TLC (AcOEt 40% in hexane) till completion. The hot mixture was poured into fine crushed ice and acidified (pH~3). A solid precipitated that was filtered and dried.

5-Carboxy-6-methyl-4-phenyl-3,4-dihydropyrimidin-2(1H)-thione (S9)

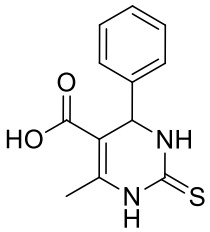

Yield 80%, orange solid, mp 145-148°C.

IR: 3240. 1685, 1460, 1176, 689 cm^{-1}.

^1H NMR (500 MHz, DMSO-d_6): δ 2.28 (s, 3H, C(6)CH_3), 5.15 (s, 1H, C(4)H), 7.00-7.50 (m, 5H, Ph), 9.57 (s, 1H, N(3)H), 10.22 (s, 1H, N(1)H) ppm.

6.8.4.2 3,4-Dihydropyrimidin-2(1H)-one/imine

The DHPM (1mmol) was dissolved in 2ml of MeOH. 10% Pd/C (10 wt % with respect of the substrate), and phenyl ethylamine (1mmol) were added to the solution under inert atmosphere. The reaction mixture was vigorously stirred at room temperature under 1atm H_2 pressure for 24 h, then it was filtered and concentrated *in vacuo* to give N18.

5-Carboxy-6-methyl-4-phenyl-3,4-dihydropyrimidin-2(1H)-one (O17)

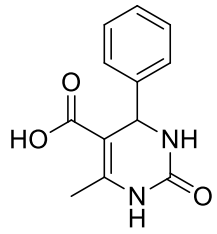

Yield 45%, white powder, mp 216-218°C

IR: 3433, 3227, 1706, 1645 cm^{-1}.

^{1}H-NMR (500 MHz, DMSO-d_6): δ 2.22 (s, 3H, C(6)CH_3), 5.10 (d, J= 4 Hz, 1H, C(4)H), 7.18-7.34 (m, 5H, Ph), 7.64 (s, 1H, N(3)H), 9.05 (s, 1H, N(3)H), 11.83 (s, 1H, OH).

ESI-MS: (m/z) 233 $[M+Na]^+$.

5-Carboxy-6-methyl-4-phenyl-3,4-dihydropyrimidin-2(1H)-imine (N15)

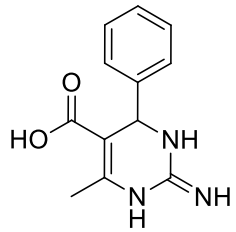

Yield 50%, light yellow solid, mp > 320°C.

IR: 3304, 2637, 1667, 1047, 833, 701cm^{-1}.

^{1}H NMR (500 MHz, DMSO-d_6): δ 2.23 (s, 3H, C(6)CH_3), 5.18 (d, 1H, J = 3.5 Hz, C(4)H), 7.21-7.65 (m, 5H, Ph), 7.65 (s, 1H, N(3)H), 9.05 (s, 1H, N(1)H), 13.12 (s, 1H, OH), ppm.

6.8.5 Synthesis of 5-carboxamide dihydropirimidinone

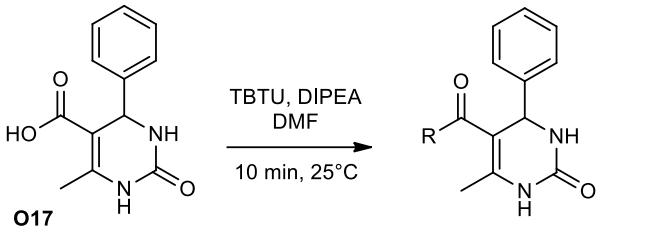

O18: R= piperidine
O19: R= n-propylamine

To a 1M DMF solution of **O17** (2 mmol) TBTU (3 mmol) and DIPEA (4 mmol) were added, under inert athmosphere . The reaction was stirred at 25°C for a few minutes, and then the appropriate amine (3mmol) was added followed by a second amount of DIPEA (4 mmol) The reaction was monitored by TLC ($CHCl_3$/MeOH: 9/1)until disappearance of the starting material. Then, 50 ml of H_2O was poured into the mixture, and the precipitated product was filtered and triturated with diisopropylether.

6-Methyl-4-phenyl-5-(piperidine-1-carbonyl)-3,4-dihydropyrimidin-2(1H)-one (O18)

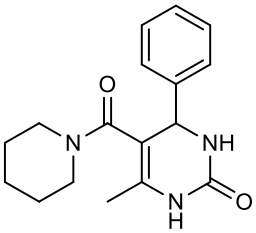

Yield: 60%, white solid.

^{1}H NMR (400 MHz, $CDCl_3$): δ 1.10 (s, 2H, CH_2), 1.33 (s, 2H, CH_2), 2.95 (s, 4H, CH_2NCH_2), 5.17 (s, 1H, C(4)H), 7.19 - 7.35 (m, 5H, Ph), 8.44 (br, 1H, N(3)H) ppm.

^{13}C NMR (100 MHz, $CDCl_3$): δ 15.73, 23.80, 25.16, 57.19, 100.81, 103.99, 126.34, 127.61, 128.02, 128.69, 144.25, 152.71, 166.69 ppm.

ESI-MS: *m/z*: 322.2 $[M+Na]^+$.

6-Methyl-2-oxo-4-phenyl-N-propyl-1,2,3,4-tetrahydropyrimidine-5-carboxamide (O19)

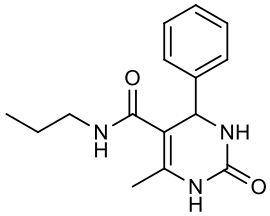

Yield 40%, yellow solid.

^{1}H NMR (400 MHz, $CDCl_3$): δ 0.68 (t, 3H, *J* = 7.2 Hz, $CH_2CH_2CH_3$), 1.20-1.32 (m, 4H, CH_2CH_2), 1.96 (s, 3H, C(6)CH_3), 5.22 (s, 1H, C(4)H), 7.13-7.35 (m, 5H, Ph), 7.40 (s, 1H, N(1)H), 7.50(m, 1H, NHC(=O)), 8.45 (br, 1H, N(3)H) ppm.

ESI-MS *m/z*: 296.2 $[M+Na]^+$.

6.8.6 *Synthesis of 3,4-dihydropyrimidin-2(1H-pyrazol-1-yl)-imine derivatives (NP1-2)*[164]

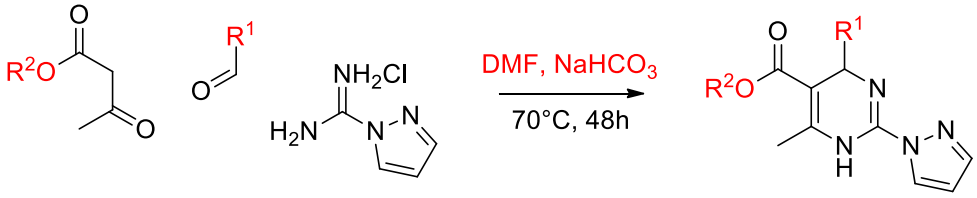

R^1	R^2	Product name
Phenyl	Ethyl	NP1
2-Naphtyl	Ethyl	NP2

0.7 M DMF solution of the appropriate aldehyde (1 mmol), β-ketoester (1.1 mmol), 1H-pyrazole-1-carboxamide hydrochloride (1.1 mmol), and sodium hydrogen carbonate (4mmol) were added and the mixture stirred at 70°C for 48 hours. After cooling to room temperature, the mixture was poured into cold water, extracted with Et_2O. The combined organic layer were dried over Na_2SO_4, filtered and concentrated *in vacuo*. The residue was purified by flash chromatography (siliga gel, Et_2O (20% to 45%) in hexane) as a mixture of tautomers, NP1-2.

5-Ethoxycarbonyl-6-methyl-4-phenyl-3,4-dihydropyrimidin-2(1H-pyrazol-1-yl)-imine (NP1)

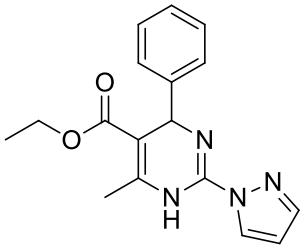

Yield 40%, pale yellow solid, mixture of tautomer (*a* and *b*).

IR: 3381, 3334, 2932, 1717, 1703, 1630, 1532, 1263, 1240, 1175, 1154, 1093 cm^{-1}.

^{1}H-NMR (400 MHz, $(CD_3)_2CO$, mixture of tautomer): δ 1.16 (t, *a,* 1.65H, *J* = 7.5 Hz, CH_2CH_3),1.18 (t, *b*, 1.35 H, *J* = 7 Hz, CH_2CH_3), 2.41 (s, *a,* 1.65 H, C(6)CH_3), 2.54 (s, *b,* 1.35 H, C(6)CH_3), 4.07 (m, *a* and *b*, 2H, *J* = 7.3 Hz, CH_2CH_3), 5.71 (s*, b,* 0.45 H, C(4)H), 5.75 (d*, a,* 0.55 H, *J* = 3.0 Hz, C(4)H), 6.48 (dd, *b*, 0.45H, *J* = 2.75 and 2 Hz, CHCHN), 6.52 (dd, *a,* 0.45H, *J* = 2.75 and 2.0 Hz, CHCHN), 7.2-7.5(m, *a* and *b,* 10H, Ph), 7.69 (d*, b*, 0.45 H, *J* = 1.5 Hz, CHNN), 7.70 (d*, a,* 0.55 H, *J* = 1.0 Hz, CHNN) 8.28 (d, *b*, 0.45 H, *J* = 3.0 Hz, CHNC(2)), (d, *a*, 0.45 H, *J* = 2.5 Hz, CHNC(2)), 8.60 (bs, *a*, 0.55H, NH), 8.78 (bs, *a,* 0.45H, NH) ppm.

13C NMR (100 MHz, $(CD_3)_2CO$) all peaks from both tautomers δ14.53, 14.56, 18.18, 18.25, 23.49, 54.58, 54.69, 59.62, 60.11, 60.17, 101.81, 101.77, 105.69, 109.28, 109.64, 127.65, 127.84, 128.02, 128.14, 128.61, 129.11, 129.25, 129.33, 142.17, 143.63, 142.18, 143.65, 157.28, 166.73, 166.90 ppm.

ESI-MS, *m/z*: 333.2 $[M+Na]^+$.

6.8.7 Derivatization of racemic DHPMs with chiral auxiliaries

For the formation of the diasteroisomers, three chiral auxiliaries (**8a**, **8b, 8c**) were taken into account with different DHPMs compounds.

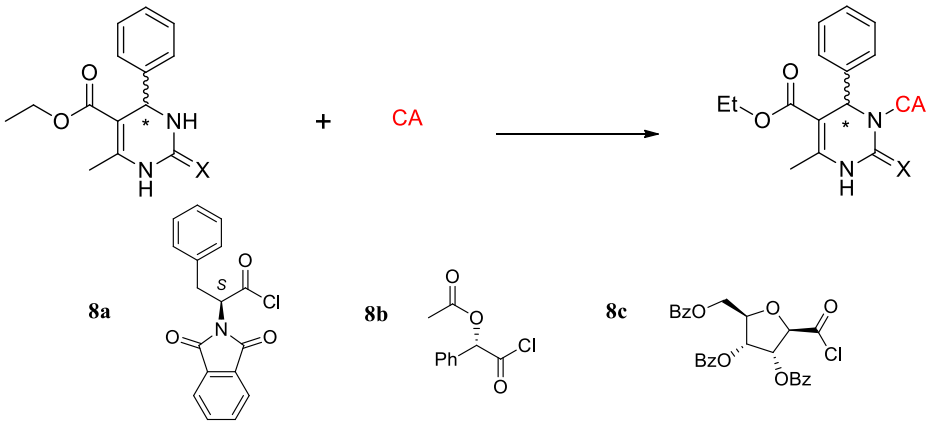

6.8.7.1 Formation of chloride:

(2S)-3-phenyl-2-phthalimidylpropanoyl chloride (8a)

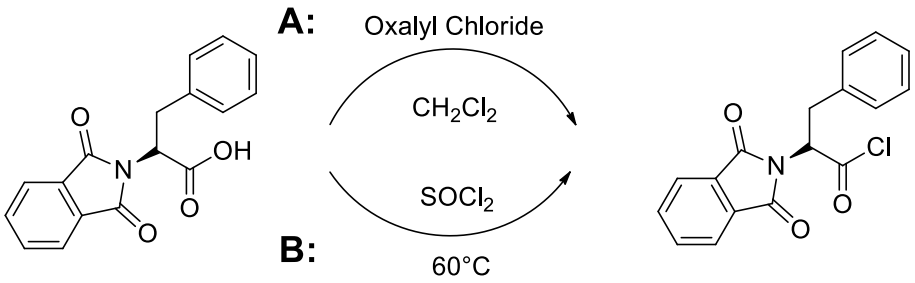

Figure 46 *Synthesis of 8a.*

Method A:

To a solution of N-phthaloyl-L-phenylalanine (1mmol) in CH_2Cl_2 (0.1M), under inert atmosphere, cooled to 0°C, oxalylchloride (1.5mmol) and a cat. Amount of DMF were added. The reaction mixture was stirred at r.t. over night. The excess oxalylchloride was removed under reduced pressure, and the residue (8a) was used in the next step without purification.

Method B:

N-phthaloyl-L-phenylalanine(1mmol) was mixed with thionyl chloride (1.2mmol) under inert atmosphere. The reaction mixture was stirred under heating at 60°C for 1.30 h, then it was cooled down and concentrated *in vacuo*. The residue was used in the next step without further purification.

(2S)-3-phenyl-2-phthalimidylpropanoyl chloride (8a)

Spectral and analytical data in accordance with the literature.[178]

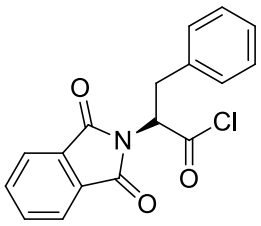

Yield 99%, white solid, mp 83°C.

^{1}H NMR (500 MHz, $CDCl_3$): δ 3.63 (m, 1H, Ph(Phe)CH_2), 3.73 (dd, 1H, J = 14.0, 5.0 Hz, Ph(Phe)CH_2), 5.43 (dd, 1H, J = 10.0, 5.0 Hz, PhCH_2CH), 7.23 (m, 5H, Ph(Phe)), 7.80 (m, 2*H,* Ph), 7.90 (m, 2*H,* Ph) ppm.

(S)-(+)-O-Acetyl mandelic chloride(8b)

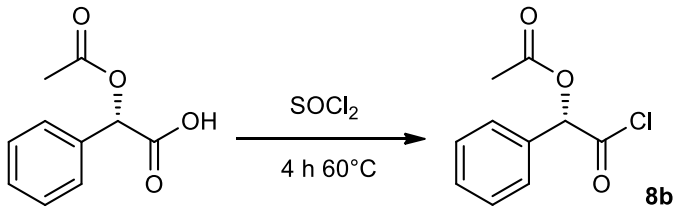

(S)-(+)-O-Acetyl mandelic acid (1mmol) was mixed with thionyl chloride (1.2mmol) under inert atmosphere. The reaction mixture was stirred under heating at 60°C for 4 h, then it was cooled down and concentrated *in vacuo*. The residue was used in the next step without further purification.

[178] S. Mallakpour, S. Sepehri *Reactive & Functional Polymers* **2008**, 68, 1459.

(S)-(+)-O-Acetyl mandelic chloride(8b)

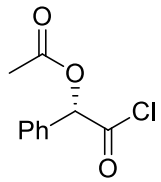

Yield 98%, yellow solid.

^{1}H NMR (270 MHz, $CDCl_3$): δ 2.22 (s, 3H, CH_3), 6.03 (s, 1H, CH), 7.45 (m, 5H, C_6H_5).

2,3,5-Tri-O-benzoyl-β-D-ribofuranosyl chloride (8c)

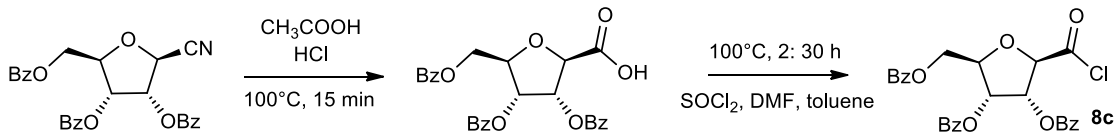

2,3,5-Tri-O-benzoyl-β-D-ribofuranosyl cianide (6.19 mmol), and conc. HCl (3 ml) in acetic acid (12 ml) was stirred at 100°C for 15 min. The solution was cooled to r.t. and poured into water (40 ml). The aqueous solution was extracted with ethyl acetate (40 ml) and the organic layer was washed with brine, dried over Na_2SO_4, and concentrated *in vacuo* to give a pale yellow oil, which was purified by flash chromatography on silica gel (gradient elution: 0–1% MeOH in DCM) to give the 2,3,5-tri-O-benzoyl-β-D-ribofuranosyl carboxylic acid as a colourless foam.
The acid was dissolved in toluene (0,5M respect to the acid), and added of thionyl chloride (1,5 eq.) under inert atmosphere. The mixture was then stirred at 100°C for 4 h. The solution was cooled down and concentrated *in vacuo*. The residue was used in the subsequent step without further purification.

2,3,5-Tri-O-benzoyl-β-D-ribofuranosyl acid

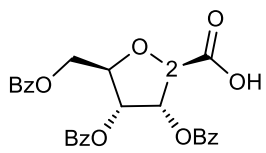

Yield: 65%, incolor oil.

^{1}H NMR (500 MHz, $CDCl_3$): δ 4.65 - 4.78 (m, 3H, H-5 and 2xH-6), 4.86 (d, 1H, H-2), 5.73 (dd, 1H, H-4), 5.97 (dd, 1H, H-3), 7.30-7.60 (m, 9H, ArH)7.87 - 8.10 (m, 6H, ArH).

ESI-MS, *m/z*: 513.2 $[M+Na]^+$.

2,3,5-Tri-O-benzoyl-β-D-ribofuranosyl chloride (8c)

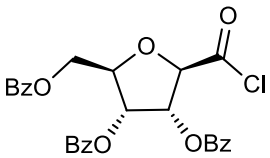

Yield: 70%, yellow oil.

^{1}H NMR(400 MHz, $CDCl_3$): δ 4.60-4.82 (m, 3H, H-5 e 2xH-6), 5.05 (d, 1H, J = 2.8 Hz, H-2), 5.87 (dd, 1H, J = 6.8, 5.2 Hz, H-4), 6.10 (dd, 1H, J = 5.4, 2.8 Hz, H-3), 7.30-7.60 (m, 9H, ArH), 7.90-8.05 (m, 6H, ArH) ppm.

6.8.7.2 Derivatization of NP1 and N1 with 8a

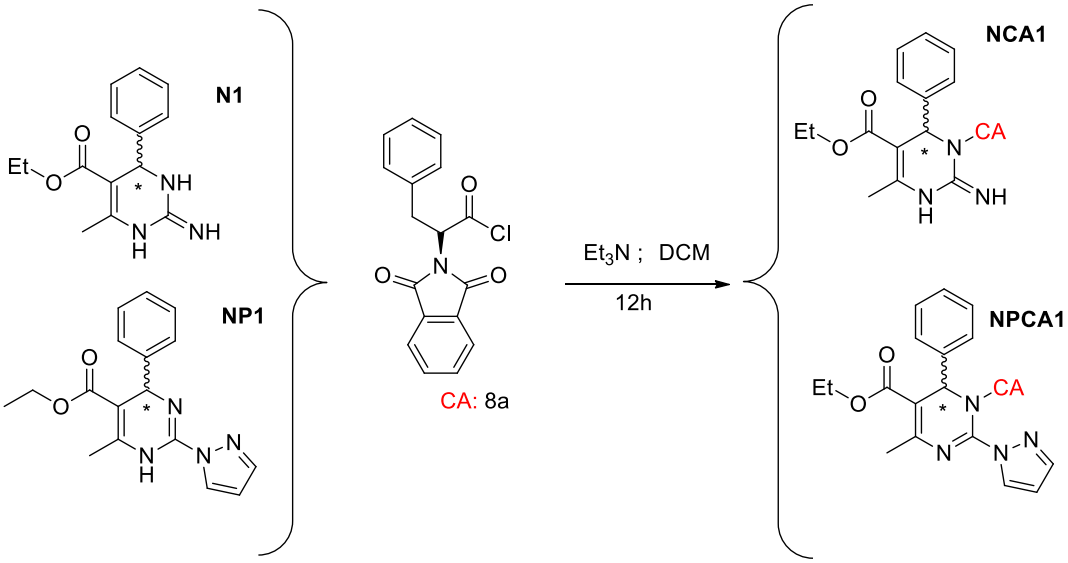

To a solution of compound N1or NP2 (1.1 mmol) in CH_2Cl_2 (0.07 M) under Ar, the chloride 8a (1mmol) and Et_3N (1mmol) were added. The reaction mixture was stirred at room temperature and monitored by TLC (AcOEt (20 or 40%) in hexane) till completion. The reaction mixture was neutralized with saturated $NaHCO_3$ solution,

and washed with water, brine, dried over Na_2SO_4, and concentrated *in vacuo*. The diasteroisomeric mixture was separated by flash chromatography (eluent AcOEt/ n-Hexane from 10% to 30%).

5 Ethoxycarbonyl-3-(2-(1,3-dioxoisoindolin-2-yl)-3-phenylpropanoyl)-6-methyl-4-phenyl-3,4-dihydropyrimidin-2(1H)-imine (NCA1)

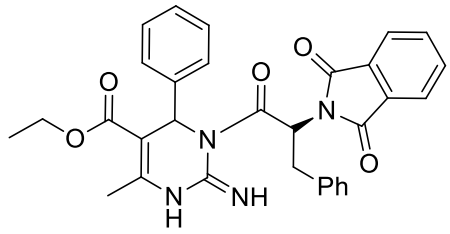

Yield 80%, light yellow solid, d.e.0% (*a* and *b*).

IR: 3233, 3062, 1774, 1713, 1634, 1281, 1072, 719 cm^{-1}

^1H NMR (400MHz, $CDCl_3$): δ 1.09 (t, 3H, J = 7.5 Hz, CH_3CH_2), 2.31 (d, 2H, J = 2.0 Hz, CH_3CH_2O), 3.37 (m, 1H, Ph(Phe)CH_2), 3.62(m, 1H, Ph(Phe)CH_2), 4.02 (m, 2H, CH_3CH_2), 4.93 (m, 1H, Ph(Phe)CH_2CH), 5.49 (s, 1H, C(4)H), 7.10 (m, 4H, Ph), 7.30 (m, 5H, Ph), 9.99(bs, 1H, C(2)=NH), 10.29 (bs, 1H, N(3)H) ppm.

^{13}C NMR (100 MHz, $CDCl_3$): δ 13.98 (*a*), 14.00 (*b*), 17.46 (*a* and *b*), 34.20 (*a*), 34.35 (*b*), 52.31 (*a*), 52.48 (*b*), 57.38 (*a*), 57.41 (*b*), 59.61 (*a*), 59.64 (*b*), 101.21 (*a*), 101.36 (*b*), 126.41 (*a*), 126.53 (*b*), 127.73 (*a*), 127.79 (*b*), 128.28 (*a*), 128.29 (*b*), 128.50 (*a* and *b*), 128.58 (*a*), 128.63(*b*), 131.08 (*a*), 131.09 (*b*), 134.59 (*a* and *b*), 138.45 (*a*), 138.42 (*b*), 143.35 (*a*), 143.44 (*b*), 146.08 (*a* and *b*), 154.39 (*a*), 154.45 (*b*), 164.67 (*a*), 164.71 (*b*), 167.59 (*a*), 167.60 (*b*) ppm.

ESI-MS, *m/z*: 322 $[M+H]^+$.

HPLC (Lux5uCell3, IPA 19% in Hex, 39bar, 1ml/min) r.t.(min): 16.5(Area: 50%), 37.4 (area 50%).

5-Ethoxycarbonyl 3-(2-(1,3-dioxoisoindolin-2-yl)-3-phenylpropanoyl)-6-methyl-4-phenyl-2-(1H-pyrazol-1-yl)- 3,4-dihydropyrimidine(NPCA1)

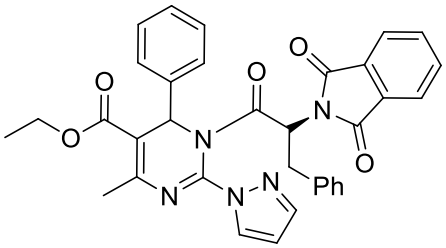

Yield 40 %, light yellow solid.

IR: 3318, 1775, 1717, 1388, 1239, 1102, 719 cm^{-1}.

^{1}H-NMR (400 MHz, $(CD_3)_2CO$, mixture of diasteroisomers): δ 1.29 (dt, 3H, CH_2CH_3), 2.58 (s, 3H, C(6)CH_3), 4.25 (m, 2H, J = 7.3 Hz, CH_2CH_3), 4.89 (m, 1H, Ph(Phe)CH_2), 5.04 (m, 1H, Ph(Phe)CH_2), 5.62 (s, 1H, C(4)H), 6.53 (dd, 1H, CHCHN), 6.73 (m, 1H, CHCHN),6.81 (dd, 1H, CHCHN), 7.0-7.45(m, 9H, Ph), 7.69 (m, 1H, CHNN), 8.0 (m, 1 H, CHNN) 8.03 (m, 1H, CHNC(2)), 8.21 (bs, 1H, NH), 8.38 (bs, 1H, NH) ppm.

6.8.7.3 Derivatization of NP1 with 8b

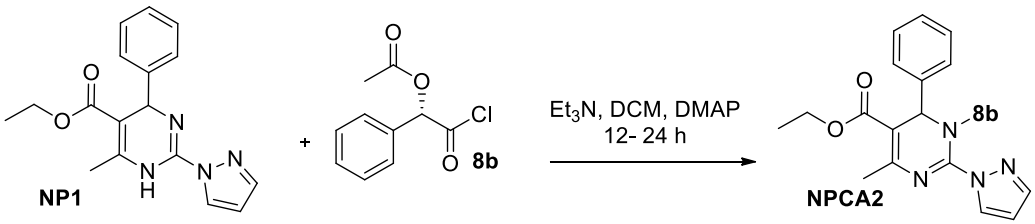

To a solution of compound **NP1** (1mmol) in CH_2Cl_2, in a round bottomed flask, were added **8b** (1 mmol), Et_3N (1 mmol) and DMAP under an inert atmosphere.

The mixture was left at r.t. 12-24h, and the reaction monitored by TLC (20-40 % AcOEt in hexane). H_2O was added and the organic layer extracted with saturated $NaHCO_3$, and brine, dried over Na_2SO_4 and evaporated to give an oily residue, identified as a 1:1 diastereoisomeric mixure of NPCA2. TFlash chromatography (eluent AcOEt/ n-Hexane from 10% to 30%) afforded one diasteroisomer in a pure form ($[\alpha]^{20°C}$= 50.4).

5-ethoxycarbonyl 3-((S)-2-acetoxy-2-phenylacetyl)-6-methyl-4-phenyl-2-(1H-pyrazol-1-yl)- 3,4-dihydropyrimidine(NPCA2)

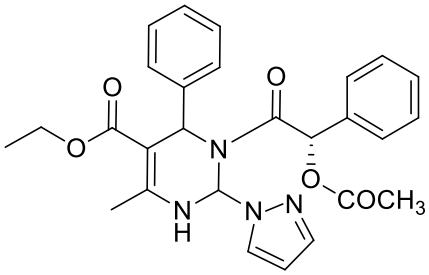

Yield:65%, white solid.

^{1}H-NMR(400 MHz, CD_3Cl_3, single diasteroisomer): δ 1.25 (t, 3H, J = 7.3 Hz, CH_2CH_3), 2.12 (s, 3H, C(6)CH_3), 2.14 (s, 3H, $OCOCH_3$), 4.20 (m, 2H, CH_2CH_3), 5.79 (s, 1H, N(3)C(=O)CH), 6.48 (dd, 1H, J = 2.4, 1.6Hz, CHCHN), 6.64 (s, 1H, C(4)H), 7,05 (dd, 1H, CHCHN), 6.98-7.48 (m, 10H, Ph), 7.83 (d, 1H, J = 1.2 Hz, CHN), 7.94 (m, 1H, J = 2.4 Hz, CHN) ppm.

6.8.7.4 Synthesis of diasteroisomers derived from 2-thioDHPMs

6.8.7.4.1 Synthesis of diasteroisomers with 8a

Method A[138]**:**

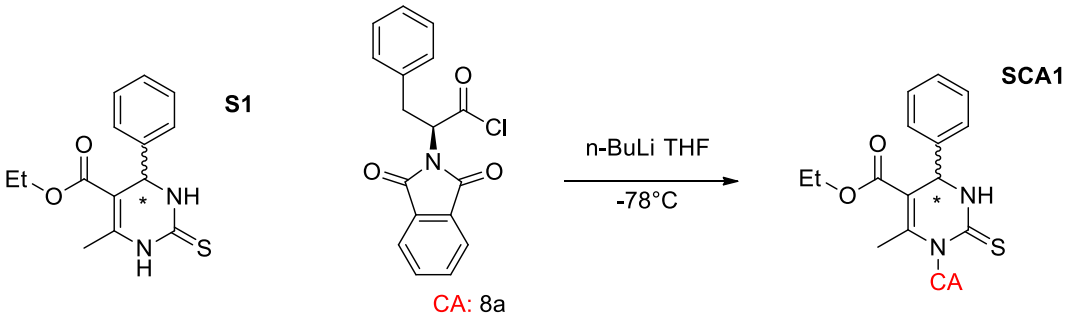

To a suspension of Thio-DHPM (1 mmol) in 10 ml dry THF under Ar, 1.6 N n-BuLi (1.1 mmol) was added drop wise at -78 °C, whereupon anion was formed. After the addition, reaction mixture was stirred at -78 °C for 30 min and quenched at -78 °C with enantiopure amino acid chloride 8a (1.5 mmol), dissolved in 10 ml dry THF.

The reaction was stirred at same low temperature till it was completed (TLC). A cold saturated aqueous solution of NH_4Cl (30 ml) was introduced at the same low temperature. The reaction contents were extracted with ethyl acetate or chloroform (3x10 ml), washed with water (2x25 ml), treated with brine, dried over anhydrous Na_2SO_4, and concentrated under reduced pressure.

Method B:

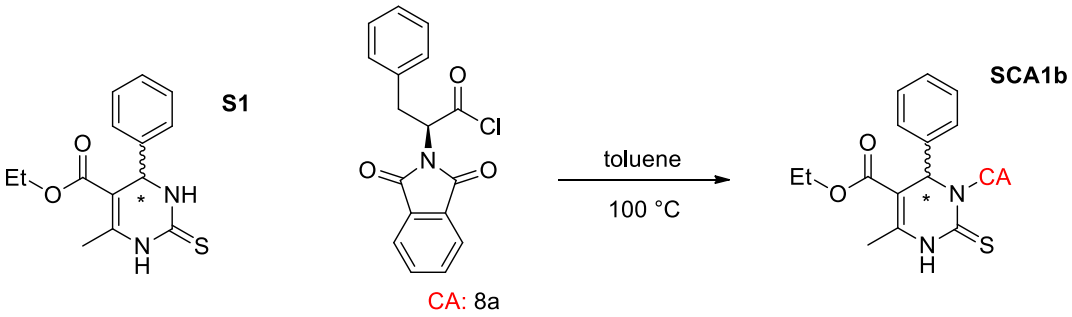

To a suspension of Thio-DHPM (1 mmol) in toluene was added 8a (0.33mmol to 1mmol). After the addition, reaction mixture was stirred at 100 °C. The reaction was stirred at same high temperature till it was completed (TLC). A cold saturated aqueous solution of NH_4Cl (30 ml) was introduced. The reaction contents were washed with water (2x25 ml), treated with brine, dried over anhydrous Na_2SO_4, and concentrated under reduced pressure.

6.8.7.4.2 *Synthesis of diasteroisomers with 8c*

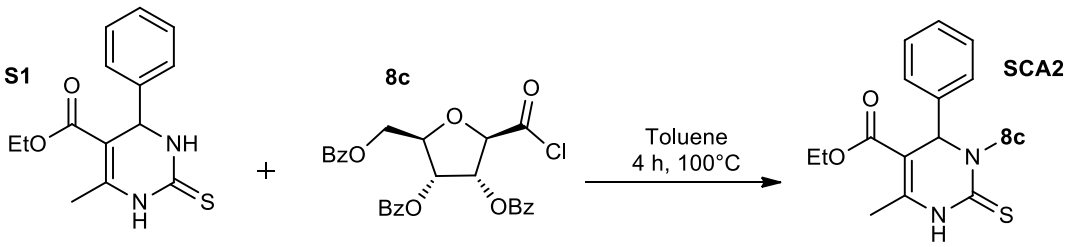

To a 0.5M toluene solution of 2,3,5-tri-O-benzoyl-β-D-ribofuranosyl chloride **8c** (1 mmol), **S1** (0.3 mmol) was added. The mixture was left for 4h at 100°C and then it was concentrated *in vacuo*.

6.8.8 Enzymatic resolution

6.8.8.1 With Subtilisine (from bacillius licheniformis)[134], α-chymotrypsin and esterase from porcine liver

A suspension of the racemic dihydropyrimidine (0.39mmol, 100mg), Trizma in water (0.044M, 8.75mL), and acetonitrile or DMSO (0.3M, 1.25mL) was heated to 37°C, sometimes to help the dissolution of the DHPM was used acetone, 1 or 2 drops. The enzyme (50mg, 12.45unit/mg solid) was added and the suspension was agitated. The pH was maintained at 7.8 with subtilisine, and 7.4 for chymotrypsin and esterase, with a solution of NaOH 1 M. The extent of the optical enrichment was followed by chiral HPLC: for N1 Lux5uCell 3, isocratic elution at ambient temperature with 10% isopropanol in hexanes, 0.5 mL/min, retention times: (+) and (–)-DHPM ester = 22.3 and 31.6 min, for O3 Lux5uCell 1 isocratic elution at ambient temperature with 20% isopropanol in hexanes, 0.8 mL/min, retention times: (+) and (–)-DHPM ester = 8.1 and 10.2 min. The reaction was stopped once the solution had been enriched with one of the two epimers. The batch was cooled to 20°C, and then AcOEt (2x10mL) was added. The combined organic layers were washed with water (2x10mL) containing Na_2CO_3. The aqueous layers were acidified with HCl acq. and estracted with chloroform (2x10mL).The organic layers were concentrated to afford the products. The starting material was only extraxted till now.

6.9 Experimental conditions for the cell free BACE1 inhibition assay

6.9.1 Intrinsic fluorescence spectra measurements.

Starting from 10 mM in DMSO stock solutions of compounds O2-11, S1-7 and N1-6, N8, N10-13, N14, 1 mM solutions in DMSO of each compound were prepared, and further diluted with a 20 mM acetate buffer soln. at pH = 4.5. to a final 10 μM concentration. The spectra were recorded in the range 450 to 600 nm with λexc = 345 nm. The excitation (Ex) and emission (Em) slits were set at 10 nm.

6.9.2 Assay conditions

The excitation and emission wavelengths were set respectively at 345 nm and 505 nm, the excitation and emission slits were 10 nm, the emission intensity was recorded for 60 minutes at 0.01 seconds intervals.

The Stock solution of the enzyme (human β-secretase) for the kinetic assay was composed of 5 μL of the commercial enzyme solution dissolved in 995 μL of 20 mM acetate buffer at pH = 4.5 in the presence of 4% of DMSO. This solution was stirred and left in the fridge for at least 2 hours to allow the protein folding. Then 200 μL was put in the quartz cell and allow the protein folding at r.t before the assay.

Starting from stock DMSO 10mM solutions of each inhibitor O2-17, S1-7 and N1-6, N8-12, N14-N16, 1 mM, 0.1 mM, 0.5 mM, 50 μM, 25 μM solutions in DMSO were prepared.

A 10 mM DMSO solution of the the substrate (Arg-Glu(EDANS)-(Asn^{670},Leu^{671})-Amyloid β/A4 Protein Precursor$_{770}$ (668-675)-Lys(DABCYL)-Arg trifluoroacetate salt) was used.

In the enzymatic assay a mixture of the enzyme solution (200 μL), and the substrate solution (2 μL), in the quartz cell was shaked and then left on standing 5 minutes before recording the fluorescence emission. The enzyme solution (200 μL) was left at r.t. for 30 minutes before the substrate solution was added, in order to allow the protein folding. An increasing of fluorescence intensity vs time was observed, due to the releasing of the fluorescent portion in the hydrolysis.

After few minutes, 2 μL of the 25 μM inhibitor solution was added in the cell, followed by the addition, at 5-10 min intervals, of 2 μL of the increasing concentration solutions of the inhibitor.

The decrease of the slope was indicative of inhibitory activity.

6.9.3 Experimental data for the determination of IC_{50} for compounds:

6.9.3.1 2-oxo-DHPMs (O2-O17)

O2	Add. N°	[I]	[I]Int	1 (%)	2 (%)	3 (%)
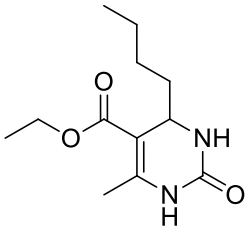	1	0	0	100.0	100.0	100.0
	2	$2.5*10^{-5}$	$2.5*10^{-7}$	82.5	72.1	57.8
	3	$5.0*10^{-5}$	$7.3*10^{-7}$	60.8	52.7	57.0
	4	$1.0*10^{-4}$	$1.7*10^{-6}$	45.8	53.0	48.3
	5	$5.0*10^{-4}$	$6.4*10^{-6}$	42.2	44.9	38.5
	6	$1.0*10^{-3}$	$1.6*10^{-5}$	30.0	32.7	30.4
	7	$1.0*10^{-2}$	$1.1*10^{-4}$	30.0	23.8	20.8
IC_{50} : 2.26 ± 0.18µM						

O3	Add. N°	[I]	[I]Int	1 (%)	2 (%)	3 (%)
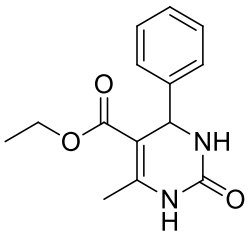	1	0	0	100.0	100.0	100.0
	2	$2.5*10^{-5}$	$2,9*10^{-7}$	81,8	85,9	85,4
	3	$5.0*10^{-5}$	$7,6*10^{-7}$	70,8	55,4	53,0
	4	$1.0*10^{-4}$	$1,7*10^{-6}$	54,2	56,8	43,8
	5	$5.0*10^{-4}$	$6,4*10^{-6}$	41,1	43,6	30,7
IC_{50} : 2.8 ± 0.1µM						

O4	Add. N°	[I]	[I]Int	1 (%)	2 (%)	3 (%)
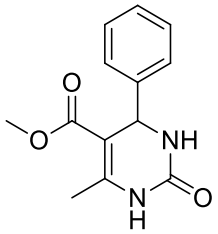	1	0	0	100.0	100.0	100.0
	2	$5.0*10^{-6}$	$5.0*10^{-8}$	72.0	66.8	80.9
	3	$1.00*10^{-5}$	$1.5*10^{-7}$	59.0	53.1	48.9
	4	$2.50*10^{-5}$	$3.9*10^{-7}$	47.1	53.6	47.9
	5	$5.00*10^{-5}$	$8.7*10^{-7}$	40.8		36.0
	6	$1.00*10^{-4}$	$1.8*10^{-6}$	32.4	31.2	38.6
	7	$5.00*10^{-4}$	$6.5*10^{-6}$	47.4	30.9	32.0
	8	$1.00*10^{-3}$	$1.6*10^{-5}$	27.8	27.1	18.3
IC_{50} : 0.3 ± 0.1µM						

Legenda: **[I]** concentration of the starting inhibitor solution; **[I]Int** concentration of inhibitor in the enzyme solution; **1,2,3 (%)** enzyme residual activity of each kinetics.

O5	Add. N°	[I]	[I]Int	1 (%)	2 (%)	3 (%)
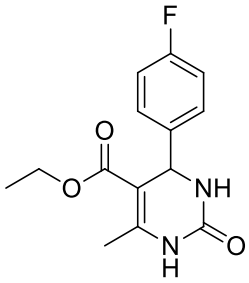	1	0	0	100.0	100.0	100.0
	2	$2.5*10^{-5}$	$2.5*10^{-7}$	59.3	89.4	77.2
	3	$5.0*10^{-5}$	$7.3*10^{-7}$	44.1	74.1	59.6
	4	$1.0*10^{-4}$	$1.7*10^{-6}$	30.9	45.3	39.8
	5	$5.0*10^{-4}$	$6.4*10^{-6}$	27.4	2.7	38.1
	6	$1.0*10^{-3}$	$1.6*10^{-5}$	20.9	17.9	32.6

IC_{50} : 1.72 ± 0.38µM

O6	Add. N°	[I]	[I]Int	1 (%)	2 (%)	3 (%)
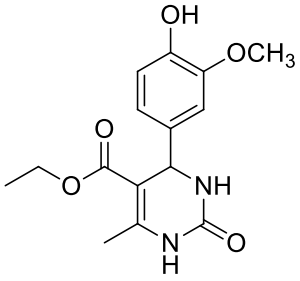	1	0	0	100.0	100.0	100.0
	2	$2.5*10^{-5}$	$2.5*10^{-7}$	72.9	71.4	61.2
	3	$5.0*10^{-5}$	$7.3*10^{-7}$	39.1	41.1	16.9
	4	$1.0*10^{-4}$	$1.7*10^{-6}$	35.2	33.8	55.1
	5	$5.0*10^{-4}$	$6.4*10^{-6}$	31.1	24.5	23.1
	6	$1.0*10^{-3}$	$1.6*10^{-5}$	16.7	19.9	20.6
	7	$1.0*10^{-2}$	$1.1*10^{-4}$	22.4	5.3	16.3

IC_{50} : 0.65 ± 0.03µM

O7	Add. N°	[I]	[I]Int	Test(%)
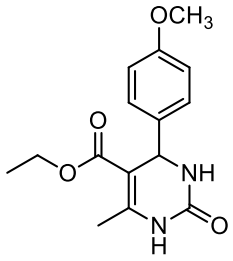	1	0	0	100.0
	2	$1*10^{-4}$	$9.8*10^{-7}$	65.9
	3	$3*10^{-4}$	$3.9*10^{-6}$	70.0
		$5*10^{-4}$	$8.7*10^{-6}$	56.2
	4	$1*10^{-3}$	$1.8*10^{-5}$	63.4
	5	$5*10^{-3}$	$6.5*10^{-5}$	51.5
	6	$1*10^{-3}$	$1.6*10^{-4}$	35.4

IC_{50} : 46 µM

Legenda: **[I]** concentration of the starting inhibitor solution; **[I]Int** concentration of inhibitor in the enzyme solution; **1,2,3 (%)** enzyme residual activity of each kinetics.

O8	Add. N°	[I]	[I]Int	1 (%)	2 (%)	3 (%)
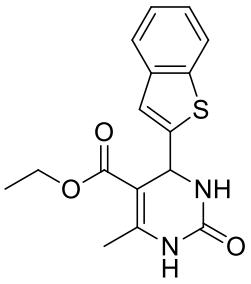	1	0	0	100.0	100.0	100.0
	2	$5.0*10^{-6}$	$4.9*10^{-8}$	73.2	78.8	88.5
	3	$2.5*10^{-5}$	$2.9*10^{-7}$	58.0	66.0	62.4
	4	$5.0*10^{-5}$	$7.7*10^{-7}$	45.2	57.4	60.3
	5	$1.0*10^{-4}$	$1.7*10^{-6}$	37.9	45.4	52.5
	6	$5.0*10^{-4}$	$6.4*10^{-6}$	30.9	47.0	52.0
	7	$1.0*10^{-3}$	$1.6*10^{-5}$	26.4	26.9	36.9
IC_{50} : 1.4 ± 0.1µM						

O9	Add. N°	[I]	[I]Int	test(%)
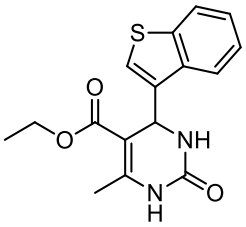	1	0	0	100.0
	2	$1*10^{-4}$	$9.8*10^{-7}$	79.4
	3	$3*10^{-4}$	$3.9*10^{-6}$	63.5
	4	$1*10^{-3}$	$1.8*10^{-5}$	52.5
	5	$5*10^{-3}$	$6.5*10^{-5}$	55.0
	6	$1*10^{-3}$	$1.6*10^{-4}$	45.7
IC_{50} : 71 µM				

O10	Add. N°	[I]	[I]Int	1 (%)	2 (%)	3 (%)
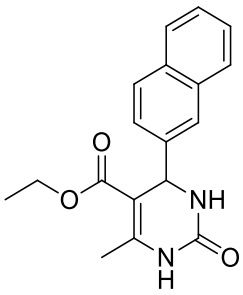	1	0	0	100.0	100.0	100.0
	2	$5.0*10^{-6}$	$5.2*10^{-8}$	94.2	80.8	63.3
	3	$1.0*10^{-5}$	$1.5*10^{-7}$	93.1	79.7	61.8
	4	$2.5*10^{-5}$	$4.1*10^{-7}$	55.0	78.8	52.6
	5	$5.0*10^{-5}$	$9.1*10^{-7}$	32.5	41.8	31.3
	6	$1.0*10^{-4}$	$1.9*10^{-6}$	23.3	31.2	11.2
	7	$5*10^{-4}$	$6.8*10^{-6}$	21.2	42.9	22.9
	8	$1.0*10^{-3}$	$1.7*10^{-5}$	/	/	4.3
IC_{50} : 0.5 ± 0.1µM						

O11	Add. N°	[I]	[I]Int	1 (%)	2 (%)	3 (%)
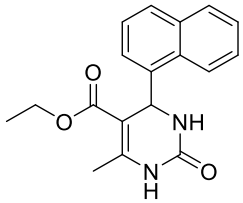	1	0	0	100.0	100.0	100.0
	2	$2.5*10^{-5}$	$2.5*10^{-7}$	94.5	79.3	68.9
	3	$5.0*10^{-5}$	$7.3*10^{-7}$	62.7	65.6	73.9
	4	$1.0*10^{-4}$	$1.7*10^{-6}$	64.0	49.6	39.7
	5	$5.0*10^{-4}$	$6.4*10^{-6}$	47.3	49.4	38.1
	6	$1.0*10^{-3}$	$1.6*10^{-5}$	39.2	37.3	28.4
	7	$1.0*10^{-2}$	$1.1*10^{-4}$	32.7	36.3	15.0
IC_{50} : 3.1 ± 0.5µM						

Legenda: **[I]** concentration of the starting inhibitor solution; **[I]Int** concentration of inhibitor in the enzyme solution; **1,2,3 (%)** enzyme residual activity of each kinetics.

O12	Add. N°	[I]	[I]Int	Test(%)
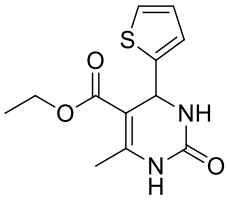	1	0	0	100.0
	2	$1*10^{-4}$	$9.8*10^{-7}$	57.5
	3	$3*10^{-4}$	$3.9*10^{-6}$	45.2
		$5*10^{-4}$	$8.7*10^{-6}$	37.4
	4	$1*10^{-3}$	$1.8*10^{-5}$	32.1
	5	$5*10^{-3}$	$6.5*10^{-5}$	28.9
	6	$1*10^{-3}$	$1.6*10^{-4}$	22.2
IC_{50} : 2.2 µM				

O13	Add. N°	[I]	[I]Int	Test(%)
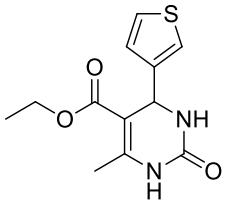	1	0	0	100.0
	2	$1*10^{-4}$	$9.8*10^{-7}$	64.1
	3	$3*10^{-4}$	$3.9*10^{-6}$	45.9
		$5*10^{-4}$	$8.7*10^{-6}$	38.7
	4	$1*10^{-3}$	$1.8*10^{-5}$	31.1
	5	$5*10^{-3}$	$6.5*10^{-5}$	25.9
IC_{50} : 3.2µM				

O14	Add. N°	[I]	[I]Int	Test(%)
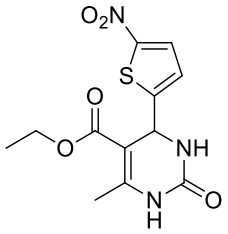	1	0	0	100.0
	2	$1*10^{-4}$	$9.8*10^{-7}$	50.9
	3	$3*10^{-4}$	$3.9*10^{-6}$	46.6
		$5*10^{-4}$	$8.7*10^{-6}$	44.9
	4	$1*10^{-3}$	$1.8*10^{-5}$	43.5
	5	$5*10^{-3}$	$6.5*10^{-5}$	45.3
	6	$1*10^{-3}$	$1.6*10^{-4}$	36.7
IC_{50} : 1.2 µM				

O16	Add. N°	[I]	[I]Int	1 (%)	2 (%)	3 (%)
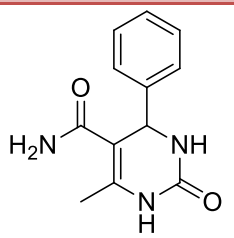	1	0	0	100	100	100
	2	$2.5*10^{-5}$	$2.5*10^{-7}$	67.1	78.5	46.2
	3	$5.0*10^{-5}$	$7.3*10^{-7}$	55.2	52.2	90.0
	4	$1.0*10^{-4}$	$1.7*10^{-6}$	34.9	46.9	31.8
	5	$5.0*10^{-4}$	$6.4*10^{-6}$	37.2	36.8	24.8
	6	$1.0*10^{-3}$	$1.6*10^{-5}$	32.9	31.0	24.3
IC_{50} : 1.60 ± 0.03µM						

Legenda: **[I]** concentration of the starting inhibitor solution; **[I]Int** concentration of inhibitor in the enzyme solution; **1,2,3 (%)** enzyme residual activity of each kinetics.

O17	Add. N°	[I]	[I]Int	1 (%)	2 (%)	3 (%)
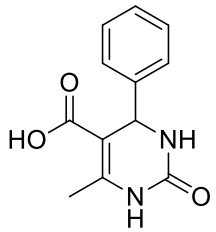	1	0	0	100	100	100
	2	$2.5*10^{-5}$	$2.5*10^{-7}$	86.9	100.3	66.8
	3	$5.0*10^{-5}$	$7.3*10^{-7}$	80.4	93.5	59.5
	4	$1.0*10^{-4}$	$1.7*10^{-6}$	80.4	80.2	45.8
	5	$5.0*10^{-4}$	$6.4*10^{-6}$	53.3	65.3	45.0
	6	$1.0*10^{-3}$	$1.6*10^{-5}$	50.6	58.8	36.9
	7	$1.0*10^{-2}$	$1.1*10^{-4}$	44.8	44.9	34.0
IC_{50} : 34 ± 8.2µM						

O18	Add. N°	[I]	[I]Int	1 (%)	2 (%)	3 (%)
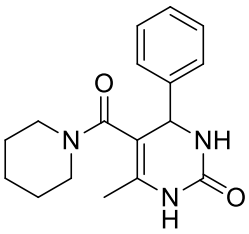	1	0	0	100.00	100.00	100.00
	2	$2.5*10^{-5}$	$2.5*10^{-7}$	72.2	73.2	89.3
	3	$5.0*10^{-5}$	$7.3*10^{-7}$	63.9	53.2	28.8
	4	$1.0*10^{-4}$	$1.7*10^{-6}$	47.5	51.6	13.3
	5	$5.0*10^{-4}$	$6.4*10^{-6}$	47.5	36.1	8.7
	6	$1.0*10^{-3}$	$1.6*10^{-5}$	42.6	36.1	25.6
	7	$1.0*10^{-2}$	$1.1*10^{-4}$	32.2	9.0	0.0
IC_{50} : 34 ± 8.2µM						

Legenda: **[I]** concentration of the starting inhibitor solution; **[I]Int** concentration of inhibitor in the enzyme solution; **1,2,3 (%)** enzyme residual activity of each kinetics.

6.9.3.2 2-thio-DHPMs (S1-2, S4-7)

S1	Add. N°	[I]	[I]Int	1 (%)	2 (%)	3 (%)
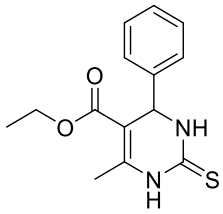	1	0	0	100.0	100.0	100.0
	2	$5.0*10^{-6}$	$5.0*10^{-8}$	100.0	100.0	100.0
	3	$2.5*10^{-5}$	$2,9*10^{-7}$	100.0	48,0	91,4
	4	$5.0*10^{-5}$	$7,6*10^{-7}$	52,1	98,1	56,2
	5	$1.0*10^{-4}$	$1,7*10^{-6}$	45,7	69,8	46,1
	6	$5.0*10^{-4}$	$6,4*10^{-6}$	38,3	28,1	49,0
IC_{50} : 1.5 ± 0.4µM						

S2	Add. N°	[I]	[I]Int	1 (%)	2 (%)	3 (%)
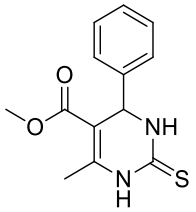	1	0	0	100.0	100.0	100.0
	2	$5.0*10^{-6}$	$5.0*10^{-8}$	81.7	92.7	98.0
	3	$1.0*10^{-5}$	$1.5*10^{-7}$	66.2	77.0	65.5
	4	$2.5*10^{-5}$	$3.9*10^{-7}$	58.6	61.2	60.4
	5	$5.0*10^{-5}$	$8.7*10^{-7}$	47.3	39.4	52.2
	6	$1.0*10^{-4}$	$1.8*10^{-6}$	27.2	31.1	41.0
	7	$5.0*10^{-4}$	$6.5*10^{-6}$	35.1	30.5	/
	8	$1.0*10^{-3}$	$1.6*10^{-5}$	27.1	24.5	29.8
	9	$1.0*10^{-2}$	$6.2*10^{-5}$	25.3	15.1	10.9
IC_{50} : 0.85 ± 0.03µM						

S4	Add. N°	[I]	[I]Int	1 (%)	2 (%)	3 (%)
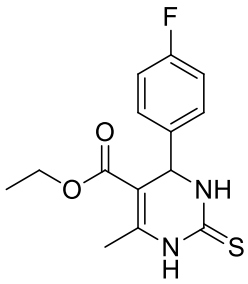	1	0	0	100.0	100.0	100.0
	2	$2.5*10^{-5}$	$2.5*10^{-7}$	41.3	46.4	53.2
	3	$5.0*10^{-5}$	$7.3*10^{-7}$	32.9	35.4	35.5
	4	$1.0*10^{-4}$	$1.7*10^{-6}$	35.9	26.6	38.2
	5	$5.0*10^{-4}$	$6.4*10^{-6}$	28.1	22.5	30.3
	6	$1.0*10^{-3}$	$1.6*10^{-5}$	6.6	21.1	18.8
	7	$1.0*10^{-2}$	$1.1*10^{-4}$	4.1	4.1	21.4
	8	$1.0*10^{-2}$	$1.9*10^{-4}$	/	/	4.3
IC_{50} : 0.24 ± 0.05µM						

S5	Add. N°	[I]	[I]Int	1 (%)	2 (%)	3 (%)
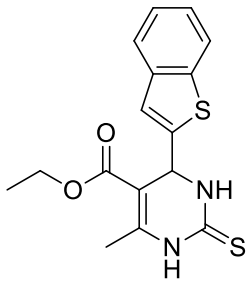	1	0	0	100.0	100.0	100.0
	2	$2.5*10^{-5}$	$2.5*10^{-7}$	59.4	63.1	74.3
	3	$5.0*10^{-5}$	$7.3*10^{-7}$	41.8	54.6	37.3
	4	$1.0*10^{-4}$	$1.7*10^{-6}$	31.2	42.4	28.1
	5	$5.0*10^{-4}$	$6.4*10^{-6}$	28.8	26.8	24.0
	6	$1.0*10^{-3}$	$1.6*10^{-5}$	13.3	32.9	8.1
	7	$1.0*10^{-2}$	$1.1*10^{-4}$	5.9	24.6	20.0
	8	$1.0*10^{-2}$	$1.9*10^{-4}$	12.8	14.4	/
IC_{50} : 0.7 ± 0.1µM						

Legenda: **[I]** concentration of the starting inhibitor solution; **[I]Int** concentration of inhibitor in the quarz cell in the enzyme solution; **1,2,3 (%)** enzyme residual activity of each kinetics

S6	Add. N°	[I]	[I]Int	1 (%)	2 (%)	3 (%)
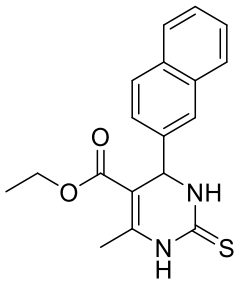	1	0	0	100.0	100.0	100.0
	2	$2.5*10^{-5}$	$2.5*10^{-7}$	64.6	59.7	79.1
	3	$5.0*10^{-5}$	$7.3*10^{-7}$	57.6	51.5	53.7
	4	$1.0*10^{-4}$	$1.7*10^{-6}$	46.5	32.5	32.8
	5	$5.0*10^{-4}$	$6.4*10^{-6}$	40.5	27.2	30.7
	6	$1.0*10^{-3}$	$1.6*10^{-5}$	9.3	21.2	22.2
IC_{50} : 1.09 ± 0.04µM						

S7	Add. N°	[I]	[I]Int	1 (%)	2 (%)	3 (%)
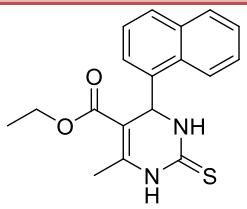	1	0	0	100.0	100.0	100.0
	2	$2.5*10^{-5}$	$2.5*10^{-7}$	56.2	50.5	59.3
	3	$5.0*10^{-5}$	$7.3*10^{-7}$	36.8	45.2	40.8
	4	$1.0*10^{-4}$	$1.7*10^{-6}$	31.1	31.0	27.3
	5	$5.0*10^{-4}$	$6.4*10^{-6}$	18.5	30.3	30.3
	6	$1.0*10^{-3}$	$1.6*10^{-5}$	18.4	17.3	34.2
IC_{50} : 0.3 ± 0.1µM	7	$1.0*10^{-2}$	$1.1*10^{-4}$	4.2	25.1	20.7

Legenda: **[I]** concentration of the starting inhibitor solution; **[I]Int** concentration of inhibitor in the quarz cell in the enzyme solution; **1,2,3 (%)** enzyme residual activity of each kinetics.

6.9.3.3 2-iminoDHPMs (N1-6, N8-12, N14-16)

N1	Add. N°	[I]	[I]Int	1 (%)	2 (%)	3 (%)
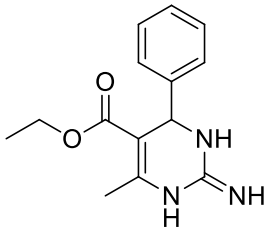	1	0	0	100.0	100.0	100.0
	2	$5.0*10^{-6}$	$4.9*10^{-8}$	78.7	81.0	95.6
	3	$2.5*10^{-5}$	$2.9*10^{-7}$	50.8	51.5	72.1
	4	$5.0*10^{-5}$	$7.7*10^{-7}$	49.6	31.5	32.3
	5	$1.0*10^{-4}$	$1.7*10^{-6}$	32.8	27.4	37.8
	6	$5.0*10^{-4}$	$6.4*10^{-6}$	27.0	26.0	27.0
IC_{50} : 0.5 ± 0.1µM						

N2	Add. N°	[I]	[I]Int	1 (%)	2 (%)	3 (%)
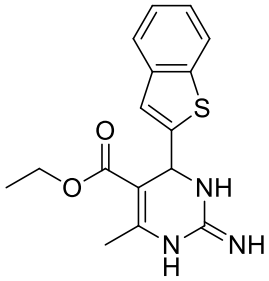	1	0	0	100.0	100.0	100.0
	2	$5.0*10^{-6}$	$4.9*10^{-8}$	82.1	83.4	85.8
	3	$1.0*10^{-5}$	$1.5*10^{-7}$	81.7	58.7	68.4
	4	$2.5*10^{-5}$	$3.9*10^{-7}$	70.7	65.0	55.0
	5	$5.0*10^{-5}$	$8.6*10^{-7}$	55.1	38.3	55.0
	6	$1.0*10^{-4}$	$1.8*10^{-6}$	58.7	32.4	40.5
	7	$5.0*10^{-4}$	$6.5*10^{-6}$	40.9	22.1	51.6
IC_{50} : 0.3 ± 0.1µM						

N3	Add. N°	[I]	[I]Int	1 (%)	2 (%)	3 (%)
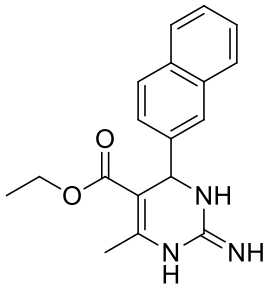	1	0	0	100.0	100.0	100.0
	2	$5.0*10^{-6}$	$4.9*10^{-8}$	64.3	88.0	/
	3	$1.0*10^{-5}$	$1.5*10^{-7}$	53.5	48.2	/
	4	$2.5*10^{-5}$	$3.9*10^{-7}$	51.1	41.2	43.2
	5	$5.0*10^{-5}$	$8.6*10^{-7}$	39.9	33.7	33.5
	6	$1.0*10^{-4}$	$1.8*10^{-6}$	37.7	33.5	18.5
	7	$5.0*10^{-4}$	$6.5*10^{-5}$	26.5	26.0	15.5
IC_{50} : 0.2 ± 0.1µM						

N4	Add. N°	[I]	[I]Int	1 (%)	2 (%)	3 (%)
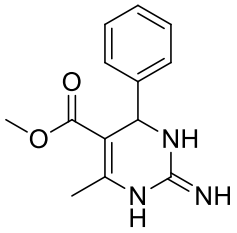	1	0	0	100.0	100.0	100.0
	2	$5.0*10^{-6}$	$4.9*10^{-8}$	76.8	62.9	66.6
	3	$2.5*10^{-5}$	$2.9*10^{-7}$	60.8	51.0	54.0
	4	$5.0*10^{-5}$	$7.7*10^{-7}$	43.1	43.6	46.2
	5	$1.0*10^{-5}$	$8.6*10^{-7}$	51.8	55.2	58.4
	6	$5.0*10^{-4}$	$5.6*10^{-6}$	35.7	30.2	31.9
	7	$1.0*10^{-3}$	$1.5*10^{-5}$	32.7	23.6	25.0
IC_{50} : 0.5 ± 0.1µM						

Legenda: **[I]** concentration of the starting inhibitor solution; **[I]Int** concentration of inhibitor in the quarz cell in the enzyme solution; **1,2,3 (%)** enzyme residual activity of each kinetics.

N5	Add. N°	[I]	[I]Int	1 (%)	2 (%)	3 (%)
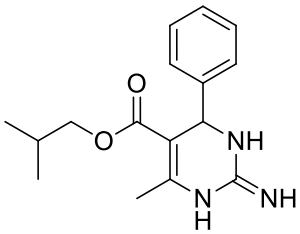	1	0	0	100.0	100.0	100.0
	2	$5.0* 10^{-6}$	$5.18* 10^{-8}$	80.5	59.5	95.8
	3	$1.0*10^{-5}$	$1.54* 10^{-7}$	66.1	76.8	56.6
	4	$2.5*10^{-5}$	$4.06* 10^{-7}$	44.8	58.2	42.4
	5	$5.0*10^{-5}$	$9.05* 10^{-7}$	46.8	42.6	
	6	$1.0* 10^{-4}$	$1.89* 10^{-6}$	46.7	39.8	44.6
	7	$5.0*10^{-4}$	$6.80* 10^{-6}$	43.1	28.0	32.2
	8	$1.0* 10^{-3}$	$1.65*10^{-5}$	39.0	13.1	54.7
	9	$1.0* 10^{-2}$	$1.13* 10^{-4}$	25.2	11.2	2.6

IC_{50} : 1.06 ± 0.19µM

N6	Add. N°	[I]	[I]Int	1 (%)	2 (%)	3 (%)
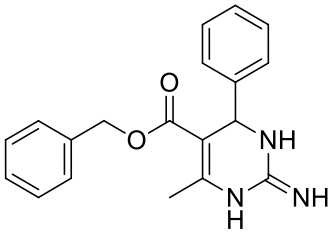	1	0	0	100.0	100.0	100.0
	2	$5.0* 10^{-6}$	$5.18* 10^{-8}$	100.0	100.0	100.0
	3	$1.0*10^{-5}$	$1.54* 10^{-7}$	96.9	82.2	83.6
	4	$2.5*10^{-5}$	$4.06* 10^{-7}$	205.1	63.5	90.6
	5	$5.0*10^{-5}$	$9.05* 10^{-7}$	71.0	27.4	117.5
	6	$1.0* 10^{-4}$	$1.89* 10^{-6}$	77.8	23.9	65.4
	7	$5.0*10^{-4}$	$6.80* 10^{-6}$	70.2	68.5	34.4
	8	$1.0* 10^{-3}$	$1.65*10^{-5}$	-180.7	-51.5	-96.3
	9	$1.0* 10^{-2}$	$1.13* 10^{-4}$	0	0	-378.1

IC_{50} : Inactive

N8	Add. N°	[I]	[I]Int	1 (%)	2 (%)	3 (%)
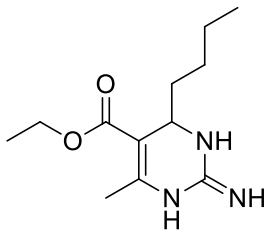	1	0	0	100.0	100.0	100.0
	2	$2.5*10^{-5}$	$2.5*10^{-7}$	95.8	56.4	81.0
	3	$5.0*10^{-5}$	$7.3*10^{-7}$	48.8	46.6	67.9
	4	$1.0*10^{-4}$	$1.7*10^{-6}$	39.9	40.7	37.2
	5	$5.0*10^{-4}$	$6.4*10^{-6}$	36.3	27.7	29.8
	6	$1.0*10^{-3}$	$1.6*10^{-5}$	31.1	24.5	22.9
	7	$1.0*10^{-2}$	$1.1*10^{-4}$	33.8	18.5	18.0
	8	$1.0*10^{-2}$	$1.9*10^{-4}$	1.9	3.3	0

IC_{50} : 1.06 ± 0.19µM

Legenda: **[I]** concentration of the starting inhibitor solution; **[I]Int** concentration of inhibitor in the quarz cell in the enzyme solution; **1,2,3 (%)** enzyme residual activity of each kinetics.

N9	Add. N°	[I]	[I]Int	1 (%)	2 (%)	3 (%)
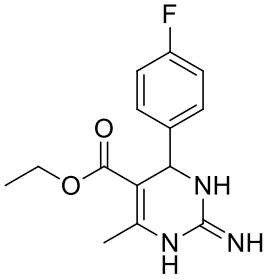	1	0	0	100.00	100.00	100.00
	2	$2.5*10^{-5}$	$2.5*10^{-7}$	76.6	37.1	54.4
	3	$5.0*10^{-5}$	$7.3*10^{-7}$	68.9	30.9	40.4
	4	$1.0*10^{-4}$	$1.7*10^{-6}$	58.4	27.8	27.6
	5	$5.0*10^{-4}$	$6.4*10^{-6}$	47.3	22.6	24.0
	6	$1.0*10^{-3}$	$1.6*10^{-5}$	36.2	15.6	16.6
	7	$1.0*10^{-2}$	$1.1*10^{-4}$	27.5	11.5	12.9
IC_{50} : 0.30 ± 0.14µM						

N10	addition N°	[I]	[I]Int	1 (%)	2 (%)	3 (%)
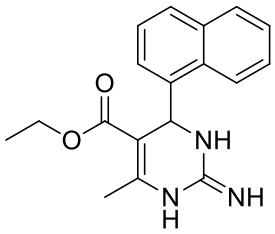	1	0	0	100.0	100.0	100.0
	2	$2.5*10^{-5}$	$2.5*10^{-7}$	77.9	66.2	74.1
	3	$5.0*10^{-5}$	$7.3*10^{-7}$	56.8	63.7	68.9
	4	$1.0*10^{-4}$	$1.7*10^{-6}$	43.4	41.6	47.2
	5	$5.0*10^{-4}$	$6.4*10^{-6}$	36.0	30.4	34.9
	6	$1.0*10^{-3}$	$1.6*10^{-5}$	26.5	39.3	10.7
IC_{50} : 1.5 ± 0.1µM						

N11	Add. N°	[I]	[I]Int	1 (%)	2 (%)	3 (%)
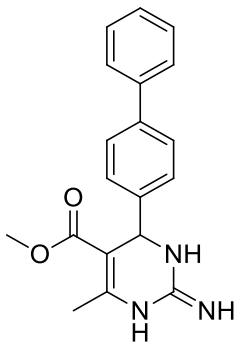	1	0	0	100.0	100.0	100.0
	2	$2.5*10^{-5}$	$2.5*10^{-7}$	115.1	50.2	81.0
	3	$5.0*10^{-5}$	$7.3*10^{-7}$	75.7	39.6	56.4
	4	$1.0*10^{-4}$	$1.7*10^{-6}$	58.5	40.2	59.5
	5	$5.0*10^{-4}$	$6.4*10^{-6}$	50.4	11.8	49.5
	6	$1.0*10^{-3}$	$1.6*10^{-5}$	56.1	19.4	46.6
	7	$1.0*10^{-2}$	$1.1*10^{-4}$	48.5	15.8	/
	8	$1.0*10^{-2}$	$1.9*10^{-4}$	/	24.2	27.7
IC_{50} : 4.65 ± 0.68µM						

Legenda: **[I]** concentration of the starting inhibitor solution; **[I]Int** concentration of inhibitor in the quarz cell in the enzyme solution; **1,2,3 (%)** enzyme residual activity of each kinetics.

N12	Add. N°	[I]	[I]Int	1 (%)	2 (%)	3 (%)
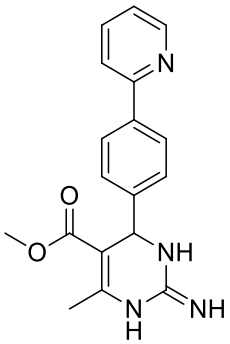	1	0	0	100.0	100.0	100.0
	2	$2.5*10^{-5}$	$2.5*10^{-7}$	66.1	68.6	65.5
	3	$5.0*10^{-5}$	$7.3*10^{-7}$	45.5	85.6	50.5
	4	$1.0*10^{-4}$	$1.7*10^{-6}$	36.8	61.2	43.4
	5	$5.0*10^{-4}$	$6.4*10^{-6}$	47.0	53.1	34.8
	6	$1.0*10^{-3}$	$1.6*10^{-5}$	74.5	36.0	26.3
	7	$1.0*10^{-2}$	$1.1*10^{-4}$	42.7	22.4	12.0
IC_{50} : 0.72 ± 0.13µM						

N14	Add. N°	[I]	[I]Int	1 (%)	2 (%)	3 (%)
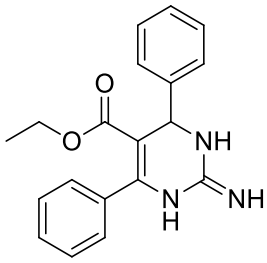	1	0	0	100.0	100.0	100.0
	2	$2.5*10^{-5}$	$2.5*10^{-7}$	53.6	57.0	52.6
	3	$5.0*10^{-5}$	$7.3*10^{-7}$	34.9	38.6	39.9
	4	$1.0*10^{-4}$	$1.7*10^{-6}$	26.2	23.8	25.3
	5	$5.0*10^{-4}$	$6.4*10^{-6}$	9.5	26.1	20.2
	6	$1.0*10^{-3}$	$1.6*10^{-5}$	17.0	21.6	13.5
	7	$1.0*10^{-2}$	$1.1*10^{-4}$	8.6	6.5	9.1
IC_{50} : 0.28 ± 0.19µM						

N15	Add. N°	[I]	[I]Int	1 (%)	2 (%)	3 (%)
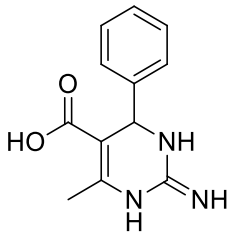	1	0	0	100	100	100
	2	$2.5*10^{-5}$	$2.5*10^{-7}$	63.5	83.3	55.3
	3	$5.0*10^{-5}$	$7.3*10^{-7}$	48.9	73.0	50.2
	4	$1.0*10^{-4}$	$1.7*10^{-6}$	42.4	74.3	42.9
	5	$5.0*10^{-4}$	$6.4*10^{-6}$	28.4	61.5	34.2
	6	$1.0*10^{-3}$	$1.6*10^{-5}$	21.2	41.0	23.7
	7	$3.00*10^{-3}$	$4.37*10^{-5}$	21.6	36.0	20.4
IC_{50} : 0.69 ± 0.19µM						

N16	Add. N°	[I]	[I]Int	1 (%)	2 (%)	3 (%)
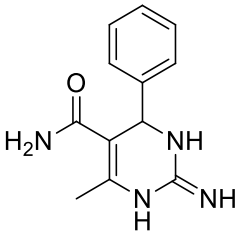	1	0	0	100.0	100.00	100.00
	2	$2.5*10^{-5}$	$2.5*10^{-7}$	78.9	70.3	77.2
	3	$5.0*10^{-5}$	$7.3*10^{-7}$	70.4	39.3	62.5
	4	$1.0*10^{-4}$	$1.7*10^{-6}$	48.6	29.8	55.3
	5	$5.0*10^{-4}$	$6.4*10^{-6}$	37.2	30.2	42.8
	6	$1.0*10^{-3}$	$1.6*10^{-5}$	38.2	23.6	37.5
	7	$1.0*10^{-2}$	$1.1*10^{-4}$	34.1	24.0	25.6
IC_{50} : 2.15 ± 0.82µM						

Legenda: **[I]** concentration of the starting inhibitor solution; **[I]Int** concentration of inhibitor in the quarz cell in the enzyme solution; **1,2,3 (%)** enzyme residual activity of each kinetics.

6.10 CNS penetration: In vitro Parallel artificial membrane permeability assay (PAMPA)-Blood brain barrier (BBB).

PAMPA assay (parallel artificial membrane permeability assay) was used as preliminary evaluation of the brain penetration. The PAMPA-BBB method was described by Di et al, which employed a brain lipid porcine membrane. [170]

Test compounds (1-2 mg of Atenolol, Caffeine, Desipramine, Enoxacin, Hydrocortisone, Ofloxacin, Piroxicam, Testosterone, Promazine and Verapamil) were dissolved in EtOH (1500 µL) and 3500 µL of PBS pH=7.4 buffer were added to reach 30% of EtOH concentration in the experiment. Meanwhile the compounds to be determined (O10, S6, N3) were also dissolved in 1500 µL of EtOH and 3500 µL of PBS pH=7.4 buffer.

These solutions were filtered. 180 µL of each test compound solution and O10, S6, N3 solution were added to a 96-well plate and the UV spetra were determined. Subsequently 180 µL of PBS/EtOH (70/30) were inserted in each plate of the acceptor 96-well microplate. The donor 96-well plate was coated with 4 µL of porcine brain lipid in dodecane (20 mg mL^{-1}) and after 5 minutes, 180 µL of each test compound solution and compound to be tested solution were added. Then the donor plate was carefully put on the acceptor plate to form a “sandwich”, which was left undisturbed for 2h and 30 min at 25 °C.

During this time the compounds diffused from the donor plate through the brain lipid membrane into the acceptor plate. After incubation, the donor plate was removed. UV plate reader determined the concentration of compounds and commercial drugs in the acceptor and the donor wells. Every sample was analyzed at three to five wavelengths, in 3 wells and in two independent runs. Results are given as the mean [standard deviation (SD)] and the average of the two runs is reported. 10 quality control compounds (previously mentioned) of known BBB permeability were included in each experiment to validate the analysis set.

6.10.1 *In vitro PAMPA-BBB assay to determine compound penetration into the brain*

The *in vitro* permeabilities (*Pe*) of commercial drugs through lipid membrane extract together with different compounds were determined (Equation 2) and described in Table 18

$$P_e = \frac{Vd \times Vr}{(Vd+Vr)St} \; Ln \; \frac{100\,Vd}{100Vd - \%T(Vd+Vr)}$$

Vd: donor plate volume (180 µL)
Vr: acceptor plate volume(180 µL)
S: area (0.266 cm^2)
t: incubation time (s)

Equation 2 *permeability (Pe)*

Compound	Bibl.[b]	*Pe* (10^{-6} cm s^{-1})[c]	Prediction
Atenolol	0.8	0.2 ± 0.3	CNS -
Caffeine	1.3	0.3 ± 0.2	CNS -
Desipramine	12	7.0 ± 0.4	CNS +
Enoxacin	1.6	0.4 ± 0.1	CNS -
Hydrocortisone	2.4	1.0 ± 0.3	CNS -
Ofloxacine	0.8	1.5 ± 0.2	CNS -
Piroxicam	2.5	3.4 ± 0.4	CNS +
Promazine	8.8	9.7 ± 1.1	CNS +
Testosterone	17	14.9 ± 0.6	CNS +
Verapamil	16	18.8 ± 0.1	CNS +
O10		8.3 ± 0.3	CNS +
S6		9.8 ± 1.0	CNS +
N3		6.9 ± 3.5	CNS +

Table 18 *Permeability (Pe 10^{-6} cm s^{-1}) in the PAMPA-BBB assay for 10 commercial drugs (used in the experiment validation) and different compounds with their predictive penetration in the CNS[a] ([a] PBS:EtOH (70:30) was used as solvent. [b]Reference Di et al. [c]Data are the mean ± SD of 2 independent experiments).*

The correlation between experimental-described values was obtained (R^2= 0.898) (Figure 47). From this equation and following the pattern established in the literature for BBB permeation prediction[171] we could classify compounds as CNS+ when they present a permeability > $3.9 \cdot 10^{-6}$ cm s^{-1} and CNS– when they present a permeability < $2.1 \cdot 10^{-6}$ cm s^{-1}.

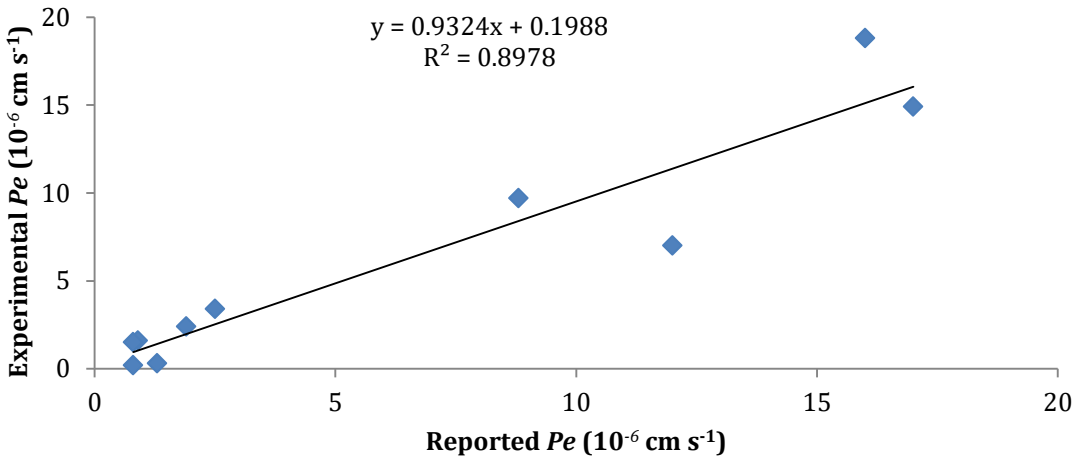

Figure 47 *Linear correlation between experimental and reported permeability of commercial drugs using the PAMPA-BBB assay.*

Article:

Fabio Benedetti, Federico Berti, Lidia Fanfoni, Michele Garbo, **Giorgia Regini** and Fulvia Felluga, "Synthesis of Chiral, Enantiopure Allylic Amines by the Julia Olefination of α-Amino Esters" , *Molecules*, **2016**, 21, 805.

Partecipation to Conferences and Congresses:

Congresso nazionale 2014 della Società Chimica Italiana (7-12 sett., 2014, Rende-CS).
Poster e Short comm.: Sintesi di allilammine da amminoacidi α- chirali.
XVI Convegno Reazioni Pericicliche e Sintesi di Etero e Carbocicli (25-27 giug., 2015, Matera).
Comm: An Old Approach For New Inhibitors of BACE I:The Biginelli Reaction.
XXXVII Convegno Nazionale della Divisione di Chimica Organica (18-22 sett., 2016, Venezia).
Comm: Dihydropyrimidines as promising BACE 1 inhibitors.

Acknowledgements

Desidero ringraziare

La mia relatrice, Prof. Fulvia Felluga, il Prof. Fabio Benedetti e il Dott. Federico Berti per avermi dato la possibilità di partecipare a questo progetto, per aver condiviso la loro profonda conoscenza, per la loro pazienza, e per i preziosi consigli durante questi tre anni.

Dott. Sara Drioli e Dott. Martina Tommasini per avermi aiutato durante questo percorso, ma anche per le chiacchiere e le risate.

Tutti gli amici con i quali ho condiviso preziosi momenti di vita.

Infine Ilir, i miei genitori, Franco e Lidia, e i miei nonni, Jvonne e Giorgio per avermi sostenuto fino a qui.